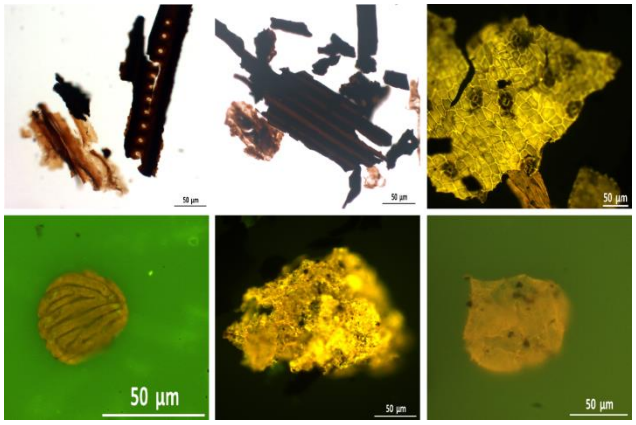

Characterization of organic facies and identification of potential source rocks in Jurassic sedimentary sequences of the Lusitanian Basin (Portugal)

Paula Alexandra Sá da Silva Gonçalves
Doutoramento em Geociências
Especialidade Petrologia e Geoquímica
Departamento Geociências, Ambiente e Ordenamento do Território
2014

Orientador
Deolinda Flores, Professora Catedrática, Faculdade de Ciências da Universidade do Porto

Coorientador
João Graciano Mendonça Filho, Professor Associado, Universidade Federal do Rio de Janeiro

FCT Fundação para a Ciência e a Tecnologia
MINISTÉRIO DA EDUCAÇÃO E CIÊNCIA
POPH PROGRAMA OPERACIONAL POTENCIAL HUMANO
QREN QUADRO DE REFERÊNCIA ESTRATÉGICO NACIONAL
UNIÃO EUROPEIA Fundo Social Europeu
GOVERNO DA REPÚBLICA PORTUGUESA

Acknowledgement

During this work I encountered several difficulties which were overcome with the help and support of many people. Thus, I must express my gratitude to all who helped me completing this project. A particular thank:

To my supervisor Professor Deolinda Flores. I am very grateful for her help and insightful guidance throughout this thesis, her constructive criticism and corrections. Thank for betting on me.

To my co-supervisor, Professor João Graciano Mendonça Filho, for the opportunity to work at the Laboratory of Palynofacies and Organic Facies (LAFO) with his fantastic team, for the fruitful discussions that largely helped improving this work and for the friendship.

To Geology Centre of the University of Porto and Professor Fernando Noronha, as the scientific coordinator, for providing all the support needed for this work.

To LAFO for all the technical support and to all the people who work there for receiving and making me feel welcome. In particular I would like to express my gratitude to Joalice Oliveira Mendonça, Frederico Sobrinho and Taís Freitas for the friendship and support during my stay at Rio de Janeiro.

To Dr. Teresinha Abecassis and Doutor José Miguel Martins from DPEP (Divisão para a Pesquisa e Exploração de Petróleo) for the easy access to the available data in their library and Dr. Rita Silva from LNEG (Laboratório Nacional de Energia e Geologia) for the support during the sampling.

To my friends and colleagues at the Department of Geosciences, Environment and Spatial Planning (DGAOT), Joana Ribeiro, Anabela Costa, Violeta Ramos, Cândida Garcia and Irene Lopes. Thanks for your patience and support.

To Nadi Poças Ribeiro with whom I had the opportunity to share my first stay in Rio de Janeiro. Thanks for the nice and fun company that really helped reduce homesickness.

To my friends, Luís, Bernardo, António, Natália, Diana, Tiago and Alexandre who always supported me during this journey.

To my very good friend Ana Gomes for the unquestionable friendship, cherished support and encouragement since we met in the hallways of the Azores University.

Most importantly, I must thank to my family. Thank you all for always being beside me. Your presence was felt even when we were separated thousands of kilometers apart. Your love and support has made all this possible.

Financially, this work was supported by a scholarship from the Fundação para a Ciência e Tecnologia, Portugal (Ref: SFRH/BD/60875/2009) and by Scientific and Technical Cooperation Agreement FCT (Portugal)/CAPES (Brazil) project titled “Caracterização das variações organofaciológicas e identificação dos horizontes potencialmente geradores de petróleo no Jurássico da Bacia Lusitânica”; and partially funded by FEDER funds through the Operational Program Competitiveness Factors - COMPETE and by national funds through FCT - Fundação para a Ciência e Tecnologia, under the project PEst-OE/CTE/UI0039/2014.

Abstract

The Lusitanian Basin is one of the main Portuguese sedimentary basins that reveal potential to generate hydrocarbons (presence of source rocks, sealed reservoirs and traps). The sedimentary record of the Lusitanian Basin, deposited between Upper Triassic and the end of the Cretaceous (mainly during the Jurassic), is associated with the opening of the North Atlantic. Their geological setting has been intensely documented, but studies about type, content and maturation of the organic matter of its source rocks are scarce.

The main objective of this thesis is the determination of the hydrocarbon generative potential in some of the sub-basins of the Lusitanian Basin based on a comparative multidisciplinary study (organic petrology and organic geochemistry) of four boreholes. The Ramalhal-1 borehole was drilled in the Bombarral sub-basin, the Freixial-1 and Benfeito-1 boreholes were drilled in the Arruda sub-basin and the Barreiro-4 borehole was drilled in Lower Tagus sub-basin.

One hundred eighty nine cuttings samples were analyzed for organic petrology (mean random reflectance and palynofacies) and geochemistry (total organic carbon, total sulfur and insoluble residue, Rock-Eval pyrolysis and gas chromatography coupled with mass spectrometry) for determination of type, content and quality of the dispersed organic matter present in the Meso - Cenozoic sediments (mainly Jurassic).

Concerning to the type and quantity of organic matter as well as the depositional palaeoenvironments no major differences in the four boreholes were observed. The sedimentary sequence intercepted by the Ramalhal-1 borehole reveals a terrestrial origin for the organic matter (type III kerogen). The organic matter of the studied sequence was preserved in a proximal - distal environment and oxic conditions. The boreholes drilled in the Arruda sub-basin showed a mainly terrestrial organic matter (type III and IV kerogen) with TOC content usually lower than 1wt.%. However, some strata from the Montejunto, Cabaços and Brenha (Callovian) Formations showed an increase of marine organic matter (mixture type II/III kerogen). In this sub-basin the organic matter was deposited in a marine environment with variations in the redox condition (anoxic to oxic). The Barreiro-4 borehole is characterized by continental organic matter punctuated by marine palynomorphs that were preserved in a marine environment under anoxic-oxic conditions.

Regarding the potential to generate hydrocarbons, the Jurassic successions studied have poor potential as oil source rock. Nevertheless, some intervals of Abadia, Montejunto,

Cabaços and Brenha (Callovian age) Formations, in Arruda sub-basin, showed a good generative potential. In these intervals the organic matter reached the oil window.

The presence of solid bitumens is common in all the sub-basins. In the Central Sector (Bombarral and Arruda sub-basins) solid bitumens were preferentially in Candeeiros and Cabaços Formations whereas in Lower Tagus sub-basin they were identified in the Montejunto Formation and in the Tithonian - Cretaceous age samples.

Resumo

A Bacia Lusitânica é uma das principais bacias sedimentares portuguesas e apresenta potencial para a geração e acumulação de hidrocarbonetos (rocha mãe, reservatórios e armadilhas petrolíferas). O registo sedimentar da Bacia Lusitânica, depositado entre o Triássico Superior e o fim do Cretácico (sobretudo durante o Jurássico), está associado com a abertura do Atlântico Norte. Do ponto de vista estratigráfico e sedimentológico esta Bacia já foi intensamente estudada, no entanto estudos sobre o tipo, o conteúdo e a maturação da matéria orgânica das suas rochas mãe ainda são escassos.

Os principais objectivos deste trabalho são a caracterização de rochas geradoras e a avaliação do seu potencial de geração de hidrocarbonetos em algumas das sub-bacias da Bacia Lusitânica baseado num estudo comparativo (petrologia e geoquímica orgânica) de quatro poços de sondagem. O poço de sondagem Ramalha-1 foi executado na sub-bacia de Bombarral, os poços de sondagem Freixial-1 e Benfeito-1 na sub-bacia de Arruda enquanto o poço Barreiro-1 foi perfurado na sub-bacia do Baixo Tejo.

Cento e oitenta e nove amostras (*cuttings*) foram analisadas através de técnicas de petrologia orgânica (determinação da reflectância da vitrinite e dos betumes sólidos e palinofácies) e geoquímicas (carbono orgânico total, enxofre total e resíduo insolúvel, pirólise Rock-Eval e cromatografia gasosa acoplada a espectrómetro de massa) para determinação do conteúdo e tipo da matéria orgânica dispersa nos sedimentos Meso - Cenozóicos (maioritariamente Jurássicos).

Relativamente ao tipo e quantidade da matéria orgânica bem como o ambiente deposicional não existem grandes diferenças entre os quatro poços de sondagem. A sequência sedimentar interceptada pelo poço de sondagem Ramalhal-1 revela uma origem continental para a matéria orgânica (cerogénio tipo III). A matéria orgânica estuda nesta sequência foi preservada num ambiente óxico proximal - distal. Os poços de sondagem perfurados na sub-bacia de Arruda apresentam matéria orgânica essencialmente terrestre (cerogénio tipo III e IV) e valores de carbono orgânico total geralmente inferiores a 1%. Contudo, alguns níveis das Formações de Montejunto, Cabaços e Brenha (Caloviano) mostram um aumento em matéria orgânica marinha (mistura de cerogénio tipo II/III). Nesta sub-bacia a matéria orgânica foi depositada num ambiente marinho onde existiram condições redox variáveis (períodos óxicos a anóxicos). O poço de sondagem Barreiro-4 é

caracterizado por matéria orgânica continental, pontuada por palinomorfos marinhos, preservada em ambiente marinho sob condições óxicas-anóxicas.

No que diz respeito ao potencial de geração de hidrocarbonetos, as sucessões estudadas apresentam pouco potencial. No entanto, alguns níveis das Formações de Abadia, Montejunto, Cabaços e Brenha (Caloviano), na sub-bacia de Arruda, mostraram bom potencial para geração de hidrocarbonetos, tendo a matéria orgânica atingido a janela de geração.

A presença de betumes sólidos é comum a todas as sub-bacias. No Setor Central (sub-bacias do Bombarral e de Arruda), os betumes sólidos encontram-se, preferencialmente, nas Formações de Candeeiros e Cabaços enquanto na sub-bacia do Baixo Tejo foram observados na Formação Montejunto e nas amostras de idade Titoniana - Cretácica.

Contents

Contribution of the co-authors

Professor Deolinda Flores from Department of Geosciences, Environment and Spatial Planning of Faculty of Sciences of the University of Porto (Portugal) and Professor João Graciano Mendonça Filho from the Palynofacies and Organic Facies Laboratory (LAFO), Geosciences Institute, Federal University of Rio de Janeiro (Brazil), as my PhD supervisors, with whom I discussed firsthand the results and contributed to the improvement of the manuscripts.

Dr. Joalice Oliveira Mendonça from LAFO (Brazil) contributed as expert in palynofacies analysis.

Dr. Taís Freitas da Silva from LAFO (Brazil) provided GC - MS analysis and supported the biomarker data analysis.

Dr. Frederico Sobrinho da Silva from LAFO (Brazil) provides the photomicrographs of SEM observations.

List of Figures

List of Tables

List of Acronyms

AA: amino acids

AF: Aveiro Fault;

AOM: Amorphous organic matter

Bac: Bacteria

Bf-1: Benfeiro-1 borehole

Bpd: barrels per day

BR: Bitumen reflectance

Br-4: Barreiro-4 borehole

C/S: Carbon/sulfur

C: Carbon

C27/C29 sterane: C27ααα 20R/C29ααα 20R steranes

C29 sterane (%): content of C29 ααα (20S +20R) sterane

CH: carbohydrates

CH_4: methane

CO_2: carbon dioxide

CPI: Carbon Preference Index

CPP: Companhia Portuguesa dos Petróleos

DES: algae from the Desmidiales Order

DIC: Differential interference contrast light

DIN: Dinoflagellate cysts

DM: weight of the decarbonated sample

EOM: Extractable organic matter

FA: fulvic acids

FID: flame ionization detector

Fm.: Formation

FM: Incident blue light

Fo: Foraminiferal test linings

FRESH: Freshwater microplankton

Fx-1: Freixial-1 borehole

GC - MS: Gas Chromatography coupled to Mass Spectrometry

GF: Grândola Fault

Gr. Group

H/C: Hydrogen/ Carbon

H: Hydrogen

H29: 17α(H),21β(H)-30-norhopane

H30: 17α,21β(H)-hopane

H31: 17α(H),21β(H)-homohopane (22S and 22R)

H32: 17α, 21β(H)-bishomohopane (22S and 22R)

H34: 17α,21β (H)-tetrakishomohopane (22S-22R)

H35: 17α, 21β(H)-pentakishomohopane (22S-22R)

HA: humic acids

HC: hydrocarbons

HCl: Hydrochloric acid

HF: Hydroflouric acid

HI: Hydrogen Index

IR: Insoluble residue

L: Lipids

LAFO: Palynofacies and Organic Facies Laboratory

LB: Lusitanian Basin

LC: Liquid Chromatography

M29: 17β(H),21α(H)-30-normoretane

M30: 17β(H),21α(H)-hopane (moretane)

MAR: Marine microplankton

N: Nitrogen

NF: Nazaré Fault;

NOP: Non-opaque phytoclast

NSO: Nitrogen, Sulfur and Oxygen

O/C: Oxygen/ Carbon

O: Oxygen

OI: Oxygen Index

OM: Organic matter

OP: Opaque phytoclast

PAL: Palynomorph

Ph: Phytane

PHY: Phytoclast

PI: Production or productivity Index

Pr: Pristane

Res: Resin

RL: Reflect light

Rm-1: Ramalhal-1 borehole

R_r: Mean random reflectance

S: Sulfur

S1, S2 and S3: Peak 1, Peak 2 and Peak 3 of pyrolysis

SB: Solid bitumen

SEM: Scanning Electron Microscope

SO_2: Sulfur dioxide

Spo: Spore

SPO: Sporomorphs

Stdev: standard deviation

Ster/17α-hop: C27, C28, C29 ααα(20S + 20R) and αββ(20S + 20R) regular steranes / 17α-hopanes of the C29 to C33 pseudo-homologue (including 22S and 22R epimers)

Tetra 24: C24 tetracyclic terpane

TF: Tagus Fault

TL: Transmitted light

Tm: 22,29,30-Trisnorhopane

TM: total weight of the sample before acidification

T_{max}: Pyrolysis maximum temperature

TOC: Total Organic Carbon

Tr 20 to Tr 26: C20 to C26 tricyclic terpane

Ts: 22,29,30-Trisnorneohopane

TS: Total Sulfur content

U.C.: Upper Cretaceous;

ZC, Zo or Zooc: Zooclast

ZIG: Zygospores

Zm: Zoomorph

$ZnCl_2$: Zinc chloride

Part I - Introduction

1. Subject

In the pursuit of energy, the mankind evolved from the simple combustion of wood to drill wells with several kilometer, in increasingly hostile environments, in order to explore hydrocarbons that are used daily to produce electric energy, transport fuels, plastics, etc. Currently, much of the hydrocarbon technology is already developed and allows that the exploitation is done better and more productively and in progressively deeper intervals.

Despite the increasing use of renewable energy, the demand for hydrocarbons is still tremendous. Data from 2010 indicate that petroleum consumption in the United States of America (the largest consumer of petroleum in the world) was about 19150000 barrels per day (bpd) whereas in Portugal was around 277400 bpd (Index Mundi, 2014). According to Bob Dudley (BP CEO) is expected that the global energy consumption rises by 41% (2012 to 2035), with the demand for oil and other liquid fuels being 19 million bpd higher in 2035 than 2012 (Hydrocarbon Processing, 2014).

In Portugal, the search for hydrocarbons began at the end of XIX century and continued until the present day. Several sedimentary basins in Portugal have been studied and the well data were often encouraging. Currently, there are no doubts about the presence (at least in some of the basins) of mature source rocks, sealed reservoirs and traps that are necessary for potential economic accumulations. Although showing evidence of petroleum system, the generation potential of the Portuguese basins still needs to be better evaluated. Even if the stratigraphy and sedimentology of the Lusitanian Basin is well established, the characterization of organic matter present in its sequences is fundamental to characterize their potential as oil source rocks. The determination of organopetrographic and organo - geochemical parameters and their variations along the sedimentary sequences with organic matter is a valuable tool in modeling generated oil deposits with immediate application in the construction of exploratory models.

The exploration and production of hydrocarbons in Portugal would have a huge social, economic and technological value. This can be materialized in a reducing dependence on foreign energy, in creating capital gains for the State (concession agreements, royalties, etc.), job creation, introducing industrial valences and promote training of qualified staff to perform the needed for drilling and production operation tasks.

2. Objectives

The main objectives of this thesis are: i) to characterize, through palynofacies, organic geochemistry and petrographic studies, the organic matter of sedimentary sequences; ii) to study the behavior of the carbonate rocks in relation to the processes of generation and storage of hydrocarbons; iii) to determine the potential of oil generation and the identification of potential source rocks; and iv) to define the paleoenvironments of the horizons of the Lusitanian Basin.

In order to reach the main objectives, several specific objectives were defined:

- Characterization of the organic matter origin and content of carbonate/pelitic Jurassic sequences from the Lusitanian Basin;
- Determination of petrological and geochemical parameters;
- Determination of the organic constituent preservation in the carbonate/pelitic studied sequences;
- Determination of the terrigenous inputs (proximal-distal relationship relatively to the origin of sediments);
- Identification of the trends regarding the depth and regression-transgression in stratigraphic sequences;
- Definition of the paleoenvironments;
- Assessment of the organic matter thermal evaluation;
- Evaluation of the petroleum generation potential source rocks of the study sequences to assist in the identification of petroliferous systems.

In order to achieve the proposed objectives, four boreholes (Ramalhal-1, Benfeito-1, Freixial-1 and Barreiro-4) were selected comprising a total of 189 cutting samples that were submitted to organic petrographic and organic geochemical analyses. Due to the aims of this study, preference was given to the informal names of the formations because they are used by the oil companies operating in Portugal.

3. Thesis structure

This thesis is presented in an article-based format, compose by five parts. The part comprising the bulk of this thesis was prepared as research papers published in national and international peer-reviewed journals. Partial results of the research were additionally presented in scientific conferences that were not included in this thesis. Their present status is as follows:

Part I includes a general overview of the subject, objectives, current state of art as well as an overview about organic matter and geological setting of the Lusitanian Basin.

Part II is divided in two chapters. The first describes the analytical procedures applied and methods used for the characterization of the organic matter both kerogen and bitumen. The second chapter presents the samples selected for this study.

Part III includes the results and their respective discussion obtained during this research. It includes five scientific papers (published or submitted to national or international referred journals). This part is divided into three chapters, according the sub-basin where the studied boreholes were drilled.

Chapter one is related with the Bombarral sub-basin and includes a paper which deals with the organic matter present in the sediments cut by Ramalhal-1 borehole:

- Gonçalves, P.A., Mendonça Filho, J.G., Mendonça, J.O., Silva, T.F., Flores, D., 2013. Paleoenvironmental characterization of a Jurassic sequence on the Bombarral sub-basin (Lusitanian basin, Portugal): insights from palynofacies and organic geochemistry. International Journal of Coal Geology 113, 27 - 40.

Chapter two comprises three papers related with the Arruda sub-basin. The first one deals with the palynofacies and hydrocarbon potential of the sedimentary sequences cut by Benfeito-1 and Freixial-1 boreholes. The second is related with the characterization of solid bitumens present in Cabaços and Candeeiros Formations on the Benfeito-1 and Freixial-1 boreholes and, the third, discusses the presence of zoomorphs and zooclasts in Candeeiros Formation.

- Gonçalves, P.A., Mendonça Filho, J.G., Silva, T.F., Flores, D., 2014. Palynofacies and source rock potential of Jurassic sequences on the Arruda sub-basin (Lusitanian Basin, Portugal). Marine and Petroleum Geology (submitted).
- Gonçalves, P.A., Mendonça Filho, J.G., Silva, F.S., Flores, D., 2014. Solid bitumen occurrences in the Arruda sub-basin (Lusitanian Basin, Portugal): petrographic features. International Journal of Coal Geology. . International Journal of Coal Geology 131, 239 – 349.
- Gonçalves, P.A., Mendonça Filho, J.G., Oliveira, J.M., Flores, D., 2014. The presence of zooclasts and zoomorphs in the carbonate Candeeiros formation (Arruda sub-basin, Lusitanian Basin, Portugal): paleoenvironmental evidences. Comunicações Geológicas (accepted for publication).

Chapter three focuses on the Lower Tagus sub-basin and presents an approach about the organic matter existing in the sediments of Barreiro-4 borehole and includes the following paper:

- Gonçalves, P.A., Mendonça Filho, J.G., Silva, T.F., Mendonça, J.O., Flores, D., 2014. The Mesozoic–Cenozoic organic facies in the Lower Tagus sub-basin (Lusitanian Basin, Portugal): Palynofacies and organic geochemistry approaches. Marine and Petroleum Geology 52, 42-56.

Part IV refers to general conclusions of the performed research, highlighting the most important aspects and the way forward.

Part V is an atlas which aims to show microscopic (reflected and transmitted white lights, blue incident light and SEM) aspects of the particulate organic matter observed during this study. This part is divided in four chapters. The first three chapters are dedicated to the three major morphological groups of kerogen (phytoclasts, amorphous organic matter and palynomorphs) and the last one shows the aspects of the solid bitumen.

4. State of art

The first reference to hydrocarbons in Portugal dates from 1844 (Carvalho, 1983; Gomes, 1981) in the sequence of the discovery of the Canto de Azeche asphalt mine (Patais, Alcobaça). However, only at the end of the XIX century, with the Capela da Sismarias concession (Monte Real, Leiria) began the interest in hydrocarbons in Portugal (Gomes, 1981). According to Gomes (1981) the prospecting of petroleum in Portugal began in 1901, in the Torres Vedras area, where Portuguese and English oil companies carried out the first exploration wells. In 1904 was drilled the first exploration well in Capela da Sismarias occurrence but only reached 58 meters. In the early years of the XX century, most of the exploration was in shallow wells located near seeps. In 1907, two hundred and fifteen requests for research and prospect were asked in the Torres Vedras and Monte Real areas. From 1906 to 1912, four wells were drilled in the Torres Vedras area and the data obtained were promising due to the evidences of oil and gas. In 1928/29, six well were drilled in the Monte Real area that provided some good evidence in hydrocarbons (Gomes, 1981).

From 1938 to 1969, one hydrocarbon exploration and concession was attributed to two English men (later named Companhia Portuguesa dos Petróleos, CPP) and covering most of the Lusitanian and Algarve onshore basins (Gomes, 1981). During this period, approximately 4000 km of seismic data were acquired and 78 well were drilled in the Lusitanian Basin. Many of the wells had strong evidence of hydrocarbons and some of them revealed sub-commercial production (DPEPa, 2014).

In the 70's of the last century, Portugal approved and implemented new hydrocarbon legislation. Between the years of 1973-1979, several exploration contracts were signed, some of them to explore the offshore of the Lusitanian Basin. About 20000 km of offshore seismic plus gravity and magnetic profiles were acquired in Portugal and 14 wells were drilled in the Lusitanian Basin. Some of them (Moreia-1 and 14A-1 boreholes) showed good evidences of hydrocarbons and produced light oil during the drill stem test (DPEPa, 2014).

From the beginning of the 80's until the end of the XX century the interest in the exploration activity in the Lusitanian Basin decreased as a result of several oil crises. However, the interests in the hydrocarbon exploration in Portugal do not diminish. From 1978 to 2004, 39 areas were granted, of which 23 concessions in the onshore (2 of them with onshore and offshore lots) and 1 in the offshore the Lusitanian Basin. During this period, 23 wells were drilled in the onshore of the Lusitanian Basin. Again, many of these wells had good shows, mainly of oil. During this period conventional seismic were acquired (DPEPa,

2014). In 1996, a report was prepared by Beicip - Franlab showing detailed geochemical and petrographic data of exploration wells and outcrop samples from the most significant source rock intervals of the Lusitanian and Porto Basins (GPEP, 1996).

At the end of 2006, just one company (Mohave Oil & Gas Corporation) operated in Portugal, that holding 2 concession areas in the onshore (Alcobaça and Torres Vedras regions) of the Lusitanian Basin. The company also acquired 760 km of seismic in the offshore and 224 km in the onshore. Since 2007 there was a significant increase in oil exploration in Portugal and several concession contracts were signed (DPEPa, 2014) and several 2D, 3D and aeromagnetic surveys were acquired (Fig. 1). However, most of the information recovered by the companies operating in Portugal is still not of public knowledge and organic petrology and geochemical data is not known.

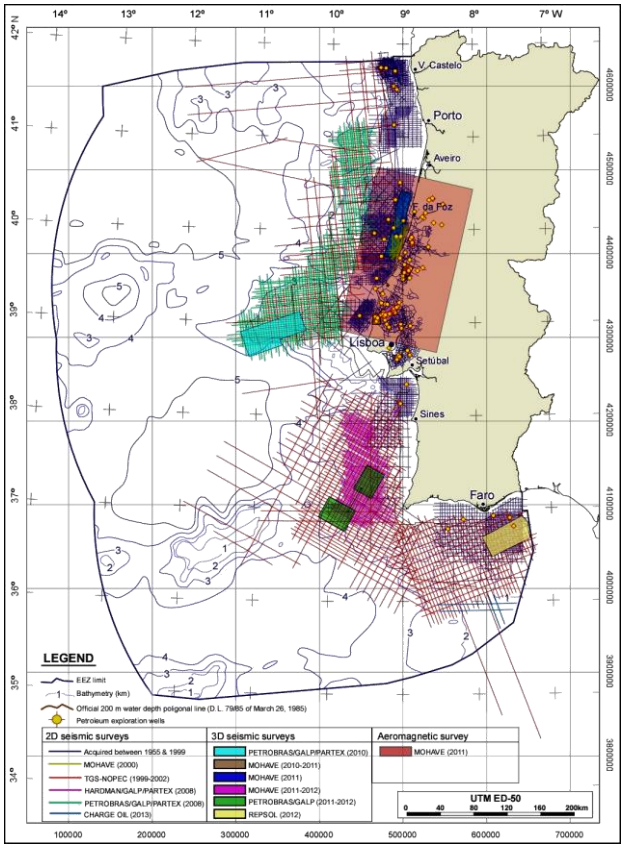

Figure 1. Exploration work carried out in the Portuguese sedimentary basins (DPEPb, 2014)

Nevertheless, in the last years, the Portuguese academic community has been studying the onshore of the Lusitanian Basin in order to determine the following: i) the occurrence and preservation of organic matter; ii) the potential of the source rocks; iii) the

definition of the depositional paleoenvironments through the palynofacies assemblages; and iv) the organic geochemical and organic carbon isotopic parameters. The majority of the studies have only been performed in outcrops existing along the Portuguese shore in the coastal plateau. These studies were focused on Jurassic age formations (Sinemurian-Pliensbachian and Oxfordian) located mainly in the western part of the basin. According to these studies (e.g., Duarte et al., 2010, 2011, 2012, 2013; Oliveira et al., 2006; Poças Ribeiro et al., 2013; Silva et al., 2010, 2011, 2013, 2014), the Lusitanian Basin includes two important interval with a potential to generate hydrocarbons: i) the Sinemurian-Pliensbachian Água de Madeiros e Vale das Fontes Formations in the northern part of the Basin; and ii) the Oxfordian Cabaços Formation in the southern part. However, the same authors referred that the organic matter do not reached the oil window.

5. Organic matter: Concepts and Classification

Sedimentary organic matter corresponds to the organic material derived directly or indirectly from living organic matter (Durand, 1980; Tissot and Welte, 1984). Its quantity and quality in sediments are basically the result of the combined influence of the biomass productivity, biochemical degradation and of the organic matter depositional processes (Tissot and Welte, 1984).

The organic matter is constituted by organic molecules, composed by elements of carbon (C), hydrogen (H), oxygen (O), nitrogen (N) and/or sulfur (S). It may be autochthonous (when it is originated in the water column above or within the sediment in which it is buried) or allochthonous (foreign to its environment of deposition). The supply of organic matter is high along the continental margins, related with the high primary productivity of coastal waters and/or of a high input of allochthonous land-derived terrestrial material. In marine environments, marine phytoplankton is the main source of organic matter, whereas in some shallow water the main source is marine phytobenthos if exits sufficient light for photosynthesis (Tissot and Welte, 1984).

From the chemical point of view, the organic matter is composed by a fraction insoluble in organic solvents - kerogen - and other soluble in organic solvents - bitumen (Fig. 2; Tissot and Welte, 1984). According to Tyson (1995), the kerogen corresponds to 95% (or more) of the total organic matter present in sedimentary rocks if migrated hydrocarbons are not considered.

Type and classification of kerogen

The nature of the organic matter and its microbial degradation are the main factors for the composition of a shallow immature kerogen (Tissot and Welte, 1984). The amount of hydrocarbons that can be generated during burial (genetic potential of sediment) is determined by the kerogen composition, principally in respect to hydrogen and oxygen (aliphatic chains and functional groups, respectively; Tissot and Welte, 1984). Taking into account this fact, van Krevelen (1993) developed a classification of the organic matter to characterize coals based on Hydrogen (H)/Carbon (C) and Oxygen (O)/Carbon (C) atomic ratios that typically distinguishes the three main types of kerogen (Type I, Type II and Type III) in the order of decreasing H/C and O/C ratios. Tissot et al. (1974) adapted the van

Krevelen diagram so that it can be used in sedimentary rocks. The modified van Krevelen diagram plots the Hydrogen Index (HI) versus Oxygen Index (OI) obtained in the Rock-Eval pyrolysis.

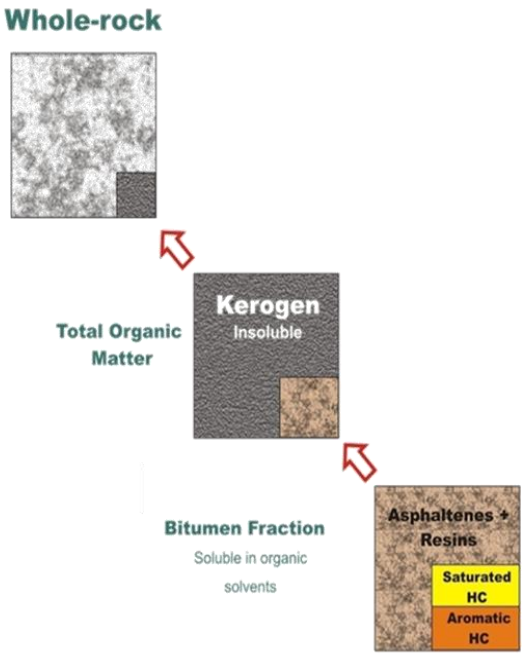

Figure 2. Composition of organic matter in ancient sedimentary rocks (Tissot and Welte, 1984).

According to Tissot and Welte (1984) the type I kerogen show high initial H/C ratio (1.5 or more) and low initial O/C ratio (usually lower than 0.1). This kerogen is rich in lipid material, particularly in aliphatic chains, and the content in polyaromatic nuclei and heteroatomic bonds is low. Type I kerogen is associated to lacustrine environments where exists a selective accumulation of algal material (fresh water algae such *Botryococcus*) or organic matter enriched in lipids by microbial activity (AOM). This kerogen presents a high potential to hydrocarbon generation (Tissot and Welte, 1984).

Type II kerogen have a relatively high H/C (lower than type I kerogen) and low O/C. The saturated material includes abundant aliphatic chains of moderate length and naphthenic rings. The polyaromatic nuclei and heteroatomic ketone and carboxylic acid groups are more important than they are in the type I kerogen (Tissot and Welte, 1984). This type of kerogen is related to open marine sediments where autochthonous organic matter derived from phyto- and zooplankton and microorganisms (bacteria) were deposited in a reducing environment, with medium to high sulfur content. Pollen grains, spores and cuticles are also related with type II kerogen. Type II kerogen have also potential to hydrocarbon

generation and is associated to many petroleum source rocks and to oil shales (Tissot and Welte, 1984).

Finally, Type III kerogen show low initial H/C ratio (less than 1) and high initial O/C ratio. The aliphatic chains are the minor constituent of the organic matter. This type of kerogen has an important proportion of the polyaromatic nuclei, heteroatomic ketone and carboxylic acid groups (Tissot and Welte, 1984). Type III kerogen is essentially derived from terrestrial plants deposited in proximal environments. The oil potential is less than in the type I and II kerogens, although it may still generate abundant gas if buried at sufficient depth (Tissot and Welte, 1984).

A secondary type of kerogen (Type IV) can be present in sedimentary rocks and it is composed practically by aromatic components. This organic matter result of carbonization processes (combustion and/or severe oxidation pre - depositional) that originated a kerogen depleted in hydrogen and oxygen and enriched in carbon. Type IV kerogen do not reveal potential to generate hydrocarbons (Mendonça et al., 2011).

Thermal maturity

The physicochemical transformations of organic matter present in sedimentary rock reflect the burial history and temperature during the geological time. From the moment that the organic matter is buried, it undergoes several compositional changes, firstly as a result of biological activity (microbial) and then, by the action of temperature and pressure. This continuous process is divided in consecutive stages of evolution (Fig. 3): diagenesis, catagenesis, metagenesis and metamorphism (Tissot and Welte, 1984).

Diagenesis

The diagenesis (Fig. 3) is characterized by physical, chemical and microbiological changes that occur during the first few hundred meters of depth. During this period the system tends to approach equilibrium under conditions of shallow burial, low temperature (to 65ºC) and pressure, and through which the sediment normally becomes consolidated. In the early diagenesis, microbial activity plays an important role in the transformation of the organic matter letting a number of low temperature reactions occur, such as: decarboxylation, deamination, polymerization and reduction. So, during sedimentation and early diagenesis, biogenic polymers or “biopolymers” (proteins, carbohydrates) are destroyed by microbial activity. Then their constituents are combined giving rise gradually to new

polycondensed structures (“geopolymers”) precursors of kerogen (Tissot and Welte, 1984). At the end of the diagenesis, the organic matter is equivalent to the boundary between brown coal and hard coal, corresponding to a vitrinite reflectance of approximately 0.5% (ICCP, 1971). Concerning to petroleum exploration, the source rocks in this stage are thermally immature (Tissot and Welte, 1984).

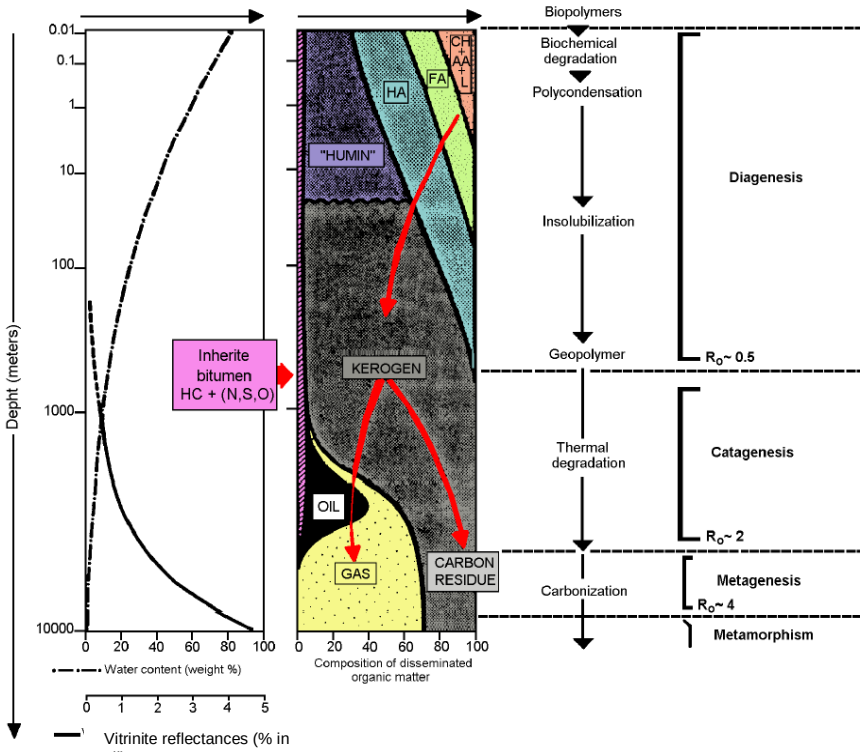

Figure 3. Stages of evolution of the organic matter (Tissot and Welte, 1984). CH: carbohydrates; AA: amino acids; L: lipids; FA: fulvic acids; HA: humic acids; HC: hydrocarbons; N, S, O: NSO compounds.

Catagenesis

The burial of layers as a result of a continued deposition of sediments that can reach several kilometers, resulting in a considerable increase of temperature (50 - 200°C) and pressure (300 to 1500 bars; Hunt, 1995; Tissot and Welte, 1984). These variations disturb the system that becomes out of equilibrium and therefore favors new changes (Tissot and Welte, 1984). During the catagenesis, the thermal degradation of organic matter is responsible for the generation of hydrocarbons (Fig. 3). The progressive evolution of the organic matter firstly produces liquid oil (correspond to the oil window) and later "wet gas" and condensate, both accompanied by substantial amounts of methane. The end of catagenesis is reached when the aliphatic chains completely disappear (Tissot and Welte, 1984). This point corresponds to a vitrinite reflectance of 2.0% that correspond to the limit between bituminous and anthracite coal rank (ISO 11760, 2005).

Metagenesis

Metagenesis (Fig. 3) represents the last stage in the thermal alteration of organic matter and corresponds to the dry gas zone (Tissot and Welte, 1984). This stage is only reached at great depth and higher temperatures, from 200 to 250°C (Hunt, 1995). The organic matter is represented by residual components with high carbon content and finally graphite, with methane liberation (Tissot and Welte, 1984). At this stage, the vitrinite reflectance ranges from 2 to 4% and, according to the ISO international standard coal classification (ISO 11760, 2005), corresponds to the Anthracite C - B sub - categories.

Metamorphism

Correspond to the last stage of the evolution of sediments where temperature and pressure reached high values. At this point the organic components that remains in the source rocks will be transform in CH_4 (methane), CO_2 (carbon dioxide) and graphite. At this phase the greenschist facies begins to appear (Hunt, 1995). Corresponding to a vitrinite reflectance of more than 4%, where coals start to be Anthracite A (ISO 11760, 2005, usually designated by metaanthracite, ICCP, 1971).

6. Lusitanian Basin

6.1. Introduction

The Lusitanian Basin (Fig. 4), located on the occidental margin of the Iberian Massif, is an Atlantic margin rift basin formed as a result of Mesozoic extension and the subsequent opening of the North Atlantic Ocean (e.g., Azerêdo et al., 2003; Rasmussen et al., 1998; Wilson et al., 1989). It is a 300 km long basin in the N-S direction and is 150 km wide (including offshore), and it is filled with approximately 5 km of sediments from the Upper Triassic to the Cretaceous that are covered with Cenozoic sediments (e.g., Azerêdo et al., 2003; Wilson, 1988). Structurally, the Lusitanian Basin is divided into three sectors - Northern, Central and Southern - bounded by faults that are most likely rooted in the Variscan basement (e.g., Kullberg et al., 2013; Wilson et al., 1989).

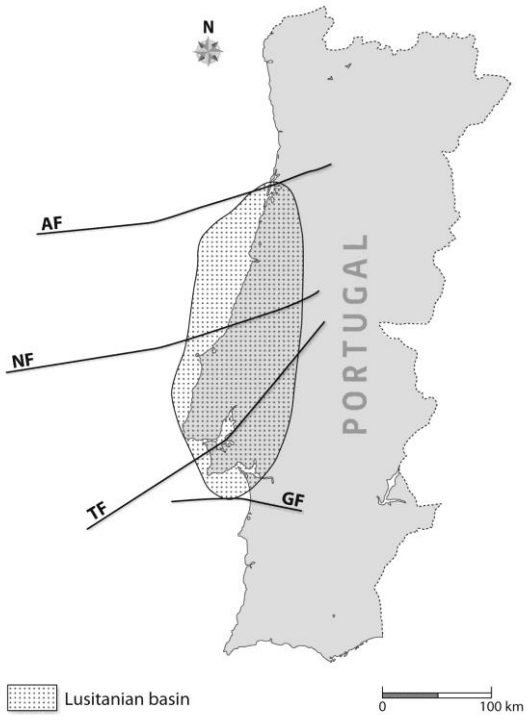

Figure 4. Localization of the Lusitanian Basin (modified from Alves et al., 2003a). AF: Aveiro Fault; NF: Nazaré Fault; TF: Tagus Fault; GF: Grândola Fault.

Four main extension and rifting events (Fig. 5) are recorded in the Lusitanian Basin: the first occurred in the Late Triassic; the second took place during the Sinemurian-Pliensbachian; the third began in the Late Jurassic and developed until the Early Cretaceous and, the fourth occurred during the Lower Cretaceous - Upper Berriasian to Upper Aptian (Alves et al., 2003b; Azerêdo et al., 2002; Kullberg, 2000; Kullberg et al., 2013; Rasmussen et al., 1998; Wilson, 1988).

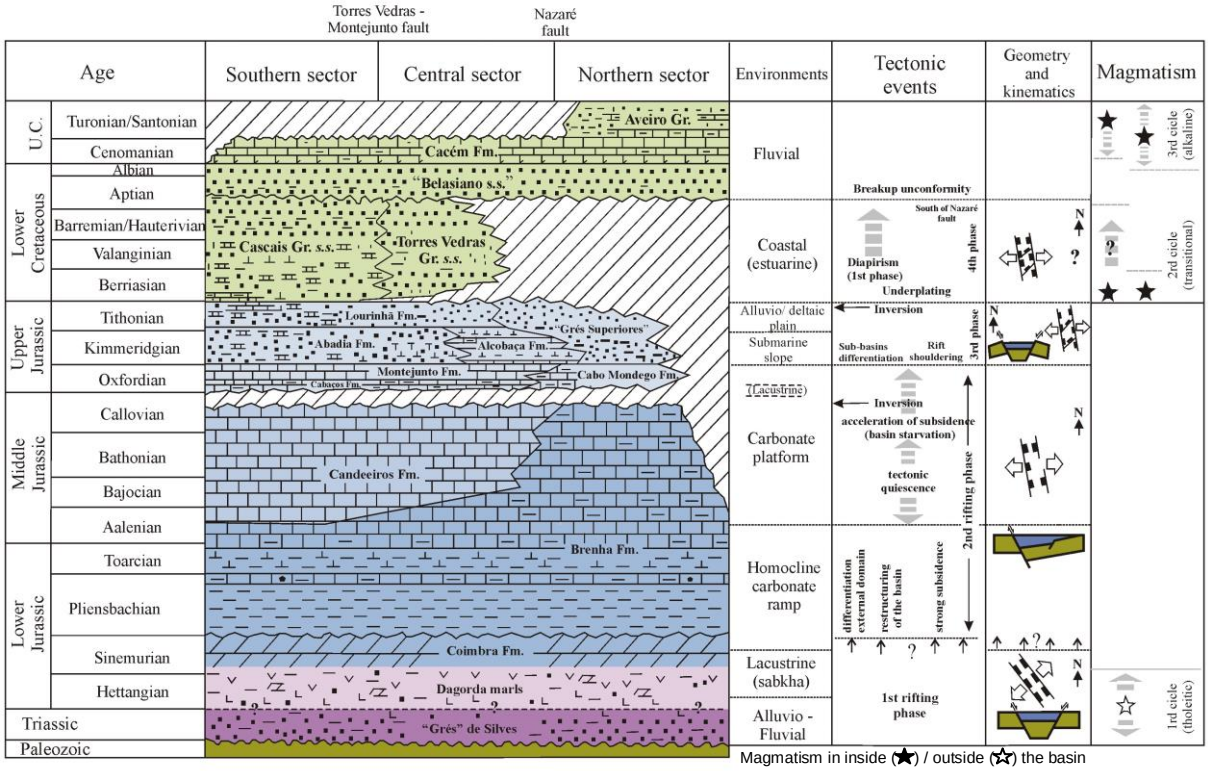

Figure 5. Synthesis of the evolution of the Lusitanian Basin (modified from Kullberg, 2000 and Kullberg et al., 2006a, and references therein). U.C.: Upper Cretaceous; Fm.: Formation; Gr. Group.

The first rifting phase (Fig. 5) was marked by the deposition of Triassic continental units and Hettangian evaporites, which were concentrated in the central part of the basin (Kullberg et al., 2013; Rasmussen et al., 1998). Following a period of regional subsidence, a second rifting phase (Fig. 5) occurred and opened the basin to marine conditions during the earliest Jurassic. Between the latest Callovian and the end of the early Oxfordian and as a result of the second rifting phase, regional uplift associated with the opening of the Central Atlantic formed a major unconformity in the basin (e.g., Mouterde et al., 1979; Rasmussen et al., 1998; Wilson, 1988). The third rifting episode (Fig. 5), which occurred between the Upper Jurassic and the Lower Berriasian, produced rapid and intense changes in the basin (Kullberg et al., 2013). The intense tectonic activity controlled the separation of the Central

Sector of the basin into the Bombarral, Turcifal and Arruda sub-basins (e.g., Kullberg et al., 2013; Leinfelder and Wilson, 1989; Montenat et al., 1988). A gap in the sedimentary record in the Lower Cretaceous is observed virtually throughout the basin and is related to the fourth rifting episode. The basin was mostly filled with siliciclastic sediments from the Hesperic Massif and the Berlengas Horst. Magmatic events occurred in the Central Sector of the basin during this period (Kullberg et al., 2013). The tectonic quiescence continued into the late Cretaceous, during which the deposition of carbonates was mixed with siliciclastic sediments, especially in the northern part of the area. The late Cretaceous was a period of volcanism in restricted areas of the basin; the volcanism is represented by units such as the Sintra intrusive complex (Rasmussen et al., 1998). From the Late Cretaceous, the deposition on the West Iberian margin was largely controlled by the reactivation of inherited Paleozoic and rift-related faults (Pinheiro et al., 1996) that together with halokynetic and thin-skinned tectonics resulted in the progressive re-organization of existing mini-basins (Alves et al., 2003c; Rasmussen et al., 1998; Ribeiro et al., 1990). Additional tectonic phases may have occurred during the Eocene and Oligocene, but they are obscured by the tectonic inversion that occurred in the Miocene as a result of the Betic compressional tectonics (Pais et al., 2012; Rasmussen et al., 1998; Ribeiro et al., 1990). Inversion in the Neogene led to the formation of uplifted areas separated by basins, including the Lower Tagus sub-basin (Rasmussen et al., 1998).

6.2. Geological setting

The first sediments were deposited in the basin during the Late Triassic-Early Jurassic (Fig. 5) and correspond to the Silves and Dagorda Formations (informal units). The Silves Formation consists of red clays, coarse sandstones and conglomerates, mostly of alluvial-fluvial origin. These are succeeded by evaporite and dolomite sediments of the Dagorda Formation (Azerêdo et al., 2003; Wilson, 1988). Some authors (e.g., Azerêdo et al., 2003; Kullberg et al., 2013; Palain, 1976) have noted that the presence of evaporites signifies a littoral, hot and dry environment similar to the current sabkhas environments. At the Hettangian the sedimentation conditions began to change. The deposition of the Coimbra, Brenha and Candeeiros Formations occurred under increasing marine influences (Azerêdo et al., 2002, 2003; Montenat et al., 1988; Wilson, 1988). The sedimentary records of the Coimbra Formation reveal dolomites at the base and limestones on the top (Azerêdo et al., 2003) with some bituminous intervals (Rasmussen et al., 1998). The Brenha Formation (informal unit) is characterized by fossiliferous and/or bioturbated marls, marly limestones

and compact limestones (Azerêdo et al., 2002); shales are interbedded in some sites of the basin (e.g., Azerêdo et al., 2003; Duarte and Soares, 2002; Duarte et al., 2010, 2011; Oliveira et al., 2006; Silva et al., 2010). The Candeeiros Formation (informal unit) reveals a predominance of carbonate facies.

The following period, between the latest Callovian and the end of the early Oxfordian, corresponds to an important basin-wide disconformity and a stratigraphic gap (e.g., Mouterde et al., 1979; Wilson, 1988). Following this hiatus, sedimentation continued and has led to the deposition of the Cabaços Formation, which comprises bituminous limestones, marly limestones, pedogenic limestones (related with subaerial exposure and pedogenesis origin) and anhydrite-limestone sequence (e.g., Azerêdo et al., 2002; Wilson, 1979). This formation shows some organic rich layers, revealing itself as a potential source rock of the Upper Jurassic in this basin (e.g., Flores and Esteves, 2008; Silva et al., 2010, 2013; Wilson, 1979). Cabaços Formation is attributed to freshwater lacustrine, brackish lagoonal and shallow-marine deposits (Azerêdo et al., 2002). During the Middle - Late Oxfordian, the deposition occurred in a low - depth marine carbonate platform, with sporadic inputs of clay resulting mainly on micritic and compact limestones interbedded with marls (Kullberg et al., 2013; Wilson, 1988). This period corresponds to the Montejunto Formation, which, in some places, overlays directly in the Middle Jurassic limestones, with the Cabaços Formation missing (Carvalho et al., 2005). Furthermore, in some areas at the top of Montejunto Formation, it is possible to find alternate beds of shales and limestones that contain coral colonies - the Tojeira Member (Wilson, 1979). In the Central sector, at some point in the Middle Oxfordian-Late Oxfordian, three sub-basins (Bombarral, Turcifal and Arruda) were differentiated as a result of the intense tectonic activity (e.g., Leinfelder and Wilson, 1989; Montenat et al., 1988). The Oxfordian - Kimmeridgian transition reveals great changes in the Lusitanian Basin, where calcareous sedimentation passes into siliciclastic sedimentation (e.g., Wilson, 1979). Along the basin, an increase can be observed in the siliciclastic sedimentation, which is composed of marls interbedded with coarse sandstones and rare limestone levels - Abadia Formation - in submarine fans and prograding slope environments (e.g., Kullberg et al, 2013; Rasmussen et al., 1998; Wilson, 1979). Covering the Abadia Formation, the Amaral Formation consists of oolitic limestone almost exclusively and was formed in a shallow - water shelf carbonate (Carvalho et al., 2005). The top of the Jurassic succession and base of the Cretaceous correspond to Lourinhã Formation (an informal formation) that is characterized by alluvial/fluvial sandstones (Alves et al., 2002; Kullberg et al., 2013), with some interbedded clays, conglomerates and marly limestones resulting from a fluvio-deltaic environment interacting with marginal marine shales (Kullberg et al., 2013; Rasmussen et al., 1998; Wilson, 1979).

In the Late Jurassic, the Central and Northern sectors of the Lusitanian Basin were uplifted and eroded and remaining the marine deposition only in the Southern sector (Alves et al., 2002). The Cretaceous began with the deposition of the Torres Vedras sediments that lies above of the unconformably of the Lourinhã Formation (Wilson et al., 1989). The Torres Vedras Formation consists of an alternation of fluvial siliciclastic and carbonate lithologies (e.g., Alves et al., 2002; Kullberg et al., 2013; Wilson et al., 1989) that was deposited as a south-west prograding wedge (Rasmussen et al., 1998). The deposition of this formation ends probably as a result of a major transgression of eustatic nature which reached a maximum in the Cenomanian - Turonian (e.g., Rasmussen et al., 1998; Witt, 1977), leading to the deposition of the shallow marine limestone and shales of Cacém Formation and the fluvio-deltaic siliciclastic of the Almargem Formation (e.g., Alves et al., 2002; Rasmussen et al., 1998; Rey et al., 2006; Wilson, 1988). Between the late Turonian and the early Campanian the sedimentation in the Northern Lusitanian Basin evolved from the fluvial/alluvial siliciclastic of the Gândara Formation to the shallow marine carbonates of the Carapau Formation and the marine siliciclastic of the Dourada Formation (Rey et al., 2006; Witt, 1977). The final period of the Cretaceous (mainly during the Campanian) reveals important occurrences of magmatism (e.g., Sintra intrusions). It is important to note that the Cretaceous sediments are not represented in the entire Basin. In fact, in some onshore sub-basins of the Central sector, part of the Lower Cretaceous and the entire Upper Cretaceous has been removed during the latest Cretaceous - Cenozoic inversion episodes (e.g., Wilson et al., 1989).

In the Paleogene, the Southern sector of the basin began to be filled with alluvial sediments (Cunha et al., 2009; Kullberg et al., 2006b). The deposits are characterized by interbedded layers of clay, silts and sands (sometimes cemented) and some limestones (Antunes and Pais, 1993). The deposition of sandstones with occasional limestone intercalations was the result of alluvial fans located on the footwalls of faults (Carvalho et al., 2005). The deposition during the Neogene was controlled by tectonic pulses and was sometimes related to glacio - eustatic sea-level curves, with the maximum transgression occurring in the Serravallian (Rasmussen et al., 1998). The Atlantic Ocean invaded the basin at the beginning of the Miocene (Kullberg et al., 2006b; Pais et al., 2012), and the marine and brackish water affected the depositional environment (Antunes and Pais, 1993). However, the deposition was, predominately, marine between Lisbon and the Arrábida hills (Carvalho et al., 2005). The Pliocene is characterized by a regressive trend (Kullberg et al., 2013). High-energy marine and fluvial environments allowed the deposition of feldspathic sandstones, coarse sandstones, gravels and conglomerates (Carvalho et al., 2005).

References

Alves, T., Moita, C., Pinheiro, L., Monteiro, J., 2003a. Evolution of deep - margin extensional basins: the continental slope basins offshore West Iberia. AAPG International Conference Barcelona (2003), p. 5.

Alves, T.M., Gawthorpe, R.L., Hunt, D.W., Monteiro, J.H., 2002. Jurassic tectono - sedimentary evolution of the Northern Lusitanian Basin (offshore Portugal). Marine and Petroleum Geology 19, 727 - 754.

Alves, T.M., Gawthorpe, R.L., Hunt, D.W., Monteiro, J.H., 2003c. Cenozoic tectono-sedimentary evolution of the western Iberian margin. Marine Geology 195, 75 - 108.

Alves, T.M., Manuppella, G., Gawthorpe, R. L., Hunt, D. W., Monteiro, J. H., 2003b. The depositional evolution of diapir- and fault-bounded rift basins: examples from the Lusitanian Basin of West Iberia. Sedimentary Geology 162, 273 - 303.

Antunes, M.T., Pais, J., 1993. The Neogene of Portugal. Ciências da Terra, Universidade Nova Lisboa, 12, 7 - 22. ISSN 0254-055x.

Azerêdo, A.C., Duarte, L.V., Henriques, M.H., Manuppella, G., 2003. Da dinâmica continental no Triásico aos mares do Jurássico Inferior e Médio. Cadernos de Geologia de Portugal. Instituto Geológico e Mineiro, Lisboa. ISBN 972-98469-9-5.

Azerêdo, A.C., Wright, V.P., Ramalho, M.M., 2002. The Middle - Late Jurassic forced regression and disconformity in central Portugal: eustatic, tectonic and climatic effects on a carbonate ramp system. Sedimentology 49, 1339 - 1370.

Carvalho, F., 1983. A problemática da pesquisa do petróleo em Portugal. Geonovas 1, 23 - 32.

Carvalho, J., Matias, H., Torres, L., Manupella, G., Pereira, R., Mendes-Victor, L., 2005. The structural and sedimentary evolution of the Arruda and Lower Tagus sub-basins, Portugal. Marine and Petroleum Geology 22, 427 - 453.

Cunha, P., Pais, J., Legoinha, P., 2009. Evolução geológica de Portugal continental durante o Cenozóico - sedimentação aluvial e marinha numa margem continental passiva (Ibéria ocidental), in: Abstracts, 6º Simpósio sobre el Margen Ibérico Atlántico MIA09 (Oviedo, España), pp. xi-xx.

DPEPa, Divisão para a Pesquisa e Exploração de Petróleo. Ministério da Economia, Governo de Portugal. http://www.dgeg.pt/dpep/en/history.htm (retrieved 5th June 2014).

DPEPb, Divisão para a Pesquisa e Exploração de Petróleo. Ministério da Economia, Governo de Portugal. http://www.dgeg.pt/dpep/en/info/explorstatus_hres.jpg (retrieved 5th June 2014).

Duarte, L.V., Silva, R.L., Mendonça Filho, J., 2013. Variação do COT e pirólise Rock-Eval do Jurássico Inferior da região de S. Pedro de Moel (Portugal). Potencial de geração de hidrocarbonetos. Comunicações Geológicas 100, Especial 1, 107 - 111.

Duarte, L.V., Silva, R.L., Mendonça Filho, J.G., 2011. The Lower Jurassic of the west coast of Portugal: stratigraphy and organic matter in carbonate sedimentation, in: Flores, D., Marques, M.M. (Eds.). 63rd ICCP Annual Meeting - Field Trip, Porto, Memória nº 17. ISSN 087.1607.

Duarte, L.V., Silva, R.L., Mendonça Filho, J.G., Poças Ribeiro, N., Chagas, R.B.A., 2012. High-resolution stratigraphy, palynofacies and source rock potential of the Água de Madeiros Formation (Lower Jurassic), Lusitanian Basin, Portugal. Journal of Petroleum Geology 35, 205 - 126.

Duarte, L.V., Silva, R.L., Oliveira, L.C.V., Comas-Rengifo, M.J., Silva, F., 2010. Organic-rich facies in the Sinemurian and Pliensbachian of the Lusitanian Basin, Portugal: Total organic carbon distribution and relation to transgressive-regressive facies cycles. Geologica Acta 8, 325 - 340.

Duarte, L.V., Soares, A.F., 2002. Litoestratigrafia das séries margo-calcárias do Jurássico inferior da Bacia Lusitânica (Portugal). Comunicação do Instituto Geológico e Mineiro 89, 115 - 134.

Durand, B., 1980. Sedimentary organic matter and kerogen. Definition and quantitative importance of kerogen. Chapter 1, in: Durand, B. (Ed.), Kerogen - Insoluble organic matter from sedimentary rocks. Editions Technip, Paris, pp. 13 - 34.

Flores D., Esteves P., 2008. Avaliação do Potencial Petrolífero de uma Sondagem da Bacia Lusitaniana: Uma Abordagem Petrográfica e Geoquímica, in: Livro de resumos VIII Congresso de Geoquímica dos PLP, Cabo Verde, pp. 35.

Gomes, J.N., 1981. Evolução e perspectiva da prospecção de petróleo em Portugal. Geonovas 1, 25 - 42.

GPEP - Gabinete para a Pesquisa e Exploração de Petróleo, 1996. Porto and Lusitanian Basins, Geochemical Analysis BEICIP-FRANLAB: Contribution to the MILUPOBAS Project, 9 vols., Lisbon.

Hunt, J.M., 1995. Petroleum Geochemistry and Geology. Freeman, San Francisco.

Hydrocarbon Processing, 2014. http://www.hydrocarbonprocessing.com/Article/3298229/BP-predicts-slowdown-in-global-energy-demand.html (retrieved 10th June 2014).

ICCP, 1971. International Handbook of Coal Petrography, Supplement to the 2nd Edition. Centre National de la Recherche Scientifique, Paris, France.

Index Mundi, 2014. http://www.indexmundi.com/map/?v=91&l=pt (retrieved 10th June 2014).

ISO 11760, 2005. Classification of coals. International Organization for Standardization. 1st edition, Geneva, Switzerland. 9 pp.

Kullberg, J. C., Rocha, R.B., Soares, A.F., Rey, J., Terrinha, P., Callapez, P., Martins, L., 2006. A Bacia Lusitaniana: Estratigrafia, Paleogeografia e Tectónica, in: Dias, R., Araújo, A., Terrinha, P., Kullberg, J.C. (Eds.), Geologia de Portugal no contexto da Ibéria, Universidade de Évora, pp. 317 - 368. ISBN: 972-778-094-6.

Kullberg, J.C., Rocha, R.B., Soares, A.F., Rey, J., Terrinha, P., Azerêdo, A.C., Callapez, P., Duarte, L.V., Kullberg, M.C., Martins, L., Miranda, J.R., Alves, C., Mata, J., Madeira, J., Mateus, O., Moreira, M., Nogueira, C.R., 2013. III.3. A Bacia Lusitaniana: Estratigrafia, Paleogeografia e Tectónica, in: Geologia de Portugal, 2, ISBN: 978-972-592-364-1, pp. 195 - 347.

Kullberg, J.C., Terrinha, P., Pais, J., Reis, R.P., Legoinha, P., 2006b. Arrábida e Sintra: dois exemplos de tectónica pós-rifting da Bacia Lusitaniana, in: Dias, R., Araújo, A., Terrinha, P., Kullberg, J.C. (Eds). Geologia de Portugal no contexto da Ibéria. Universidade de Évora, Évora, pp. 369 - 396.

Kullberg, J.C.R., 2000. Evolução tectónica mesozóica da Bacia Lusitaniana. PhD thesis, Univ. Nova de Lisboa, 361pp.

Leinfelder, M.R.R, Wilson, R.C.L., 1989. Seismic and sedimentologic features of Oxfordian-Kimmeridgian syn-rift sediments on the eastern margin of the Lusitanian Basin. Geologische Rundschau 79, 81 - 104.

Mendonça Filho, J.G., Menezes, T.R., Mendonça, J.O., Oliveira, A.D., Souza, J.T., Sant'Anna, A.J., 2011. Kerogen: Composition and Classification. Chapter 3 in: ICCP Training Course on Dispersed Organic Matter, ISBN 978-9-89-826567-8, pp. 17 - 24.

Montenat, C., Guery, F., Jamet, M., Berthou, P.Y., 1988. Mesozoic evolution of the Lusitanian Basin: comparison with the adjacent margin, in: Boillot, G., Winterer, E.L. (Eds.), Proceedings of the Ocean Drilling Program, Scientific Results 103, pp. 757 - 775.

Mouterde, R., Rocha, R.B., Ruget, C., Tintant, H., 1979. Faciès, biostratigraphie et paléogéographie du Jurassique portugais. Ciências da Terra, Universidade Nova Lisboa 5, 29 - 52.

Oliveira, L.C.V., Rodrigues, R., Duarte, L.V., Lemos, V., 2006. Avaliação do potencial gerador de petróleo e interpretação paleoambiental com base em biomarcadores e isótopos estáveis do carbono da seção Pliensbaquiano-Toarciano inferior (Jurássico Inferior) da região de Peniche (Bacia Lusitânica, Portugal). Boletim de Geociências da Petrobras 14, 207 - 234.

Pais, J., Cunha, P., Moreira, D., Legoinha, P., Dias, R., Moura, D., Silveira, A.B., Kullberg, J.C., González-Delgado, J., 2012. The Paleogene and Neogene of Western Iberia. A Cenozoic Record in the European Atlantic Domain. Springer.

Palain, C., 1976. Une série détritique terrigène. Les “Grés de Silves”: Trias et Lias inférieur du Portugal. Memórias dos Serviços Geológicos de Portugal, 25. Serviços Geológicos de Portugal, Lisboa.

Pinheiro, L.M., Wilson, R.C.L., Reis, R.P., Whitmarsh, R.B., Ribeiro, A., 1996. The western Iberia margin: A geophysical and geological overview, in: Proceedings of the Ocean Drilling Program, Scientific results. R.B. Whitmarsh, D.S. Sawyer, A. Klaus, D.G. Masson. 149, pp. 3 - 23.

Poças Ribeiro, N., Mendonça Filho, J.G., Duarte, L.V., Silva, R.L., Mendonça, J.O., Silva, T.F., 2013. Palynofacies and organic geochemistry of the Sinemurian carbonate deposits in the western Lusitanian Basin (Portugal): Coimbra and Água de Madeiros formations. International Journal of Coal Geology 111, 37 - 52.

Rasmussen. E.S., Lomholt, S., Andersen, C., Vejbæk, O.L., 1998. Aspects of the structural evolution of the Lusitanian Basin in Portugal and the shelf and slope area offshore Portugal. Tectonophysics 300, 199 - 225.

Rey, J., Dinis, J.L., Callapez, P., Cunha, P.P., 2006. Da rotura continental à margem passiva: Composição e evolução do Cretácico de Portugal. INETI. Lisboa, Portugal.

Ribeiro, A., Kullberg, M.C., Kullberg, J.C., Manuppella, G., Phipps, S., 1990. A review of alpine tectonics in Portugal - foreland detachment in basement and cover rocks. Tectonophysics 184, 357 - 366.

Silva, R.L., Mendonça Filho, J., Azerêdo, A.C., Duarte, L.V., 2013. Palinofácies e caracterização de matéria orgânica da Formação de Cabaços (Bacia Lusitânica): contributos para a discriminação das dinâmicas paleobiológicas e paleoambientais em meios

carbonatados dominantemente não-marinhos. Comunicações Geológicas 100, Especial 1, 113 - 118.

Silva, R.L., Mendonça Filho, J.G., Azerêdo, A., Duarte, L.V., 2014. Palynofacies and TOC analysis of marine and non-marine sediments across the Middle - Upper Jurassic boundary in the central - northern Lusitanian Basin (Portugal). Facies 60, 255 - 276.

Silva, R.L., Mendonça Filho, J.G., Azerêdo, A.C., Silva, T.F., Oliveira, A.D., Duarte, L.V., 2011. Palynofacies and organic geochemistry survey of the Middle - Upper Jurassic transition in the Central-Northern sectors of the Lusitanian Basin (Portugal), in: Flores, D., Marques, M.M. (Eds). "New Trends on Coal Science", 63rd ICCP Annual Meeting, Memória nº 18. ISSN 087.1607, pp. 17 - 18.

Silva., R.L., Mendonça Filho, J.G., Duarte, L.V., Comas-Rengifo, M.J., Azerêdo, A.C., Ferreira, R., 2010. Organic-rich facies of the top Ibex - Margaritatus zones (Pliensbachian) of the Lusitanian Basin (Portugal): TOC and biomarkers variation. Geochimica et Cosmochimica Acta 74, A962.

Tissot, B., Durand, B., Espitalié, J., Combaz, A., 1974. Influence of the nature and diagenesis of organic matter in formation of petroleum. American Association of Petroleum Geologists Bulletin 58, 499 - 506.

Tissot, B., Welte, D.H., 1984. Petroleum Formation and Occurrence, Second ed. Springer Verlag, Heidelberg.

Tyson, R.V., 1995. Sedimentary Organic Matter. Chap. & Hall, London.

van Krevelen, D.W., 1993. Coal: Typology - Chemistry - Physics - Constitution, 3rd ed. Elsevier, The Netherlands.

Wilson, R.C.L., 1979. A reconnaissance study of Upper Jurassic sediments of the Lusitanian basin. Ciências da Terra, Universidade Nova de Lisboa 5, 53 - 84.

Wilson, R.C.L., 1988. Mesozoic Development of the Lusitanian Basin, Portugal. Revista de la Sociedad Geológica de España 1, 393 - 407.

Wilson, R.C.L., Hiscott, R.N., Willis, M.G., Gradstein, F.M., 1989. The Lusitanian Basin of west - Central Portugal: Mesozoic and Tertiary tectonic, stratigraphic and subsidence history. The American Association of Petroleum Geologists Bulletin 46, 341 - 362.

Witt, W.G., 1977. Stratigraphy of the Lusitanian Basin. Unpublished. Report Shell Prospex Portuguesa.

Part II - Methodologies and Samples

1. Methodologies

This chapter comprises a detailed description of the methodologies employed in this research. The techniques selected were chosen to allow the characterization of both the bitumen and kerogen. Most of the analyses were performed in the Palynofacies and Organic Facies Laboratory (LAFO). The exception was the organic petrology study that was carried out in the Department of Geosciences, Environment and Spatial Planning of Faculty of Sciences of the University of Porto. Figure 6 illustrates the petrographic and geochemical analyses used during this study.

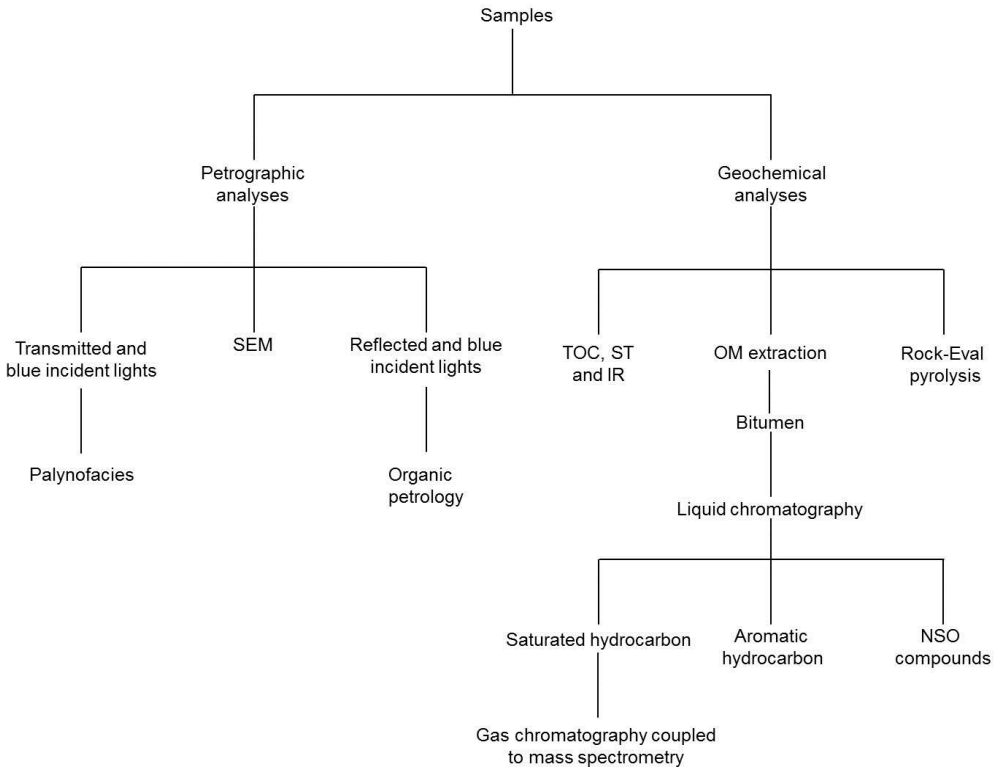

Figure 6. Flowchart of the analytic techniques carried out in this study to characterize the bitumen and the kerogen. SEM: Scanning Electron Microscope; TOC: Total organic carbon; ST: Total Sulfur; IR: Insoluble residue; OM: Organic matter; NSO: Nitrogen, Sulfur and Oxygen.

1.1. Petrographic analyses

1.1.1. Palynofacies analysis

Palynofacies is a term introduced by Combaz (1964) to define the total assemblage of particulate organic matter contained in sediments and sedimentary rocks that remains after

acidification (hydrochloric and hydrofluoric acids) used to eliminate the mineral matrix. Later, Tyson (1995) introduced a modern palynofacies concept namely: *"a body of sediment containing a distinctive assemblage of palynological organic matter thought to reflect a specific set of environmental conditions or to be associated with a characteristic range of hydrocarbon - generating potential".* To study the kerogen assemblage, microscopic techniques (transmitted white and incident blue lights) are used to acquiring data and statistical methods can be necessary for its interpretation.

Palynofacies studies allow identify, quantify and assess the state of preservation of the particulate organic matter and also determine their relative proportions (Tyson, 1995). According to Tyson (1995), palynofacies analysis can be applied in diverse studies, such as: geology (stratigraphy, sedimentology and palaeoenvironmental studies), paleontology (biostratigraphic studies) and petroleum exploration.

1.1.1.1. Sample preparation

The preparation of the slides was performed according to the palynofacies procedures through the isolation of non-oxidative organic matter proposed by Mendonça Filho et al. (2011a) and Tyson (1995) followed in LAFO. Between 20 to 40 grams of sediment were used to obtain an ideal amount of kerogen concentrate. The first step consists in crushing the rock material down to fragments (size of about 2 - 5mm) and posterior elimination of the contaminations (e.g., material added to the drilling mud in petroleum activities). For cleaning, mechanical (washing with water, detergent or alcohol) and chemical (extraction method using organic solvents, etc.) techniques can be used depending of the type or condition of the samples. The next step consists in the elimination of the mineral matrix of the rocks. For that, the crushed rocks are acidified, sequentially, with: i) chloridric acid (HCl) during 18 hours to remove the carbonates; ii) hydrofluoric acid (HF) for 24 hours to eliminate the silicates; and, finally, iii) HCl for 3 hours to remove possible fluoride silicates formed during the previous steps. After each acidification, the material needs to be neutralized with filtered water. The following step consist to apply a heavy liquid ($ZnCl_2$) during 24 hours, in order to concentrate the kerogen. The organic residue is separated by decantation and sieved at 10µm. A portion of the retained material is mounted on glass slides.

1.1.1.2. Microscopic analysis

Microscopic analysis was performed on strewn slides of kerogen concentrate sample using transmitted white and incident blue lights. The combination of these lights makes

possible the distinction of the different individual organic particles from the kerogen assemblage. The analysis involved qualitative (identification of the particles) and quantitative (counting 300 to 500 particles) examination of the groups and subgroups of kerogen components. The counting followed the classification of groups and subgroups of organic matter proposed by Mendonça Filho et al. (2011b) and Tyson (1995). Counting is performed using an ocular with 10x and objective 20x magnification. The observer should covered the slides making a series of non - overlapping transverse lines using a vertical or horizontal cross graduated reticule (scale) and counting only those particles which pass under the very center of the field of view in the crossed lines from the reticule. All the particles that pass under the field of view of the crossed lines of the reticule are counted except those which have the size less than 10µm and any contaminants (identified by color, relief, or form); unrecognizable fragments of palynomorphs which have less than half of the original form are ignored. The final data is recalculated to percentages. After counting, the slide must be systematically scanned for any rare palaeoecological indicators that were not recognized during the counting process.

1.1.1.3. Kerogen groups

The classification of dispersed kerogen is still not standardized and, until now, several classifications systems have been proposed (e.g., Mendonça Filho et al., 2010; Mendonça Filho, 1999; Traverse, 1988; Tyson, 1995; Vicent, 1995). These classifications are based primarily on the appearance and preservation state of the particulate organic matter and their biological origin (e.g., plant debris, phytoplankton, etc.) using transmitted white light with additional observation employing fluorescence methods (blue or UV modes). According to Tyson (1995) there are several criteria that should be used in the kerogen classification, such as: origin, structure, morphology, measurable optical properties, geochemical composition and preservation state. It is important to use a classification system that provides as much information as possible to achieve the objectives of the study.

Tables 1, 2 and 3 show in detailed the classification system used in this work. This classification system is based on Tyson (1995), Vicent (1995), Mendonça Filho (1999) and Mendonça Filho et al. (2010, 2011b, 2012), indicating the appropriate use of the nomenclature for the observation of the kerogen under transmitted white light. According to this classification three major morphological kerogen groups can be recognized in the associations of particulate organic matter: i) phytoclasts; ii) amorphous (AOM); and iii) palynomorphs.

Phytoclast Group

Bostick (1971) introduced the term phytoclast to describe the particles with clay or fine-sand sizes derived from higher terrestrial plants tissues and fungi, sometimes with autofluorescence depending on their origin. They are representative of lingo-cellulosic tissues that can correspond to fragments of lignified mechanical support and vascular tissues of gymnosperms and angiosperms (Tyson, 1995). Phytoclast Group (Table 1) is divided in opaque (dark), non-opaque (translucent, including cuticular tissues and fungal hyphae) and sclereids.

Table 1. Detailed classification system from Phytoclast Group (Mendonça Filho et al., 2011b and references therein).

Subgroup			Description
Opaque	**Equidimensional (Equant)** Length : width ratio <2	Black or opaque in color even at grain boundary; Sharp outline; Mostly no internal structure.	
	Lath Length : width ratio>2	Black or opaque in color even at grain boundary; Sharp outline; It may shows pits.	
	Corroded	Black in color; more diffuse outline; irregular.	
Non-opaque (translucent)		**Fungal Hyphae**	Fragments of hyphae; Brown in color; Individual filaments of the mycelium of the vegetative phase of eumycote (higher) fungi.
	Undegraded Sharp outline (may be slightly irregular). May be splintered. or **Degraded** Irregular and diffuse outline. or **Pseudoamorphous/ "Amorphous"** Diffuse outline, it may light brown, brown and dark brown in color. Starting to show features of AOM, but homogeneous in appearance, not pyrite specked, no inclusions. It may exhibits fluorescence. or **In decomposition (gelified) "highly preserved"** Irregular outline in transmitted white light, it exhibits coloration of fluorescence. The characteristics indicate a highly degree of chemistry preservation due to specific conditions.	**Non-biostructured**	No botanical structure; Translucent, generally brown in color; Lath or equant in shape.
		Biostructured	Generally brown in color; Lath to equant in shape; Clearly visible internal structure. Striate: shown thin (regular fibrous lineation). Striped: irregular or unequal stripes (may be thickenings). Banded: regular and equal parallel sided thickenings. Pitted: bordered or scalariform pits.
		Cuticle	Epidermal tissue of higher plants. Pale yellow-green, yellow, reddish-yellow in color particle. Regular cells outlines; Sheet-like, in some cases with visible stomata. It may occur in thick translucent phytoclasts that under fluorescence, present a yellow fluorescing cuticle overlaying ("coating") on these phytoclasts. This particular feature (cuticular layer fragments associated with innermost part of epidermis) could be indicating that the land plants fragments derived from leaves.
		Membrane	Pale yellow in color; thin; sheet-like; irregular. They often fluorescent; Highly translucent; Lack of diagnostic internal structure.
Sclereids	Generally opaque, but may be translucent (dark brown). Sclerenchymatic tissue cells, with thickened secondary wall and impregnated with lignin. Found in different parts of the plants (root, stem and leaf) with the sustention function and mechanical resistance.		

Phytoclast particles generally became less abundant, smaller and more oxidized with the increasing of the distance to the terrestrial source. Their high percentage in the kerogen assemblage is related with several aspects, such as: i) high supply; ii) preferential preservation; iii) selective sedimentation due the hydrodynamic equivalence of the particles; and/or iv) preferential sedimentation (Tyson, 1995).

Amorphous Group

The Amorphous Group (Table 2) consists of all particulate organic components that appear structureless at the scale of the optical microscopy; it includes phytoplankton derived from amorphous organic matter (traditionally referred to as “AOM”), bacterially derived amorphous organic matter (also traditionally referred to as “AOM”), higher plant resins and amorphous products of the diagenesis of macrophyte tissues (Mendonça et al., 2011b; Tyson, 1995). A large part of the marine organic matter dispersed in sediments belongs to this group; however it is easily degraded when exposed to aerobic conditions (Tyson, 1995).

Table 2. Detailed classification system from Amorphous Group (Mendonça Filho et al., 2011b and references therein).

Subgroup		Description
“AOM” Phytoplankton or bacterially derived amorphous organic matter - derived from microbiological rework.		Structureless material no morphology or form; Color: yellow-orange-red, orange-brown, ash; often has palynomorphs and pyrite inclusions; It can exhibit or nor fluorescence colorations.
Resin Mostly produced by terrestrial higher plants in tropical climates.		Structureless particle (glassy shards), hyaline, usually round, homogeneous, strongly fluorescence.
Amorphous products	**Products of macrophyte tissues** (Pseudoamorphous/“Amorphous”)	Diffuse outline, it may light brown, brown and dark brown in color; Starting to show some features of AOM, but homogeneous in appearance (flat fluorescence); not pyrite specked, no inclusions; It may exhibits fluorescence.
	Microbial mats	They consist predominantly of maceral lamalginite when examined in reflected white light. They form rather uniformly and strongly fluorescent cohesive particles which show relatively sharp and distinct (sometimes quite angular) outlines after maceration.
	Products from bacteria Bacterial Extracellular Polymeric Substance (EPS)	Mucilaginous sheat. Diffuse outlines, thin, it may pale yellow, yellow, orange, ash in color. Not pyrite specked no inclusions. It may exhibits intense fluorescence.

Reducing environments (at least temporarily dysoxic to anoxic) or distal depositional (sedimentation removed from active sources of terrestrial organic matter) environments are two possible explanation for the dominance of AOM in total assemblage of kerogen (Tyson, 1995). The fluorescent intensity of the AOM is related with the redox conditions under which

it was deposited; in dysoxic-anoxic conditions the labile hydrogen-rich components of the AOM are easily preserved (Tyson, 1995).

Palynomorph Group

The term of palynomorph (Table 3) was introduced by Tchudy (1961) to refer to all discrete HCl and HF - resistant, organic-walled microfossil that may be present in palynological preparations.

Table 3. Detailed classification system from Palynomorph Group (modified from Mendonça Filho et al., 2011b and references therein).

Subgroups			Description
Sporomorphs	**Spores**	Terrestrial palynomorphs produced by *Pteridophyte*, *Briophyte* and *Fungi*.	Triangular or circular form palynomorph, trilete mark ("Y") or monolete (scar). They can occur as massulae of freshwater fern (Azolla), agglomerates and tetrad. "First spores" (Cambrian): Cryptospores (spore-like bodies) and Embryophyte Spores: Upper Ordovician - Recent.
	Pollen grain	Terrestrial palynomorphs produced by Gymnosperms and Angiosperms	Palynomorph with varied ornamentation, most with outline circular or oval; could present opening or not. They can occur as agglomerates or tetrads. Devonian - Recent.
Freshwater Microplankton	***Botryococcus***	*Chlorococcales Algae*	Irregular globular colonies: size 30 to 2000μm, sometimes with several lobes (like miniature cauliflower). Ordovician - Recent.
	Pediastrum		Colonial green algae (coenobia). Rounded colonies with 30-200μm of diameter. Polygonal form cells with concentric arrangement; cells with horns in the external side. Jurassic (?) - Recent.
	zygospores of *Zygnema*-type	Zygnemataceae Family	Extinct filamentous green algae. Only the filamentous algae spore is preserved. Inhabited a wide range of hydro-terrestrial habitats nevertheless they preferred fluvial and lacustrine environments. Carboniferous - Recent.
	Desmidiales	Desmidiales Order	Green algae found mostly, but not exclusively, in freshwater habits. Most desmids are unicellular organisms however many species grow as long filamentous colonies. Jurassic (?) - Recent.
Marine Microplankton	**Dinoflagellate Cysts**	Cell produced during the sexual phase of the dinoflagellate life cycle	The fossil record of dinocysts is almost entirely confined to forms that have a meroplanktonic life cycle. Major dinoflagellate cyst morphotypes: proximate, cavate and chorate. Triassic - Recent.
	Prasinophyte	Structure fossilized produced by small quadric-flagellate motile phase	Majority, like *Tasmanites*, are spherical; diameter 50 to 2000μm. Exit current freshwater species. Precambrian - Recent.
	Acritarchs	Fossilized cysts, unicellular of organic wall. They have no formal taxonomic status.	The acritarchs are a polyphyletic group of palynomorph whose name means "of uncertain origin". Acritarchs (*akritos*= uncertain, mixed and *arche*=origin). Small dimension organism (5 to 150μm). They possess symmetry, it structures very varied ornamentation. They first appeared in the late Precambrian, attained their acme during the Ordovician - Devonian.
Zoomorph	**Foraminiferal test-linings**	Chitinous organic linings to calcareous shells of foraminifera	The linings are typically dark brown color, although their outer chambers are often more thin-walled and translucent. Good indicator of marine conditions.
	Scolecodonts	Elements of the jaw of benthic polychaete annelids worms	They are part-calcified and scleroprotenaceous ("chitinous") mouth parts ("pharyngeal jaws") of benthic polychaete annelid worms. Inner Ordovician - Recent.
	Chitinozoa	Vesicles in format of flasks or small hollow bottles.	They constitute an extinct group of organic-walled microfossils found in Palaeozoic marine sediments. Early Ordovician - Late Devonian.
Others	Zooclasts (e.g., Graptolite, Crustacean eggs); *Spongiophyton*.		

Palynomorphs are usually the group of particulate organic matter underrepresented in the kerogen assemblage. The interpretation of these particles depends on the nature of the assemblage being dependent of the proximity to a terrestrial source area and on the primary productivity microplankton (Tyson, 1995).

1.1.2. Organic petrology

1.1.2.1. Sample preparation

Optical petrography was performed on whole rock polished blocks prepared according to standard procedures (ISO 7404-2, 2009).

1.1.2.2. Microscopic analysis

The mean random reflectance were measured in vitrinite and solid bitumen (if present) on a Leica DM4000 microscope equipped with a Discus-Fossil system using a 50x oil immersion objective following the standard procedures of the ASTM D7708 (2011). The microscope was calibrated with a YAG standard (0.905% R_r) and an optical black glass (zero). The vitrinite reflectance was measured as a parameter for rank determination as recommend by the International Committee for Coal and Organic Petrology (ICCP, 1998).

1.1.3. Scanning Electron Microscope (SEM)

The concentrated organic matter obtained for palynofacies analysis was placed on a carbon ribbon on a plug of aluminum. After 24h it was metallized with a coating of gold-palladium. The observation was made in a Scanning Electron Microscope model MA10 Zeiss, with voltage (EHT) 20.00 kV and working distance (WD) of 8.5 mm under vacuum conditions.

1.2. Geochemical analyses

1.2.1. Total organic carbon, total sulfur content and insoluble residue

The total organic carbon determination provides a simple measure of organic matter content in sediments and sedimentary rocks. The content of organic matter is usually expressed as the relative percentage of organic carbon on a dry weight basis (Bordenave et al., 1993; Jarvie, 1991). The organic content includes both the organic matter insoluble in

organic solvents (kerogen) and the soluble organic matter (bitumen) in organic solvents (Tissot and Welte, 1984). The total organic carbon is controlled by a set of factors: i) the input of organic matter; ii) the preservation of organic matter; and, iii) the dilution of the organic matter by the mineral matter (Tyson, 1995).

The procedure to determine the total organic carbon (TOC) and total sulfur contents (TS) and insoluble residue (IR) obeyed to the follow: 0.26 g of crushed sediment was weighed into a sample holder porcelain filter and was added HCl to eliminate the carbonate fraction for 24 hours. Then it was washed with hot distilled water (100°C) to eliminate chloride for one hour, and neutralized with distilled water. The excess of water was discarded and the sample was dried in an oven at 65°C (about 3 hours). At the end of this procedure the weight of each sample was recorded. TOC and TS were quantified simultaneously by a LECO® analyzer SC-144DR. The equipment is an oven with an oxygen atmosphere (superdry) at a temperature of 1350°C which leads to complete combustion of the elements. The equipment records the concentrations of carbon and sulfur gases (CO_2 and SO_2) being the result expressed in percentage of weight.

The insoluble residue (IR) corresponds to the sample fraction that has not been eliminated by the acid treatment, assuming that a complete elimination of the carbonates was achieved. The IR is calculated by the following equation:

$$IR= (DM/TM)*100$$

where DM is the weight of the decarbonated sample and TM is the total weight of the sample before acidification. The results are expressed in percentage.

1.2.2. Rock-Eval pyrolysis

Rock-Eval pyrolysis, developed by Espitalié et al. (1977), simulates the natural process of hydrocarbons generation in the laboratory. This technique is one of the standard analyses in the petroleum industry. The samples were submitted to high experimental temperatures (up to 850°C) in order to promote thermochemical reactions in a short period of time (Lafargue et al., 1998). The products (vapors) are analyzed with a flame ionization detector (FID) and are expressed by three different peaks (P1, P2 and P3) and their correspondent areas (S1, S2 and S3; Fig. 7), and by the maximum temperature (T_{max}) of pyrolysis (Behar et al., 2001; Lafargue et al., 1998).

The S1 area (peak P1) represents the amount of free hydrocarbons (in mgHC/g rock) in the sample that either was present at time of deposition or was generated from the kerogen since deposition. S2 (peak P2) corresponds to the amount of hydrocarbons (in

mgHC/g rock) generated through thermal cracking of the kerogen. S3 (peak P3) represents the amount of CO_2 (in $mgCO_2$/g rock) produced during the pyrolysis of the kerogen (Behar et al., 2001; Lafargue et al., 1998).

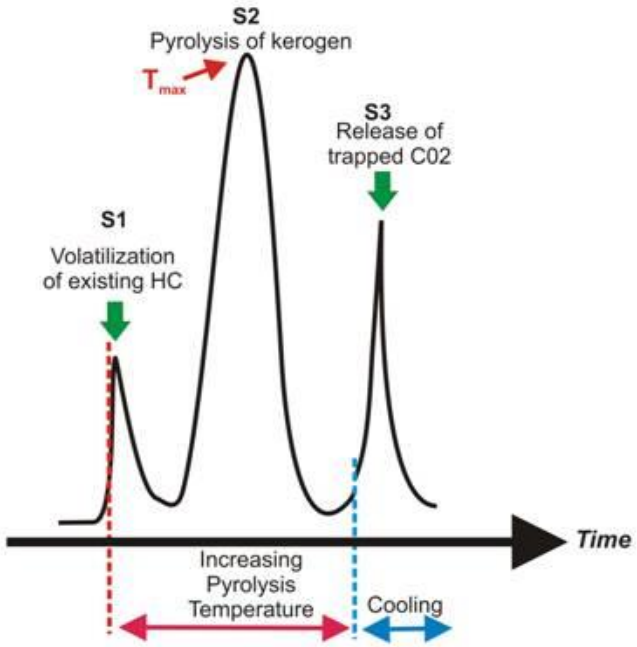

Figure 7. Schematic pyrogram showing result from Rock-Eval pyrolysis (modified from Tissot and Welte, 1984)

Directly in the pyrogram is still possible to read the maximum temperature of the pyrolysis (T_{max}). The T_{max} correspond to the temperature at which the maximum release of hydrocarbons from cracking of the kerogen occurs during pyrolysis (top of S2 peak). T_{max} is an indicator of the stage of maturation of the organic matter. T_{max} values < 435°C indicate immature organic matter; values between 435 to 470°C represent the oil window (mature organic matter) and T_{max} > 470°C represents the overmature zone matter (Tissot and Welte, 1984). T_{max} is partially dependent on other factors, such as type of organic matter (Tissot and Welte, 1984) and concentration of S2 peak (<0.2 mg HC/g rock; Peters, 1986) nevertheless is not affected by migration process (Tissot and Welte, 1984).

Based on the results of Rock-Eval pyrolysis two indices could be calculated. The Hydrogen Index [HI = (100 x S2)/TOC] and the Oxygen Index [OI = (100 x S3)/TOC] are used to characterize the origin of organic matter. On the van Krevelen-type diagram (HI versus OI) the type and maturity of kerogen could be estimated (Tissot and Welte, 1984). Other parameters, such as production or productivity index [PI = S1/(S1+S2)] and genetic

potential (S1+S2) can also give information about type, general potential and maturity of kerogen (e.g., Peters et al., 2005; Tissot and Welte, 1984).

1.2.3. Molecular compounds

1.2.3.1. Extraction

The bitumen was obtained by extraction in a Soxhlet extractor, using dichloromethane as solvent. In this procedure, approximately 50g of crushed and dried rock is transferred to cellulose extraction thimble, and covered with glass wool. The thimble is placed in the extraction flask sitting in a tube containing the solvent. Them it was boiled, traveling the vapor upward through the extraction tube into the condenser tube. Cool water flowing around the outside of the condenser tube leading to condensate the vapor, which then drips into the thimble. This procedure runs during approximately 8 hours. The free sulfur is removed with active copper filings. Then the solvent was removed by evaporation and the extractable organic matter (EOM) is weighed.

1.2.3.2. Liquid Chromatography (LC)

A 25 mm i.d. column is packed with pre-activated silica gel (28 - 200 mesh). The bitumen sample is poured on the column, and fractions are collected by successive elution of solvents with increasing polarity. The extracts were fractionated into saturated hydrocarbons, aromatic hydrocarbons and NSO compounds. The solvents employed were, respectively, *n*-hexane, a mixture of *n*-hexane / dichloromethane (8:2) and a mixture of methanol / dichloromethane (1:1).

1.2.3.3. Gas Chromatography coupled to Mass Spectrometry (GC - MS)

The saturated fraction was analyzed in an Agilent ® 7890 gas chromatograph (GC) equipped with an Agilent ® 7683 autosampler coupled to a mass spectrometer (MS). The carrier gas was helium (He) at 1.2 ml/min, in constant flow mode. A capilar column DB-5 Agilent (5% phenyl, 95% methylsiloxane, 30 m x 0.25 mm i.d.; film thickness 0.25 µm) was used. The injector temperature was 280°C. The GC was programmed with an initial temperature of 70°C (1 min), then programmed to rise 170°C at 20°C/min and 310°C at 2°C/min (10 min). The transfer line temperature was 280°C. The MS was operated with the following conditions: ion source temperature 280°C, interface temperature 300°C, quadrupole temperature 150°C and ionization voltage 70 eV. In this study, the ions *m/z* 85 and *m/z* 191

were monitored for the analysis of *n*-alkanes and terpanes (respectively) and the *m/z* 217 and *m/z* 218 for steranes.

1.2.3.4. Biomarkers

Biomarkers (chemical fossils, biological markers) are complex organic compounds whose basic skeletons do not suffered significant alterations despite the biological and/or geochemical processes they have undergone during burial. So, its structure can be linked with its biologic precursor. They can be found in oils, rock extracts, recent sediment extracts, and soil extracts. Biomarkers are able to give specific information about the origin of sedimentary organic matter, its thermal evolution and degree of degradation in crude oils (e.g., Eglinton et al., 1964; Peters et al., 2005).

Table 4 summarizes the information that can be obtained through the study of biomarkers present in the saturated fraction of bitumen.

Table 4. Main biomarkers used in organic geochemistry (e.g., Peters et al., 2005; Waples and Machihara, 1991).

Biomarker	Precursor	Information
n-alkane (C15, C17, C19)	Marine algae	OM origin
n-alkane (C25, C27, C29, C31)	Terrestrial plants	OM origin
Pristane and phytane	Photosynthetic organisms	Depositional environment
Tricyclic terpanes	Prokaryotic organisms	Thermal maturation
Hopanes	Prokaryotic organisms	Thermal maturation
Gammacerane	Protozoa	Hypersalinity conditions
Steranes	Eukaryotic organisms	Thermal maturation and OM origin
Diasteranes	Eukaryotic organisms	Thermal maturity

OM: Organic matter.

1.3. Statistic treatment

In order to group a set of elements and to check their similarity and/or differences a cluster analysis was used.

Cluster analysis is an exploratory technique, i.e., does not aim to explain but reveal structures in empirical data. Thus, clusters analysis is an exploratory multivariate analysis where the original data are organized and grouped into homogeneous or compact groups

with respect to one or more common characteristics, named clusters. The information contained in a cluster is similar to all the information contained in the same cluster but different from other clusters (Maroco, 2003; Reis, 1993, 1997). According to Maroco (2003), this technique does not have solid theoretical basis and just try to group more or less homogeneous objects according to more or less heuristic criteria.

In this study the cluster analysis was carried out based on the percentage and composition of the particulate organic matter (R-mode and Q-mode, cluster of kerogen groups and cluster of samples, respectively). This analysis allowed the establishment of groups and recognizes the relationship between the different kerogen components. The Statistica 7.0 software was used for this propose. The linear correlation coefficient of Pearson (*r*-Pearson) was applied to quantify the linear dependence between the elements. The results are displayed as dendrograms.

2. Samples

For the development of this research four boreholes were selected, containing carbonate and pelitic samples, drilled in the Central and Southern sectors of the Lusitanian Basin. The location of the boreholes is shown in Figure 8.

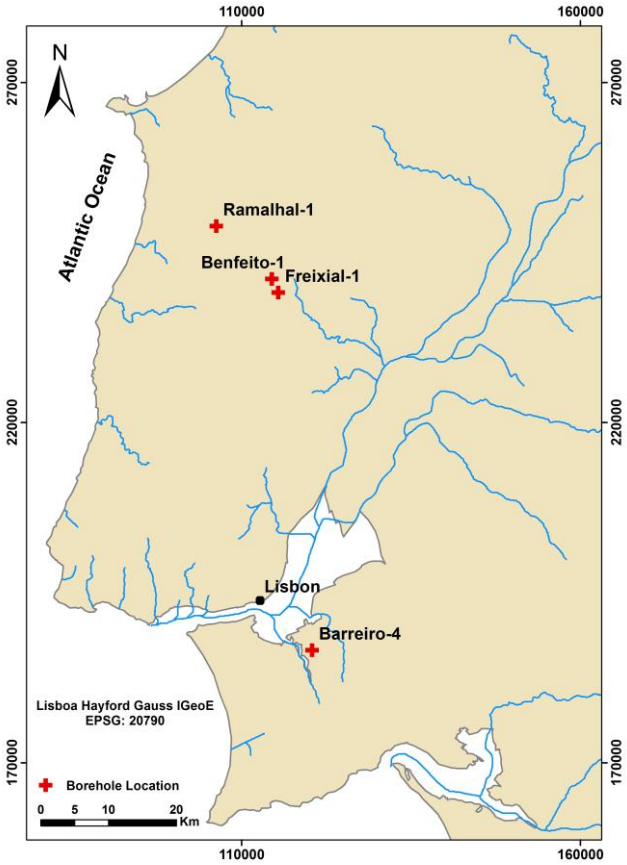

Figure 8. Location of the studied boreholes. Rm-1: Ramalhal-1; Bf-1: Benfeito-1; Fx-1: Freixial-1; Br-4: Barreiro-4.

Table 5 gives some information about the selected boreholes. The samples were provided by the archives of the Geology Centre of the University of Porto (Portugal). No published data were available from the selected samples.

Table 5. General information about the studied samples (data from the geological reports).

Borehole	Oil company	Sub-basin	Number of sample	Age	Depth (m)
Ramalhal-1 (Rm-1)	CPP/ Mobil	Bombarral	33	Bathonian? to Tithonian	3521
Benfeito-1 (Bf-1)	Petrogal	Arruda	77	Hettangian to Tithonian	3343
Freixial-1 (Fx-1)	EURAFREP	Arruda	36	Bathonian to Tithonian	2503
Barreiro-4 (Br-4)	Petrogal	Lower Tagus	43	Middle Jurassic to Neogene	2833

CPP: Companhia dos Petróleos de Portugal.

All the information presented bellow was gathered from the geological reports of the studied boreholes available on request at DPEP (Divisão para a Pesquisa e Exploração de Petróleo, Ministério da Economia, Governo Português).

Brief information on the boreholes is given as follow:

Ramalhal-1 borehole

The Ramalhal-1 borehole (Fig. 9) penetrated lithologies (Table 6) whose ages fall within the temporal interval between Bathonian? to Tithonian, recording an important gap in the transition between the Middle and the Upper Jurassic.

Table 6. Summary of the lithologies crossed by Ramalhal-1 borehole (data from Ramalhal-1 geological report).

Formation	Depth (m)	Number of samples	Lithologies
Lourinhã	0 - 1024	6	Fine to medium-grained sand with beds of red clay (on top); Red clays beds of course to medium-grained sandstone and marl; Marl intercalated with fine to medium-grained sandstone.
Abadia	1024 - 2027	7	Gray marl interbedded by layers of fine to medium-grained sandstone and limestone. On the top, there are thin layers of oolitic limestone.
Montejunto	2027 - 3190	16	Reef limestone with interbedded grey-brown compact limestones (on top). Compact limestone with calcite layers.
Brenha	3170 - 3521	4	Compact limestone with interbedded oolitic limestone and thin layers of calcite.

This borehole was drilled in the Bombarral sub-basin that correspond to a salt withdrawal structure flanked by diapiric structures (e.g., Leinfelder and Wilson, 1989; Wilson

et al., 1989). Bombarral sub-basin is separated from the Arruda and Turcifal sub-basins by a 70 km long northeast- to east-trending structural lineament, the Torres Vedras-Montejunto lineament. In this sub-basin, early Jurassic units show evidences of halokinesis (Montenat and Guéry, 1984).

Benfeito-1 borehole

The Benfeito-1 borehole crossed several lithologies (Table 7) whose ages cover a wide period of time, since the Hettangian to Tithonian (Fig. 9), i.e., all the Jurassic period. It was drilled in the Arruda sub-basin. This sub-basin corresponds to a half-graben developed during the Middle Oxfordian - Late Oxfordian as a consequence of transtensional rifting episodes that have affected the Estremadura Basin. The Arruda sub-basin represents an intra-continental pull-apart basin with a rhomb - like shape (Leinfelder and Wilson, 1989).

Table 7. Summary of the lithologies crossed by Benfeito-1 borehole (data from Benfeito-1 geological report).

Formation	Depth (m)	Number of samples	Lithologies
Lourinhã	20 - 135	6	Sandstone with intercalations of clay-calcareous.
Amaral	135 -165	1	Oolitic limestone.
Abadia	165 - 1137	19	Claystone with intercalations of compact sandstones and biogenic limestone. From 1062-1137m, clay schist, limestone and calcarenite.
Montejunto	1137 - 1399	9	Compact limestone, sometime with fractures, and brown limestones thinly stratified.
Cabaços	1399 - 1585	8	From 1410-1499m, anhydrite and organogenic limestones with ostracod. Organic limestone thinly stratified and compact.
Brenha (Callovian)	1585 - 1740	3	Micritic limestone, very compact with stylolite sometimes pseudoolitic.
Candeeiros	1740 - 2627	18	Alternation of limestone, mainly oolitic in part dolomitized, and dolomites.
Brenha	2627 - 2963	7	Argillaceous micritic limestone and carbonate claystone.
Coimbra	2963 - 3174	4	Limestones, sometimes argillaceous and fossiliferous, and compact microcrystalline dolomite.
Dagorda	3174 - 3343	2	Argillaceous dolomite, dolomitic claystone and anhydrite.

Freixial-1 borehole

The Freixial-1 borehole was drilled in the same sub-basin that Benfeito-1 borehole, i.e., the Arruda sub-basin. The Freixial-1 borehole (Table 8) through a section continues from the Bathonian until the Tithonian.

Table 8. Summary of the lithologies crossed by Freixial-1 borehole (data from Freixial-1 geological report).

Formation	Depth (m)	Number of samples	Lithologies
Lourinhã	0 - 100	1	Silty clay, argillaceous limestones and very fine sandstone.
Amaral	100 - 157	2	Oolitic limestone.
Abadia	157 - 1412	11	Silty clay; Rare layers of limestone and dolomite; Fine sandstone argillaceous with pyrite and lignite; Compact sandstones; quartz sand and subangular quartz.
Montejunto	1412 - 1885	9	Recrystallized micritic limestones; Calcareous clay, silty.
Cabaços	1885 - 2184	6	Limestones and anhydrite.
Brenha	2184 - 2327	3	Limestones weakly argillaceous.
Candeeiros	2327 - 2503	4	Recrystallized limestones.

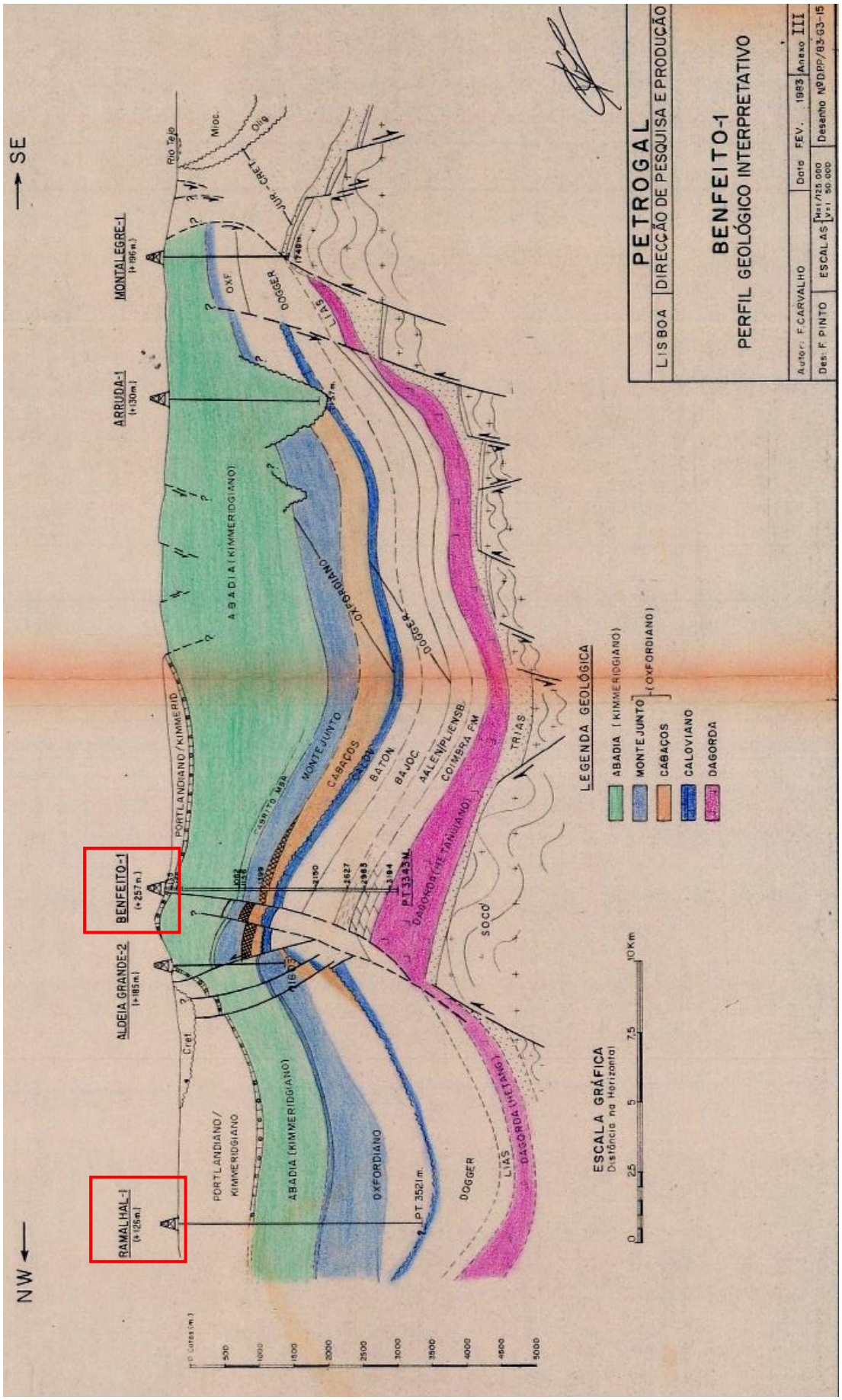

Figure 9. Interpretive geological profile of Rm-1 and Bf-1 boreholes (data from Benfeito-1 geological report).

Barreiro-4 borehole

Forty - four samples were collected from the Barreiro-4 borehole, which cut a sedimentary sequence (siliciclastic and carbonate; Table 9) from the Middle Jurassic (Bathonian) to the Neogene (Fig. 10). It was drilled in the Lower Tagus sub-basin. This sub-basin developed as a NNW-SSW elongated saucer - shaped basin. Sedimentological and seismic data indicate that this sub-basin was a platform (Middle Oxfordian - Late Kimmeridgian) that was most likely controlled by the Setúbal-Pinhal Novo fault (Carvalho et al., 2005). During the Late Cretaceous, the sub-basin had the geometry of a foredeep basin as a result of the extensional tectonics induced by NW-SE compressive episodes of the Alpine orogeny (Carvalho et al., 2005; Rasmussen et al., 1998; Ribeiro et al., 1990). During this period, the sub-basin was filled with more than 2 km of siliciclastic sediments that alternate from coarse sandstones to silty mudstones.

Table 9. Summary of the lithologies crossed by Barreiro-4 borehole (data from Barreiro-4 geological report).

Formation	Depth (m)	Number of samples	Lithologies
	0 - 1215	5	0-180m: Arkosic and subarkosic sandstone; Micaceous and argillaceous sandstones. 180-890m: Sandy limestones; Sandstones with calcareous cements; Silty clay. 890-1215m: microcrystalline limestone; Silty and sandy clay; Argillaceous limestone.
Torres Vedras	1215 - 1432	9	Argillaceous sandstones; Presence of dead oil (after 1345m).
Lourinhã	1432 - 1717	6	Coarse sandstones; fossiliferous calcareous cement with dead oil; Silty clay; Dolomite and dolomitic limestone.
Amaral	1717 - 1816	1	Limestone and dolomitic limestone; Dead and heavy oil; Clays.
Abadia	1816 - 2148	7	Limestone breccia and reef limestone. Thin layers of dolomite. Some layers of anhydrite and dolomitic clay.
Montejunto	2148 - 2470	7	Limestone; Thin layers of marls.
Brenha	2470 - 2833	6	Until 2588m: Dolomite and dolomitic limestones. From 2588 to 2833, calcareous fossiliferous microcrystalline; Some layers of clastic and oolitic limestone.

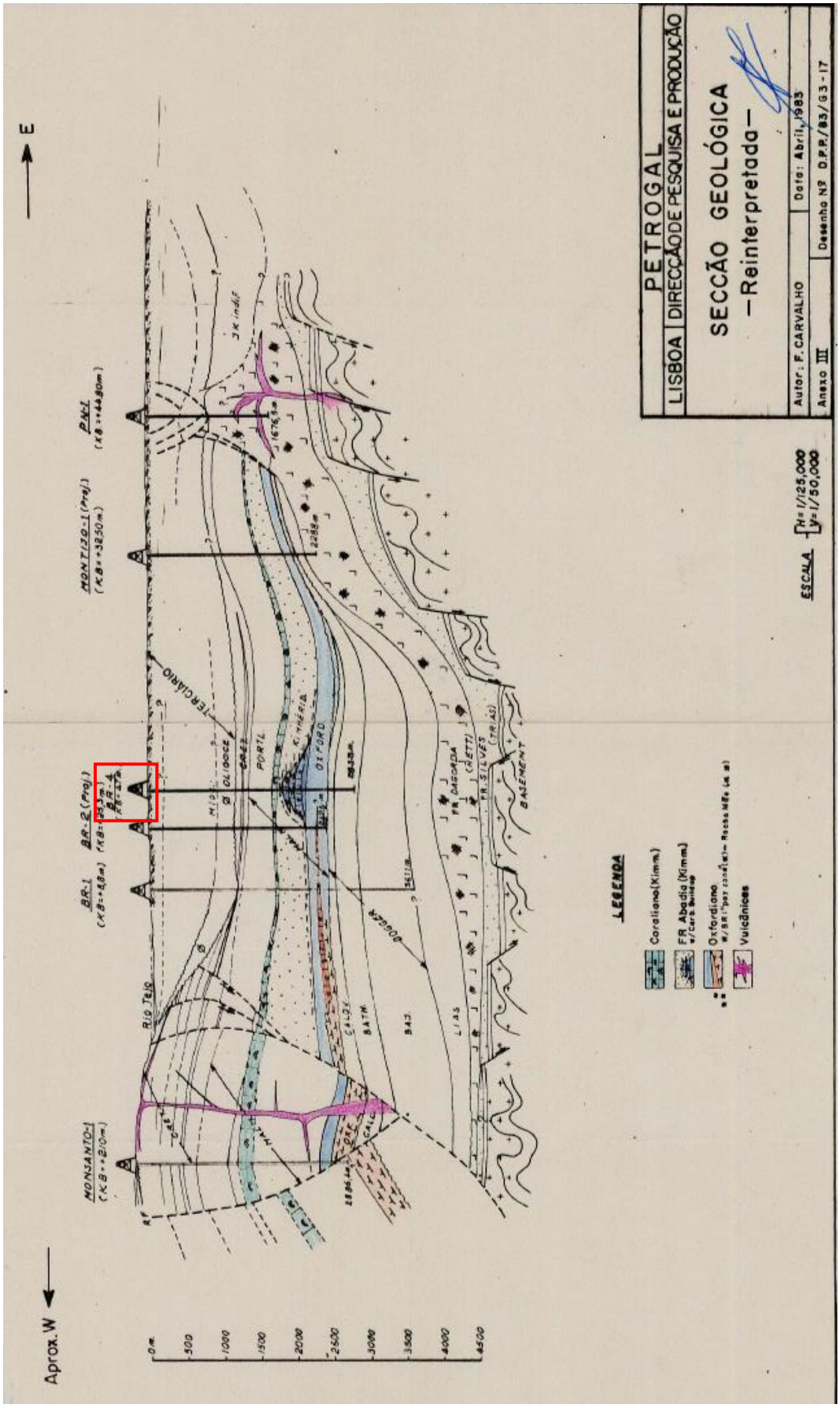

Figure 10. Interpretive geological profile of Br-4 borehole (data from Barreiro-4 geological report)

References

ASTM D7708, 2011. Standard Test Method for Microscopical Determination of Reflectance of Vitrinite Dispersed in Sedimentary Rocks. ASTM International, 8 pp.

Behar, F., Beaumont, H.L., Penteado, H.L., 2001. Rock-Eval 6 Technology: Performance and Developments. Oil & Gas Science and Technology-Revue de l'Institut Français du Pétrole 56, 111 - 134.

Bordenave, M.L., Espitalié, L., Leplat, P., Oudin, J.L., Vandenbroucke, M., 1993. Screening techniques for source rock evaluation, in: Bordenave, M.L. (Ed.), Applied Petroleum Geochemistry. Editions Technip, Paris, pp. 217 - 278.

Bostick, N.H., 1971. Thermal alteration of clastic organic particles as an indicator of contact and burial metamorphism in sedimentary rocks. Geosciences & Man, Baton Rouge 3, 83 - 92.

Carvalho, J., Matias, H., Torres, L., Manupella, G., Pereira, R., Mendes-Victor, L., 2005. The structural and sedimentary evolution of the Arruda and Lower Tagus sub-basins, Portugal. Marine and Petroleum Geology 22, 427 - 453.

Combaz, A., 1964. Les palynofacies. Reveu de Micropaléontologie 7, 204 - 218.

Eglinton, G., Scott, P.M., Besky, T., Burlingame, A.L., Calvin, M., 1964. Hydrocarbons of biological origin from a one-billion-year-old sediment. Science 145, 263 - 264.

Espitalié, J., Laporte, J.L., Madec, M., Marquis, F., Leplat, P., Paulet, J., Boutefeu, A., 1977. Méthode rapide de caractérisation des roches mètres, de leur potentiel pétrolier et de leur degré d'évolution. Revue de l'Institut Français du Pétrole 32, 23 - 42.

ICCP, 1998. The new vitrinite classification (ICCP System 1994). Fuel 77, 349 - 358.

ISO 7404-2, 2009. Methods for the petrographic analysis of coals - Part 2: Methods of preparing coal samples. International Organization for Standardization, 12pp.

Jarvie, D.M., 1991. Total Organic Carbon (TOC) analysis, in: Merril, R.K. (Ed.), Source and Migration Processes and Evaluation Techniques, Tulsa, Treatise of Petroleum Geology. American Association of Petroleum Geologists, pp. 113 - 118.

Lafargue, E., Marquis, F., Pillot, D., 1998. Rock-Eval 6 applications in hydrocarbon exploration, production, and soil contamination studies. Revue de l'Institut Français du Pétrole 53, 421 - 437.

Leinfelder, M.R.R, Wilson, R.C.L., 1989. Seismic and sedimentologic features of Oxfordian-Kimmeridgian syn-rift sediments on the eastern margin of the Lusitanian Basin. Geologische Rundschau 79, 81 - 104.

Maroco, J., 2003. Análise estatística - com utilização do SPSS. 2º Edição, Edições Sílabo.

Mendonça Filho, J.G., Carvalho, M.A., Menezes, T.R., 2002. Palinofácies, in: Dutra, T.L. (Ed.), Técnicas e procedimentos para o trabalho com fósseis e formas modernas comparativas. Unisinos, São Leopoldo, 20 - 24.

Mendonça Filho, J.G., 1999. Aplicação de estudos de palinofácies e fácies orgânica em rochas do Paleozóico da Bacia do Paraná, Sul do Brasil. Universidade Federal do Rio Grande do Sul. PhD thesis, 338 pp.

Mendonça Filho, J.G., Menezes, T.R., Mendonça, J.O., 2011b. Organic Composition (Palynofacies Analysis). Chapter 5 in: ICCP Training Course on Dispersed Organic Matter, ISBN 978-9-89-826567-8, pp. 33 - 81.

Mendonça Filho, J.G., Menezes, T.R., Mendonça, J.O., Oliveira, A.D., Carvalho, M.A., Sant'Anna, A.J., Souza, J.T., 2010. Palinofácies, in: Sousa, C.I. (Ed.), Paleontologia. Rio de Janeiro, Interciência, pp.379 - 413

Mendonça Filho, J.G., Menezes, T.R., Mendonça, J.O., Oliveira, A. D., Souza, J.T., Sant'Anna, A.J., 2011a. Kerogen: Composition and Classification. Chapter 3 in: ICCP Training Course on Dispersed Organic Matter, ISBN 978-9-89-826567-8, pp. 17 - 24.

Mendonça Filho, J.G., Menezes, T.R., Mendonça, J.O., Oliveira, A.D., Silva, T.F., Rondon, N.F., Silva, F.S., 2012. Organic Facies: Palynofacies and Organic Geochemistry Approaches, in: Panagiotaras, D. (Org.), Geochemistry Earth's system processes. InTech, Patras, ISBN 978-9-53-510586-2, vol. 1, pp. 211 - 245.

Montenat, C., Guéry, F, 1984. L'intrusion diapirique de Caldas da Rainha et l'halocinèse jurassique sur la marge portugaise. C.R. Acad. Sci. Paris 298, 901 - 906

Peter, K.E., 1986. Guidelines for evaluating petroleum source rocks using programmed pyrolysis. AAPG Bulletin 70, 318 - 329.

Peters, K.E., Walters, C.C., Moldowan, J.M., 2005. The Biomarker Guide, vol. 2, Biomarkers and Isotopes in Petroleum Exploration and Earth History, second ed. Cambridge University Press, London.

Rasmussen. E.S., Lomholt, S., Andersen, C., Vejbæk, O.L., 1998. Aspects of the structural evolution of the Lusitanian Basin in Portugal and the shelf and slope area offshore Portugal. Tectonophysics 300, 199 - 225.

Reis, E., 1993. Análise de clusters: um método de classificação sem preconceitos. ISCTE, Grupo de Investigação Estatística e Análise de Dados. Edições Sílabo, Lda.

Reis, E., 1997. Estatística multivariada aplicada. Edições Sílabo, Lda.

Ribeiro, A., Kullberg, M.C., Kullberg, J.C., Manuppella, G., Phipps, S., 1990. A review of alpine tectonics in Portugal - foreland detachment in basement and cover rocks. Tectonophysics 184, 357 - 366.

Tchudy, R.H., 1961. Palynomorphs as indicators of facies environments in Upper Cretaceous and Lower Tertiary strata, Colorado and Wyoming. Wyoming Geological Society, 16th Annual Field Conference, Guidebook, 53 - 59.

Tissot, B., Welte, D.H., 1984. Petroleum formation and occurrence, second ed. Springer Verlag, Hidelberg.

Traverse, A., 1988. Paleopalynology. Unwin Hyman, London.

Tyson, R.V., 1995. Sedimentary Organic Matter. Chap. & Hall, London.

Vicent, A.J., 1995. Palynofacies analysis of Middle Jurassic sediments from the Inner Hebrides. PhD Thesis, University of Newcastle upon Tyne. 475p.

Waples, D.W., Machihara, T., 1991. Biomarkers for Geologists: A Practical Guide to the application of Steranes and Triterpanes in Petroleum Geology. American Association of Petroleum Geologists, Methods in Exploration, Series 9.

Wilson, R.C.L., Hiscott, R.N., Willis, M.G., Gradstein, F.M., 1989. The Lusitanian Basin of west-Central Portugal: Mesozoic and Tertiary tectonic, stratigraphic and subsidence history. The American Association of Petroleum Geologists Bulletin 46, 341 - 362.

Part III - Results and discussion

1. Bombarral sub-basin

1. 1. Paleoenvironmental characterization of a Jurassic sequence on the Bombarral sub-basin (Lusitanian basin, Portugal): insights from palynofacies and organic geochemistry

Adapted from Paula Alexandra Gonçalves, João Graciano Mendonça Filho, Joalice Oliveira Mendonça, Taís Freitas da Silva, Deolinda Flores

International Journal of Coal Geology (2013) 113, 27 - 40

Accepted 25th March 2013

Abstract

A Middle - Upper Jurassic sedimentary succession has been cut by the Ramalhal-1 borehole in the Bombarral sub-basin (Lusitanian Basin, Portugal). The succession comprises the Brenha, Montejunto, Abadia and Lourinhã Formations, which are composed of limestones, marls, sandstones and clays. The main objective of this study was to characterize the organic matter using palynofacies and geochemical analyses to determine the depositional paleoenvironments and the hydrocarbon generation potential. The Total Organic Carbon content is generally less than 1 wt. % but reaches 4.1 wt.% in one sample, due to the presence of perhydrous coal. The Rock-Eval pyrolysis results reveal lower values HI, usually nether to 100 mgHC/gTOC, showing that the studied samples have type III kerogen and a low potential for oil generation. The T_{max} values (varies between 319 and 443ºC) and biomarker data obtained for these samples indicate a maturation ranging between immature and, eventually, mature. The palynofacies data indicate predominance of the Phytoclast group (>80%), with different degradation degrees and a modest contribution of Palynomorph group, especially sporomorphs, and the Amorphous Organic Matter (AOM) group. Solid bitumen was observed in some samples from the Montejunto and Brenha Formations. Determining the relative percentages of the kerogen groups allowed for the identification of seven intervals that established variations in the depositional environment.

1.1.1. Introduction

The Lusitanian Basin (Portugal) is an important Mesozoic basin that has caught the attention of the scientific community since the 1950s, driven by the constant interest of oil companies. This basin is located on the occidental sector of the Iberian Peninsula and

comprises an important Mesozoic onshore record (Leinfelder and Wilson, 1989; Wilson, 1988), including a thick marine carbonated series whose potential source rocks and hydrocarbon occurrences have been one of the main objectives of the numerous drillings conducted by various oil companies.

The Mesozoic sequence of the Lusitanian Basin (hereinafter called LB) is well known for its stratigraphic, sedimentological and structural characteristics (e.g., Azerêdo et al., 2003; Duarte et al., 2004; Kullberg et al., 2006; Leinfelder and Wilson, 1989; Rasmussen et al., 1998; Rey et al., 2006; Wilson, 1979, 1988; Wilson et al., 1989). However, organic petrology and geochemical studies have only been performed in the recent years in the excellent outcrops existing along the Portuguese shore in the coastal plateau to determine the following: the occurrence and preservation of organic matter; the potential of the source rocks; the definition of the depositional paleoenvironments through the palynofacies assemblages; and the organic geochemical and organic carbon isotopic parameters. These studies were focused on the Lower - Middle Jurassic age formations located mainly in the western part of the basin. They revealed immature organic rich facies with high values of Total Organic Carbon (TOC) preserved in a marine environment under variable redox conditions (e.g., Duarte et al., 2010, 2011, 2012; Oliveira et al., 2006; Poças Ribeiro et al., 2013; Silva et al., 2010, 2011). Studies from Masson and Miles (1986) revealed, also, that the offshore Jurassic deposits have potential for the generation of hydrocarbons (oil and/or gas).

Although there are studies conducted in the sedimentary sequences intercepted by the drillings performed in the LB (ordered by the Portuguese government), further studies using new methodologies are needed that focus on the understanding of the organic matter, which is the main purpose of this study. Thus, the objectives of this study are as follows: (i) to characterize the organic matter content of the Jurassic sedimentary succession cut by the Ramalhal-1 (Rm-1) borehole; (ii) to define the type and maturation of the source rock and its hydrocarbon generation potential; and iii) to characterize the depositional paleoenvironment of the sedimentary sequence intercepted by this borehole. Palynofacies analysis and organic geochemistry techniques (TOC and Sulfur content, Rock-Eval pyrolysis and biomarker analysis) were used to achieve these goals.

1.1.2. Geological setting

Please see section 6 on Part I for detailed description of geological setting.

1.1.3. Samples and methods

This paper focused on the sedimentary succession intercepted by the Ramalhal-1 borehole (Rm-1) drilled to a depth of 3521 m. This borehole was drilled in the Central Sector of the LB at the Bombarral sub-basin (Fig. 11), and crossed sediments of Jurassic age (Bathonian? to Tithonian). The lithological log (Fig. 12) was prepared according to the information included in the Geological Report available on request at DPEP (Divisão para a Pesquisa e Exploração de Petróleo, Ministério da Economia, Governo Português).

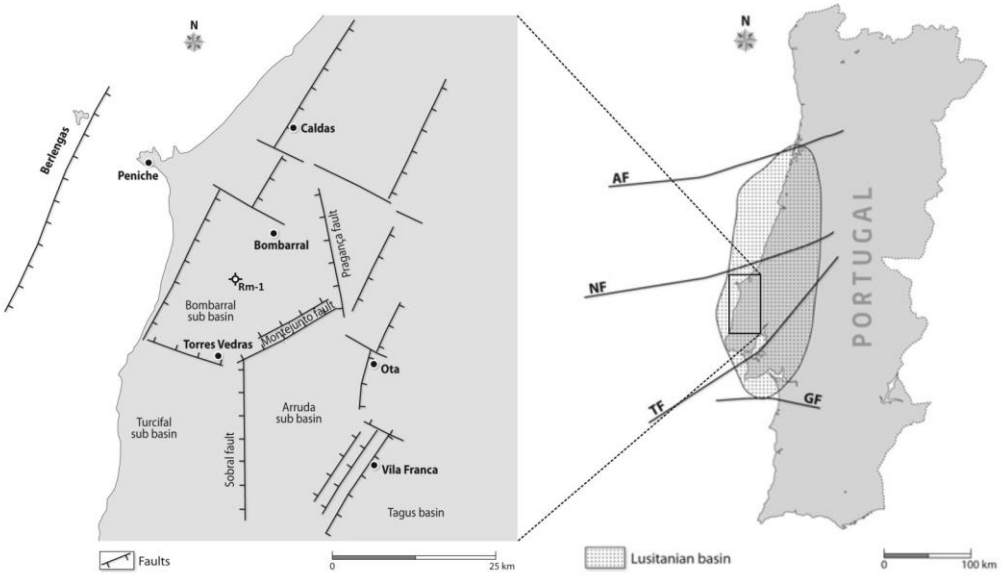

Figure 11. Geographic and tectonic settings of the Lusitanian Basin. Rm-1 - Ramalhal-1 borehole.

Thirty-three samples (Table 10) were taken and submitted for palynofacies and geochemical analyses (TOC, Rock-Eval pyrolysis and molecular biomarker analysis), and some of the obtained results were statistically (cluster analysis) evaluated. These analyses were performed in the Palynofacies and Organic Facies Laboratory (LAFO) of the Federal University of Rio de Janeiro (Brazil), except for the Rock-Eval pyrolysis, which was performed at Baseline Resolution INC., Analytical Laboratories (USA).

Geochemical analyses

Please see section 1.2. on Part II for detailed description of the geochemical analyses procedures.

Palynofacies analysis

Please see section 1.1.1. on Part II for detailed description of the palynofacies procedures.

Statistical analyses

Please see section 1.3 on Part II for detailed description of the statistical analyses.

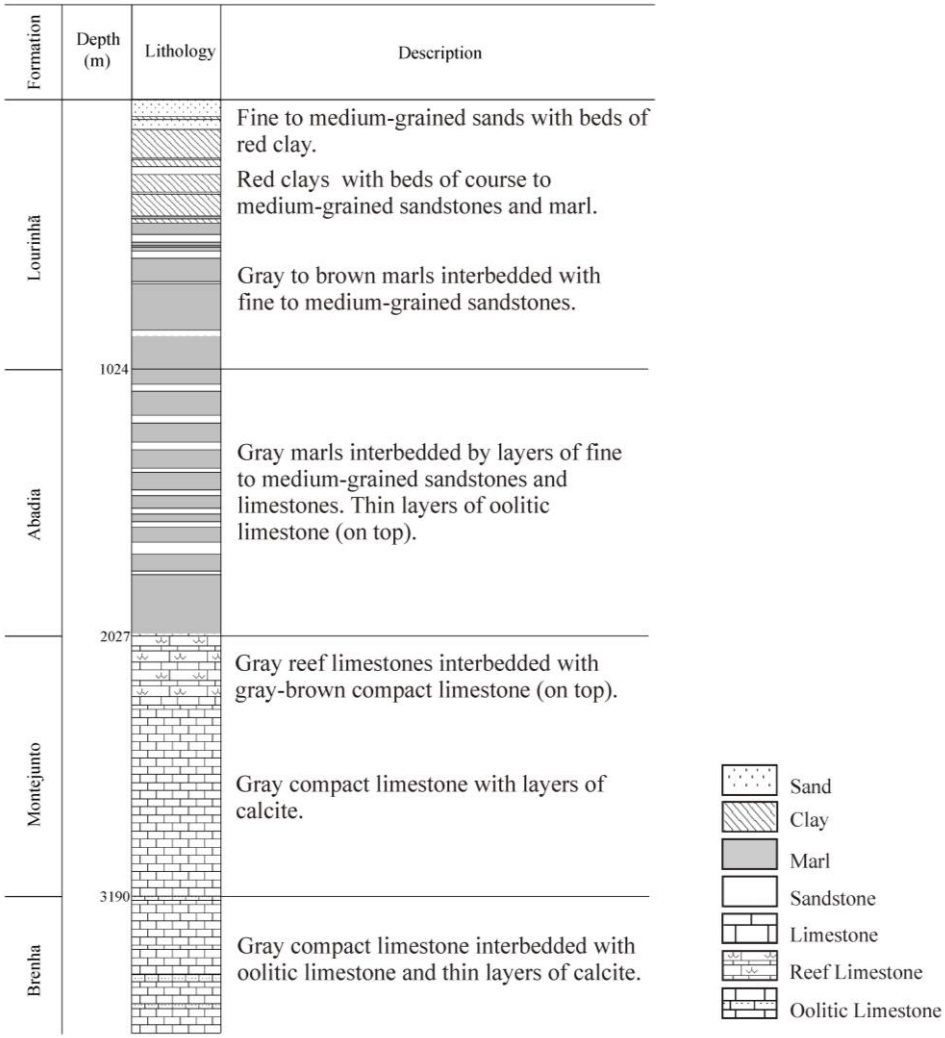

Figure 12. Simplified stratigraphic column of the sedimentary sequence cut by the Rm-1 borehole (data from the geological report of CPP).

1.1.4. Results and discussion

The organic matter of the studied samples does not show evidence of weathering using both the fluorescence mode observation as well as the pyrite crystal appearance. The

organic matter shows, in fluorescence, a high level of preservation and, in addition, pyrite crystals appear unchanged. According to Littke et al. (1991) the microscopic appearance of pyrite seems to be the most reliable indicator of source rock weathering because pyrite is a ubiquitous constituent in most organic matter-rich sediments. In sediments affected by weathering many pyrite crystals seem to be completely replaced by iron oxide or iron hydroxide. Thus, the organic matter in these studied samples contains exclusively fresh pyrite revealing according to these authors that they are not affected by weathering.

1.1.4.1. Total Organic Carbon and Total Sulfur

The TOC values (Table 10) range between 0.27 (Am.33) and 4.10 wt.% (Am.4),with a mean of 0.88 wt.%, pointing out a poor to good content of organic carbon according to the limits suggested by Peters and Cassa (1994). Although the TOC content of sample Am.4 was unexpected, it may be due to the identification of traces of perhydrous coal in the core and reported in the LB Upper Jurassic (Costa et al., 2010). The TS content (Table 10) is low, ranging between 0.01 and 0.49 wt.%. Marls and sandstone beds show higher TOC (mean of 1.75 wt.%) and TS contents than the limestones. Tissot and Welte (1984) have reported that black shales and carbonates with TOC values higher than 0.5 and 0.3 wt.%, respectively, can be considered as potential source rocks for oil or gas. However, Tyson (1995) asserts that TOC values higher than 2 or 3 wt.% are usually associated with the assemblage of organic matter dominated by AOM; in siliciclastic facies, lower values are associated with the dominance of phytoclasts, which are the main organic matter for the gas source rock. This relationship will be discussed later in the paper.

Furthermore, according to Berner (1995) and Borrego et al. (1998), the carbon (C)/sulfur (S) ratio can be used to identify the occurrence of sulfate reduction, where values below and above 3 indicate more reducing or more oxic environments, respectively. The C/S ratios (Table 10) in the studied samples were higher than 3 (except sample Am.22, which reached 2.97), indicating an oxygenated water column.

1.1.4.2. Rock-Eval pyrolysis

The Rock-Eval pyrolysis data are listed in Table 10, and Fig. 13 plots OI versus HI. The S1 and S2 values vary from 0.02 to 1.19 mgHC/g rock and 0.01 to 1.01 mgHC/g rock, respectively. The samples with the highest HI values are from the Montejunto (Am.14, Am.21, Am.22 and Am.23) and Brenha (Am.33) Formations and range between 120 and 222 mgHC/gTOC (see also Table 10). Fig. 13 indicates that the organic matter of the samples consists of type III kerogen derived primarily from terrestrial higher plants.

Table 10. Geochemical results of Rm-1 borehole samples.

Sample	Depth (m)	Lithology	TOC	TS	C/S	IR	S1	S2	HI	OI	T_{max}
Lourinhã Formation											
Am.1	150	Clay	0.42	n.d.	n.d	95	0.06	0.01	2	33	434
Am.2	300	Clay	0.41	n.d.	n.d	83	0.03	0.02	5	17	356
Am.3	450	Clay	0.62	n.d.	n.d	87	0.05	0.03	5	35	299
Am.4	600	Sandstone and perhydrous coal	4.10	0.49	8.37	76	0.03	0.25	6	5	451
Am.5	750	Marl	0.84	0.13	6.38	70	0.02	0.04	5	15	319
Am.6	900	Marl	1.81	0.19	9.53	76	0.09	0.22	12	20	393
Abadia Formation											
Am.7	1050	Limestone	0.87	0.27	3.25	45	0.17	0.34	39	40	426
Am.8	1200	Marl	1.56	0.40	3.93	67	0.09	0.45	29	25	426
Am.9	1350	Marl	1.45	0.13	10.82	60	0.04	0.29	20	20	439
Am.10	1500	Sandstone	1.77	0.29	6.05	64	0.06	0.40	23	19	442
Am.11	1650	Marl	1.40	0.15	9.05	61	0.04	0.12	9	24	427
Am.12	1800	Marl	1.36	0.13	10.46	62	0.07	0.22	16	26	426
Am.13	1950	Marl	1.45	0.18	8.19	56	0.04	0.20	14	19	443
Montejunto Formation											
Am.14	2050	Limestone	0.62	0.06	9.72	11	0.42	0.94	153	114	429
Am.15	2125	Limestone	0.46	0.01	35.44	4.3	0.07	0.16	35	102	427
Am.16	2200	Limestone	0.76	0.18	4.13	10	0.05	0.13	17	33	416
Am.17	2275	Limestone	0.72	0.03	21.59	7.1	0.17	0.38	53	78	419
Am.18	2350	Limestone	0.73	0.17	4.25	7.4	0.10	0.18	25	49	448
Am.19	2425	Limestone	0.52	0.02	21.19	4.2	0.05	0.15	29	75	423
Am.20	2500	Limestone	0.39	0.04	9.01	5.1	0.05	0.09	23	93	425
Am.21	2575	Limestone	0.84	0.21	4.00	16	1.14	1.01	120	70	428
Am.22	2650	Limestone	0.68	0.23	2.97	16	0.69	0.82	121	90	428
Am.23	2725	Limestone	0.51	0.08	6.07	7.5	0.60	0.66	129	137	431
Am.24	2800	Limestone	0.35	0.04	7.83	3.5	0.24	0.23	66	135	430
Am.25	2875	Limestone	0.50	0.08	5.94	9.5	0.11	0.29	59	79	431
Am.26	2950	Limestone	0.41	0.08	4.92	5.2	0.23	0.15	37	80	420
Am.27	3025	Limestone	0.35	0.03	11.74	4.4	0.20	0.25	71	100	422
Am.28	3100	Limestone	0.40	0.04	9.53	4.7	0.16	0.28	70	105	433
Am.29	3175	Limestone	0.42	0.04	10.85	3.0	0.09	0.24	57	102	426
Brenha Formation											
Am.30	3250	Limestone	0.62	0.03	18.49	6.4	0.12	0.27	43	61	423
Am.31	3325	Limestone	0.75	0.07	10.71	12	0.16	0.30	40	61	386
Am.32	3400	Limestone	0.63	0.05	12.55	11	0.44	0.38	61	75	422
Am.33	3475	Limestone	0.27	0.04	6.65	4.0	0.36	0.60	222	226	427

n.d. Not detected. TOC: Total Organic Carbon (wt.%); TS: Total Sulfur content (wt.%); C/S: carbon/sulfur ratio; IR: Insoluble residue (wt.%); S1 and S2: mgHC/g rock; HI: hydrogen index (mgHC/g TOC); OI: Oxygen index (mgCO2/g); T_{max}: pyrolysis maximum temperature.

According to Tissot and Welte (1984), this type of kerogen has a low potential of oil generation but can generate gas if buried at a sufficient depth. The T_{max} (°C) values (Table 10) indicate that the majority of the samples are in an immature stage (T_{max} varies between

299 and 434°C). The low T_{max} values that were observed correspond to samples with small S2 peaks (<0.2 mgHC/g rock) or that are impregnated with migrated bitumen (Peters and Cassa, 1994).

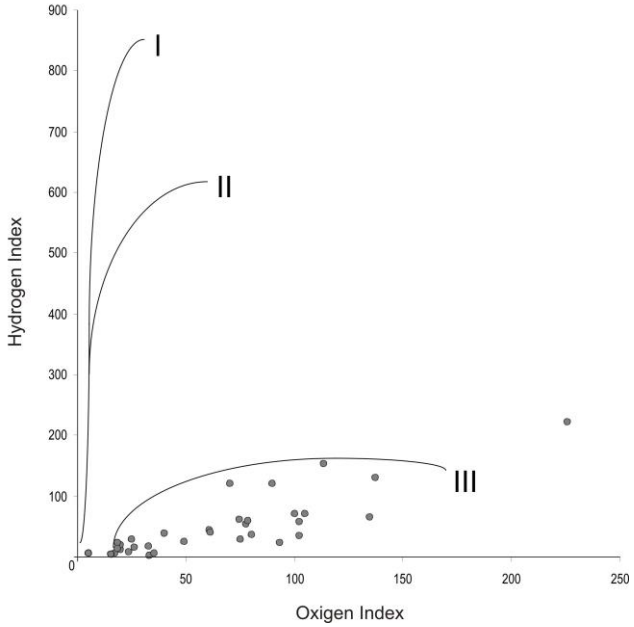

Figure 13. Van Krevelen-type diagram for the Rm-1 samples.

1.1.4.3. Palynofacies

The palynofacies analysis (Table 11) revealed the presence of the three main groups of particulate organic matter (Phytoclast, Amorphous Organic Matter and Palynomorph), with a predominance of the phytoclast group in all samples.

In the phytoclast group (Fig. 14, Table 11), the tissues derived from terrestrial higher plants (Bostick, 1971), were mainly composed of non-opaque non-biostructured phytoclast (43.5% of total phytoclast, Fig. 14B) with a dark brown color under transmitted white light and, usually, without fluorescence. These particles did not show botanical structure, had irregular outlines and, in most cases, were degraded. According to Tyson (1995), this type of phytoclast is characteristic of proximal environments (near or nearest to the fluvio-deltaic point source), and the dark color is related to the oxidation process.

Non-opaque biostructured phytoclast (Fig. 14C-E) was the second most abundant subgroup of phytoclast in the samples; it exhibited pale to dark brown color under white transmitted light and usually did not display fluorescence; some striate phytoclasts, however, revealed a yellow-brown color.

Table 11. Palynofacies results from Rm-1 borehole samples.

Sample	Depth (m)	Phytoclast (%)	AOM (%)	Sporomorphs (%)	Freshwater Palynomophs (%)	Marine Palynomophs (%)	Palynofacies Association	Interval
Lourinhã Formation								
Am.1	150	n.d.	n.d.	n.d.	n.d	n.d	n.d.	
Am.2	300	96.46	2.25	1.29	0.00	0.00	I	
Am.3	450	n.d.	n.d.	n.d.	n.d.	n.d.	n.d.	
Am.4	600	97.05	0.98	1.97	0.00	0.00	I	7
Am.5	750	97.73	0.65	1.62	0.00	0.00	I	
Am.6	900	98.36	0.66	0.99	0.00	0.00	I	
Abadia Formation								
Am.7	1050	98.01	0.99	0.99	0.00	0.00	I	
Am.8	1200	97.42	0.32	2.26	0.00	0.00	II	
Am.9	1350	96.76	0.65	2.59	0.00	0.00	I	
Am.10	1500	94.08	2.30	3.62	0.00	0.00	II	6
Am.11	1650	94.48	1.62	3.90	0.00	0.00	II	
Am.12	1800	81.37	16.46	2.17	0.00	0.00	II	
Am.13	1950	78.39	14.52	7.10	0.00	0.00	IV	
Montejunto Formation								
Am.14	2050	67.52	27.33	5.14	0.00	0.00	VI	
Am.15	2125	80.39	13.50	6.11	0.00	0.00	IV	
Am.16	2200	83.80	12.46	3.74	0.00	0.00	IV	
Am.17	2275	84.19	10.00	5.81	0.00	0.00	IV	5
Am.18	2350	65.27	30.55	2.25	0.00	1.93	VI	
Am.19	2425	80.13	17.03	2.84	0.00	0.00	IV	
Am.20	2500	84.16	12.11	3.42	0.31	0.00	V	
Am.21	2575	66.88	23.97	9.15	0.00	0.00	IV	
Am.22	2650	84.84	9.68	5.16	0.00	0.32	IV	
Am.23	2725	78.12	18.54	2.74	0.61	0.00	V	
Am.24	2800	89.04	10.39	0.56	0.00	0.00	I	4
Am.25	2875	76.36	18.53	3.83	0.32	0.96	II	
Am.26	2950	80.66	11.48	2.62	0.33	4.92	III	
Am.27	3025	88.85	4.92	1.97	0.66	3.61	III	3
Am.28	3100	87.87	4.26	3.28	0.33	4.26	III	
Am.29	3175	93.71	1.32	4.97	0.00	0.00	II	
Brenha Formation								2
Am.30	3250	88.49	7.24	3.29	0.99	0.00	II	
Am.31	3325	98.68	0.66	0.66	0.00	0.00	II	
Am.32	3400	89.09	0.00	10.62	0.00	0.29	V	1
Am.33	3475	90.76	0.00	7.88	1.36	0.00	V	

n.d. Not detected. AOM: Amorphous organic matter.

The striate and striped phytoclasts usually showed more irregular outlines than the banded and pitted ones. The striate and striped phytoclasts were dominant in all samples, however, in the Montejunto Formation, the banded phytoclasts occurred in higher contents.

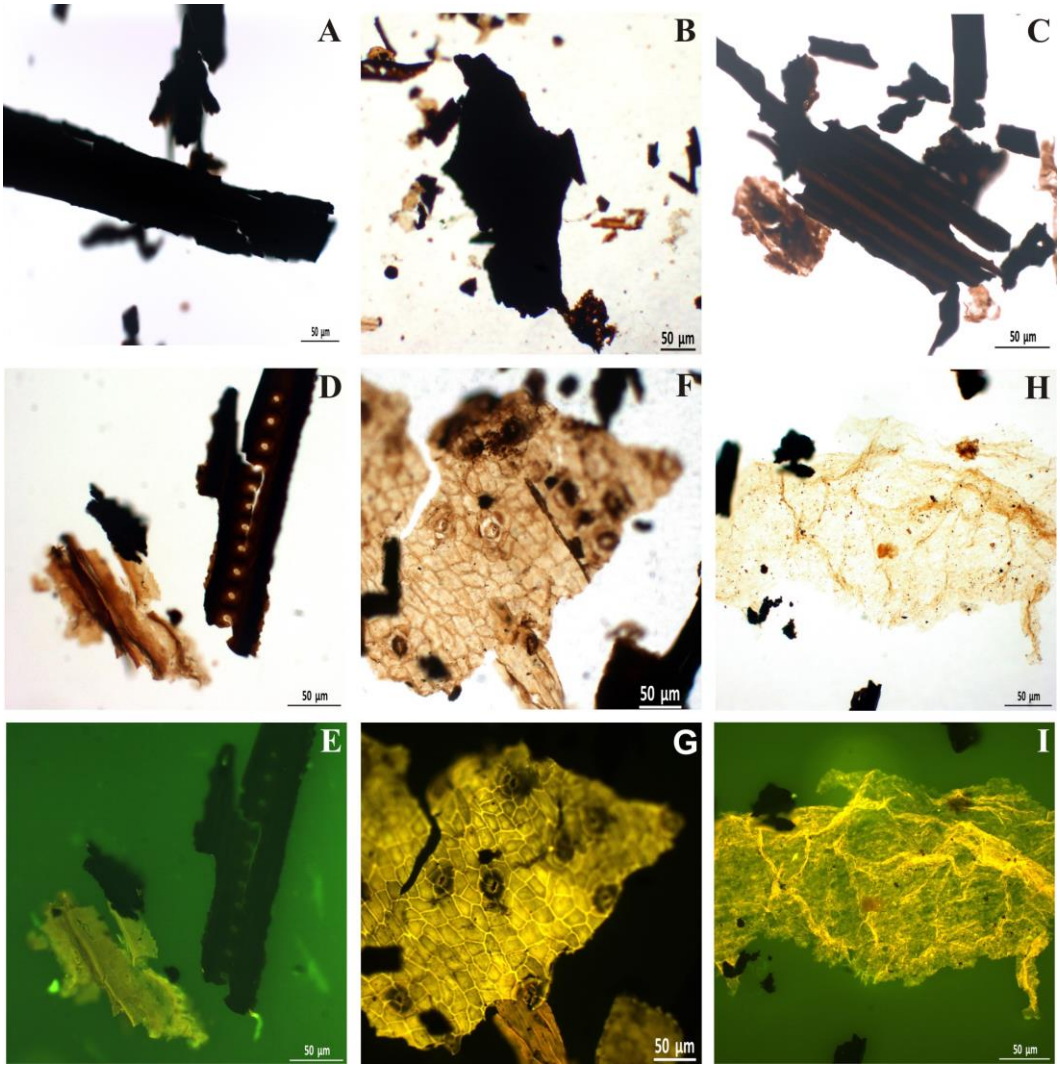

Figure 14. Photomicrographs of Phytoclast group taken under transmitted white light (TL) and fluorescence mode (FM). A (Am.6): opaque phytoclast; B (Am.21): non-opaque non-biostructured phytoclast; C (Am.15): striped phytoclast; D-E (Am.4): striate and pitted phytoclast; F-G (Am.5): cuticle; H-I (Am.20): membrane. TL: A, B, C, D, F, H; FM: E, G, I.

The opaque phytoclasts (Fig. 14A) were also present in all samples, and the Brenha Formation exhibited the highest values. The opaque phytoclasts were black, had no internal structure and had clear to diffuse outlines for the lath and corroded phytoclasts, respectively. The equidimensional opaque phytoclast was rare, most likely due to the transport. In general, the opaque phytoclast was related to more distal environments than its non-opaque (Tyson, 1995). The cuticles (Fig. 14F - G), some of which had visible stomas, exhibited orange to brown color in white transmitted light and relatively high fluorescence with intense yellow to orange colors. In some cases, the cuticles appeared degraded, whereas in others, they preserved the innermost part of the epidermis. In the Abadia Formation, the cuticle content reached 15% of the total organic matter analyzed in the sample (Am.8). The high percentages of cuticles could be related to fluvio-deltaic environments (Batten, 1973; Tyson,

1995). Membranes (Fig. 14H - I), derived primarily from leaves or branches of higher plants, were also present in most of the studied samples; they were very thin, pale yellow or even transparent with no visible cellular structures and revealing an intense yellow fluorescent color.

The AOM group (Fig. 15, Table 11) consists of all particulate organic components that appear structureless at the scale of light microscopy. These components include phytoplankton-derived amorphous organic matter (AOM), bacterially derived amorphous organic matter (AOM) and amorphous products of the diagenesis of macrophyte tissues (Mendonça Filho et al., 2010, 2011b, 2012; Tyson, 1995). The amorphous products of the diagenesis of macrophyte tissues (Fig. 15A-B) showed different amorphization stages ranging from subangular particles with neat boundaries to particles with diffuse limits or even completely unstructured. This type of AOM did not show inclusions of palynomorphs or pyrite and had a brown color under white transmitted light and, in most of the cases, fluorescence was absent.

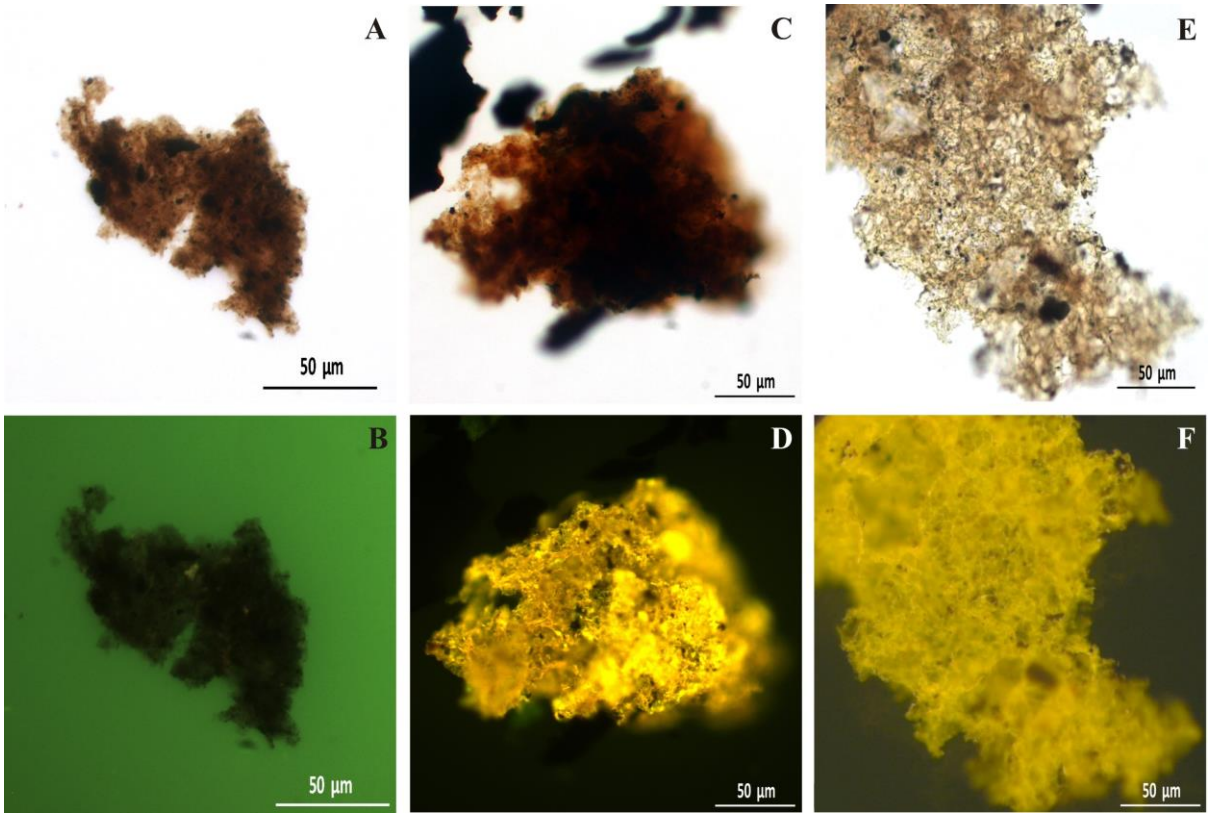

Figure 15. Photomicrographs of the Amorphous Organic Matter group taken under transmitted white light (TL) and fluorescence mode (FM). A-B (Am.18): AOM terrestrially derived; C-D (Am.19): AOM; E-F (Am.33): AOM bacterially derived. TL: A, C, E; FM: B, D, F.

The phytoplankton-derived AOM is structureless, homogeneous or heterogeneous particles, frequently with inclusions of palynomorphs, phytoclasts and pyrite (Fig. 15C - D). Under white transmitted light, these particles usually had an orange to brown color, and in incident blue light, they exhibited moderate to intense fluorescence (yellow to orange color). Some AOM showed a euhedral crater aspect (Fig. 15E - F) resulting from the dissolution of carbonate minerals by the HCl treatment. This type of AOM is considered bacterially derived amorphous organic matter and is generally related to lower TOC values (Mendonça Filho et al., 2010). It exhibited a pale yellow color in white transmitted light and intense yellow fluorescence color, under incident blue light. The Montejunto Formation revealed the highest contents of AOM (Table 11), reaching 30.55% (of the total organic matter) on the Am.18 sample.

The Palynomorph group (Fig. 16, Table 11) was the least abundant of the three main kerogen groups in the studied samples. The sporomorph subgroup had a relative abundance higher than the algae (see also Table 8). This abundance can indicate a proximal area, with lower salinity near the source area (Mendonça Filho et al., 2011b; Tyson, 1995). Spores (Fig. 16A to D) were the most common sporomorph in the organic matter assemblage. The spores displayed different sizes, shapes (from oval to triangular), and ornamentations, with some of them exhibiting the trilete or monolete mark on the surface. The color varied from pale yellow to black in white transmitted light and revealed fluorescence that varied from dark yellow to brown. According to Mendonça Filho et al. (2011b) and Tyson (1995), when spores are inefficiently transported (short distance), the relative percentage and variety indicate that the original flora was near the deposition location. Pollen grains (Fig. 16E - F) were also observed, and they exhibited various ornamentations, form, sizes and colors (pale yellow to black). The presence of bisaccate grain pollens was relatively minor. In a few samples, it was possible to observe the agglomerates (dyads, tetrads and polyads, Fig. 16G - H), which are indicative of the source area proximity (Mendonça Filho et al., 2011b). Some dyads and tetrads were from one type of extinct coniferous, genus *Classopollis* (bottom and top of Montejunto Formation) with important paleoenvironmental significance. These plants were adapted to hot and dry climates and to a wide range of salinity conditions (Mendonça Filho et al., 2011b; Tyson, 1995). The presence of *Classopollis* is, in general, associated with proximal environments with high sedimentation rate (Tyson, 1995).

In a few samples (Brenha and Montejunto Formations, Table 11; Fig. 21), it was possible to find freshwater algae from *Botryococcus* genus, which was brown in white transmitted light and intense yellow when observed in blue light. These algae can occur in lagoonal and lacustrine facies and have the ability to adapt to different salinity conditions, although they are limited to lakes (Mendonça Filho et al., 2011b; Tyson, 1995). The presence

of Azolla, a massula of microspore of an aquatic plant, was also confirmed in the samples from the Abadia Formation; additionally, Zygospore of *Zygnema*-type (spores from Zygnemataceae Family) was observed in the Montejunto and Brenha Formations.

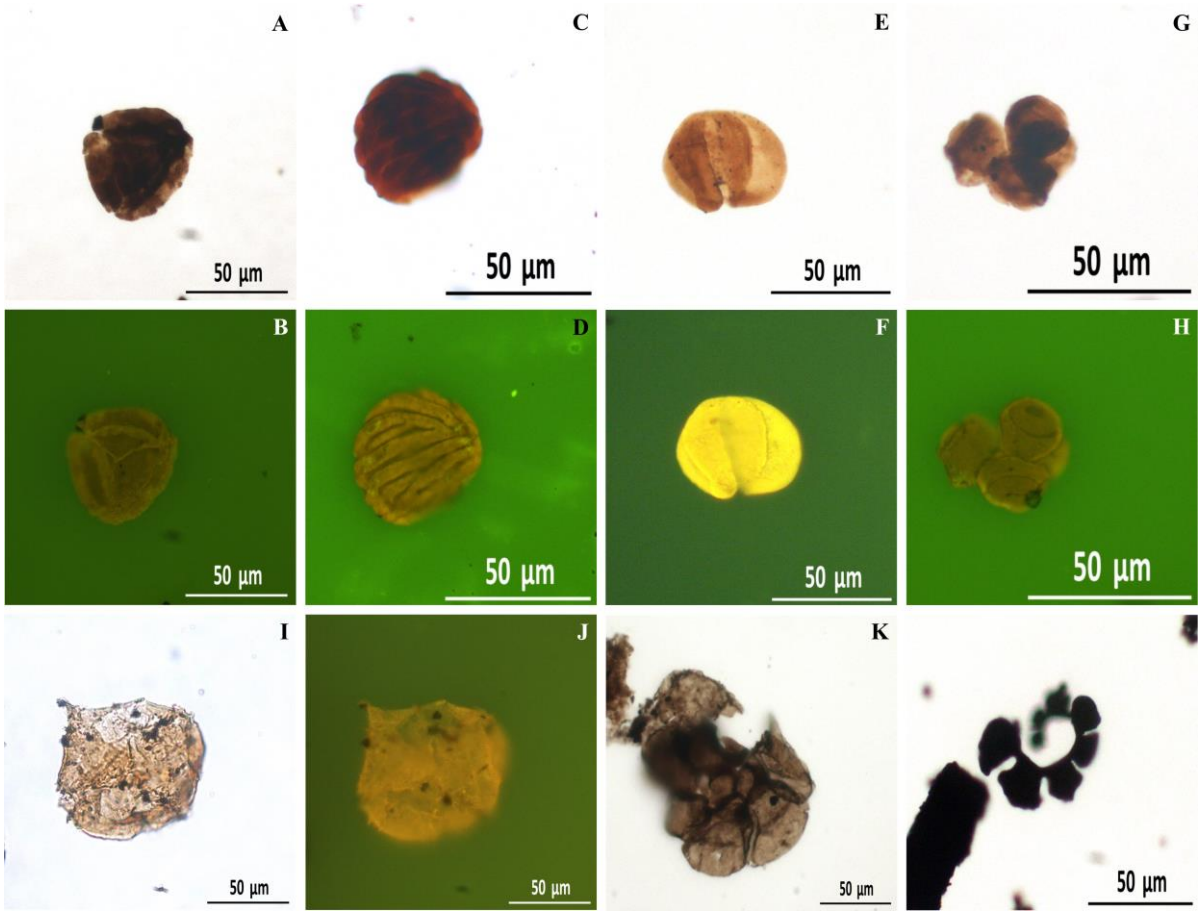

Figure 16. Photomicrographs of the Palynomorph group taken under transmitted white light (TL) and fluorescence mode (FM). A - D (A/B - Am.17; C/D - Am.25): spores; E - F (Am.4): pollen grains; G - H (Am.16): tetrad of sporomorph; I - K (Am.25): dinocysts; J - L (Am.28 and Am.33, respectively): foraminiferal test linings. TL: A, C, E, G, I, K, L; FM: B, D, F, H, J.

The occurrence of marine microplankton was identified in the Abadia, Montejunto and Brenha Formations (Table 11, Fig. 21), mainly as dinoflagellate cysts (Fig. 16I - J). According to Mendonça Filho et al. (2011b), the dinocysts are the predominant form of fossilized microplankton in marine sediments. In the studied samples, the dinocysts were, in some cases, degraded and exhibited a pale brown color in white transmitted light and yellow (sometimes intense) color when observed in blue light. Small acritarchs were also present but only in a restricted number of samples from the Brenha Formation. Some foraminiferal test linings were also identified (Fig. 16K - L) in the samples from the Montejunto and Brenha Formations. These foraminiferal linings showed different degrees of alteration (especially in Brenha Formation), varying in color from pale brown to black (non-fluorescing). According to

several authors (e.g., Tyson, 1995), foraminiferal linings are good indicators of normal marine conditions.

Solid bitumen was observed in some samples from the Montejunto and Brenha Formations and sometimes, as in the case of Brenha Formation, represented more than 50% of the organic matter present in the samples. This solid bitumen was dark in color in transmitted light. When observed in a whole rock sample and under reflected white light, this bitumen was found to infill the inter-mineral spaces.

1.1.4.4. Cluster analysis

Cluster analysis was employed, based on the composition (R-mode) and percentage (Q-mode) of the kerogen components, to establish groups and recognize the relationships between them. The results obtained using the R-mode (Table 12) allowed for the classification of the organic matter components into four groups (A to D) according to the degree of similarity regarding the origin criterion. Group A includes some of the fluvio-deltaic components (cuticles, membrane and non- opaque non-biostructured phytoclasts). Group B comprises the marine components (marine microplankton and foraminiferal test linings) and non-opaque biostructured phytoclasts. Group C contains only the amorphous organic matter (AOM). Group D includes the opaque phytoclasts and continental palynomorphs (spores, pollen grains and freshwater algae).

Q-mode cluster analysis of the Rm-1 borehole data subdivided the samples into six palynofacies associations (Table 11) according to the abundance of the different groups and subgroups of particulate organic matter. It is important to emphasize that all the defined associations are characterized by a high presence of phytoclasts (see also Table 11). The relative variations in the phytoclast subgroups, as well as the variation in the AOM and palynomorphs, were the main components allowing for the distinction of the associations established in this work.

Table 12. Description of R-mode cluster analysis.

Group	Description
A	Cuticles + membranes + non-opaque non-biostructured phytoclasts
B	Marine microplankton + foraminiferal test linings + non-opaque biostructured phytoclasts
C	AOM
D	Opaque phytoclasts + continental palynomorphs

The Palynofacies Association I corresponds to a predominance of the non-opaque non-biostructured phytoclast, which constitutes an average of 67.90% of the total organic matter. The AOM and palynomorph groups appeared in much lower percentages (2.37 and 1.43%, respectively). The presence of large amounts of non-opaque, non-biostructured phytoclast could be related to the proximity to the source area. Marine microplankton and foraminiferal test linings are absent in this association. In the Palynofacies Association II, the non-opaque phytoclast represents, in average, approximately 79.45% of the organic matter. In this association, the cuticles are present in a major percentage relative to the other associations, with one sample (Am.8) exhibited a relative percentage of 14.84%. Palynofacies Association III reveals a major contribution from the phytoclast group, mainly non-opaque phytoclasts (73.99% on average). The presence of marine microplankton, dinocysts, and foraminiferal test linings increases in this association (approximately 4% on average). This increase could be due to the water level variation related to the occasional input of salt water in the system. In the Palynofacies Association IV, the phytoclast group (approximately 79.80% on average) is predominant in the organic matter assemblage, with an increase of opaque phytoclast percentage (on average 16.43%). Moreover, in this association, the relative percentage of the AOM increases, reaching 14.45%. The Palynofacies Association V maintains the dominance of phytoclasts and exhibits an increase in the opaque phytoclasts (27.53% on average). The AOM content is lower than in the previous association. The continental palynomorphs, mainly spores, are higher than in other associations. Finally, the Palynofacies Association VI is characterized by non-opaque, non-biostructured phytoclasts and AOM with relative percentages of 39.87% and 28.94% (on average), respectively. In this association, marine microplankton and foraminiferal test linings are present in very small amounts (approximately 1% on average).

1.1.4.5. Molecular composition

Figure 17 shows the selected chromatograms of the studied samples. In the majority of the samples, the *n*-alkanes typically reach peak abundance in the *n*C15-*n*C23 range, extending for long-chain *n*-alkanes, and predominantly consist of algal and/or microorganism sources and some continental contribution (Tissot and Welte, 1984). Some samples of the Lourinhã Formation had a dominance of long-chain *n*-alkanes, reflecting a major continental contribution (Tissot and Welte, 1984).

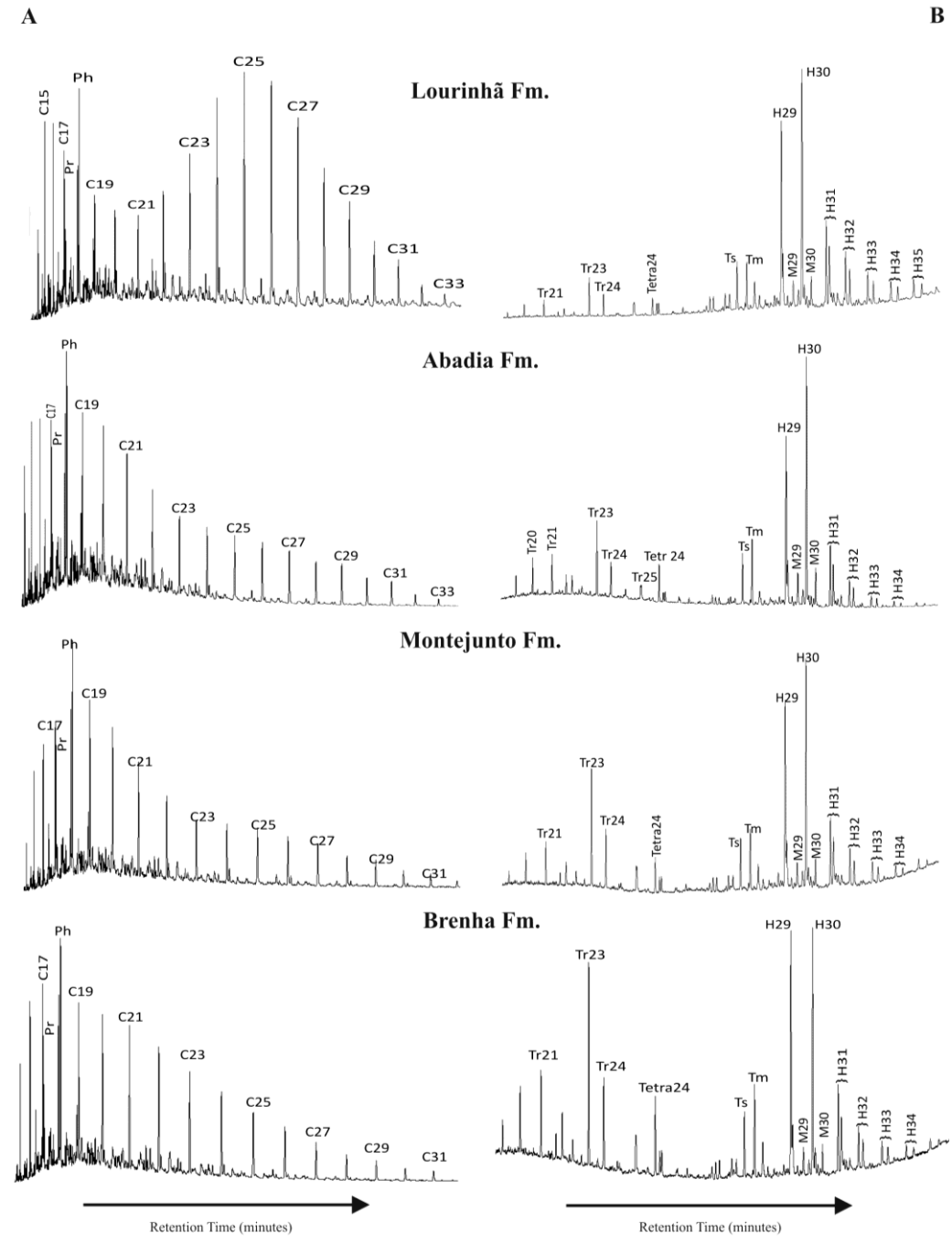

Figure 17. *n*-Alkanes (A, ion *m/z* 85) and terpanes (B, ion *m/z* 191) distributions in selected samples from the Ramalhal-1 borehole.

Phytane (Ph) is the predominant acyclic isoprenoid in the studied samples (Table 13). The pristane (Pr)/phytane (Ph) ratio (see also Table 13) is low and varies between 0.25 and 0.79,which seems to indicate a reduction in the depositional conditions, according to several authors (e.g., Brooks et al., 1969; Didyk et al., 1978; Peters et al., 2005). Peters et al. (2005) reported a Pr/Ph ratio less than 0.8, which is indicative of anoxic conditions in hypersaline or carbonate environments. However, these results must be interpreted carefully due to the

interference of other factors with regard to this ratio, such as the organic matter maturity (Peters et al., 2005; Waples and Machihara, 1991).

The relationship between the Pr/*n*-C17 and Ph/*n*-C18 ratios can be used to classify the extracts of rocks and oils (Hunt, 1979). In the present case, the Pr/*n*-C17 ratio (Table 13) has relatively low values and, in most cases, does not exceed one. In contrast, the Ph/*n*-C18 ratio (Table 13) has higher values that were generally higher than one. According to Palacas et al. (1984), a Ph/*n*-C18 ratio > 1 is typical of oils produced in carbonate source rocks.

The Carbon Preference Index (CPI) values from samples of the Ramalhal-1 borehole are listed in Table 13. The values of CPI are close to one (0.92 to 1.34, with a mean of 1.02), indicating a probable marine origin for the kerogen (except some samples of Lourinhã Formation) or the maturity of the organic matter (Hunt, 1979; Tissot and Welte, 1984).

Typical terpane distributions (Fig. 17) are characterized by a high content of pentacyclic terpanes compared to tricyclic and tetracyclic terpanes. The relation between some tricyclic and tetracyclic terpanes (Fig. 18) reveals a more continental origin for the organic matter present in the samples from Lourinhã and Abadia Formations. The content of C24 tetracyclic terpane exceeds that of the C26 tricyclic terpane.

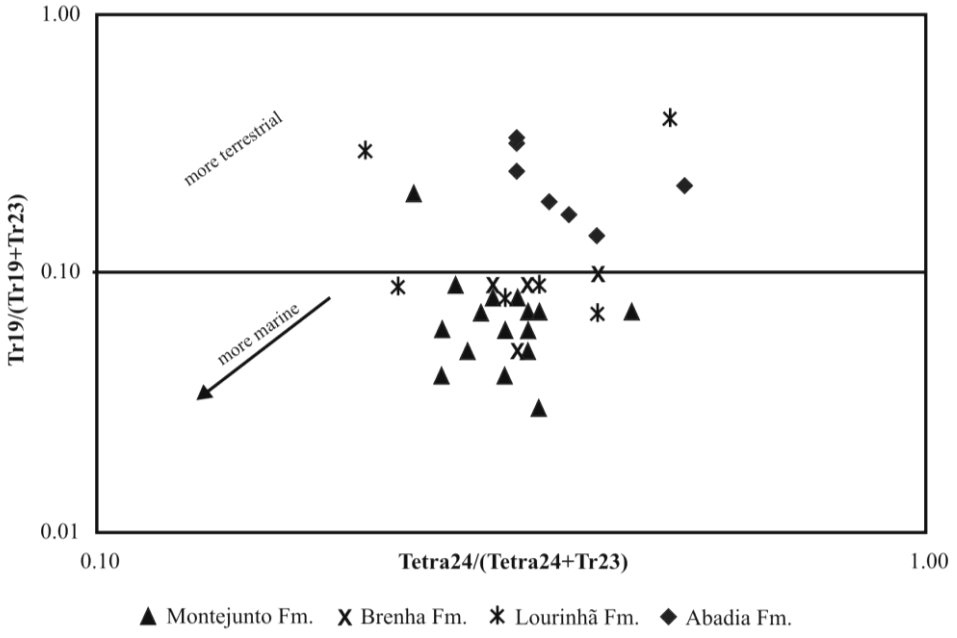

Figure 18. Relation between the C24 tetracyclic terpane/(C24 tetracyclic terpane + C23 tricyclic terpane) and C19 tricyclic terpane/(C19 tricyclic terpane + C23 tricyclic terpane) ratios (modified from George et al., 2007).

Table 13. Molecular parameters derived from biomarkers assemblage.

Formation	Sample	EOM	*n*-Alkanes				Terpanes					Steranes		
		(mg/g rock)	Pr/Ph	Pr/*n*-C17	Ph/*n*-C18	CPI	Ts/Tm	M30/H30	H32 S/(S+R)	H35/H34	Ster/17α-Hop	C27/C29 sterane	C29 S/(S + R)	C29 ββ/(αα+ββ)
Lourinhã	Am.1	0.09	0.44	0.86	2.05	1.06	1.03	0.12	0.61	1.04	0.38	1.06	0.49	0.52
	Am.2	0.12	0.45	0.99	1.91	1.01	0.84	0.14	0.56	0.50	0.16	0.68	0.36	0.52
	Am.3	0.12	0.47	2.42	7.21	1.02	1.17	0.11	0.59	0.81	0.33	1.47	0.46	0.54
	Am.4	0.23	0.49	0.51	1.06	0.99	1.05	0.13	0.52	0.82	1.59	0.58	0.18	0.47
	Am.5	0.19	0.39	0.64	1.71	0.96	0.95	0.12	0.58	0.84	0.38	1.40	0.46	0.52
	Am.6	0.77	0.43	0.56	1.48	1.02	0.89	0.15	0.57	0.45	0.12	0.89	0.32	0.45
Abadia	Am.7	0.85	0.25	0.51	1.22	0.92	0.99	0.14	0.59	0.69	0.35	1.33	0.37	0.54
	Am.8	0.53	0.39	1.33	4.2	1.06	0.86	0.15	0.56	0.36	0.12	0.97	0.33	0.45
	Am.9	0.30	0.42	0.84	1.81	0.96	0.79	0.15	0.57	0.62	0.24	1.02	0.39	0.50
	Am.10	0.30	0.55	0.60	1.21	1.04	0.67	0.16	0.59	0.68	0.36	0.99	0.42	0.51
	Am.11	0.16	0.49	0.54	1.27	1.04	0.87	0.13	0.58	0.72	0.35	1.02	0.39	0.55
	Am.12	0.33	0.43	0.47	0.97	0.94	0.8	0.14	0.60	0.51	0.25	1.30	0.42	0.52
	Am.13	0.15	0.79	0.88	1.35	1.00	0.6	0.14	0.61	0.43	0.30	1.38	0.45	0.54
Montejunto	Am.14	0.45	0.40	0.59	1.35	0.99	0.86	0.13	0.59	0.58	0.23	1.21	0.39	0.50
	Am.15	0.11	0.37	0.78	1.76	0.98	0.82	0.11	0.59	0.79	0.45	1.31	0.44	0.52
	Am.16	0.19	0.37	0.99	2.66	0.96	0.84	0.12	0.59	0.68	0.56	1.23	0.46	0.53
	Am.17	0.28	0.42	1.10	2.95	1.01	0.88	0.12	0.57	0.73	0.35	1.25	0.43	0.53
	Am.18	0.24	0.43	0.98	2.95	1.02	0.94	0.11	0.59	0.74	0.56	1.27	0.42	0.54
	Am.19	0.12	0.47	0.81	1.66	1.00	0.87	0.12	0.58	0.80	0.51	1.09	0.48	0.50
	Am.20	0.11	0.41	0.94	1.85	1.00	0.86	0.11	0.57	0.91	0.39	1.11	0.40	0.56
	Am.21	0.76	0.41	0.38	0.82	1.02	0.56	0.10	0.57	0.70	0.57	1.46	0.46	0.58
	Am.22	0.46	0.34	0.57	1.80	1.34	0.63	0.12	0.59	0.63	0.46	1.52	0.41	0.62
	Am.23	0.41	0.39	0.51	1.16	1.32	0.61	0.11	0.59	0.67	0.47	1.15	0.45	0.59
	Am.24	0.19	0.38	0.42	1.05	1.00	0.61	0.1	0.57	0.82	1.26	0.83	0.33	0.42

(Continue on next page)

Table 13. (cont.) - Molecular parameters derived from biomarkers assemblage.

Formation	Sample	EOM	*n*-Alkanes				Terpanes					Steranes		
		(mg/g rock)	Pr/Ph	Pr/*n*-C17	Ph/*n*-C18	CPI	Ts/Tm	M30/H30	H32 S/(S+R)	H35/H34	Ster/17α-Hop	C27/C29 sterane	C29 S/(S + R)	C29 ββ/(αα+ββ)
Montejunto	Am.25	0.16	0.40	0.65	1.67	0.97	0.69	0.12	0.58	0.73	0.42	1.31	0.44	0.57
	Am.26	0.18	0.40	0.43	0.96	0.95	0.61	0.1	0.59	0.74	0.49	1.29	0.45	0.57
	Am.27	0.19	0.31	0.21	0.70	0.96	0.61	0.1	0.58	0.64	0.52	1.44	0.43	0.60
	Am.28	0.11	0.42	0.42	0.96	0.97	0.73	0.1	0.58	0.83	0.46	1.28	0.43	0.56
	Am.29	0.12	0.41	0.91	2.93	0.99	0.78	0.12	0.58	0.74	0.46	1.32	0.43	0.54
Brenha	Am.30	0.14	0.39	0.73	2.18	1.25	0.79	0.12	0.58	0.73	0.40	1.29	0.40	0.56
	Am.31	0.34	0.41	0.78	1.73	0.98	0.71	0.11	0.56	0.83	0.52	1.25	0.43	0.58
	Am.32	0.28	0.29	0.58	1.89	0.98	0.56	0.09	0.58	0.84	0.55	1.46	0.44	0.60
	Am.33	0.18	0.25	0.33	1.30	0.97	0.66	0.10	0.59	0.96	0.62	1.47	0.44	0.59

EOM: extractable organic matter; Pr: Pristane; Ph: Phytane; CPI: Carbon Preference Index [2*(C23+C25+C27+C29)/C22+2*(C24+C26+C28)+C30]; Ts: 22,29,30-Trisnorneohopane; Tm: 22,29,30-Trisnorhopane; M30: 17β,21α(H)-Hopane (Moretane); H30: 17α,21β(H)-Hopane; H32: 17α, 21β(H)-bishomohopane; (Ster/17α-hop): regular steranes consist of the C27, C28, C29 ααα(20S + 20R) and αββ(20S + 20R) / 17α-hopanes consist of the C29 to C33 pseudo-homologue (including 22S and 22R epimers); H34: 17α,21β(H)-tetrakishomohopane (22S-22R); H35: 17α, 21β(H)-pentakishomohopane (22S-22R); C27/C29 sterane: C27ααα 20R/C29ααα 20R; C29 (%): content of C29 ααα (20S +20R).

Regarding the pentacyclic terpanes, the C29 and C30 hopanes are the most abundant in the samples, with a preference for C30 hopane (except sample Am.1). Extended hopanes C31 to C35 are present in all samples (Fig. 17) and occur as doublets; this stereoisomeric pair decreases in abundance with an increasing molecular weight.

The 22, 29, 30-Trisnorneohopane (Ts) is more resistant to thermal degradation than the 22, 29, 30-Trisnorhopane (Tm), thus, the Ts/Tm ratio increases with increasing thermal evolution (Seifert and Moldowan, 1978). However, this ratio also depends on the source of the organic matter. In the studied samples, the Tm content was higher than the Ts content, except in some samples from Lourinhã Formation, for which the Ts/Tm ratio (Table 13) was approximately 1. It was also ob served that the Ts/Tm ratio decreases with depth probably influenced by the source lithology.

The regular steranes/17α-hopanes (Est/Hop; Table 13) ratio is used as an indicator of organic matter input to the source rock, assuming that the steranes originated from algae and higher plants, whereas the hopanes originated mainly from bacteria. The results showed that the steranes/17α-hopanes ratios were lower, which is indicative of terrigenous and/or microbial reworked organic matter (Fig. 19).

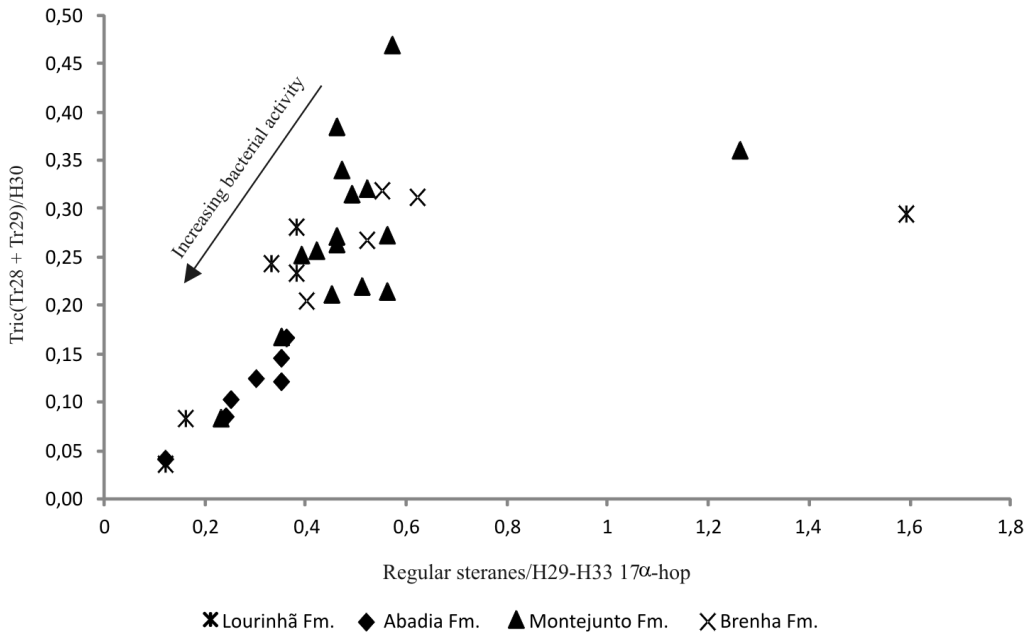

Figure 19. Relation between regular steranes/C29-C33 17α(H)-hopanes vs. C28-C29 (22R and 22S)tricyclic terpanes/C30-hopane (regular steranes:C27, C28, C29 ααα(20S + 20R) and αββ(20S + 20R); C29-C33 17a(H)-hopanes: C29 to C33 pseudo-homologues, including 22S and 22R epimers). (Modified from Marynowski et al., 2000)

In this study, the C29 20S/(20S + 20R) sterane, C29ββ/(αα + ββ) sterane, H32 22S/(22S + 22R) and the M30/H30 hopane (Table 13) were used as indicators of the source rock's maturity. The 20S/(20S + 20R) and ββ/(αα + ββ) isomerization ratios in C29 sterane, calculated for the studied samples, had ranges of 0.18 to 0.49 and 0.42 to 0.62, respectively, which are below the proposed equilibrium values. The values of the ratio 22S/(22S + 22R) epimer of C32 homohopanes revealed that the majority of the samples had reached equilibrium values (0.57 to 0.62, Seifert and Moldowan, 1980). The M30/H30 ratio generally decreases with increasing thermal maturity because moretane is less stable than hopane (Waples and Machihara, 1991). The values of this ratio are approximately 0.80 for immature stages and less than 0.15 for mature stages (Peters and Moldowan, 1993). For the Ramalhal-1 samples, the ratio M30/H30 (Table 13) varied between 0.09 and 0.16, corresponding to an early mature stage.

C27 sterane was more abundant than the C28 and C29 steranes, especially in the Montejunto and Brenha Formations. However, C29 sterane was dominant in some samples (Table 13) from the Lourinhã and Abadia Formations and in Am.24 sample (Montejunto Formation). The predominance of C27 sterane is indicative of a high contribution of planktonic organic matter, and C29 sterane is associated with a strong continental contribution (Huang and Meinschein, 1979). Thus, the studied samples have a combination of continental and marine organic matter preserved in an open marine environment, as illustrated in Fig. 20.

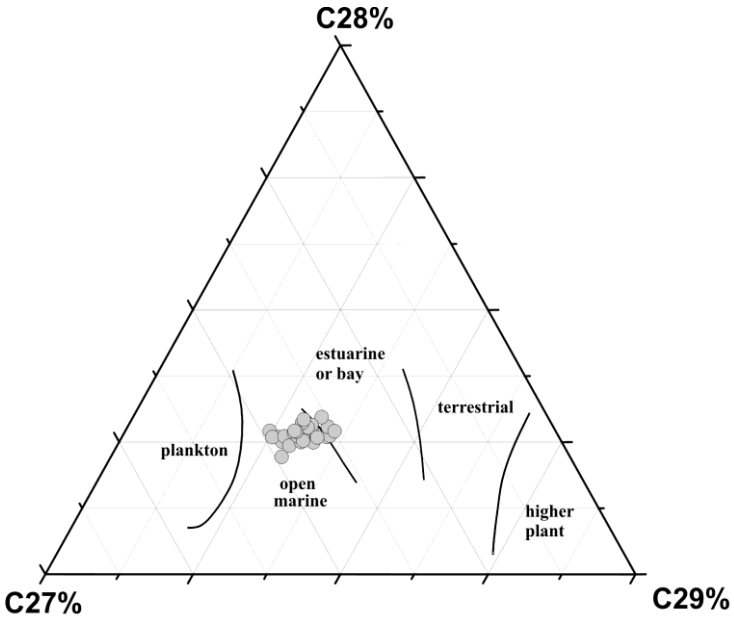

Figure 20. Ternary diagram showing the relative abundance of C27, C28 and C29 regular steranes [C27, C28, C29 ααα(20S + 20R) and αββ(20S + 20R)].

1.1.5. Paleoenvironmental interpretation

Seven intervals were defined based on the Palynofacies Associations established for the sedimentary sequence of the Ramalhal-1 borehole (Table 11, Fig. 21). The variation in the organic matter groups and subgroups, from the bottom to the top of the sequence, was the main parameter considered in defining the intervals, whose paleoenvironmental characteristics are very similar and are directly related to the input of phytoclasts in the system.

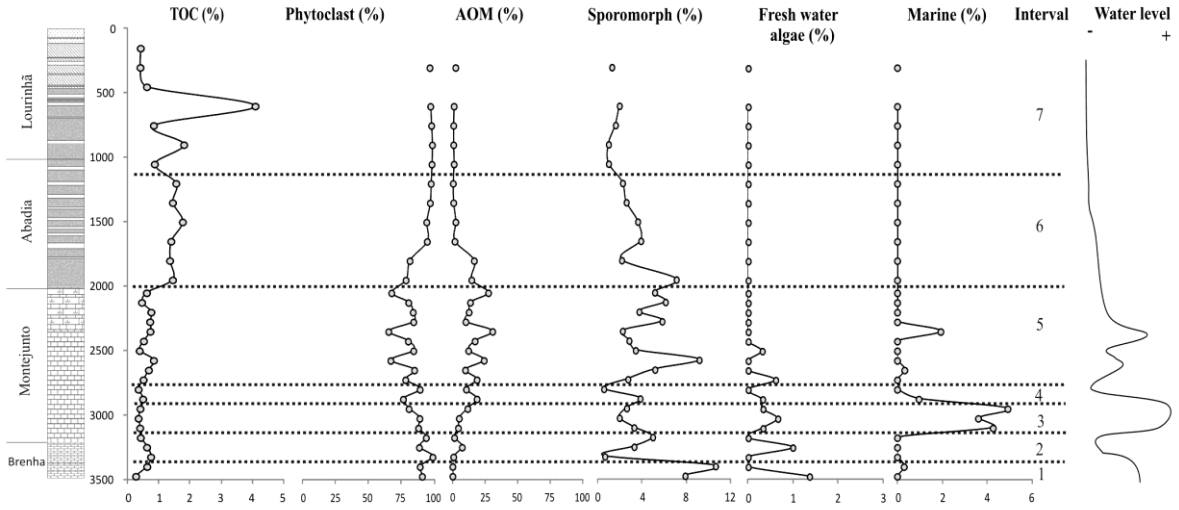

Figure 21. Palynofacies and TOC parameters variation showing the water level oscillations

Interval 1 (3475 to 3400 m) corresponds to Palynofacies Association V (see Fig. 21 and Table 11), which includes samples from the Brenha Formation. The absence of AOM associated with the abundance of opaque phytoclasts (29%) and the highest percentage of spores (8.8%) in the whole sequence seems to be related to an oxidizing environment, in which the AOM and the less refractory particles were rapidly degraded. A small quantity of marine palynomorphs is present, especially degraded foraminiferal linings. This characteristic is usually related to a more distal environment.

Interval 2 (3325 to 3175 m) overlaps the Palynofacies Associations II (see Fig. 21 and Table 11) and includes samples from the Brenha and Montejunto Formations. In relation to the previous interval, this interval contains a slight increase in the AOM and a decrease in the opaque phytoclasts. Marine palynomorphs are absent. According to Azerêdo et al. (2002), the hiatus (latest Callovian and the end of the early Oxfordian) observed in the LB was preceded by a complex regression that led to several variations in the carbonate ramp

environments. Therefore, the presence of *Botryococcus* (in Brenha Formation samples) and the increase in the AOM are most likely associated with a decrease in the water level and, consequently, an increase in the luminosity and salinity.

Intervals 3, 4 and 5 are related to the Montejunto Formation (see Fig. 21 and Table 11), and correspond to a period of reestablishment of a carbonate ramp condition. Interval 3 (3100 to 2950 m) is associated with Palynofacies Association III. Additionally, the opaque phytoclast and the AOM are increased. This interval exhibits the greatest amount of marine palynomorphs (4%). The increase in dinocysts associated with the decrease in sporomorphs suggests the entrance of seawater into the system, which induced the rise in the water level and the reestablishment of saline conditions.

Interval 4 (2875 to 2800 m) includes Palynofacies Associations I and II and reveals high percentages of phytoclasts, especially the non-biostructured non-opaque phytoclasts characteristic of proximal environments. A slight increase in the AOM was observed in relation to the previous interval. This AOM is derived from macrophyte tissues (terrestrially derived AOM).

Interval 5 (2725 to 1950 m) comprises Palynofacies Associations IV, V and VI (see Fig. 21 and Table 11) and represents a period of water level oscillation. The C/S ratios (Table 10) showed a wide interval (between 2.97 and 35.44) corresponding to more or less oxic environments, probably, related with the water level oscillation during this period. The terrestrially derived AOM is still present in moderate percentages. The increase in the opaque phytoclast content in the first half of the interval could be related to an increase in the distance from the terrestrial source area. In this period, there was a fluctuation of the relative abundance of dinocysts that should be related to the oscillation of the water level and the establishment of a more distal environment in the middle of this interval. From the middle to the top of this interval, the increase in the non-opaque phytoclasts and sporomorphs is indicative of reduction in the water level, and consequentially a progressive more proximal environment.

Interval 6 (1800 to 1200 m) is associated with the Palynofacies Associations I, II and VI (see Fig. 21 and Table 11) and is linked to the Abadia Formation. The high percentages of phytoclasts associated with an increase in non-opaque phytoclasts and a decrease in AOM are indicators of a more proximal environment. The presence of cuticles, some with stomata and others with a preserved inner part of the epidermis, confirms the proximity to the terrestrial source area, as well as a humid climate. The presence of Azolla and spores also suggests a humid climate In this case, the TOC values (1.51 wt.% on average) found in the samples of this interval were most likely controlled by the high phytoclast content that

resulted from high discharges in submarine fans and prograding slope environments. The relation between some tricyclic and tetracyclic terpanes also confirmed the proximity to the source area.

Lastly, interval 7 (900 to 150 m) is related to the Palynofacies Association I (see Fig. 21 and Table 11) and corresponds to the Lourinhã Formation. The biomarker data for this interval revealed the major continental contribution of all sequence, with a predominance of the long-chain *n*-alkanes. In fact, interval 7 is dominated by non-opaque non-biostructured phytoclasts and rare AOM, indicating extreme proximity to the source area and a high input of continental organic matter, characteristic of a fluvio-deltaic environment.

1.1.6. Conclusions

A combination of palynofacies and organic geochemistry techniques was used to characterize the organic matter content, assess the potential source rocks and establish the depositional paleoenvironment of the sedimentary sequence intercepted by the Rm-1 borehole. The following conclusions were drawn:

1) Rock-Eval pyrolysis and palynofacies data reveal a terrestrial origin for the organic matter (type III kerogen). In general, all formations contain lower values of TOC, S2 and HI, indicating that they are not potential source rocks for oil. Combining the data from palynofacies and pyrolysis demonstrated that the anomalous TOC value of sample Am.4 was influenced by the presence of perhydrous coal in the sample.

2) The phytoclast dominance, principally the non-opaque non-biostructured phytoclasts, in the kerogen assemblage suggests a higher terrigenous input due to the greater proximity to the continental source area. This proximity is more marked in the Lourinhã and Abadia Formations. This observation is also corroborated by the significant predominance of sporomorphs (especially spores) regarding marine microplankton and zooplankton. Montejunto Formation revealed the major contributions of marine phytoplankton of all the sequence. Biomarker data also suggest a major continental contribution for Lourinhã Formation and a combination of continental and marine organic matter preserved in an open marine environment for the other formations.

3) The T_{max} data indicate that studied samples are immature-early mature. C29 20S/(20S + 20R) sterane, C29ββ/(αα + ββ) sterane, H32 22S/(22S + 22R) and other biomarker maturity data suggest an immature to early mature stage for the extracted bitumen.

4) The organic matter of the studied sequence was preserved in a proximal - distal environment and oxic conditions. These environment characteristics are directly related to the input of phytoclasts in the system. The presence of the sporomorphs subgroup is indicative of a humid climate and determines the proximal - distal relationship of the terrestrial continental source area. The increasing of marine palynomorphs in Montejunto Formation corresponds to a period of major input of salt water in the system and reflects a more distal environment.

References

Alves, T.M., Gawthorpe, R.L., Hunt, D.W., Monteiro, J.H., 2002. Jurassic tectono-sedimentary evolution of the Northern Lusitanian Basin (offshore Portugal). Marine and Petroleum Geology 19, 727 - 754.

Alves, T.M., Manuppella, G., Gawthorpe, R.L., Hunt, D.W., Monteiro, J.H., 2003. The depositional evolution of diapir- and fault - bounded rift basins: examples from the Lusitanian Basin of West Iberia. Sedimentary Geology 162, 273 - 303.

Azerêdo, A.C., Duarte, L.V., Henriques, M.H., Manuppella, G., 2003. Da dinâmica continental no Triásico aos mares do Jurássico Inferior e Médio. Cadernos de Geologia de Portugal. Instituto Geológico e Mineiro, Lisboa ISBN 972-98469-9-5.

Azerêdo, A.C., Wright, V.P., Ramalho, M.M., 2002. The Middle - Late Jurassic forced regression and disconformity in central Portugal: eustatic, tectonic and climatic effects on a carbonate ramp system. Sedimentology 49, 1339 - 1370.

Batten, D.J., 1973. Use of palynologic assemblage-types in Wealden correlation. Palaeontology 16, 1 - 40.

Behar, F., Beaumont, H.L., Penteado, H.L., 2001. Rock-Eval 6 technology: performance and developments. Oil & Gas Science and Technology - Rev. IFP 56, 111 - 134.

Berner, R.A., 1995. Sedimentary organic matter preservation: an assessment and speculative synthesis - a comment. Marine Chemistry 49, 1121 - 1122.

Borrego, J., Lopez, M., Pedon, J.G., Morales, J.A., 1998. C/S ratios in estuarine sediments of the Odiel River-mouth, S.W. Spain. Journal of Coastal Research 14, 1276 - 1286.

Bostick, N.H., 1971. Thermal alteration of clastic organic particles as an indicator of contact and burial metamorphism in sedimentary rocks. Geosciences and Man 3, 83 - 92.

Brooks, J.D., Gould, K., Smith, J.W., 1969. Isoprenoid hydrocarbons in coal and petroleum. Nature 222, 257 - 259.

Carvalho, J., Matias, H., Torres, L., Manupella, G., Pereira, R., Mendes-Victor, L., 2005. The structural and sedimentary evolution of the Arruda and Lower Tagus sub-basins, Portugal. Marine and Petroleum Geology 22, 427 - 453.

Costa, A., Flores, D., Suárez-Ruiz, I., Pevida, C., Rubiera, F., Iglesias, M.J., 2010. The importance of thermal behaviour and petrographic composition for understanding the characteristics of a Portuguese perhydrous Jurassic coal. International Journal of Coal Geology 84, 237 - 247.

Didyk, B.M., Simoneit, B.R.T., Brassell, S.C., Eglinton, G., 1978. Organic geochemical indicators of paleoenvironmental conditions of sedimentation. Nature 272, 216 - 222.

Duarte, L.V., Silva, R.L., Mendonça Filho, J.G., 2011. The Lower Jurassic of the west coast of Portugal: stratigraphy and organic matter in carbonate sedimentation in: Flores, D., Marques, M.M. (Eds.), 63rd ICCP Annual Meeting - Field Trip, Porto: Memória, nº 17 (ISSN 087.1607).

Duarte, L.V., Silva, R.L., Mendonça Filho, J.G., Poças Ribeiro, N., Chagas, R.B.A., 2012. High-resolution stratigraphy, palynofacies and source rock potential of the Água de Medeiros Formation (Lower Jurassic), Lusitanian Basin, Portugal. Journal of Petroleum Geology 35, 105 - 126.

Duarte, L.V., Silva, R.L., Oliveira, L.C.V., Comas-Rengifo, M.J., Silva, F., 2010. Organic-rich facies in the Sinemurian and Pliensbachian of the Lusitanian Basin, Portugal: total organic carbon distribution and relation to transgressive-regressive facies cycles. Geologica Acta 8, 325 - 340.

Duarte, L.V., Soares, A.F., 2002. Litoestratigrafia das séries margo-calcárias do Jurássico inferior da Bacia Lusitânica (Portugal). Comunicação do Instituto Geológico e Mineiro 89, 115 - 134.

Duarte, L.V., Wright, V.P., Fernández-López, S., Elmi, S., Krautter, M., Azerêdo, A., Henriques, M.H., Rodrigues, R., Perilli, N., 2004. Early Jurassic carbonate evolution in the Lusitanian Basin (Portugal): facies, sequence stratigraphy and cyclicity, in: Duarte, L.V., Henriques, M.H. (Eds.), Carboniferous and Jurassic Carbonate Platforms of Iberia: Field Trip Guide Book of the 23rd IAS Meeting of Sedimentology, 1, pp. 45 - 71.

Espitalié, J., Laporte, J.L., Madec, M., Marquis, F., Leplat, P., Paulet, J., Boutefeu, A., 1977. Méthode rapide de caractérisation des roches mètres, de leur potentiel pétrolier et de leur degré d'évolution. Revue de l'Institut Français du Pétrole 32, 23 - 42.

Flores, D., Esteves, P., 2008. Avaliação do Potencial Petrolífero de uma Sondagem da Bacia Lusitaniana: Uma Abordagem Petrográfica e Geoquímica. Livro de resumos VIII Congresso de Geoquímica dos PLP, Cabo Verde, 35.

George, S.C., Volk, H., Ahmed, M., Pickel, W., Allan, T., 2007. Biomarker evidence for two sources for solid bitumens in the Subu wells: Implications for the petroleum prospectivity of the East Papuan Basin. Organic Geochemistry 38, 609 - 642.

Huang, W.Y., Meinschein, W.G., 1979. Sterols as ecological indicators. Geochimica et Cosmochimica Acta 43, 739 - 745.

Hunt, J.M., 1995. Petroleum Geochemistry and Geology. Freeman, San Francisco.

Kullberg, J.C., Rocha, R.B., Soares, A.F., Rey, J., Terrinha, P., Callapez, P., Martins, L., 2006. A Bacia Lusitaniana: Estratigrafia, Paleogeografia e Tectónica, in: Dias, R., Araújo, A., Terrinha, P., Kullberg, J.C. (Eds.), Geologia de Portugal no contexto da Ibéria, Universidade de Évora. ISBN: 972-778-094-6, pp. 317 - 368.

Lafargue, E., Marquis, F., Pillot, D., 1998. Rock-Eval 6 applications in hydrocarbon exploration, production, and soil contamination studies. Revue de l'Institut Français du Pétrole 53, 421 - 437.

Leinfelder, M.R.R., Wilson, R.C.L., 1989. Seismic and sedimentologic features of Oxfordian-Kimmeridgian syn - rift sediments on the eastern margin of the Lusitanian Basin. Geologische Rundschau 79, 81 - 104.

Littke, R., Klussmann, U., Krooss, B., Leythaeuser, D., 1991. Quantification of loss of calcite, pyrite, and organic matter due to weathering of Toarcian black shales and effects on kerogen and bitumen characteristics. Geochimica et Cosmochimica Acta 55, 3369 - 3378.

Marynowski, L., Narkiewicz, M., Grelowski, C., 2000. Biomarkers as environmental indicators in a carbonate complex, example from the Middle to Upper Devonian, Holy Cross Mountains, Poland. Sedimentary Geology 137, 187 - 212.

Masson, D.G., Miles, P.R., 1986. Development and hydrocarbon potential of Mesozoic sedimentary basins around margins of North Atlantic. American Association of Petroleum Geologists Bulletin 70, 721 - 729.

Mendonça Filho, J.G., Chagas, R.B.A., Menezes, T.R., Mendonça, J.O., Silva, F.S., Sabadini-Santos, E., 2010. Organic facies of the Oligocene lacustrine system in the Cenozoic Taubaté Basin, Southern Brazil. International Journal of Coal Geology 84, 166 - 178.

Mendonça Filho, J.G., Menezes, T.R., Mendonça, J.O., 2011b. Organic composition (palynofacies analysis). Chapter 5 ICCP Training Course on Dispersed Organic Matter. ISBN: 978-9-89-826567-8, pp. 33 - 81.

Mendonça Filho, J.G., Menezes, T.R., Mendonça, J.O., Oliveira, A.D., Souza, J.T., Sant'Anna, A.J., 2011a. Kerogen: composition and classification. Chapter 3 ICCP Training Course on Dispersed Organic Matter, 2. ISBN: 978-9-89-826567-8, pp. 17 - 24.

Mendonça Filho, J.G., Menezes, T.R., Mendonça, J.O., Oliveira, A.D., Silva, T.F., Rondon, N.F., Silva, F.S., 2012. Organic Facies: Palynofacies and Organic Geochemistry Approaches, in: Panagiotaras, D. (Org.), Geochemistry Earth's system processes. InTech, Patras, ISBN 978-9-53-510586-2, vol. 1, pp. 211 - 245.

Montenat, C., Guery, F., Jamet, M., Berthou, P.Y., 1988. Mesozoic evolution of the Lusitanian basin: comparison with the adjacent margin, in: Boillot, G., Winterer, E.L. (Eds.), Proceedings of the Ocean Drilling Program: Scientific Results, 103, pp. 757 - 775.

Mouterde, R., Rocha, R.B., Ruget, C., Tintant, H., Mouterde, R., Rocha, R.B., Ruget, C., Tintant, H., 1979. Faciès, biostratigraphie et paléogéographie du Jurassique portugais. Ciências da Terra, Universidade Nova Lisboa 5, 29 - 52.

Oliveira, L.C.V., Rodrigues, R., Duarte, L.V., Lemos, V., 2006. Avaliação do potencial gerador de petróleo e interpretação paleoambiental com base em biomarcadores e isótopos estáveis do carbono da seção Pliensbaquiano - Toarciano inferior (Jurássico inferior) da região de Peniche (Bacia Lusitânica, Portugal). Boletim de Geociências da Petrobras 14, 207 - 234.

Palacas, J.G., Anders, D.E., King, J.D., 1984. South Florida Basin: a prime example of carbonate source rocks in petroleum, in: Palacas, J.C. (Ed.), Petroleum Geochemistry and Source Rock Potential of Carbonate Rocks: Studies in Geology, 18. American Association of Petroleum Geologists (AAPG), Tulsa, pp. 71 - 96.

Palain, C., 1976. Une série détritique terrigène. Les “Grés de Silves”: Trias et Lias inférieur du Portugal. Memórias dos Serviços Geológicos de Portugal, 25. Serviços Geológicos de Portugal, Lisboa.

Peters, K.E., Cassa, M.R., 1994. Applied source rock geochemistry, in: Magoon, L.B., Dow, W.G. (Eds.), The Petroleum System - From Source to Trap. APPG Memoir 60. American of Petroleum Geologists Memoir 60, Tulsa, pp. 93 - 120.

Peters, K.E., Moldowan, J.M., 1993. The Biomarker Guide: interpreting molecular fossils in petroleum and ancient sediments. Prentice - Hall Inc., New Jersey.

Peters, K.E., Walters, C.C., Moldowan, J.M., 2005. The Biomarker Guide, vol. 2, Biomarkers and Isotopes in Petroleum Exploration and Earth History. Second ed., Cambridge University Press, London.

Poças Ribeiro, N., Mendonça Filho, J.G., Duarte, L.V., Silva, R.L., Mendonça, J.O., Silva, T.F., 2013. Palynofacies and organic geochemistry of the Sinemurian carbonate deposits in the western Lusitanian Basin (Portugal): Coimbra and Água de Madeiros formations. International Journal of Coal Geology 111, 37 - 52.

Rasmussen, E.S., Lomholt, S., Andersen, C., Vejbæk, O.L., 1998. Aspects of the structural evolution of the Lusitanian Basin in Portugal and the shelf and slope area offshore Portugal. Tectonophysics 300, 199 - 225.

Rey, J., Dinis, J.L., Callapez, P., Cunha, P.P., 2006. Da rotura continental à margem passiva. Composição e evolução do Cretácico de Portugal. Cadernos de Geologia de Portugal. Instituto Geológico e Mineiro, Lisboa.

Seifert, W.K., Moldowan, J.M., 1978. Applications of steranes, terpanes and monoaromatics to the maturation, migration and source of crude oils. Geochimica et Cosmochimica Acta 42, 77 - 95.

Seifert, W.K., Moldowan, J.M., 1980. The effect of thermal stress on source-rock quality as measured by hopane stereochemistry. Physics and Chemistry of the Earth 12, 229-237.

Silva, R.L., Mendonça Filho, J.G., Azerêdo, A.C., Sila, T.F., Oliveira, A.D., Duarte, L.V., 2011. Palynofacies and organic geochemistry survey of the Middle - Upper Jurassic transition in the Central - Northern sectors of the Lusitanian Basin (Portugal), in: Flores, D., Marques, M.M. (Eds.), New Trends on Coal Science: 63rd ICCP Annual Meeting, Memória, nº 18, pp. 17-18 (ISSN 087.1607).

Silva, R.L., Mendonça Filho, J.G., Duarte, L.V., Comas-Rengifo, M.J., Azerêdo, A.C., Ferreira, R., 2010. Organic - rich facies of the top Ibex - Margaritatus zones (Pliensbachian) of the Lusitanian Basin (Portugal): TOC and biomarkers variation. Geochimica et Cosmochimica Acta 74, A962.

Tissot, B., Welte, D.H., 1984. Petroleum Formation and Occurrence, Second ed. Springer Verlag, Hidelberg.

Tyson, R.V., 1995. Sedimentary Organic Matter. Chap. & Hall, London.

Waples, D.W., Machihara, T., 1991. Biomarkers for geologists: a practical guide to the application of steranes and triterpanes in petroleum geology. American Association of Petroleum Geologists Methods in Exploration, Series 9.

Wilson, R.C.L., 1979. A Reconnaissance Study of Upper Jurassic Sediments of the Lusitanian Basin. Ciências da Terra, Universidade Nova de Lisboa 5, 53 - 84.

Wilson, R.C.L., 1988. Mesozoic development of the Lusitanian basin, Portugal. Revista de la Sociedad Geológica de España 1, 393 - 407.

Wilson, R.C.L., Hiscott, R.N., Willis, M.G., Gradstein, F.M., 1989. The Lusitanian basin of west-central Portugal: mesozoic and tertiary tectonic, stratigraphic and subsidence history. American Association of Petroleum Geologists Bulletin 46, 341 - 362.

2. Arruda sub-basin

2.1. Palynofacies and source rock potential of Jurassic sequences on the Arruda sub-basin (Lusitanian Basin, Portugal)

Adapted from Paula Alexandra Gonçalves, Taís Freitas da Silva, João Graciano Mendonça Filho, Deolinda Flores

Marine and Petroleum Geology

Submitted

Abstract

The study of the organic matter present in sedimentary rocks is fundamental for the characterization of the potential source rocks as well as to define the depositional paleoenvironments. Parameters of organic petrology and organic geochemistry, and their variations along sedimentary successions are essential tools to achieve these goals. Two borehole successions (Freixial-1 and Benfeito-1) from Arruda sub-basin (Lusitanian Basin), that comprise siliciclastic-carbonate deposits of Jurassic age, have been studied in order to characterize the organic matter and its vertical variability as well as its hydrocarbon potential. Palynofacies and geochemical data indicate both, marine (including zooclasts) and terrestrial organic matter where the phytoclasts predominated despite an important contribution of the amorphous organic matter (AOM). Different types of solid bitumen were observed. Most of the analyzed samples have total organic carbon content (TOC) lower than 1wt.% and Hydrogen Index (HI) values lower than 100mgHC/g TOC, revealing types III and IV kerogen. However, one set of samples exhibit TOC values higher than 1wt.% and higher HI values depicting a type II kerogen. The biomarker data showed a dominance of *n*-alkanes with 15 to 30 carbon atoms having a unimodal distribution. Pristane/Phytane ratio varies between 0.04 and 1.84 indicating an alternation of oxic-anoxic conditions along the sequences. Typical terpane distributions are characterized by the presence of tricyclic and tetracyclic terpanes as well as pentacyclic terpanes (rare in carbonated samples from Freixial-1 borehole). The amount of 17α (H),22,29,30-trisnorhopane (Tm) usually exceeds the amount of 18α (H),22,29,30-trinorneohopane (Ts). The values of the ratio 22S/(22S + 22R) epimers of C32 homohopanes revealed that most samples reached equilibrium values. The 20S/(20S +2 0R) and ββ/(αα + ββ) isomerization ratios in C29 sterane, calculated for the studied samples, range between 0.19 - 0.61 and 0.20 - 0.70, respectively, with several samples reaching the equilibrium values. The vitrinite reflectance values are higher than 0.5% indicating that the

organic matter reached the oil generation window. According to the data obtained in this study, the Abadia, Montejunto, Cabaços and Brenha Formations can be considered potential source rocks of hydrocarbons (gas and/or oil) in this section of the Lusitanian Basin.

2.1.1. Introduction

The Lusitanian Basin (Portugal) located on the western board of the Iberian Peninsula, filled with a maximum of 5km sedimentary thickness of sediments (e.g., Azerêdo et al., 2003; Wilson, 1988), presents evidence of a petroleum system. Even the stratigraphy and sedimentology of this Basin is well established (e.g., Azerêdo et al., 2003; Carvalho et al., 2005; Duarte et al., 2004; Kullberg et al., 2013; Leinfelder and Wilson, 1989; Rasmussen et al., 1998; Rey et al., 2006; Wilson et al., 1989; Wilson, 1979, 1988). However, its organic matter content is not well known and the petroleum generation potential has not yet been fully evaluated. In recent years, some studies have emerged aiming to characterize organic matter and provide clues regarding ancient depositional environments thus allowing to evaluate the potential as hydrocarbon source rocks (e.g., Duarte et al., 2010, 2011, 2012; Gonçalves et al., 2013, 2014; Oliveira et al., 2006; Poças Ribeiro et al., 2013; Silva et al., 2014). The integrated geochemical and petrographic data portrayed a wide range of terrestrial and marine organic matter preserved in a marine environment under variable redox conditions. Lower - Middle Jurassic and Oxfordian sequences show evidence of a potential source rocks although the organic matter is not yet in the generation window (e.g., Duarte et al., 2012; Gonçalves et al., 2013, 2014; Poças Ribeiro et al., 2013; Silva et al., 2014).

The purpose of this study is to characterize the organic matter (OM) present in two Jurassic sedimentary successions drilled in the Arruda sub-basin (Lusitanian Basin), in order to: i) determine the type of organic matter (OM); ii) assess the maturation of the potential source rocks and its hydrocarbon generation potential; and, iii) define the sedimentary depositional environment. Petrographic analysis and organic geochemical techniques (total organic carbon and total sulfur, Rock-Eval pyrolysis and biomarker analysis) were used for these purposes. Attending the objectives of this work, preference was given to the informal names of the formations because these names are well-known by the oil companies operating in Portugal.

2.1.2. Geological setting

The Lusitanian Basin is an Atlantic margin rift basin formed in the Mesozoic (Rasmussen et al., 1998) located on the occidental margin of the Iberian Massif. According

to several authors (e.g. Azerêdo et al., 2003; Rasmussen et al., 1998; Wilson et al., 1989) this basin is related to the opening of the North Atlantic Ocean and is filled with approximately, 5 km of sediments from the Upper Triassic to the Cretaceous covered with Cenozoic sediments (Fig. 22).

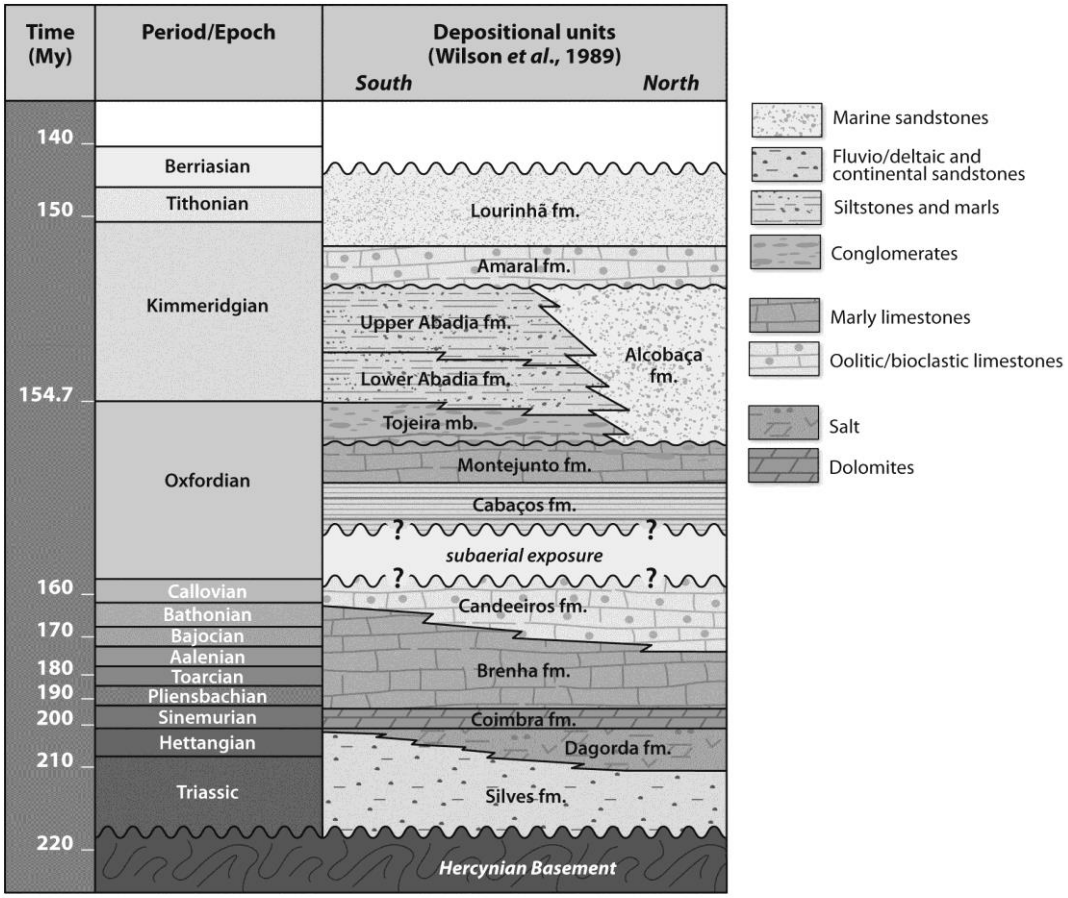

Figure 22. Simplified lithostratigraphy of the Central sector of the Lusitanian basin (modified from Alves et al., 2003).

The Arruda sub-basin (Fig. 23) corresponds to a half-graben developed during the Middle Oxfordian - Late Oxfordian as a consequence of transtensional rifting episodes that have affected the Estremadura Basin. This sub-basin represents an intra-continental pull-apart basin with a rhomb-like shape (Leinfelder and Wilson, 1989).

Please see section 6 on Part I for detailed description of geological setting.

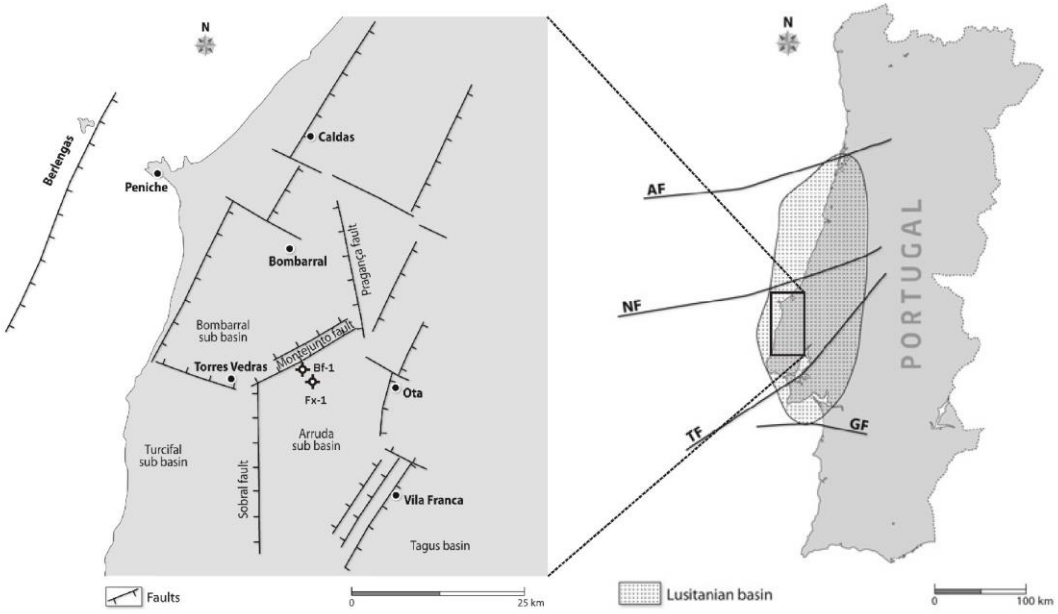

Figure 23. Geographic and tectonic settings of the Lusitanian basin (modified from Alves et al., 2002) and location of the Benfeito-1 and Freixial-1 boreholes. AF: Aveiro Fault; NF: Nazaré Fault; TF: Tagus Fault; GF: Grândola Fault; Bf-1: Benfeito-1 borehole; Fx-1: Freixial-1 borehole.

2.1.3. Samples and methods

One hundred and thirteen cutting samples were collected from two boreholes (Benfeito-1 and Freixial-1) drilled in the Arruda sub-basin (Fig. 23) providing two continuous Jurassic age sediment sections. Benfeito-1 (hereinafter called Bf-1; Fig. 24A) borehole crossed sediments since the Hettangian until the Tithonian, while the Freixial-1 (hereinafter called Fx-1; Fig. 24B) borehole sequence just began at the Bathonian and ends at the Tithonian. Both boreholes have cut siliciclastic and carbonate rocks. The cited unpublished reports and corresponding thin sections belong to the Direcção Geral de Energia e Geologia in Lisbon, where they can be studied. In order to achieve the proposed goals, the cutting samples were taken and submitted to petrographic and geochemical analyses.

Petrographic analyses

Please see section 1.1 on Part II for detailed description of the petrographic analyses.

Geochemical analyses

Please see section 1.2 on Part II for detailed description of the geochemical analyses.

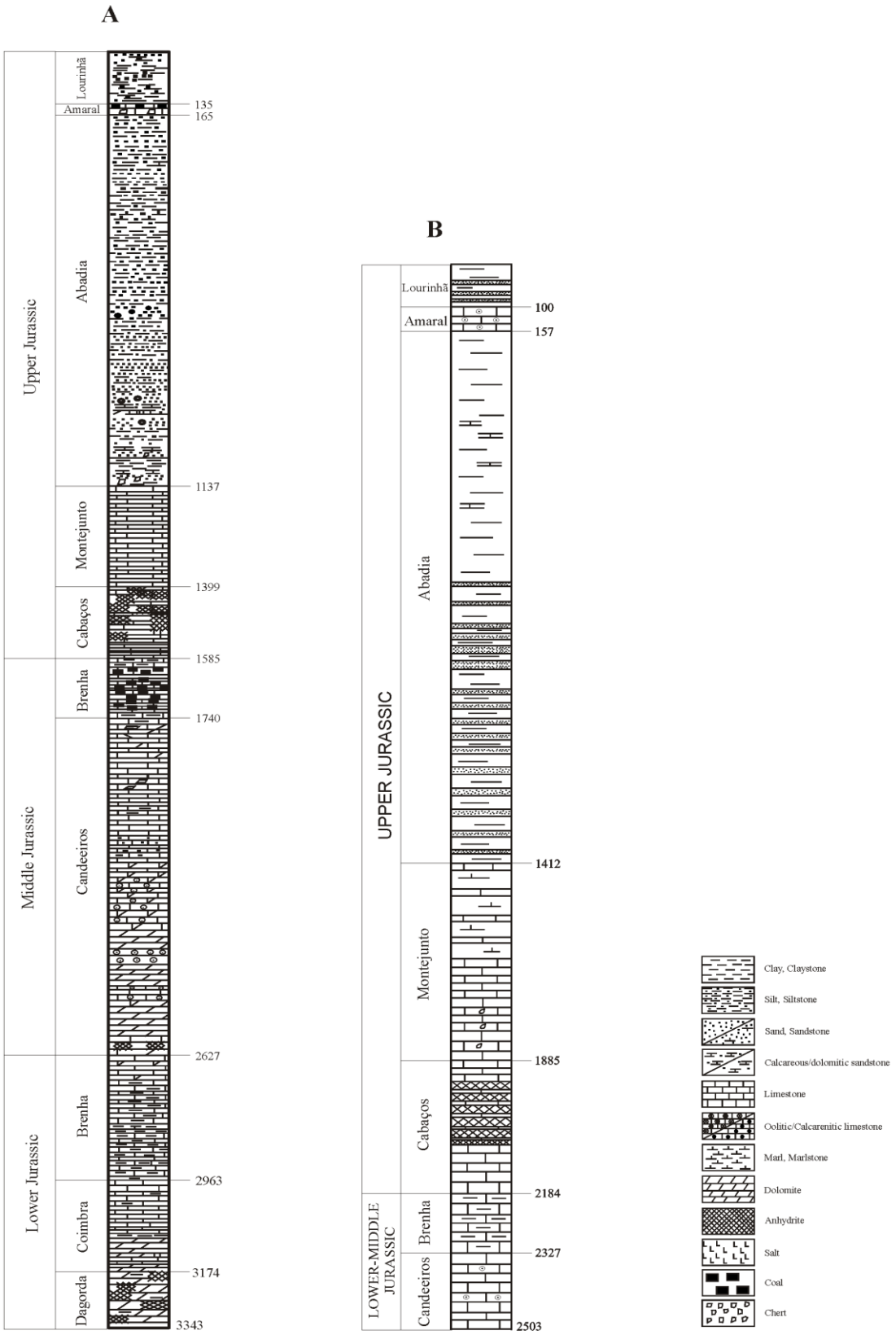

Figure 24. Simplified stratigraphic columns of the sedimentary sequences cut by A) Benfeito-1 and B) Freixial-1 boreholes (data from the geological report of Petrogal and EURAFREP, respectively).

2.1.4. Results

2.1.4.1. Organic petrographic characteristics

The palynological assemblages of two Jurassic successions (Benfeito-1 and Freixial-1 boreholes) drilled in the Arruda sub-basin were studied. The kerogen assemblages included the three main groups: Phytoclast, Amorphous and Palynomorph (Figs. 25 and 26). Phytoclast group (tissues derived from terrestrial higher plants; Bostick, 1971) is the predominant kerogen group (Tables 14 and 15; Figs. 25 and 26A to I), reaching 98.41% on sample Bf66. Some exceptions were observed in few samples from the Montejunto, Cabaços, Brenha (Callovian age), Candeeiros and Coimbra Formations (see Tables 14 and 15). The non-opaque phytoclast subgroup is generally the most representative, corresponding mainly to the non-opaque non-biostructured phytoclasts, often degraded. Their dominance suggests proximal environments and the dark color can be linked with sub-aerial oxidation due to water column fluctuation and transport (Ercegovac and Kostić, 2006; Mendonça Filho et al., 2011b, 2012; Tyson, 1995). Non-opaque biostructured phytoclasts were also observed, with predominance of banded phytoclast in both boreholes. Opaque phytoclast (Fig. 25A) subgroup is mainly represented by the corroded phytoclast and also includes charcoal particles especially in the Candeeiros Formation. Generally, opaque phytoclast is related to more distal environments than the non-opaque (Tyson, 1995), and charcoal is associated with the occurrence of natural fires that can be deposited in distal areas (Mendonça Filho et al., 2011b). Opaque phytoclasts occur in higher relative percentages in the Bf-1 borehole (Table 15) than in the Fx-1 borehole (Table 14). Cuticles, some of them with preserved stomata (Fig. 25B), occur in low percentages, except in Lourinhã and Abadia Formations, reaching up to 34% (sample Bf3; Table 15) of the total OM present in the samples. They constitute different degrees of degradation and some preserved the innermost part of the epidermis. The percentage of cuticles could be associated to the fluvio-deltaic environments (Batten, 1973; Tyson, 1995) where these sediments were deposited.

The Amorphous Group (Fig. 25C to F) represents 3.03 to 60.16% (Fx-1 borehole; Table 14) and 1.59 to 87.57% (Bf-1 borehole; Table 15) of the kerogen assemblage. This group includes phytoplankton-derived amorphous organic matter (AOM), bacterially derived amorphous organic matter (Bacterial AOM), amorphous products of the diagenesis of macrophyte tissues and resin (Mendonça Filho et al., 2010, 2011b, 2012; Tyson, 1995).

Table 14. Petrographic results from Fx-1 borehole samples.

		Palynofacies Analysis						Vitrinite reflectance	
Sample	Depth (m)	OP (%)	NOP (%)	AOM (%)	SPO (%)	FRESH (%)	MAR (%)	$\%R_r$	Stdev
Lourinhã Formation									
Fx1	50	4.32	84.72	9.97	1.00	0.00	0.00	-	-
Amaral Formation									
Fx2	100	11.11	81.70	5.23	1.31	0.65	0.00	-	-
Fx3	150	12.25	80.13	7.62	0.00	0.00	0.00	-	-
Abadia Formation									
Fx4	200	10.31	68.25	9.47	11.70	0.00	0.28	-	-
Fx5	350	10.30	71.76	14.95	2.99	0.00	0.00	-	-
Fx6	500	16.12	63.82	8.55	11.51	0.00	0.00	-	-
Fx7	650	10.42	61.41	16.06	12.11	0.00	0.00	-	-
Fx8	800	6.02	64.16	19.30	10.53	0.00	0.00	-	-
Fx9	950	3.31	65.36	18.67	12.35	0.30	0.00	-	-
Fx10	1100	2.98	63.58	26.49	6.62	0.33	0.00	-	-
Fx11	1250	5.19	61.67	29.11	4.03	0.00	0.00	-	-
Fx12	1300	5.11	56.16	32.43	6.31	0.00	0.00	-	-
Fx13	1350	6.54	62.31	26.48	4.67	0.00	0.00	-	-
Fx14	1400	4.35	69.57	19.25	5.90	0.00	0.93	-	-
Montejunto Formation									
Fx15	1450	4.58	54.90	22.55	14.05	1.96	1.96	-	-
Fx16	1500	2.17	50.77	24.46	8.05	8.98	5.57	-	-
Fx17	1550	4.67	55.00	16.33	8.33	7.67	8.00	-	-
Fx18	1600	6.48	53.40	23.77	8.02	1.54	6.79	-	-
Fx19	1650	5.06	55.95	16.96	4.17	9.23	8.63	-	-
Fx20	1700	3.62	67.76	6.25	7.24	8.55	6.58	-	-
Fx21	1750	3.26	58.63	16.61	2.93	7.82	10.75	-	-
Fx22	1800	2.93	55.70	36.81	2.93	0.00	1.63	-	-
Fx23	1850	18.97	50.29	30.75	0.00	0.00	0.00	-	-
Cabaços Formation									
Fx24	1900	11.65	48.22	38.83	1.29	0.00	0.00	1.13	0.11
Fx25	1950	2.99	72.46	20.06	4.19	0.00	0.30	1.37	0.10
Fx26	2000	1.33	72.76	22.59	2.99	0.00	0.33	1.48	0.10
Fx27	2050	7.64	34.55	57.14	0.33	0.00	0.33	1.20	0.11
Fx28	2100	9.80	48.41	41.50	0.29	0.00	0.00	1.11	0.05
Fx29	2140	5.79	71.32	18.95	2.89	0.26	0.79	1.47	0.08
Brenha Formation									
Fx30	2200	14.60	72.70	10.48	1.27	0.63	0.32	1.29	0.05
Fx31	2250	0.26	23.18	60.16	13.54	1.04	1.82	1.28	0.03
Fx32	2300	1.81	83.43	5.72	7.83	0.30	0.90	1.29	0.08
Candeeiros Formation									
Fx33	2350	11.36	31.82	13.07	0.85	0.00	42.90	-	-
Fx34	2400	22.42	61.82	3.03	1.21	0.00	11.52	-	-
Fx35	2450	19.87	43.71	15.56	0.66	0.00	20.20	-	-
Fx36	2500	11.81	33.25	4.58	1.69	0.00	48.67	-	-

OP: Opaque phytoclasts; NOP: Non-opaque phytoclasts; AOM: Amorphous organic matter; SPO: Sporomorphs; FRESH: Freshwater microplankton; MAR: Marine palynomorphs and zooclasts. $\%R_r$: vitrinite mean random reflectance (%): Stdev: standard deviation (%).

The phytoplankton - derived AOM (Fig. 25C, 25F) are structureless, with homogeneous or heterogeneous particles, frequently with inclusions of palynomorphs, phytoclasts and pyrite. Some AOM showed a euhedral crater aspect (Fig. 25D - E) resulting from the dissolution of carbonate minerals by the HCl treatment. This type of AOM is considered bacterially derived amorphous organic matter and is generally related to lower TOC values (Mendonça Filho et al., 2010).

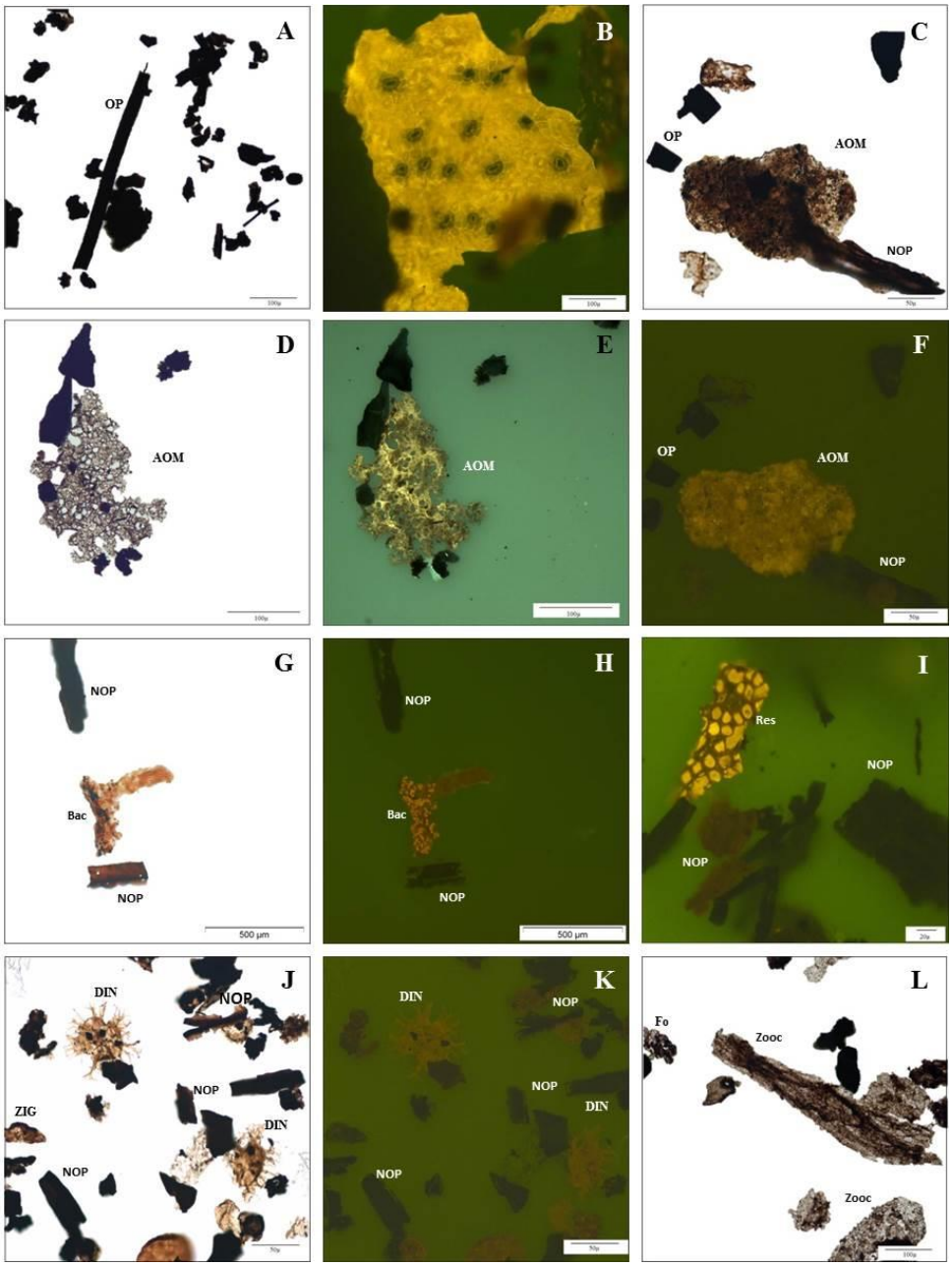

Figure 25. Photomicrographs of particulate organic matter taken under transmitted white light (TL) and fluorescence mode (FM). A (Fx23): opaque phytoclasts; B (Bf3): cuticle; C, F (Fx13) AOM; D, E (Bf41): bacterial AOM; G, H (Fx5): bacteria; I (Bf5): resin filling out structures; J, K (Fx21): general view; L (Fx33): zooclasts. Op: opaque phytoclasts; NOP: non-opaque phytoclasts; Bac: Bacteria; Res: Resin filling out structures of organic particles; DIN: dinoflagellate cysts; ZIG: zygospores; Fo: foraminiferal test linings; Zooc: zooclast. TL: A, C, D, G, J, L; FM: B, E, F, H, I, K.

Table 15. Petrographic results from Bf-1 borehole samples.

		Palynofacies analysis						Vitrinite reflectance	
Sample	Depth (m)	OP (%)	NOP (%)	AOM (%)	SPOR (%)	FRESH (%)	MAR (%)	%R_r	Stdev
Lourinhã Formation									
Bf1	20	n.r.	n.r.	n.r.	n.r.	n.r.	n.r.	-	-
Bf2	40	23.60	71.39	2.36	2.65	0.00	0.00	-	-
Bf3	60	13.44	73.75	10.94	1.88	0.00	0.00	-	-
Bf4	80	21.59	69.89	3.69	4.83	0.00	0.00	-	-
Bf5	100	26.73	59.74	10.56	2.97	0.00	0.00	-	-
Bf6	120	n.r.	n.r.	n.r.	n.r.	n.r.	n.r.	-	-
Amaral Formation									
Bf7	150	3.24	31.18	61.47	3.82	0.00	0.29	-	-
Abadia Formation									
Bf8	200	22.29	59.87	11.15	6.37	0.00	0.32	0.80	0.11
Bf9	250	17.09	68.59	5.03	9.05	0.00	0.25	0.81	0.11
Bf10	300	22.94	63.82	6.76	6.47	0.00	0.00	0.84	0.10
Bf11	350	17,.22	67.22	9.17	6.39	0.00	0.00	0.83	0.11
Bf12	400	16.34	71.19	2.22	10.25	0.00	0.00	0.81	0.11
Bf13	450	11.48	78.03	4.26	6.23	0.00	0.00	0.85	0.09
Bf14	500	15.51	68.09	7.42	8.09	0.22	0.67	0.83	0.10
Bf15	550	18.00	72.33	3.33	6.00	0.00	0.33	0.81	0.10
Bf16	600	17.32	75.82	3.92	2.94	0.00	0.00	0.80	0.11
Bf17	650	16.08	72.86	5.64	4.80	0.42	0.21	0.83	0.10
Bf18	700	11.28	76.52	8.84	3.35	0.00	0.00	0.81	0.10
Bf19	750	14.50	66.34	14.00	4.91	0.00	0.25	0.82	0.09
Bf20	800	15.27	73.03	9.16	2.54	0.00	0.00	0.81	0.11
Bf21	850	9.41	75.88	12.35	2.35	0.00	0.00	0.82	0.11
Bf22	900	10.97	72.10	11.29	5.64	0.00	0.00	0.83	0.10
Bf23	950	30.14	61.41	5.35	3.10	0.00	0.00	0.83	0.10
Bf24	1000	18.04	70.03	6.12	5.81	0.00	0.00	0.83	0.10
Bf25	1050	14.60	70.56	11.92	2.68	0.24	0.00	0.87	0.08
Bf26	1100	2.74	73.42	20.00	3.29	0.27	0.27	0.88	0.09
Montejunto Formation									
Bf27	1140	17.00	41.00	14.67	1.33	1.33	24.67	-	-
Bf28	1170	17.22	51.66	22.52	0.66	2.32	5.63	-	-
Bf29	1200	23.59	55.48	10.30	0.66	2.33	7.64	-	-
Bf30	1230	9.06	39.06	37.50	0.31	1.56	12.50	-	-
Bf31	1260	14.21	49.45	33.33	0.55	0.55	1.91	-	-
Bf32	1290	13.62	50.50	24.92	1.66	1.66	7.64	-	-
Bf33	1310	5.62	60.95	31.66	1.48	0.30	0.00	-	-
Bf34	1340	0.00	11.05	87.57	1.10	0.00	0.28	-	-
Bf35	1370	2.78	26.23	70.37	0.62	0.00	0.00	-	-
Cabaços Formation									
Bf36	1400	30.19	63.64	3.90	0.97	0.00	1.30	1.46	0.01
Bf37	1425	26.67	30.00	36.00	0.67	0.00	6.67	-	-
Bf38	1450	18.15	36.96	42.57	1.98	0.00	0.33	1.41	0.11
Bf39	1475	28.57	36.88	32.23	0.00	0.00	2.33	1.25	0.14
Bf40	1500	28.06	42.09	25.07	1.79	0.00	2.99	1.20	0.12
Bf41	1525	23.55	50.15	25.38	0.61	0.00	0.31	1.26	-
Bf42	1550	21.24	52.61	25.16	0.00	0.33	0.65	1.24	0.06
Bf43	1575	15.09	51.26	33.02	0.00	0.00	0.63	1.24	0.07

(Continue on next page)

Table 15 (cont.). Petrographic results from Bf-1 borehole samples.

		Palynofacies analysis						Vitrinite reflectance	
Sample	Depth (m)	OP (%)	NOP (%)	AOM (%)	SPO (%)	FRESH (%)	MAR (%)	$\%R_r$	Stdev
Brenha Formation									
Bf44	1600	9.47	20.33	67.69	0.00	0.00	2.51	-	-
Bf45	1650	28.02	43.95	23.33	1.77	0.00	2.95	-	-
Bf46	1700	23.92	42.19	29.90	0.33	0.00	3.65	-	-
Candeeiros Formation									
Bf47	1750	4.36	21.50	71.34	2.18	0.00	0.62	-	-
Bf48	1800	8.94	35.10	54.97	0.66	0.00	0.33	-	-
Bf49	1850	4.93	44.41	47.04	3.29	0.00	0.33	-	-
Bf50	1900	n.r.	n.r.	n.r.	n.r.	n.r.	n.r.	-	-
Bf51	1950	n.r.	n.r.	n.r.	n.r.	n.r.	n.r.	-	-
Bf52	2000	4.53	26.54	12.94	0.32	0.00	54.69	-	-
Bf53	2050	n.r.	n.r.	n.r.	n.r.	n.r.	n.r.	-	-
Bf54	2100	n.r.	n.r.	n.r.	n.r.	n.r.	n.r.	-	-
Bf55	2150	n.r.	n.r.	n.r.	n.r.	n.r.	n.r.	-	-
Bf56	2200	27.30	32.57	31.25	0.66	0.00	7.24	-	-
Bf57	2250	n.r.	n.r.	n.r.	n.r.	n.r.	n.r.	-	-
Bf58	2300	40.53	37.21	18.94	0.66	0.00	0.00	-	-
Bf59	2350	25.40	28.62	28.94	0.32	0.00	15.76	-	-
Bf60	2400	n.r.	n.r.	n.r.	n.r.	n.r.	n.r.	-	-
Bf61	2450	32.78	63.25	3.31	0.33	0.33	0.00	-	-
Bf62	2500	15.48	79.68	2.58	1.94	0.32	0.00	-	-
Bf63	2550	21.71	74.34	2.96	0.00	0.99	0.00	-	-
Bf64	2600	16.67	81.05	1.63	0.00	0.65	0.00	-	-
Brenha Formation									
Bf65	2650	15.68	78.70	4.14	0.59	0.89	0.00	-	-
Bf66	2700	9.52	88.89	1.59	0.00	0.00	0.00	-	-
Bf67	2750	54.05	36.04	9.61	0.00	0.30	0.00	-	-
Bf68	2800	13.65	79.79	4.99	0.52	0.00	0.79	-	-
Bf69	2850	15.58	76.32	7.79	0.00	0.00	0.31	-	-
Bf70	2900	16.81	79.83	3.08	0.00	0.28	0.00	-	-
Bf71	2950	20.00	73.43	5.97	0.60	0.00	0.00	-	-
Coimbra Formation									
Bf72	3000	14.19	70.00	15.16	0.00	0.32	0.32	-	-
Bf73	3050	n.r.	n.r.	n.r.	n.r.	n.r.	n.r.	-	-
Bf74	3100	18.11	45.13	36.49	0.28	0.00	0.00	-	-
Bf75	3150	8.92	27.38	63.38	0.00	0.00	0.00	-	-
Dagorda Formation									
Bf76	3200	n.r.	n.r.	n.r.	n.r.	n.r.	n.r.	-	-
Bf77	3300	47.33	32.33	20.00	0.33	0.00	0.00	-	-

OP: Opaque phytoclasts; NOP: Non-opaque phytoclasts; AOM: Amorphous organic matter; SPO: Sporomorphs; FRESH: Freshwater microplankton; MAR: Marine palynomorphs and zooclasts. n.r.: not recoverable. $\%R_r$: vitrinite mean random reflectance (%): Stdev: standard deviation (%).

The amorphous products of the diagenesis of macrophyte tissues showed different amorphization stages ranging from subangular particles with neat boundaries to particles with diffuse limits or even completely unstructured, usually without fluorescence. This type of AOM did not show inclusions of palynomorphs or pyrite. In most of the samples of

Abadia Formation is still possible to observe terrestrial material covered by bacteria (Fig.25G - H). Some samples from Candeeiros Formation presented a homogeneous AOM with weak fluorescence and remnants fragments of zooclasts and zoomorphs (Foraminiferal test linings). These features may be evidence of this AOM may have originated from these components. Resin (substance produced by terrestrial higher plants; Tyson, 1995) was observed in some samples of Lourinhã, Amaral, Abadia and Candeeiros Formations and sometimes it was found filling out structures in other organic particles (Fig. 25I), mainly phytoclasts.

The least abundant kerogen group was the palynomorphs (Fig. 25J to L and Fig. 26J to M) that includes continental (sporomorphs and freshwater algae) and marine (marine algae, zoomorph and zooclast) organic matter. The sporomorph subgroup had a relative abundance higher than the marine organic matter with some exceptions in Montejunto, Cabaços, Brenha (Callovian) and Candeeiros Formations (see Tables 14 and 15). The predominance of sporomorphs may indicate proximity to the terrestrial source area associated to oxygenated environments with lower energy. On the other hand, the prevalence of marine palynomorphs may refer to more distal environments (Mendonça Filho et al., 2011b; Tyson, 1995). Spores and pollen grains displayed different sizes, shapes (from oval to triangular) and ornamentations. In some samples (mostly in Abadia Formation) it was possible to observe agglomerates, dyads, and tetrads from the genus *Classopollis*. These plants were adapted to hot and dry climates and their presence is, generally, associated to proximal environments with high sedimentation conditions (Mendonça Filho et al., 2011b; Tyson, 1995). Freshwater microplankton was detected in both boreholes. Algae from *Botryococcus* genus and zygospores of *Zygnema*-type (spores from Zygnemataceae Family) were observed mostly in Montejunto Formation and appear degraded. Green algae from the Desmidiales Order were observed in Amaral Formation. The occurrence of freshwater algae in marine sediment may be referred to transport or redeposition (Mendonça Filho et al., 2010, 2012; Tyson, 1995). Marine microplankton were represented by dinoflagellate cysts and some Prasinophyte phycomata (including *Tasmanites* genus), mainly in the Montejunto Formation (reaches 24.67% on sample Bf27). In the studied samples, the dinocysts (Fig. 25J - K) exhibited a pale brown color in white transmitted light and yellow (sometimes intense) fluorescence color when observed in blue incident light. Zoomorph subgroup (animal-derived palynomorphs; e.g., Tyson, 1995), more accurately foraminiferal test linings, were present in a few samples of the Montejunto, Cabaços, Brenha (Callovian age) and Candeeiros Formations. They showed brown to black color and revealed different degrees of preservation. Some carbonate samples (Fx33 to Fx36, Bf52, Bf56, Bf58 and Bf59) of Candeeiros Formation presented great amounts of degraded animal-derived organic

particles that were classified as zooclasts (Tyson, 1995; Fig. 25L). Marine microplankton, foraminiferal test linings and zooclasts are reliable indicators of a normal marine condition (e.g., Ercegovac and Kostić, 2006; Tyson, 1995).

Solid bitumen was observed in some samples from Montejunto, Cabaços, Brenha (Callovian age), Candeeiros and Dagorda Formations and drops of hydrocarbons were identified in some samples from Candeeiros, Coimbra and Dagorda Formations (Benfeito-1 borehole).

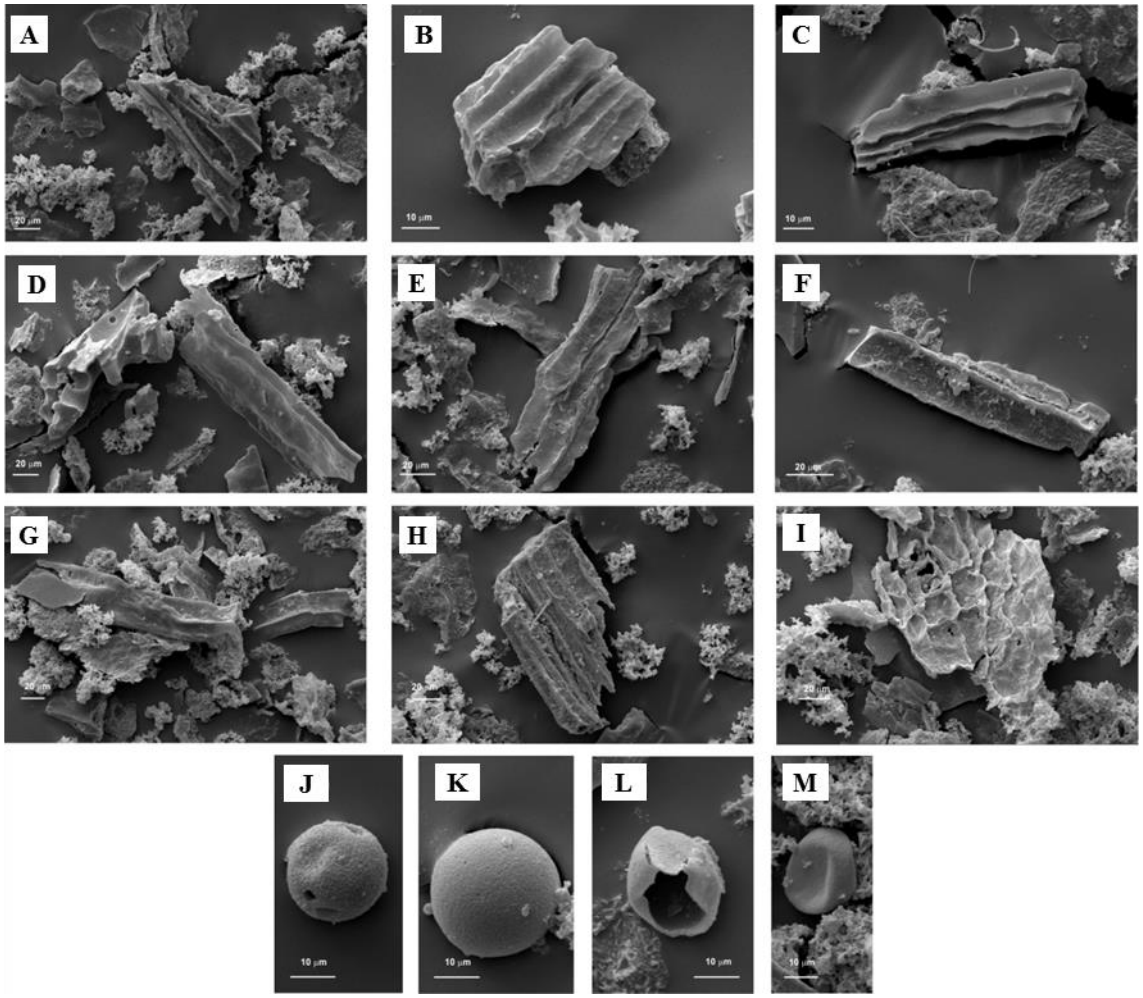

Figure 26. Photomicrographs of particulate organic matter (Fx25) taken by Scanning Electron Microscope (SEM). A-H: phytoclast; I: cuticle; J-M: palynomorphs.

Additionally, whole rock samples were prepared and vitrinite reflectance was measured (Tables 14 and 15). Samples have mean random vitrinite reflectance in a range of 0.80-1.47%R_r (Tables 14 and 15). The observation of the whole rock samples allowed to verify that the pyrite crystals appear unchanged and, in addition, the organic matter shows, in fluorescence, a high level of preservation. According to Littke et al. (1991), in sediments

affected by weathering, many pyrite crystals seem to be completely replaced by iron oxide or iron hydroxide as pyrite is very sensitive to the weathering.

2.1.4.2. Total Organic Carbon, Total Sulfur and Rock-Eval pyrolysis

TOC contents (Tables 16 and 17) varied between 0.06wt.% (Fx1) and 2.10wt.% (Fx4). Siliciclastic samples showed higher TOC contents than the limestone.

Table 16. Geochemical data of Fx-1 borehole samples.

Sample	TOC	TS	C/S	IR	S1	S2	S2/S3	HI	OI	T_{max}
Lourinhã Formation										
Fx1	0.06	0.20	0.31	64	-	-	-	-	-	-
Amaral Formation										
Fx2	0.53	0.37	1.45	33	-	-	-	-	-	-
Fx3	0.41	0.32	1.28	43	-	-	-	-	-	-
Abadia Formation										
Fx4	2.10	0.19	10.85	75	0.03	0.58	0.50	27.6	54.8	441
Fx5	1.00	0.13	7.48	63	0.02	0.21	0.21	20.9	99.7	442
Fx6	1.58	0.30	5.26	66	0.03	0.41	0.44	26.0	59.6	442
Fx7	1.20	0.25	4.81	68	0.04	0.41	0.59	34.1	58.2	440
Fx8	1.36	0.42	3.24	61	0.06	0.55	0.86	40.4	47.1	444
Fx9	1.28	0.25	5.11	72	0.06	0.52	0.46	40.7	89.2	439
Fx10	0.17	0.08	2.05	90	-	-	-	-	-	-
Fx11	1.22	0.42	2.88	52	0.11	1.09	2.48	89.3	36.1	443
Fx12	1.05	0.30	3.51	53	0.10	0.73	2.21	69.4	31.4	446
Fx13	0.43	0.09	4.67	57	-	-	-	-	-	-
Fx14	1.10	0.34	3.24	60	0.08	0.63	1.85	57.3	30.9	440
Montejunto Formation										
Fx15	0.62	0.28	2.20	42	0.12	0.49	1.53	79.0	51.6	443
Fx16	0.81	0.25	3.24	49	0.10	0.77	0.88	95.1	108.6	435
Fx17	0.61	0.37	1.65	34	0.14	0.52	1.27	85.2	67.2	441
Fx18	0.63	0.38	1.66	40	0.05	0.35	0.81	55.6	68.3	444
Fx19	0.50	0.23	2.19	26	-	-	-	-	-	-
Fx20	0.30	0.12	2.41	14	-	-	-	-	-	-
Fx21	0.32	0.51	0.62	11	-	-	-	-	-	-
Fx22	0.26	0.15	1.72	5.5	-	-	-	-	-	-
Fx23	0.58	0.20	2.84	5.0	0.25	0.82	2.65	141.9	53.6	451
Cabaços Formation										
Fx24	0.40	0.12	3.35	5.4	-	-	-	-	-	-
Fx25	1.05	4.20	0.25	23	0.50	4.85	9.90	463.0	46.8	425
Fx26	1.00	6.12	0.16	30	0.53	4.22	6.81	422.7	62.1	427
Fx27	0.53	0.20	2.63	2,4	0.16	0.38	0.78	71.7	92.5	460
Fx28	0.53	0.13	3.99	2,0	0.29	0.78	1.59	147.2	92.5	425
Fx29	1.22	0.84	1.45	23	0.84	6.47	10.44	531.9	51.0	421
Brenha Formation										
Fx30	0.50	0.76	0.67	17	-	-	-	-	-	-
Fx31	0.33	0.44	0.76	7.2	-	-	-	-	-	-
Fx32	0.32	0.36	0.89	6.4	-	-	-	-	-	-
Candeeiros Formation										
Fx33	0.14	0.04	3.78	< 0.5	-	-	-	-	-	-
Fx34	0.15	0.04	4.19	< 0.5	-	-	-	-	-	-
Fx35	0.15	0.11	1.43	< 0.5	-	-	-	-	-	-
Fx36	0.10	0.02	5.61	< 0.5	-	-	-	-	-	-

TOC: Total Organic Carbon (wt. %); TS: Total Sulfur content (wt. %); C/S: carbon/sulfur ratio; IR: Insoluble residue (%); S1 and S2: Peak 1 and Peak 2 (mgHC/g rock); HI: hydrogen index (mgHC/g TOC); OI: Oxygen index (mgCO2/g); T_{max}: pyrolysis maximum temperature (ºC).

The highest TOC values were observed in the Abadia Formation with the majority of the samples showing values above 1 wt.% (see Tables 16 and 17). This trend is consistent with published data for this formation in other sub-basins of the Lusitanian Basin (Gonçalves et al., 2013, 2014). Candeeiros Formation presented the lowest TOC values that just reached 0.30 wt.% (mean values of 0.12 wt.%).

Table 17. Geochemical data of Bf-1 borehole samples.

Sample	TOC	TS	C/S	IR	S1	S2	S2/S3	HI	OI	T_{max}
Lorinhã Formation										
Bf1	0.17	0.07	2.28	76	0.04	0.03	0.38	18	47	403
Bf2	0.52	0.52	1.01	81	0.04	0.05	0.56	10	17	323
Bf3	1.33	1.35	0.99	87	0.10	0.60	1.67	45	27	427
Bf4	0.52	0.65	0.79	77	0.02	0.04	0.29	8	27	433
Bf5	1.12	1.00	1.12	86	0.03	0.34	1.10	30	28	422
Bf6	1.28	1.06	1.02	72	0.02	0.11	0.48	10	21	424
Amaral Formation										
Bf7	0.25	0.31	0.81	34	0.02	0.05	0.50	20	40	377
Abadia Formation										
Bf8	0.74	0.14	5.12	80	0.02	0.13	0.39	18	44	431
Bf9	1.61	0.28	5.76	82	0.01	0.14	0.25	9	34	436
Bf10	1.09	0.27	4.02	80	0.02	0.22	0.55	20	37	400
Bf11	1.61	0.27	5.95	80	0.05	0.47	0.92	29	32	431
Bf12	1.40	0.29	4.83	75	0.04	0.34	1.00	24	24	432
Bf13	1.08	0.16	6.59	81	0.02	0.25	1.39	23	17	451
Bf14	0.77	0.06	12.24	77	0.05	0.35	0.97	45	47	466
Bf15	1.28	0.28	4.53	79	0.07	0.31	0.94	24	26	438
Bf16	1.65	0.57	2.91	77	0.06	0.41	1.64	25	15	458
Bf17	1.17	0.27	4.34	77	0.04	0.35	1.25	30	24	431
Bf18	1.55	0.45	3.41	80	0.06	0.36	1.57	23	15	437
Bf19	1.51	0.38	3.98	76	0.08	0.57	2.19	38	17	434
Bf20	1.28	0.59	2.18	84	0.07	0.37	1.03	29	28	431
Bf21	0.93	0.29	3.21	78	0.18	0.17	0.85	18	21	452
Bf22	0.80	0.30	2.67	83	0.06	0.21	1.31	26	20	417
Bf23	1.00	0.36	2.82	71	0.05	0.31	1.35	31	23	431
Bf24	0.87	0.24	3.55	66	0.10	0.49	1.29	56	44	434
Bf25	0.60	0.24	2.51	72	0.10	0.30	5.00	50	10	433
Bf26	0.39	0.39	5.12	55	0.05	0.08	0.35	21	59	346
Montejunto Formation										
Bf27	0.53	0.35	1.53	41	0.10	0.28	2.00	53	26	433
Bf28	0.81	0.49	1.65	34	0.11	0.46	1.84	57	31	429
Bf29	0.41	0.22	1.86	29	0.07	0.11	0.58	27	46	412
Bf30	0.32	0.20	1.56	9	0.12	0.15	1.00	47	47	418
Bf31	0.36	0.23	1.57	17	0.11	0.18	1.20	50	42	439
Bf32	0.31	0.33	0.93	16	0.12	0.19	1.19	61	52	435
Bf33	0.34	0.16	2.19	14	0.01	0.06	0.55	17	32	385
Bf34	1.28	0.30	4.21	18	0.21	0.28	1.47	22	15	436
Bf35	0.50	0.22	2.23	14	0.48	2.28	9.50	456	48	442
Cabaços Formation										
Bf36	0.73	0.28	2.66	14	0.21	0.55	2.89	75	26	443

(Continue on next page)

Table 17 (cont.). Geochemical data of Bf-1 borehole samples.

Sample	TOC	TS	C/S	IR	S1	S2	S2/S3	HI	OI	T_{max}
Cabaços Formation										
Bf37	0.67	0.98	0.68	17	0.33	0.55	2.39	82	34	439
Bf38	0.63	0.55	1.14	18	0.19	0.40	2.00	64	32	432
Bf39	0.52	0.94	0.56	18	0.11	0.26	1.44	50	34	442
Bf40	0.64	0.76	0.84	17	0.20	0.23	1.53	36	24	460
Bf41	0.46	0.11	4.05	12	0.20	0.28	1.22	60	49	455
Bf42	0.61	0.18	3.39	13	0.28	0.41	1.86	67	36	437
Bf43	0.53	0.14	3.84	11	0.26	0.38	2.00	72	36	454
Brenha Formation										
Bf44	1.48	0.55	2.69	7	0.73	1.92	6.19	130	21	448
Bf45	0.58	0.82	0.71	15	0.23	0.57	1.39	98	71	447
Bf46	0.45	0.68	0.66	11	0.18	0.25	1.09	56	51	433
Candeeiros Formation										
Bf47	0.30	0.54	0.56	6.2	0.07	0.09	1.00	30	30	376
Bf48	0.10	0.02	4.99	<1	0.05	0.05	0.42	50	120	391
Bf49	0.09	0.05	1.90	<1	0.02	0.01	1.00	11	11	-
Bf50	0.13	0.04	3.54	5	0.12	0.26	0.79	200	254	455
Bf51	0.11	0.05	2.44	2	0.06	0.07	0.88	64	73	402
Bf52	0.07	0.06	1.14	<1	0.04	0.07	1.17	100	86	313
Bf53	0.09	0.06	1.36	<1	0.01	0.01	0.25	11	44	-
Bf54	0.09	0.07	1.20	<1	0.01	0.01	0.25	11	44	-
Bf55	0.09	0.02	3.55	<1	0.01	0.05	0.56	56	100	301
Bf56	0.08	0.02	3.42	<1	0.02	0.03	0.50	38	75	304
Bf57	0.08	0.01	6.74	<1	0.01	0.02	0.50	25	50	-
Bf58	0.11	0.03	3.36	<1	0.04	0.07	0.70	64	91	312
Bf59	0.07	0.02	3.62	<1	0.03	-	-	-	88	-
Bf60	0.16	0.11	1.45	<1	0.05	0.13	0.76	81	106	419
Bf61	0.07	0.03	2.50	<1	0.06	0.16	1.14	229	200	352
Bf62	0.12	0.04	3.05	<1	0.04	0.04	0.40	33	83	312
Bf63	0.18	0.09	1.97	<1	0.06	0.11	1.38	61	44	332
Bf64	0.20	0.19	1.05	4	0.44	0.11	0.17	5	30	-
Brenha Formation										
Bf65	0.27	0.20	1.38	4	0.05	0.05	0.56	19	33	372
Bf66	0.27	0.19	1.44	4,2	0.05	0.01	0.11	4	33	-
Bf67	0.34	0.24	1.42	16	0.05	-	-	-	26	-
Bf68	0.26	0.35	0.73	15	0.03	0.04	0.36	14	39	307
Bf69	0.39	0.34	1.14	15	0.05	0.03	0.12	8	67	418
Bf70	0.38	0.56	0.68	24	0.04	0.02	0.13	5	42	345
Bf71	0.31	0.41	0.77	22	0.07	0.20	1.54	64	42	336
Coimbra Formation										
Bf72	0.32	0.37	0.86	18	0.08	0.08	0.22	25	113	393
Bf73	0.13	0.19	0.65	21	-	-	-	-	-	-
Bf74	0.33	0.26	1.25	9	0.04	0.01	0.20	3	15	-
Bf75	0.21	0.41	0.52	20	0.02	0.02	0.50	10	19	-
Dagorda Formation										
Bf76	0.12	0.13	0.94	11	0.03	-	-	-	93	-
Bf77	0.73	0.35	2.10	12	0.36	0.43	0.07	59	822	376

TOC: Total Organic Carbon (wt. %); TS: Total Sulfur content (wt. %); C/S: carbon/sulfur ratio; IR: Insoluble residue (%); S1 and S2: Peak 1 and Peak 2 (mgHC/g rock); HI: hydrogen index (mgHC/g TOC); OI: Oxygen index (mgCO2/g); T: pyrolysis maximum temperature (ºC).

The total sulfur (TS) content (Tables 16 and 17) ranged between 0.01wt.% (Bf57) and 6.12wt.% (Fx26). The carbon (C)/sulfur (S) ratio (see Tables 16 and 17) varied between 0.16 (Fx26) and 12.24 (Bf14). This ratio can be used to identify the occurrence of sulfate reduction, once values below 3 indicate more reducing environments and values above 3 more oxic (e.g., Berner, 1995; Borrego et al., 1998). The studied sequences showed variation in the redox conditions during the depositional process.

The amount of hydrocarbon yield (S2; Tables 16 and 17) expelled during the pyrolysis is, according to several authors (e.g., Bordenave et al., 1993; Peter and Cassa, 1994), a good parameter to evaluate the generative potential of a source rock. Most of the samples have less than 2.5 mg HC/g rock pointing to a poor generative potential. There are few exceptions (see Tables 16 and 17) that indicate a fair to good potential to generate hydrocarbons, according to the classification proposed by Peter and Cassa (1994).

Generally, both boreholes have lower hydrogen index (HI) values ranging from 3 to 456 in the Bf-1 borehole, and from 20.9 to 531.9 in the Fx-1 borehole (see Tables 16 and 17). The oxygen index (OI) values are also low. The higher values of pyrolysis S2 parameter and consequently higher HI of the samples Fx25, Fx26 and Fx29 seems to be related with the presence of migrated hydrocarbons. The T_{max} values varied between 301 and 466ºC in the Bf-1 borehole, and from 421 to 460ºC in the Fx-1 borehole. The lower T_{max} values in the Bf-1 borehole may be connected with the smaller values of the pyrolysis S2 peak (<0.20 mgHC/g rock) that led to unreliable data. In the case of Fx-1 samples, it can be associated with the presence of large amounts of migrated bitumen. According to Peter and Cassa (1994), lower T_{max} values can be related with the presence of migrated bitumen.

2.1.4.3. Biomarker distribution

Saturated biomarkers are used to characterize the sedimentary OM and provide useful information in order to determine the paleodeposicional environment. The data obtained correspond to *m/z* 85 for normal alkanes and isoprenoids, *m/z* 191 for terpanes, and *m/z* 217 and *m/z* 218 for steranes.

Normal alkanes and isoprenoids

The saturated hydrocarbon fraction (Fig. 27A) is dominated by *n*-alkanes with 15 to 30 carbon atoms and usually showed a unimodal distribution with the predominance of low to medium molecular weight compounds (*n*C15 to *n*C21).

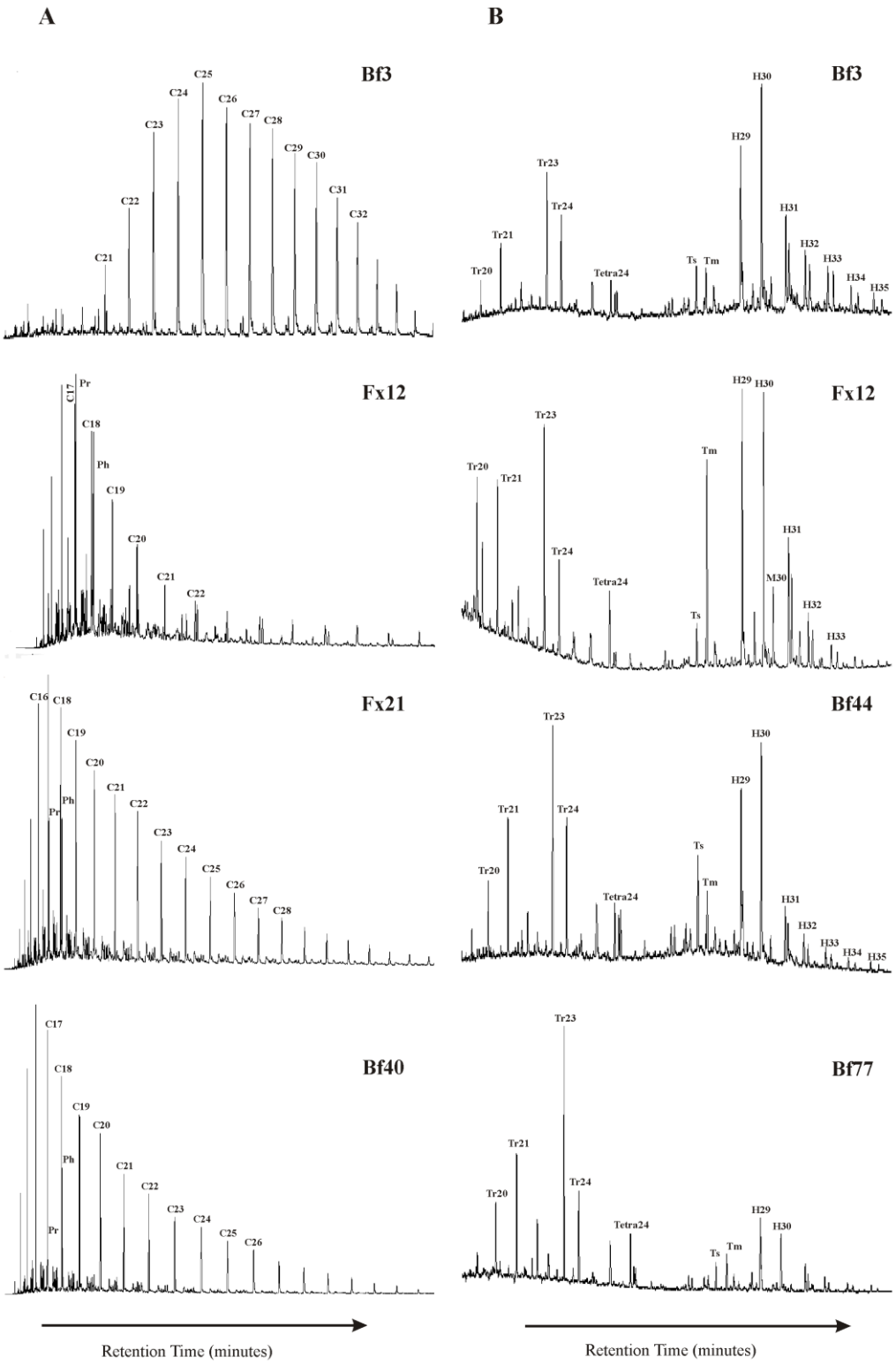

Figure 27. Gas chromatograms (*m/z* 85 and *m/z* 191) of saturated fractions showing the distributions of *n*-alkanes and acyclic isoprenoids (A) and terpanes (B) of selected samples from the Freixial-1 and Benfeito-1 boreholes. Tr 20 to Tr 26: C20 to C26 tricyclic terpane; Tetra 24: C24 tetracyclic terpane; Ts: 22,29,30-trisnorneohopane; Tm: 22,29,30-trisnorhopane; H29: 17α(H),21β(H)-30-norhopane; H30: 17α(H),21β(H)-hopane; H31(22S and 22R): 17α(H),21β(H)-homohopane; H32: 17α(H),21β(H)-bishomohopane (22S and 22R); H33: 17α(H),21β(H)-trishomohopane (22S and 22R); H34: 17α(H),21β(H)-tetrakishomohopane (22S and 22R); H35: 17α(H),21β(H)-pentakishomohopane (22S and 22R); M29: 17β(H),21α(H)-30-normoretane; M30: 17β(H),21α(H)-hopane (moretane).

The predominance of short chain *n*-alkanes can be associated to organic matter derived from algae and/or plankton (e.g., Peters et al., 2005; Tissot and Welte, 1984) or with high temperatures that led to the cracking of the long chain *n*-alkanes (Peter et al., 2005). Some samples of Cabaços and Lourinhã Formations (Fig. 27A; Bf3) had a predominance of medium to long weight compounds (*n*C19 to *n*C30) characteristic of terrestrial origin for the organic matter (Peters et al., 2005; Tissot and Welte, 1984).

The main acyclic isoprenoids, pristane (Pr) and phytane (Ph), are present in all samples with the Pr/Ph ratio raging between 0.12 - 1.84 in the Fx-1 borehole, and 0.04 - 0.82 in the Bf-1 borehole (see Table 18). Pr and Ph can be derived from the phytol side chain of the chlorophyll by oxidation and reduction process, respectively (Brooks et al., 1969). Thus, the Pr/Ph ratio is usually used to determine the redox condition in the depositional environment, but must be interpreted carefully due to the interference with other factors such as maturity and origin of the organic matter (Peters et al., 2005; Waples and Machihara, 1991). According to several authors (e.g., Brooks et al, 1969; Didyk et al, 1978; Peters et al., 2005), Pr/Ph< 1 is indicative of reducing conditions in the depositional environment, while 1>Pr/Ph<3 reflects oxic conditions. Ratio values >3 are related with terrestrial sediments (Hunt, 1979). Plotting the Pr/*n*C17 versus the Ph/*n*C18 data (Fig. 28), it was noticed that the samples contain a mixture of type II and III kerogen.

The carbon preference index (CPI) parameter is affected by the organic matter source and maturity, and obtained by the sum of the odd carbon-numbered *n*-alkanes to the sum of the even carbon-numbered from *n*C22 until *n*C30 (Tissot and Welte, 1984). The values of CPI varied from 0.49 (Fx13) to 1.21 (Fx7) with a mean of 0.91 (Fx-1 borehole; Table 18). According to Peters et al. (2005) CPI values substantially larger or smaller than 1 are indicative of low thermal maturity whereas CPI values near 1 (CPI≈1) suggest thermal maturity. The same authors refer that CPI values <1 are unusual and can be related to immature oil or bitumen from carbonate or hypersaline environments.

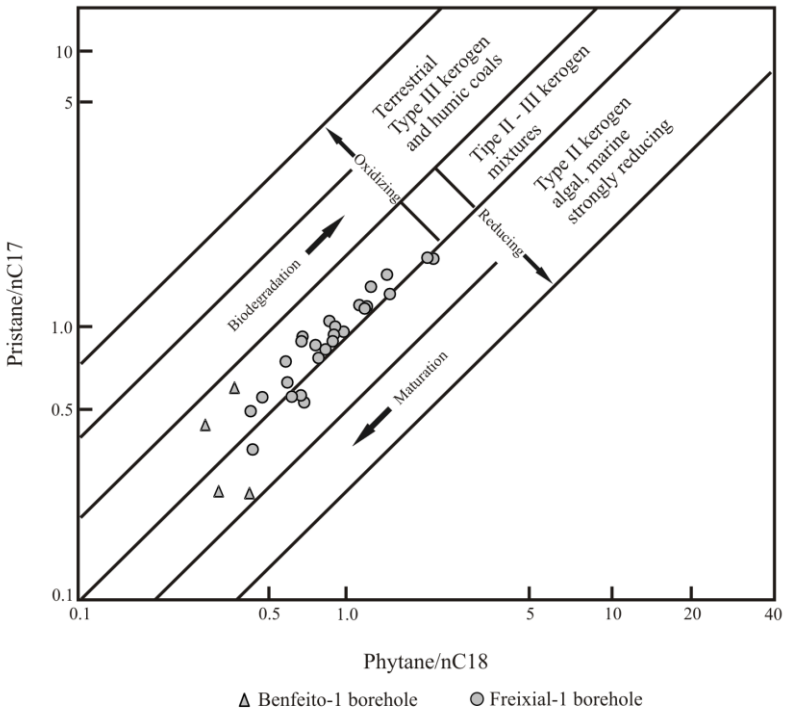

Figure 28. Pristane/*n*C17 versus phytane/*n*C18 from the bitumen extracted from Freixial-1 and Benfeito-1 boreholes (modified from Hunt, 1979).

Terpanes and steranes

The terpane distribution pattern (Fig. 27B) in the studied boreholes showed different behaviors. Regarding to Fx-1 borehole samples, the typical terpane distributions were characterized by a higher content of tricyclic and tetracyclic in the siliciclastic samples and higher content of pentacyclic terpanes in the carbonate samples. C23 terpane is the dominant tricyclic terpane and the C24 tetracyclic content usually exceeds the C26 tricyclic terpane. In the few samples of the Bf-1 borehole analyzed, the terpane distribution was the opposite, being the pentacyclic terpanes predominant in the siliciclastic samples. The 22,29,30-Trisnorhopane (Tm) content dominates over the 22,29,30-Trisnorneohopane (Ts) content, except in samples Fx21, Fx22, Bf3 and Bf44 (see Table 18). Regarding to the hopanes, the C29 and C30 hopanes are the most abundant in all the samples with the preference for C30 hopane, except in the samples Fx22, Fx27, Fx29 and Bf77. The predominance of C29 norhopane is frequently associated with anoxic carbonate or marl source rocks (e.g., Peters et al., 2005; Waples and Machihara, 1991).

Extended hopanes C31 to C35 are not present in all samples but when appears they occur as doublets that decreases in abundance with the increase of the molecular weight. The hopanes from C33 to C35 are just preserved in anoxic environments, so low homohopane index values are evidence of more anoxic conditions during the deposition process (Peter and Moldowan, 1993).

Table 18. Molecular parameters derived from biomarkers assemblage of Fx-1 and Bf-1 samples.

Sample	EOM	*n*-Alkanes				Terpanes					Steranes		
	(mg/g rock)	Pr/Ph	Pr/*n*-C17	Ph/*n*-C18	CPI	Ts/Tm	H32 S/(S+R)	M30/H30	H34/H35	Ster/17α-Hop	C27/C29 sterane	C29 S/(S + R)	C29 ββ/(αα+ββ)
Freixial-1 borehole													
Fx1	0.04	0.97	1.33	1.44	-	0.93	0.56	-	0.90	0.20	0.79	-	0.50
Fx2	0.15	1.05	1.79	2.08	-	0.80	0.52	0.18	1.37	0.15	0.68	-	0.59
Fx3	0.10	1.28	1.80	1.98	-	0.37	0.18	0.30	-	0.09	0.75	-	0.39
Fx4	0.38	1.27	1.56	1.40	-	0.42	0.21	0.18	-	0.43	0.31	-	0.40
Fx5	0.32	1.04	1.41	1.22	-	0.43	0.28	0.28	-	0.23	0.68	-	0.40
Fx6	0.14	1.84	1.06	0.86	1.19	0.28	0.31	0.38	-	0.41	0.70	-	0.45
Fx7	0.10	1.21	0.97	0.97	1.21	0.35	0.42	0.33	-	0.39	0.65	-	0.48
Fx8	0.60	1.55	0.93	0.68	0.56	0.64	0.54	0.20	1.88	0.33	0.55	-	0.59
Fx9	4.31	-	-	-	-	0.20	0.50	0.36	1.88	0.74	0.40	0.19	0.30
Fx10	0.10	0.51	1.01	0.90	0.94	0.79	0.60	0.16	1.68	0.41	0.77	0.46	0.44
Fx11	0.42	-	-	-	-	0.26	0.59	0.27	1.94	0.36	0.44	0.47	0.32
Fx12	0.35	1.14	1.21	1.11	1.01	0.22	0.58	0.29	-	0.24	0.46	0.49	0.31
Fx13	0.50	0.85	1.20	1.18	0.49	0.56	0.58	0.20	-	0.34	0.74	0.34	0.50
Fx14	0.30	1.05	0.94	0.89	0.75	0.13	0.58	0.32	-	0.18	0.65	0.41	0.34
Fx15	0.51	0.66	0.83	0.83	0.50	0.30	0.60	0.22	-	0.22	0.81	0.52	0.41
Fx16	0.62	1.57	0.89	0.67	0.98	0.69	0.58	0.13	1.38	0.39	11.06	-	0.97
Fx17	0.74	1.35	0.75	0.59	0.93	0.53	0.60	0.12	-	0.15	1.30	-	0.75
Fx18	0.32	0.12	0.05	0.50	1.00	0.55	0.61	0.12	-	0.15	1.06	-	0.67
Fx19	0.19	1.50	0.86	0.76	0.97	0.64	0.59	0.12	-	0.18	1.27	-	0.67
Fx20	0.10	1.12	0.77	0.78	-	0.64	0.63	0.10	-	0.14	0.71	-	0.66
Fx21	0.23	1.20	0.63	0.60	0.98	11.39	0.64	-	-	1.91	1.29	-	0.72
Fx22	0.17	0.80	0.53	0.69	0.95	3.47	-	-	-	-	-	-	-
Fx23	0.85	0.80	0.56	0.67	0.93	-	-	-	-	-	-	-	-

(Continue on next page)

Table 18 (cont.). Molecular parameters derived from biomarkers assemblage of Fx-1 and Bf-1 samples.

Sample	EOM	*n*-Alkanes				Terpanes					Steranes		
	(mg/g rock)	Pr/Ph	Pr/*n*-C17	Ph/*n*-C18	CPI	Ts/Tm	H32 S/(S+R)	M30/H30	H34/H35	Ster/17α-Hop	C27/C29 sterane	C29 S/(S + R)	C29 ββ/(αα+ββ)
Fx24	0.37	0.91	0.56	0.48	0.95	-	-	-	-	-	-	-	-
Fx25	6.76	0.46	0.89	0.88	0.98	0.61	0.61	-	0.98	0.43	1.48	-	0.70
Fx26	8.77	0.65	1.17	1.16	0.99	0.64	0.60	0.10	0.94	0.37	1.23	0.50	0.52
Fx27	0.62	0.69	0.36	0.44	0.89	0.77	0.60	0.10	1.08	0.57	1.57	-	0.68
Fx28	0.75	0.81	0.49	0.44	0.97	0.81	0.62	-	0.85	0.23	0.88	-	0.70
Fx29	9.56	0.43	0.56	0.62	0.98	0.87	0.59	0.10	-	0.56	1.20	0.53	0.53
Benfeito-1 borehole													
Bf3	-	0.44	0.60	0.38	1.03	1.13	0.61	-	1.44	0.26	0.95	0.44	0.20
Bf18	-	0.82	0.44	0.30	1.24	0.77	0.57	-	1.32	0.45	0.93	0.29	0.49
Bf35	-	0.04	0.02	0.47	0.88	-	0.65	-	1.20	-	0.78	0.61	0.58
Bf40	-	0.36	0.09	0.25	0.93	-	0.68	-	1.06	-	-	-	-
Bf44	-	0.57	0.36	0.33	0.91	1.77	0.61	-	-	0.74	1.00	0.35	0.49
Bf77	-	0.49	0.25	0.43	0.76	0.81	0.59	-	0.92	-	-	-	-

EOM: extractable organic matter; Pr: Pristane; Ph: Phytane; CPI: Carbon Preference Index [2*(C23+C25+C27+C29)/C22+2*(C24+C26+C28)+C30]; Ts: 22,29,30-Trisnorneohopane; Tm: 22,29,30-Trisnorhopane; M30: 17β,21α(H)-Hopane (Moretane); H30: 17α,21β(H)-Hopane; H32: 17α, 21β(H)-bishomohopane; (Ster/17α-hop): regular steranes consist of C27, C28, C29 ααα(20S + 20R) and αββ(20S + 20R) / 17α-hopanes consist of the C29 to C33 pseudo-homologue (including 22S and 22R epimers); H34: 17α,21β(H)-tetrakishomohopane (22S-22R); H35: 17α, 21β(H)-pentakishomohopane (22S-22R); C27/C29 sterane: C27ααα 20R/C29ααα 20R; C29 (%): content of C29 ααα (20S +20R).

C32 homohopane isomerization ratios 22S/(22S + 22R) range from 0.57 to 0.68 in the Bf-1 borehole and between 0.18 and 0.64 in the Fx-1 borehole, showed that the organic matter is marginally mature in all samples of the Bf-1 borehole and immature to early mature in the Fx-1 borehole (Tables 18). The C27/C29 sterane ratios range from 0.31 to 11.06 (Tables 18). The C29 sterane were more abundant in the siliciclastic samples. The predominance of C27 sterane can be related with high contribution of planktonic organic matter whereas the C29 sterane is usually associated to continental contribution (Huang and Meinschein, 1979). These data proved to be consistent in the palynofacies analysis.

2.1.5. Discussion

2.1.5.1. Type and origin of the organic matter

The type of organic matter has an important role on the nature of hydrocarbons that can be generated from a given source rock. Kerogen characterization by palynofacies analysis allowed to verify that the major organic matter input comes from continental source (terrestrial higher plants), with some marine contribution (principally in Montejunto, Cabaços and Candeeiros Formations). Rock-Eval pyrolysis results are consistent with the ones observed in the palynofacies analysis. Data from Rock-Eval confirmed that these Jurassic successions contain mostly types III and IV kerogen with minor type II kerogen. Regarding the biomarker compounds, the presence of hopanes is an evidence of contribution of higher plants or prokaryotes (Peter et al., 2005; Tissot and Welte, 1984) while the high tricyclic terpanes concentration can be associated with algae and bacteria (Aquino Neto et al., 1983) or with constituents that exist in prokaryote membranes (Ourisson et al., 1982). The regular steranes/17α-hopanes ratio is used as an indicator of organic matter input to the source rock, assuming that the steranes originated from algae and higher plants, whereas the hopanes originated mainly from bacteria (Marynowski et al., 2000). The results showed the steranes/17α-hopanes ratios (Table 18) were usually low, which is an indicative of terrigenous and/or microbial reworked organic matter (Fig. 29).

The C27/C29 sterane ratios (Table 18) were less than 1 in samples from Lourinhã, Amaral and Abadia Formations reflecting a predominance of terrestrial organic matter, whereas Montejunto and Cabaços displayed a more algal contribution, as observed in palynofacies analysis.

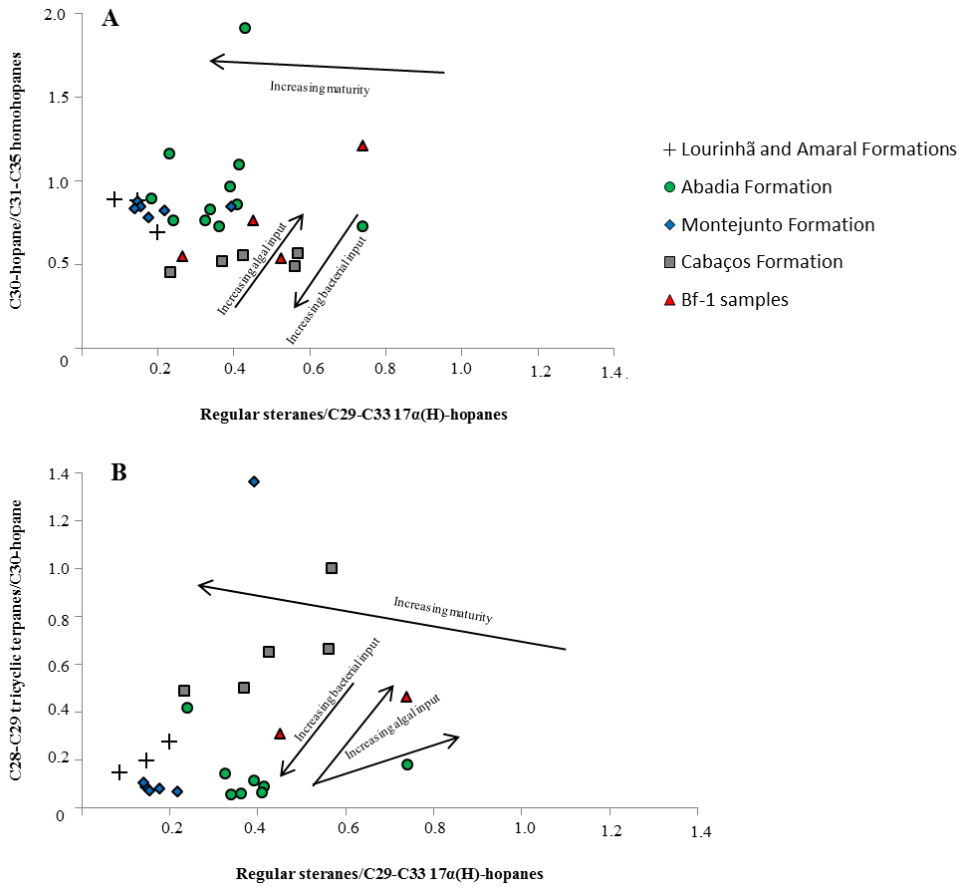

Figure 29. Relation between regular steranes/C29-C33 17α(H)-hopanes versus: A) C28-C29 (22R and 22S) tricyclic terpanes/C30-hopane; B) C30-hopane/C31-C35 homohopanes (modified from Marynowski et al., 2000).

2.1.5.2. Thermal maturity of organic matter

Several thermal markers such as vitrinite reflectance (%R_r), T_{max}, CPI, moretane (M30) /hopane (H30) ratio, hopane and sterane ratios can be used to evaluate the thermal maturity of sediments. But some of them must be used with careful since they can be influenced by other parameters such source lithology (e.g., Peter et al., 2005; Seifert and Moldowan, 1978). Data obtained through the vitrinite reflectance (Tables 14 and 15) indicated that the organic matter reached the oil generation window. Based on the T_{max} values (Tables 16 and 17), the Jurassic succession crossed Fx-1 borehole seems to be in a mature stage. Regarding the Bf-1 borehole samples, this parameter is unreliable as previously explained and cannot be used as a maturation parameter in the majority of the samples. However, in the samples where S2 > 0.20mgHC/g rock, the organic matter seems to have reached the oil generation window. The M30/H30 ratio generally decreases with increasing thermal maturity since moretane is less stable than hopane. The values of approximately 0.80 correspond to immature stages and values less than 0.15 suggest mature stages (Waples and Machihara, 1991). The M30 /H30 ratio (Table 18) varied

between 0.10 and 0.32 pointing to an immature to mature stage for the organic matter. The lowest values of M30/H30 correspond to Cabaços samples, more specifically, the samples that are impregnated with solid bitumen. The 22S/(22R + 22S) C32 homohopane ratio and αββ/(ααα + αββ) isomerization ratio in the C29 sterane escalate with the increasing maturity until they reached the equilibrium values (0.57 - 0.62 and 0.67 - 0.71, respectively; Seifert and Moldowan, 1980). In the case of the C32 homohopane ratios they are found in the range of 0.18 to 0.68, indicating that the majority of the samples have reached the interval of equilibrium reflecting a mature and, in some cases, overmature thermal stage. The ratio for C29 sterane varied between 0.31 and 0.97 which suggest thermally mature (early to over mature) samples. The data above indicate that the studied samples are sufficiently thermally mature for hydrocarbon generation.

2.1.5.3. Hydrocarbon potential

The Bf-1 and Fx-1 sequences contain variable amounts of organic matter content and consequently different hydrocarbon generation potential. According to Tissot and Welte (1984), black shales and carbonates with TOC values higher than 0.5 and 0.3 wt.%, respectively, can be considered as potential source rocks for oil and/or gas. With the exception of some samples (see Tables 16 and 17), these two Jurassic successions have TOC values lower than 1wt.% and pyrolysis S2 yields minor than 2.0 mgHC/g rock. Therefore, a large number of the studied samples are poor concerning liquid hydrocarbon potential. The ratio of S2/S3 suggests the quality of the organic matter. Ratio values lower than 1 indicate absence to generate any hydrocarbon (Peter and Cassa, 1994). Samples from the Lower Jurassic always showed S2/S3 values < 1. In contrast, the bulk of samples from the Middle and Upper Jurassic (Abadia, Montejunto, Cabaços and Brenha Formations) showed S2/S3 values higher than 1 (Tables 16 and 17). In fact, some layers of Abadia, Montejunto, Cabaços and Brenha (Callovian age) Formations can be considered as potential source - rocks with capacity to generate hydrocarbons. In regards to Abadia Formation, despite the important TOC content (in most cases higher than 1%), the OM present was almost of continental origin (type III kerogen), thus only with the capacity to generate gas (e.g., Tissot and Welte, 1984). Concerning to Montejunto, Cabaços and Brenha (Callovian age) Formations, despite the lower TOC content, they showed a mixed type III/II kerogen, where the AOM has an important role. The presence of AOM, principally fluorescent AOM, is an indicator of potential source rocks of both oil and gas (Tyson, 1995). Furthermore, the higher pyrolysis S2 yield (> 2mg HC/g rock) and consequently the higher HI values of some of these samples (see Tables 16 and 17) implies from fair to good hydrocarbon potential.

2.1.5.4. Paleoenvironmental interpretation

The paleoenvironmental interpretation herein present takes into account the data obtained in this study. However, the presence of solid hydrocarbons in some samples makes impossible to distinguish the biomarkers of autochthonous and migrated bitumens. Thus, when solid hydrocarbons were detected in the palynofacies analysis, the biomarker data were not used for this interpretation.

Lateral and vertical variations of the type and content of organic matter were observed during this study. Generally, the Jurassic sequences crossed by the Benfeito-1 and Freixial-1 boreholes have been deposited in a marine environment, proximal to the terrestrial source area, under variable energy and redox conditions. Continental organic matter prevails in most samples.

Deposition of Dagorda sediments (Hettangian age) occurred in a shallow environment like an evaporitic lake or lagoon (e.g., Azerêdo et al., 2003; Palain, 1976). The presence of nearly 50% of opaque phytoclasts revealed periods of subaerial exposure of the organic matter and/or oxic environments. Furthermore, the high opaque phytoclast content associated to a high OI (822 mgCO2/g TOC) and lower HI (59 mgHC/g TOC) suggests the existence of oxic conditions during the deposition of the continental organic matter (Tissot et al., 1974). At the Sinemurian there is a depth increase of the basin that began to show more marine influences (Azerêdo et al., 2010). The Coimbra Formation was deposited in a low - energy shallow marine environment sometimes with higher - energy as a result of storms or flooding (Azerêdo et al., 2010; Duarte et al., 2008) where the terrigenous influx is notorious, mainly at the top (Table 15). The C/S ratio (Table 17) refers to anoxic periods that allowed the production of AOM. The deposition of Brenha Formation (Pliensbachian to Aalenian) occurred in a normal marine environment, probably in suboxic to anoxic conditions, but with low preservation of the organic matter. The amounts of opaque phytoclasts, some of them charcoal particles, are probably the result of long transport of the organic particles. In the case of charcoal, they usually are deposited in distal environments carried by currents. The input of terrestrial sediments still decreases (IR < 1%, in Candeeiros Formation) as well as the preservation of the organic matter (TOC mean value of 0.12 wt.%) until Bathonian. The marine influence increased (Tables 14 and 15) attaining its maximum exponent during the Lower to Middle Bathonian. In fact, this period is characterized by high primary productivity that led to an increase of the zooplankton (zooclasts and some foraminiferal test linings). However, the very low content in OM (TOC content lower than 0.30 wt.%) suggests a restrict environment and/or unfavorable conditions for preservation. Considering the zooclasts preservation is difficult due the organic composition (more proteinaceous organic matter; Tyson, 1995) its presence in the kerogen assemblage can refer to periods of high

productivity (both phytoplankton and zooplankton) where oxic conditions prevail (C/S ratio >3; Tables 16 and 17). The amounts of opaque phytoclasts support the idea of an oxygenated environment. From the middle to late Bathonian (Candeeiros Formation), the environmental conditions are changed and they remain until the end of Callovian. The decline in phytoclast and marine particles abundance accompanied by AOM enrichment confirm changes in the depositional environment. These changes are probably related with fluctuations in oxygenation system (C/S ratio < 3, Pr/Ph <1). The different types of AOM suggest periods of reworking by bacterial activity (heterotrophic) and others by primary productivity (autotrophic). The marine influence corresponds to dinoflagellate cysts, Prasinophyte algae and foraminiferal test linings. The end of the Middle Jurassic was marked by the occurrence of a complex regression that led to several variations in the carbonate ramp environment (e.g., Azerêdo et al., 2002). The increase of phytoclasts, most pronounced in Freixial-1 borehole (Table 14), revealing a wide continental influence that might have been the result of a drop in sea - level which allowed more terrestrial components, were transported deeper into the basin. During the deposition of Cabaços Formation the carbonated sedimentation remains. The abundance of fluorescence AOM is related to high primary productivity with good preservation of lipid - rich materials, which was possible by reducing environmental conditions (Tyson, 1995). The biomarker data for this formation is ambiguous due to the presence of solid bitumen. Carbonate sedimentation continued during the deposition of the Montejunto Formation with increasing of siliciclastic sediments at the top. Continental and marine organic matter were deposited in a marine environment under variable energy conditions and oscillations in the water column. These conditions controlled the fluctuations in oxygen content, leading to oxic to anoxic environments (Pr/Ph varied from 0.04 - 1.50; C/S varied from 0.62 - 4.21). The presence of marine organic microplankton and foraminiferal test linings as well as the biomarker data (*n*-alkanes from *n*C15 - *n*C21; C27/C29 steranes >1) confirm the marine conditions during this period. The occurrence of sporomorphs (increase from the bottom to top) and freshwater algae can be related to the presence of fluvial systems along the coastline, which carried these organic particles to marine depositional areas. The sedimentary condition began to change at the end of the Oxfordian - beginning of the Kimmeridgian with an increasing of the siliciclastic sediments (see IR values; Tables 16 and 17). The kerogen assemblage changed and the continental organic matter becomes dominant in the Abadia Formation (Tables 14 and 15), mainly the non-opaque phytoclasts. The siliciclastic Abadia sediments showed an increase in the organic matter content (TOC values higher than 1wt.%) most likely controlled by the phytoclast content resulting from high discharges in submarine fans and prograding slope environments (Leinfelder, 1993). The environment was favorable for the preservation of the organic matter probably due to the higher sedimentation rates and faster burial rate of the

organic matter (Hofmann et al., 2000). The relation between some tricyclic and tetracyclic terpanes also confirmed the proximity to the source area as well as the C27/C29 steranes ratios lower than 1 (Table 18). The Amaral Formation had a small expression in the study area. The continental influence prevailed and corresponds to a more than 90% of the total organic matter. Its deposition revealed a carbonate character (IR < 45; Tables 16 and 17) that took place in an intertidal to subtidal environment with some marine influences (e.g., Kullberg et al., 2013). The continental influences remains during the Tithonian with the deposition of Lourinhã Formation. This siliciclastic formation was deposited in a near shore environment with significant inputs of terrestrial organic material (mainly non-opaque non-biostructured phytoclasts). Large amounts of cuticles (some with the inner part) were preserved in low energy environment and indicating extreme proximity to the terrestrial source as well as a humid climate. The opaque fraction may be the result of regressive periods in which the organic matter was exposed.

2.1.6. Conclusions

The integrated palynological and geochemical studies of the Jurassic successions of the Benfeito-1 and Freixial-1 boreholes have indicated variations in the type of kerogen, depositional environment and potential for generate hydrocarbons. The organic matter is mainly terrestrial (type III and IV kerogen) with TOC content usually lower than 1wt.%. The carbonated successions from Montejunto, Cabaços and Brenha (Callovian) Formations showed different characteristics and revealed an increasing of the marine organic matter (mixture type II/III kerogen). The organic matter was deposited in a marine environment with variations in the redox condition (anoxic to oxic). Based on Rock-Eval pyrolysis data, the overall generative potential of these sequences are classified as mostly being poor to fair. Nevertheless, some intervals of Abadia, Montejunto, Cabaços and Brenha (Callovian age) Formations showed a good generative potential and can be consider as potential source rocks in the Arruda sub-basin. Abadia Formation has potential for gas generation while the remaining formations presented potential for generation of liquid hydrocarbons. Biomarker maturity parameters as well as vitrinite reflectance and T_{max} indicate that the organic matter reached the generation oil window.

References

Alves, T.M., Gawthorpe, R.L., Hunt, D.W., Monteiro, J.H., 2002. Jurassic tectono-sedimentary evolution of the Northern Lusitanian Basin (offshore Portugal). Marine and Petroleum Geology 19, 727 - 754.

Alves, T.M., Manuppella, G., Gawthorpe, R.L., Hunt, D.W., Monteiro, J.H., 2003. The depositional evolution of diapir- and fault-bounded rift basins: examples from the Lusitanian Basin of West Iberia. Sedimentary Geology 162, 273 - 303.

Aquino Neto, F.R., Trendel, J.M., Restle, A., Connan, J., Albrecht, P., 1983. Occurrence and formation of tricyclic and tetracyclic terpanes in sediments and petroleum, in: Bjorøy, M. et al. (Eds.), Advances in Organic Geochemistry 1981. Wiley, pp. 659-667.

ASTM D 7708: 2011. Standard Test Method for Microscopical Determination of the Reflectance of Vitrinite Dispersed in Sedimentary Rocks.

Azerêdo, A.C., Duarte, L.V., Henriques, M.H., Manuppella, G., 2003. Da dinâmica continental no Triásico aos mares do Jurássico Inferior e Médio. Cadernos de Geologia de Portugal. Instituto Geológico e Mineiro, Lisboa.

Azerêdo, A.C., Silva, R.L., Duarte, L.V., Cabral, M.C., 2010. Subtidal stromatolites from the Sinemurian of the Lusitanian Basin (Portugal). Facies 56, 211 - 230.

Azerêdo, A.C., Wright, V.P., Ramalho, M.M., 2002. The Middle - Late Jurassic forced regression and disconformity in central Portugal: eustatic, tectonic and climatic effects on a carbonate ramp system. Sedimentology 49, 1339 - 1370.

Batten, D.J., 1973. Use of palynologic assemblage-types in Wealden correlation. Palaeontology 16, 1 - 40.

Behar, F., Beaumont, H.L., Penteado, H.L., 2001. Rock-Eval 6 Technology: Performance and Developments. Oil & Gas Science and Technology-Rev. IFP 56, 111 - 134.

Berner, R.A., 1995. Sedimentary organic matter preservation: an assessment and speculative synthesis - a comment. Marine Chemistry 49, 1121 - 1122.

Bordenave, M.L., Espitalié, L., Leplat, P., Oudin, J.L., Vandenbroucke, M., 1993. Screening techniques for source rock evaluation, in: Bordenave, M.L. (Ed.), Applied Petroleum Geochemistry. Editions Technip, Paris, pp. 217 - 278.

Borrego, J., Lopez, M., Pedon, J.G., Morales, J.A., 1998. C/S ratios in estuarine sediments of the Odiel River-mouth, S.W. Spain. Journal of Coastal Research. 14, 1276-1286.

Bostick, N.H., 1971. Thermal alteration of clastic organic particles as an indicator of contact and burial metamorphism in sedimentary rocks. Geosci. Man, Baton Roude 3, 83 - 92.

Brooks, J.D., Gould, K., Smith, J.W., 1969. Isoprenoid hydrocarbons in coal and petroleum. Nature 222, 257 - 259.

Carvalho, J., Matias, H., Torres, L., Manupella, G., Pereira, R., Mendes-Victor, L., 2005. The structural and sedimentary evolution of the Arruda and Lower Tagus sub-basins, Portugal. Marine and Petroleum Geology 22, 427 - 453.

Didyk, B.M., Simoneit, B.R.T., Brassell S.C., Eglinton, G., 1978. Organic geochemical indicators of paleoenvironmental conditions of sedimentation. Nature 272, 216 - 222.

Duarte, L.V., Soares, A.F., 2002. Litoestratigrafia das séries margo-calcárias do Jurássico inferior da Bacia Lusitânica (Portugal). Comunicações do Instituto Geológico e Mineiro 89, 115 - 134.

Duarte, L.V., Silva, R.L., Duarte, C.B., Azerêdo, A.C., Comas-Rengifo, M.J., 2008. Litostratigrafia do Jurássico Inferior da região de S. Pedro de Moel (Bacia Lusitânica), in: Callapez, P.M., Rocha, R.B., Marques, J.F., Cunha, L.S., Dinis, P.M. (Eds), A Terra, Conflitos e Ordem. Homenagem ao Professor Ferreira Soares. Museu Laboratório Mineralógico e Geológico da Universidade de Coimbra, Coimbra, pp. 175 - 185.

Duarte, L.V., Silva, R.L., Mendonça Filho, J.G., 2011. The Lower Jurassic of the west coast of Portugal: stratigraphy and organic matter in carbonate sedimentation, in: Flores, D., Marques, M.M. (Eds). “New Trends on Coal Science”, 63rd ICCP Annual Meeting - Field Trip, Porto.

Duarte, L.V., Silva, R.L., Mendonça Filho, J.G., Poças Ribeiro, N., Chagas, R.B.A., 2012. High-resolution stratigraphy, palynofacies and source rock potential of the Água de Medeiros formation (Lower Jurassic), Lusitanian basin, Portugal. Journal of Petroleum Geology 35, 105 - 126.

Duarte, L.V., Silva, R.L., Oliveira, L.C.V., Comas-Rengifo, M.J., Silva, F., 2010. Organic-rich facies in the Sinemurian and Pliensbachian of the Lusitanian Basin, Portugal: Total organic carbon distribution and relation to transgressive-regressive facies cycles. Geologica Acta 8, 325 - 340.

Duarte, L.V., Wright, V.P., Fernández-López, S., Elmi, S., Krautter, M., Azerêdo, A.C., Henriques, M.H., Rodrigues, R., Perilli, N., 2004. Early Jurassic carbonate evolution in the Lusitanian Basin (Portugal): facies, sequence stratigraphy and cyclicity, in: Duarte, L.V., Henriques, M.H. (Eds.), Carboniferous and Jurassic Carbonate Platforms of Iberia. Field Trip Guide Book of the 23rd IAS Meeting of Sedimentology 1, pp. 45 - 71.

Ercegovac, M., Kostić, A., 2006. Organic facies and palynofacies: nomenclature, classification and applicability for petroleum source rock evaluation. International Journal of Coal Geology 68, 70 - 78.

Espitalié, J., Laporte, J.L., Madec, M., Marquis, F., Leplat, P., Paulet, J., Boutefeu, A., 1977. Méthode rapide de caractérisation des roches mètres, de leur potentiel pétrolier et de leur degré d'évolution. Rev. IFP 32, 23 - 42.

Gonçalves, P.A., Mendonça Filho, J.G., Mendonça J.O., Silva, T.F., Flores, D., 2013. Paleoenvironmental characterization of a Jurassic sequence on the Bombarral sub-basin (Lusitanian basin, Portugal): Insights from palynofacies and organic geochemistry. International Journal of Coal Geology 113, 27 - 40.

Gonçalves, P.A., Mendonça Filho, J.G., Silva, T.F., Mendonça, J.O., Flores, D., 2014. The Mesozoic-Cenozoic organic facies in the Lower Tagus sub-basin (Lusitanian Basin, Portugal): Palynofacies and organic geochemistry approaches. Marine and Petroleum Geology 52, 42 - 56.

Hofmann, P., Ricken, W., Schwark, L., Leythaeuser, D., 2000. Carbon–sulfur–iron relationships and δ13C of organic matter for late Albian sedimentary rocks from the North Atlantic Ocean: paleoceanographic implications. Palaeogeography, Palaeoclimatology, Palaeoecology 163, 97 - 113.

Huang, W.Y., Meinschein, W.G., 1979. Sterols as ecological indicators. Geochimica, Cosmochimica Acta 43, 739 - 745.

Hunt, J.M., 1979. Petroleum Geochemistry and Geology. Freeman, San Francisco.

ISO 7404-2, 2009. Methods for the petrographic analysis of coals - Part 2: Methods of preparing coal samples. International Organization for Standardization. 12pp.

Kullberg, J.C., Rocha, R.B., Soares, A.F., Rey, J., Terrinha, P., Azerêdo, A.C., Callapez, P., Duarte, L.V., Kullberg, M.C., Martins, L., Miranda, J.R., Alves, C., Mata, J., Madeira, J., Mateus, O., Moreira, M., Nogueira, C.R., 2013. III.3. A Bacia Lusitaniana: Estratigrafia, Paleogeografia e Tectónica, in: Geologia de Portugal, 2, ISBN: 978-972-592-364-1, pp. 195 - 347.

Leinfelder, M.R.R, Wilson, R.C.L., 1989. Seismic and sedimentologic features of Oxfordian-Kimmeridgian syn-rift sediments on the eastern margin of the Lusitanian Basin. Geologische Rundschau 79, 81 - 104.

Leinfelder, R.R., 1993. A sequence stratigraphic approach to the Upper Jurassic mixed carbonate - siliciclastic succession of the central Lusitanian Basin, Portugal. Profil 5, 119 - 140.

Littke, R., Klussmann, U., Krooss, B., Leythaeuser, D., 1991. Quantification of loss of calcite, pyrite, and organic matter due to weathering of Toarcian black shales and effects on kerogen and bitumen characteristics. Geochimica et Cosmochimica Acta 55, 3369 - 3378.

Marynowski, L., Narkiewicz, M., Grelowski, C., 2000. Biomarkers as environmental indicators in a carbonate complex, example from the Middle to Upper Devonian, Holy Cross Mountains, Poland. Sedimentary Geology 137, 187 - 212.

Mendonça Filho, J.G., Chagas, R.B.A., Menezes, T.R., Mendonça, J.O., Silva, F.S., Sabadini-Santos, E., 2010. Organic facies of the Oligocene lacustrine system in the Cenozoic Taubaté Basin, Southern Brazil. International Journal of Coal Geology 84, 166 - 178.

Mendonça Filho, J.G., Menezes, T.R., Mendonça, J.O., 2011b. Organic Composition (Palynofacies Analysis). Chapter 5 in: ICCP Training Course on Dispersed Organic Matter, 33 - 81.

Mendonça Filho, J.G., Menezes, T.R., Mendonça, J.O., Oliveira, A.D., Silva, T.F., Rondon, N.F., Silva, F.S., 2012. Organic Facies: Palynofacies and Organic Geochemistry Approaches, in: Panagiotaras, D. (Org.), Geochemistry Earth's system processes. InTech, Patras, ISBN 978-9-53-510586-2, vol. 1, pp. 211 - 245

Mendonça Filho, J.G., Menezes, T.R., Mendonça, J.O., Oliveira, A.D., Souza, J.T., Sant'Anna, A.J., 2011a. Kerogen: Composition and Classification. Chapter 3 in: ICCP Training Course on Dispersed Organic Matter, 17 - 24.

Oliveira, L.C.V., Rodrigues, R., Duarte, L.V., Lemos, V., 2006. Avaliação do potencial gerador de petróleo e interpretação paleoambiental com base em biomarcadores e isótopos estáveis do carbono da seção Pliensbaquiano-Toarciano inferior (Jurássico inferior) da região de Peniche (Bacia Lusitânica, Portugal). Boletim de Geociências da Petrobras 14, 207 - 234.

Ourisson, G., Albrecht, P., Rohmer, M., 1982. Predictive microbial biochemistry from molecular fossils to prokaryotic membranes. Trends in Biochemical Sciences 7, 236 - 239.

Palain, C., 1976. Une série détritique terrigène. Les "Grés de Silves": Trias et Lias inférieur du Portugal. Memórias dos Serviços Geológicos de Portugal nº. 25, Lisboa.

Peters, K.E., Cassa, M.R., 1994. Applied source rock geochemistry, in: Magoon, L.B., Dow, W.G. (Eds.), The petroleum system - from source to trap, American Association of Petroleum Geologists Memoir 60, Tulsa, pp. 93 - 120.

Peters, K.E., Moldowan, J.M., 1993. The Biomarker Guide: Interpreting Molecular Fossils in Petroleum and Ancient Sediments, New Jersey, Prentice-Hall Inc.

Peters, K.E., Walters, C.C., Moldowan, J.M., 2005. The Biomarker Guide, vol. 2, Biomarkers and Isotopes in Petroleum Exploration and Earth History, second ed. Cambridge University Press, London.

Poças Ribeiro, N., Mendonça Filho, J.G., Duarte, L.V., Silva, R.L., Mendonça, J.O., Silva, T.F., 2013. Palynofacies and organic geochemistry of the Sinemurian carbonate deposits in the western Lusitanian Basin (Portugal): Coimbra and Água de Madeiros formations. International Journal of Coal Geology 111, 37 - 52.

Rasmussen. E.S., Lomholt, S., Andersen, C., Vejbæk, O.L., 1998. Aspects of the structural evolution of the Lusitanian Basin in Portugal and the shelf and slope area offshore Portugal. Tectonophysics 300, 199 - 225.

Rey, J., Dinis, J.L., Callapez, P., Cunha P.P., 2006. Da rotura continental à margem passiva. Composição e evolução do Cretácico de Portugal. Cadernos de Geologia de Portugal. Instituto Geológico e Mineiro, Lisboa.

Seifert, W.K., Moldowan, J.M., 1978. Applications of steranes, terpanes and monoaromatics to the maturation, migration and source of crude oils. Geochimica Cosmochimica Acta 42, 77 - 95.

Seifert, W.K., Moldowan, J.M., 1980. The effect of thermal stress on source-rock quality as measured by hopane stereochemistry. Physics and Chemistry of the Earth 12, 229 - 237.

Silva, R.L., Mendonça Filho, J.G., Azerêdo, A.C., Duarte, L.V., 2014. Palynofacies and TOC analysis of marine and non-marine sediments across the Middle - Upper Jurassic boundary in the central-northern Lusitanian Basin (Portugal). Facies 60, 255 - 276.

Tissot, B., Durand, B., Espitalie, J., Combaz A., 1974. Influence of Nature and Diagenesis of Organic Matter in Formation of Petroleum. AAPG Bulletin 58, 499 - 506.

Tissot, B., Welte, D.H., 1984. Petroleum formation and occurrence, second ed. Springer Verlag, Heidelberg.

Tyson, R.V., 1995. Sedimentary Organic Matter. London, Chap. & Hall.

Waples, D.W., Machihara, T., 1991. Biomarkers for Geologists: A Practical Guide to the application of Steranes and Triterpanes in Petroleum Geology. AAPG Methods in Exploration, Series 9.

Wilson, R.C.L., 1979. A reconnaissance study of Upper Jurassic sediments of the Lusitanian basin. Ciências da Terra, Universidade Novo Lisboa 5, 53 - 84.

Wilson, R.C.L., 1988. Mesozoic development of the Lusitanian Basin, Portugal. Revista de la Sociedad Geológica de España 1, 393 - 407.

Wilson, R.C.L., Hiscott, R.N., Willis, M.G., Gradstein, F.M., 1989. The Lusitanian Basin of west - Central Portugal: Mesozoic and Tertiary tectonic, stratigraphic and subsidence history. Bulletin of the American Association of Petroleum Geologists 46, 341 - 362.

2.2. Solid bitumen occurrences in the Arruda sub-basin (Lusitanian Basin, Portugal): petrographic features

Adapted from Paula Alexandra Gonçalves, João Graciano Mendonça Filho, Frederico Sobrinho da Silva, Deolinda Flores

International Journal of Coal Geology (2014), 131, 239 - 249

Accepted 27th June 2014

Abstract

The Middle Jurassic to Cretaceous sedimentary record in the Lusitanian Basin (Portugal) reveals the presence of disseminated solid bitumen. The present work is focused on the petrographic characteristics of solid bitumen identified in the Freixial-1 and Benfeito-1 boreholes (Arruda sub-basin, Lusitanian Basin) that display different thermal maturities. Microscopy techniques (reflected and transmitted white light, incident blue light and SEM) and organic geochemistry analyses (total organic carbon, total sulfur and insoluble residue) were used to study these samples.

From the results obtained by optical microscopy (fluorescence and reflectance) it was possible to distinguish three types of solid bitumen. They were labelled as solid bitumen A, present in all the samples, solid bitumen B and solid bitumen C, these ones observed in some of them. They correspond to allochthonous (migrated) bitumens. In blue incident light, some bitumen do not show fluorescence while others reveal fluorescence that range from yellow (solid bitumen B) to dark brown (solid bitumen A). All bitumens are optically isotropic. Bitumen reflectance varies between 0.70 and 2.60%R_r, and the vitrinite reflectance ranges from 1.11 to 1.48%R_r. Based on the %R_r values, the solid bitumen identified in these samples are classified as impsonite (epi- and cata-) or pyrobitumen. No relation can be established with confidence for the reflectance of bitumens with the reflectance of vitrinite.

2.2.1. Introduction

Solid bitumen occurs in several basins all over the world associated to source rocks as well as reservoirs rocks. Solid bitumens (“migrabitumen”) are secondary organic matter products that are filling voids and fractures in rocks (Jacobs, 1989) resulting from advanced stages of thermal maturation (Curiale, 1986) and can occur in carbonate and siliciclastic rocks. Its occurrence in petroliferous basins becomes a topic of interest for organic petrologists and organic geochemists. Their presence can be an oil and/or gas indicator as

well as an indicator of maturity, especially in sedimentary sequences that are destitute of vitrinite, and can also provide some information on the migration path (e.g., Gentzis and Goodarzi, 1990; Jacob, 1989; Landis and Castaño, 1995). Furthermore, the presence of certain types of solid bitumen (e.g., pyrobitumen) can deteriorate the reservoir quality since it acts as cement reducing the porosity and permeability of the reservoir (e.g., Huc et al., 2000; Walters et al., 2006).

Generally, solid bitumens are accumulations of organic matter that contain an important solid phase and are found in petroliferous systems (e.g., Landis and Castaño, 1995) but it definition depends on whether it is being studied by organic petrologists or by organic geochemists. For organic petrologists, solid bitumen correspond to solid organic matter that filling voids and fractures in sedimentary rocks. The parameters used for its classification are based on the physical properties such as reflectance, fluorescence intensity, micro-solubility and micro - flowpoint (Jacob, 1989). Attending to these parameters, Jacob (1989) classified the solid bitumen as ozocerite, wurtzilite, albertite, asphalt, gilsonite, glance pitch, grahamite and impsonite (epi-, meso- and cata-impsonite). On the other hand, the organic geochemists define solid bitumen as the organic matter soluble in organic solvents (Tissot and Welte, 1984). Curiale (1986), using biomarker data from organic rich source rocks, defined two types of bitumen: a pre - oil bitumen with low maturity and that migrates small distances, and a post - oil bitumen, usually called pyrobitumen, that represents the residue of the oil. Despite the different definitions, the use of petrographic and geochemical techniques allows a better understanding of this type of organic material. Many studies enable a better understanding on the origin of solid bitumen and using their characteristics to evaluate the thermal maturity of the sequences: some studies are focused on geochemical analyses (Curiale et al, 1983; Curiale, 1986; George et al., 2007; Huc et al., 2000; Hwang et al., 1998; Kelemen et al., 2008, 2010); and others also include petrographic analysis (e.g., Bertrand and Héroux, 1987; Bertrand, 1990, 1993; Fowler et al., 1993; Gentzis and Goodarzi, 1990; Jacob, 1989; Landis and Castaño, 1995; Riediger, 1993; Schoenherr et al., 2007; Shalaby et al., 2012; Stasiuk, 1997).

The Lusitanian Basin (LB) is an Atlantic margin rift basin located on the western board of the Iberian Peninsula that was filled with sediments from the Upper Triassic to the Cretaceous covered with Cenozoic sediments (e.g., Azerêdo et al., 2003; Wilson, 1988).

Benfeito-1 and Freixial-1 boreholes (Arruda sub-basin, Central Sector of LB; Fig. 30) revealed the presence of dispersed solid bitumen in two carbonate formations (Candeeiros and Cabaços Formations). Candeeiros Formation (Bathonian) consists predominantly of carbonate facies deposited in a carbonate ramp with shallow waters (Carvalho et al., 2005). The Cabaços Formation, the lowermost formation of the Upper Jurassic from the LB,

comprises limestone, marls and anhydrites beds (e.g. Azerêdo et al., 2002; Leinfelder and Wilson, 1989; Wilson, 1979) and corresponds to a lacustrine marginal marine environment (e.g., Azerêdo et al., 2002; Carvalho et al., 2005; Leinfelder and Wilson, 1989).

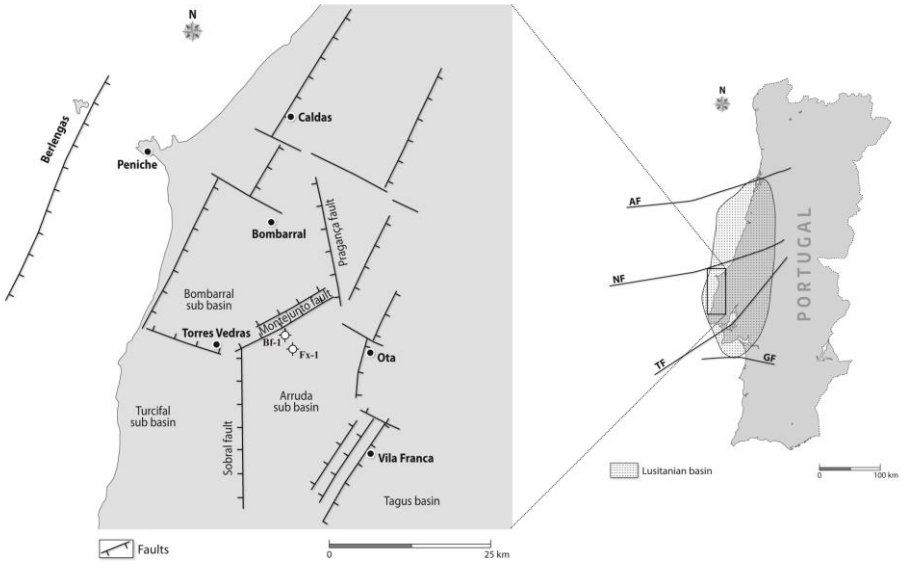

Figure 30. Geographic and tectonic settings of the Lusitanian basin (modified from Alves et al., 2002) and location of the Benfeito-1 and Freixial-1 boreholes. AF: Aveiro Fault; NF: Nazaré Fault; TF: Tagus Fault; GF: Grândola Fault; Bf-1: Benfeito-1 borehole; Fx-1: Freixial-1 borehole.

So far, there is no published data on the characteristics and origin of solid bitumen in the Lusitanian Basin but its occurrence has been reported in the Bombarral sub-basin (Central Sector of LB; Gonçalves et al., 2013) and in Lower Tagus sub-basin (Southern Sector of LB; Gonçalves et al., 2014). This paper is a first approach to the study of solid bitumen existing in the Lusitanian Basin. The main purpose of this work is to study the optical characteristics of the different solid bitumen identified in the carbonate rocks of the Candeeiros and Cabaços Formations using incident and transmitted light microscopy, and scanning electron microscopy (SEM).

2.2.2. Samples and methods

Eighteen samples were chosen for this research, twelve from Cabaços Formation and six from Candeeiros Formation (Table 19). The samples belong to Benfeito-1 (Bf-1) and Freixial-1 (Fx-1) boreholes drilled in the Arruda sub-basin (Lusitanian Basin, Portugal, Fig. 30).

Table 19. List of the studied samples ordered by borehole, depth and lithostratigraphy as well as the lithological composition

Borehole	Samples	Depth (m)	Lithostratigraphy	Lithological description
Freixial - 1	Fx24	1900	Cabaços Fm.	Limestones
	Fx25	1950	Cabaços Fm.	Limestones, silty marl and anhydrite
	Fx26	2000	Cabaços Fm.	Limestones, silty marl and anhydrite
	Fx27	2050	Cabaços Fm.	Limestones
	Fx28	2100	Cabaços Fm.	Limestones
	Fx29	2140	Cabaços Fm.	Limestones
	Fx33	2350	Candeeiros Fm.	Limestones
	Fx34	2400	Candeeiros Fm.	Limestones
	Fx35	2450	Candeeiros Fm.	Limestones
	Fx36	2500	Candeeiros Fm.	Limestones
Benfeito - 1	Bf36	1400	Cabaços Fm.	Limestones and some anhydrite
	Bf37	1425	Cabaços Fm.	Limestones and some anhydrite
	Bf38	1450	Cabaços Fm.	Limestones and some anhydrite
	Bf39	1475	Cabaços Fm.	Limestones and some anhydrite
	Bf40	1500	Cabaços Fm.	Limestones
	Bf41	1525	Cabaços Fm.	Limestones
	Bf51	1950	Candeeiros Fm.	Limestones
	Bf52	2000	Candeeiros Fm.	Limestones

The selected samples do not show evidence of weathering. According to Littke et al. (1991) the microscopic appearance of pyrite seems to be the most reliable indicator of source rock weathering because pyrite is a ubiquitous constituent in most organic matter-rich sediments. In sediments affected by weathering many pyrite crystals seem to be completely replaced by iron oxide or iron hydroxide. Thus, the organic matter in the studied samples contains exclusively fresh pyrite revealing according to these authors that they are not affected by weathering.

Please see section 1.2.1 on Part II for description of the determination of total organic carbon, total sulfur content and insoluble residue.

Please see section 1.1 on Part II for detailed description of the petrographic analyses (palynofacies and organic petrology).

2.2.3. Results and discussion

2.2.3.1. Total organic carbon, total sulfur and insoluble residue

TOC content (Table 20) varies between 0.07 wt.% (Bf52) and 1.22 wt.% (Fx29) pointing out a poor to good content of organic carbon according to the limits suggested by Peters and Cassa (1994) for carbonated rocks. Values greater than 1 wt.% occur in samples from Cabaços Formation. The lowest TOC values belong to the Candeeiros Formation reaching just 0.15 wt.% with a mean value of 0.12 wt.%. The TS content varies between 0.02 wt.% (Fx36) and 6.12 wt.% (Fx26), with an average of 0.86 wt.% (Table 20). The higher values correspond to the samples less carbonated with anhydrite of Cabaços Formation. The IR values (Table 20) reach 30%, displaying the Candeeiros Formation the lowest values (less than 2%) confirming the carbonated character of the samples.

Table 20. Geochemical and palynofacies data of the studied samples.

Formation	Samples	Geochemical data			Palynofacies data			
		TOC	TS	IR	PHY	AOM	PAL	SB
Cabaços	Fx24	0.40	0.12	5.4	59.43	34.29	1.14	5.14
	Fx25	1.05	4.20	23	52.94	14.08	2.94	30.04
	Fx26	1.00	6.12	30	45.51	13.88	2.04	38.57
	Fx27	0.53	0.20	2.4	44.06	48.99	0.58	6.38
	Fx28	0.53	0.13	2.0	54.63	37.65	0.00	7.72
	Fx29	1.22	0.84	23	69.43	17.06	3.32	10.19
Candeeiros	Fx33	0.14	0.04	<0.5	37.81	11.44	37.56	13.18
	Fx34	0.15	0.04	<0.5	65.26	2.35	8.92	23.47
	Fx35	0.15	0.11	<0.5	48.24	11.81	15.33	24.62
	Fx36	0.10	0.02	<0.5	41.01	4.17	44.30	10.53
Cabaços	Bf36	0.73	0.28	14	65.38	2.71	1.58	30.32
	Bf37	0.67	0.98	17	41.87	26.60	5.42	26.11
	Bf38	0.63	0.55	18	48.83	37.72	2.05	11.40
	Bf39	0.52	0.94	18	60.80	29.94	2.16	7.10
	Bf40	0.64	0.76	17	50.54	18.06	3.44	27.96
	Bf41	0.46	0.11	12	66.57	22.93	0.83	9.67
Candeeiros	Bf51	0.11	0.05	2	n.r.	n.r.	n.r.	n.r.
	Bf52	0.07	0.06	<1	29.03	11.73	49.56	9.65

TOC: Total organic carbon (wt.%); TS: Total sulfur (wt.%); IR: Insoluble residue (%); PHY: Phytoclast (%); AOM: Amorphous organic matter (%); PAL: Palynomophs (%); SH: Solid hydrocarbon (%); n.r.: not recoverable.

2.2.3.2. Palynofacies data

The summarized palynofacies data are listed in Table 20. Although the phytoclast group was the most expressive group of particulate organic matter, some samples revealed substantial quantities of the AOM group (up to 49%) and palynomorphs (up to 50%). Non-opaque degraded phytoclasts dominated the organic matter (OM) assemblage. Samples from Benfeito-1 borehole presented a significant percentage of opaque phytoclast (maximum of 30% of the total OM). The AOM is mostly homogeneous without fluorescence but small percentages of these particles show a brown fluorescence. Most of the AOM seems to be the result of the phytoclast and zooclasts reworking.

Palynomorphs are scarce in Cabaços samples. The color of these palynomorphs, mostly sporomorphs, varied from orange to brown (Fig. 31C) in white transmitted light, and from yellow to brown under incident blue light.

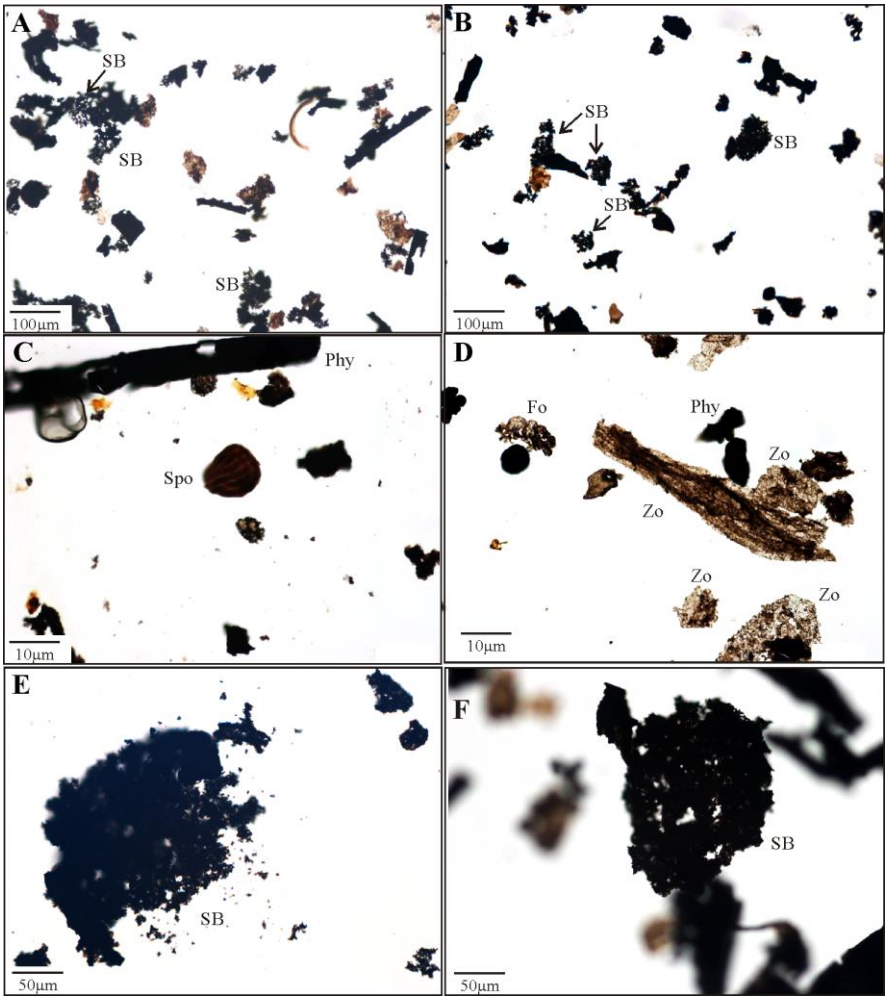

Figure 31. Photomicrographs of particulate organic matter taken under transmitted white light. A, B: general aspect (Bf40 and Fx25, respectively); C (Fx35): sporomorph; D (Fx33): zooclast and zoomorphs; E - F (Fx25 and Bf37, respectively): solid bitumen. SB: Solid bitumen; Spo: spore; Phy: phytoclast; Zo: zooclast; Fo: foraminiferal test linings.

Candeeiros Formation revealed important percentages of degraded remains of zooclasts and some zoomorphs (Fig. 31D). Solid bitumen (Fig. 31) was identified in all the studied samples, sometimes representing more than 25% of the organic matter in the samples (Table 20). This percentage increases in the anhydrite layers (Fx25, Fx26 and Bf36; Table 20). Adjacent samples, from other formations, contain also solid bitumen but in a very small proportion (less than 5% of the OM).

2.2.3.3. Optical characteristics of the solid bitumens

In transmitted white light, solid bitumen (Fig. 31) had amorphous aspect with dark brown to dark color and no fluorescence under incident blue light. SEM observations showed the amorphous aspect of this bitumen (see Fig. 32). In both methods of observation was noticed the cratered aspect (Fig. 31 and 32) of the bitumen resulting from the dissolution of carbonate minerals by the HCl treatment.

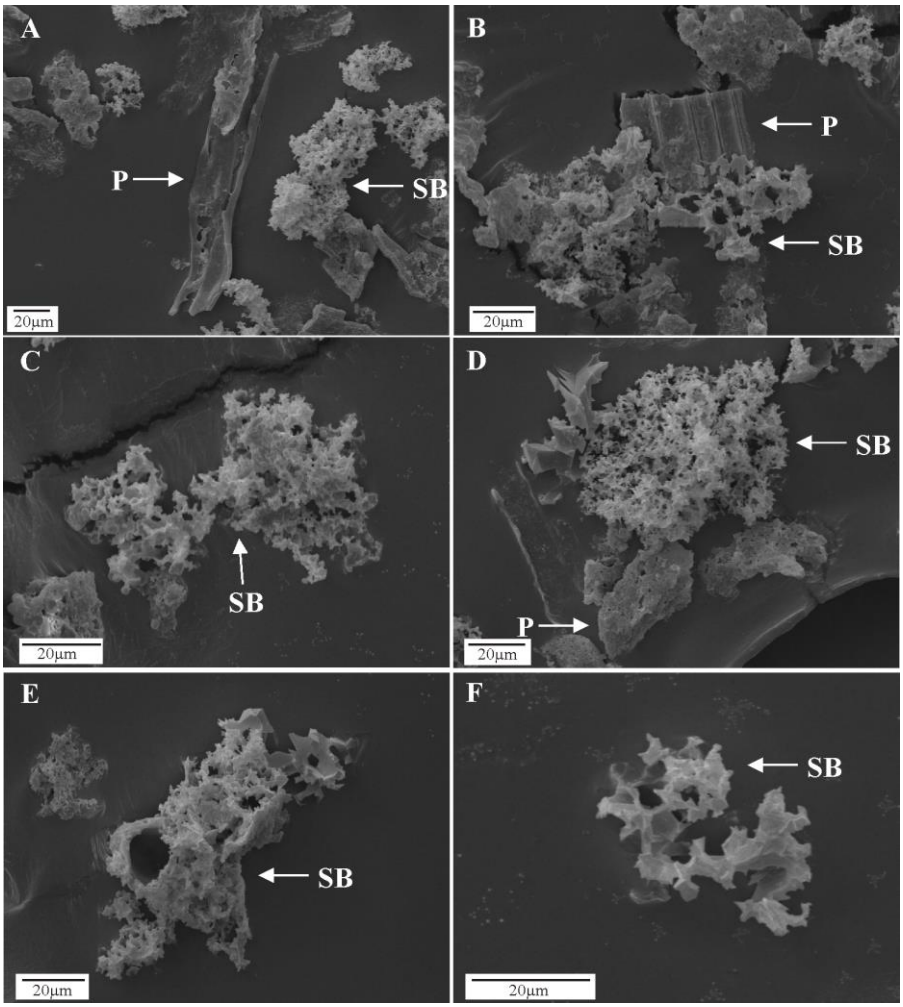

Figure 32. Photomicrographs of solid bitumen taken by SEM. A, B: solid bitumen and phytoclasts (Fx25); C to F: solid bitumen (Fx25). SB: Solid bitumen; P: Phytoclast.

The petrographic analysis under reflected white light and incident blue light was used to understand the characteristics of the organic material and its spatial relation with the mineral matrix. Petrographic observations revealed various differences in the optical characteristics (reflectance, texture and fluorescence) of the solid bitumen. This observation showed that the solid bitumen occur filling voids and fractures, and sometimes dispersed in the mineral matrix. Based on optical characteristics, three groups of solid bitumen were distinguished. Petrographic features of these solid bitumens are discussed below. All the families showed mean reflectance values higher than 0.7% and lower than 2.6%R_r (Fig. 33; Table 21) indicating high thermal maturity for the solid bitumens.

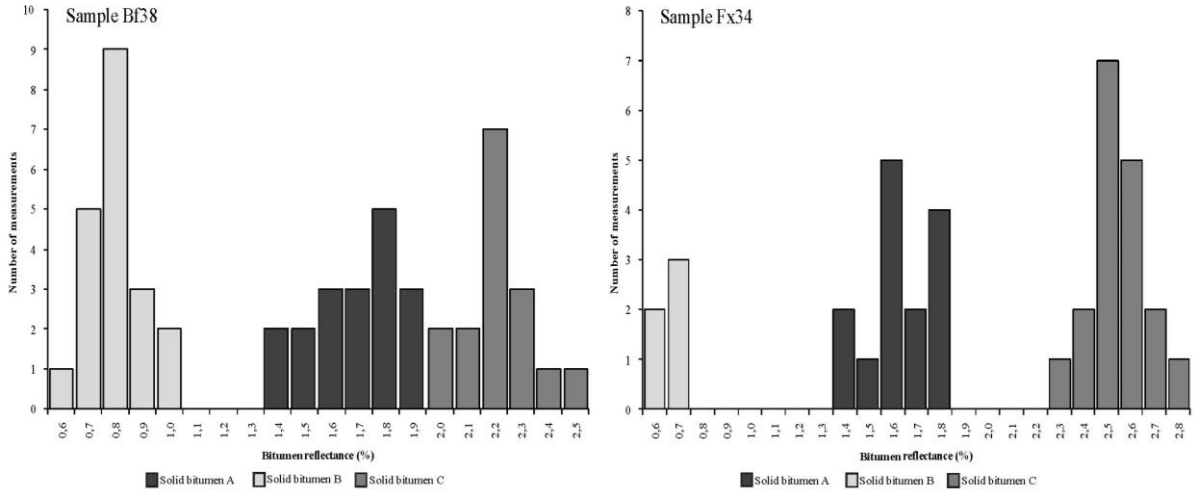

Figure 33. Histograms of solid bitumens reflectance (BR) of samples Bf38 and Fx34.

According to the reflectance data, these bitumens are classified as epi- and cata-impsonite (Jacob, 1989) or pyrobitumen (Landis and Castaño, 1995).

Solid bitumen A

Solid bitumen A (Fig. 34) was the most common of the bitumens observed and was present in all the samples selected for this study. Samples with higher IR (Fx25, Fx26, Fx29 and Bf38; see also Table 20) showed greater quantities of this bitumen. The solid bitumen A corresponds to the bitumen observed in transmitted white light and SEM (Fig. 31 and 32). In whole rock and under reflected white light, this bitumen had a grey color, brittle aspect and an irregular surface. Under blue incident light, it reveals different shades of brown. Usually the smaller particles exhibit a brown color whereas bigger particles are dark brown.

Table 21. Mean random reflectance values for vitrinite and solid bitumens

Formation	Sample	Vitrinite			Solid bitumen A			Solid bitumen B			Solid bitumen C		
		$\%R_r$	Stdev	n	$\%R_r$	Stdev	n	$\%R_r$	Stdev	n	$\%R_r$	Stdev	n
Cabaços	Fx24	1.13	0.11	20	1.48	0.15	23	-	-	-	-	-	-
	Fx25	1.37	0.10	19	1.66	0.14	20	-	-	-	2.26	0.19	2
	Fx26	1.48	0.10	2	1.79	0.11	20	-	-	-	2.33	0.17	16
	Fx27	1.20	0.11	5	1.76	0.10	21	0.89	0.07	5	2.24	0.17	4
	Fx28	1.11	0.05	4	1.68	0.10	20	-	-	-	-	-	-
	Fx29	1.47	0.08	5	1.69	0.11	26	-	-	-	2.29	0.18	8
Candeeiros	Fx33	1.22	0.09	23	1.68	0.13	4	-	-	-	2.37	0.22	17
	Fx34	1.28	0.08	17	1.62	0.17	17	0.84	0.01	2	2.58	0.12	18
	Fx35	1.27	0.13	4	1.68	0.14	8	0.70	0.05	5	2.22	0.11	22
	Fx36	1.38	0.10	11	1.69	0.12	8	0.85	0.09	10	2.44	0.24	13
Cabaços	Bf36	1.46	0.01	2	1.55	0.13	21	0.87	0.09	22	2.18	0.27	3
	Bf38	1.41	0.11	10	1.73	0.16	18	0.86	0.10	20	2.25	0.14	16
	Bf39	1.25	0.14	3	1.61	0.14	19	0.81	0.08	20	2.02	-	1
	Bf40	1.20	0.12	3	1.42	0.04	5	0.70	0.03	8	2.09	0.11	13
	Bf41	1.26	-	1	1.51	0.07	11	0.87	-	1	2.31	-	1
Candeeiros	Bf51	-	-	-	1.78	0.09	2	-	-	-	2.21	0.07	4
	Bf52	-	-	-	1.57	0.09	5	-	-	-	1.94	-	1

$\%R_r$: mean random reflectance (%): Stdev: standard deviation (%); n: number of particles measured.

Solid bitumen A appears filling the inter-mineral spaces and dispersed in the mineral matrix. It shape varies according to the pores shape where it occurs. Sometimes, pyrite was associated to this bitumen. The mean random reflectance ranges from 1.42 to 1.79$\%R_r$ (average of 1.64$\%R_r$; see Table 21) and are optically isotropic.

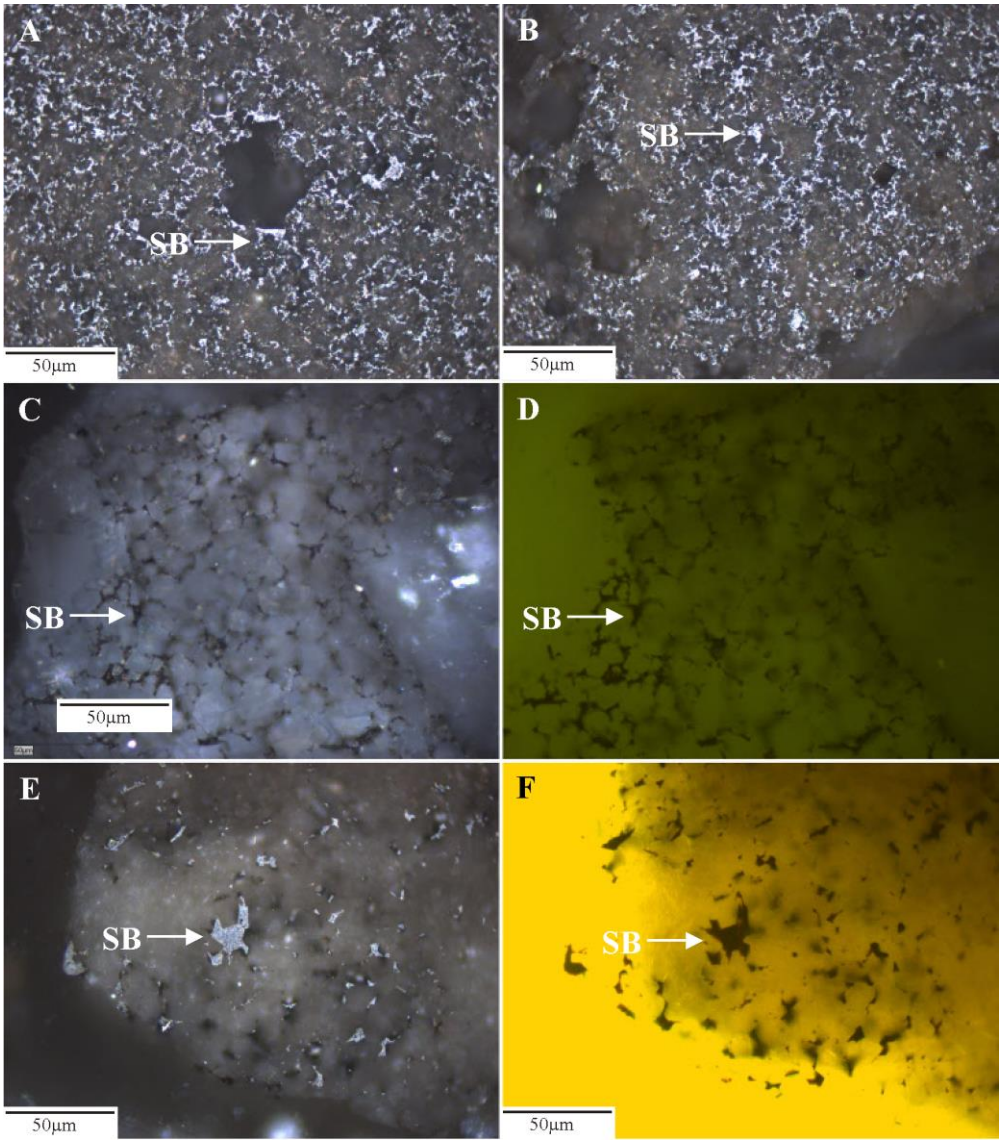

Figure 34. Photomicrographs of solid bitumen A taken under reflected white light (RL) and fluorescence mode (FM). A, B (Fx25); C, D (Fx36); E, F (Fx25). RL: A, B, C, E; FM: D, F. SB: Solid bitumen.

Solid bitumen B

Solid bitumen B (Fig. 35) was neither detected (Table 21) in the Candeeiros Formation (Benfeito-1 borehole) nor in the majority of the samples of Cabaços Formation (Freixial-1 borehole). With the exception of the top of Cabaços Formation in the Benfeito-1 borehole (Bf36, Bf38 and Bf39), this bitumen was scarce in the studied samples. When present this was regularly associated with the mineral matrix filling the voids. They had a dark grey color, brittle aspect, an irregular surface and fluorescence (from intense yellow to light brown; Fig. 35). The mean random reflectances varied between 0.70 to 0.89%R_r (Table 21).

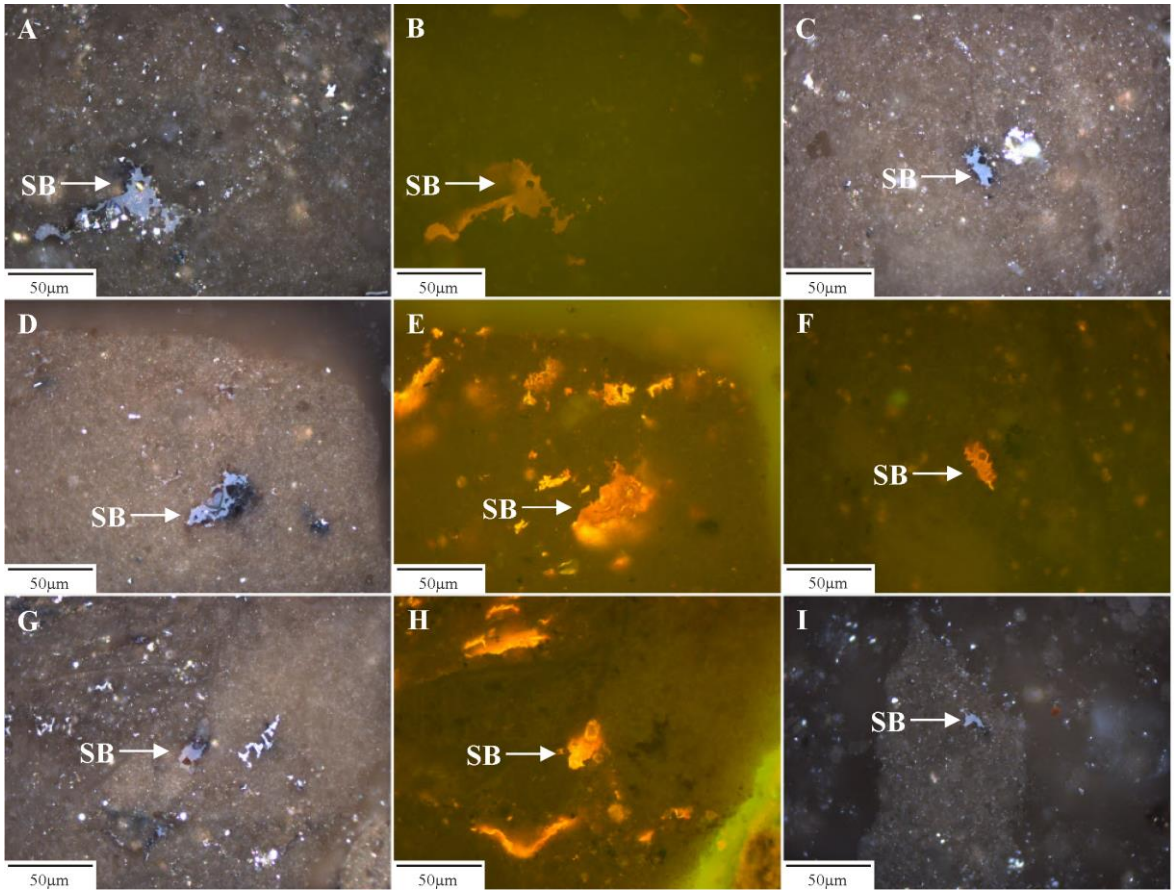

Figure 35. Photomicrographs of solid bitumen B taken under reflected white light (RL) and fluorescence mode (FM). A, B (Bf39); C, F (Fx35); D, E (Fx27); G, H (Bf40); I (Bf38). RL: A, C, D, G; FM: B, E, F, H. SB: Solid bitumen.

Solid bitumen C

This bitumen was observed in most samples (see Table 21) but in lower amount than solid bitumen A. When present it is usually associated with limestones or sparry calcite (Fig. 36). Similar features were also found by other authors (e.g., Sun et al., 1995). Typically are larger than the others described above. Solid bitumen C (Fig. 36) exhibit homogeneous optical properties, with easy polishing, smooth surfaces and mosaic structures, and was optically isotropic. This bitumen displays a mean random reflectance values from 1.94 to 2.58%R_r (mean value 2.23%R_r; Table 21).

2.2.3.4. Relationship between vitrinite and solid bitumen reflectance

In the studied samples vitrinite, inertinite and liptinite macerals (Fig. 37) were observed. In general, the samples proved to be poor or devoid of vitrinite, mainly in the samples from Benfeito-1 borehole (Table 21). Vitrinite particles are usually small size. Cutinite and sporinite were found in low quantities and inertinite (mainly semifusinite) was observed, principally in Cabaços Formation.

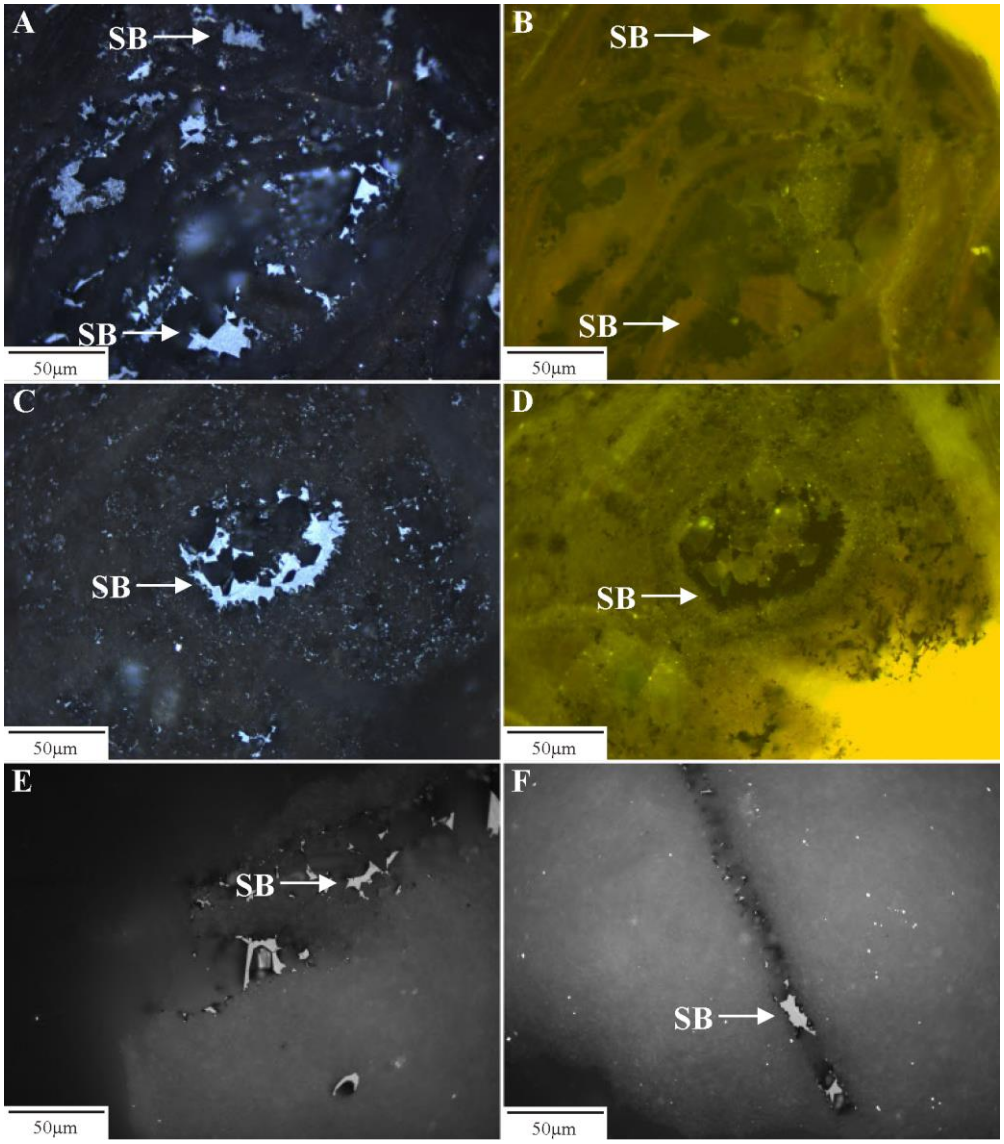

Figure 36. Photomicrographs of solid bitumen C taken under reflected white light (RL) and fluorescence mode (FM). A, B (Fx35); C, D (Fx26); E, F (Fx35). RL: A, C, E, F; FM: B, D. SB: Solid bitumen.

The mean random reflectance of vitrinite was measured in the same samples as the bitumens. The values varied between 1.13 and 1.48%R_r (Table 21), pointing out to a thermally mature to overmature sequences. Comparing the mean random reflectance for vitrinite and the solid bitumens, was possible to note that bitumens A and C show high reflectance than vitrinite. Gentzis and Goodarzi (1990) also found three bitumen families (Panartic Dundas C-80 well, Melville Island) all of them showing higher maturity than their hosted rocks.

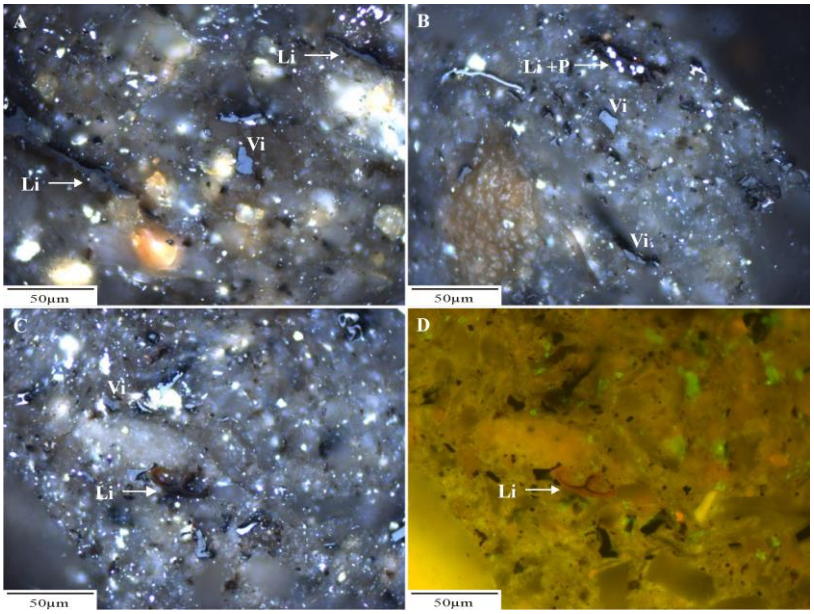

Figure 37. Photomicrographs taken under reflected white light (RL) and fluorescence mode (FM). A (Fx25); B (Fx24); C-D (Fx25). RL: A to C; FM: D. Vi: vitrinite; Li: Liptinite; P: Pyrite.

Table 22 shows some empirical relationships that were established to correlate the reflectance of vitrinite with the reflectance of solid bitumen in order to determine the thermal maturity of the samples where vitrinite was absent. Through the established relations the reflectance of the solid bitumen (BR) can be used to calculate the vitrinite reflectance equivalent (VR_{eqv}).

Table 22. Some relationships between vitrinite reflectance equivalent (VReqv) and solid bitumen reflectance (BR).

Author (s)	Correlation equation
Jacob (1989)	VR_{eqv}= (0.618*BR)+0.4
Riediger (1993)[1]	VR_{eqv}= (0.277*BR)+0.57
Landis and Castaño (1995)	VR_{eqv}=(BR+0.41)/1.09
Schoenherr et al (2007)	VR_{eqv}= (BR+0.2443)/1.0495
Bertrand and Malo (2012)	VR_{eqv}= 1.2503*$BR_{(limestones)}$ $^{0.904}$
(and references therein)	VR_{eqv}= 0.8113*$BR_{(shale-marl)}$ $^{1.2438}$

[1] Relationships established for BR > 0.52% (for smaller values, the relationship is equivalent to the one proposed by Jacob, 1989).

In samples with several bitumens the reflectance value of the autochthonous bitumen (non-migrated) should be used to correlate with the vitrinite reflectance (e.g., Bertrand, 1990; Gentzis and Goodarzi, 1990; Jacob, 1989). Plotting solid bitumen B reflectance versus vitrinite reflectance, it was observed that the correlation is poor (R = 0.30) and has no statistical significance (Fig. 38). The same is true (Fig. 38) for solid bitumen A (R = 0.39) and solid bitumen C (R = 0.17). According to these data, there is no linear relationship between bitumen and vitrinite reflectance.

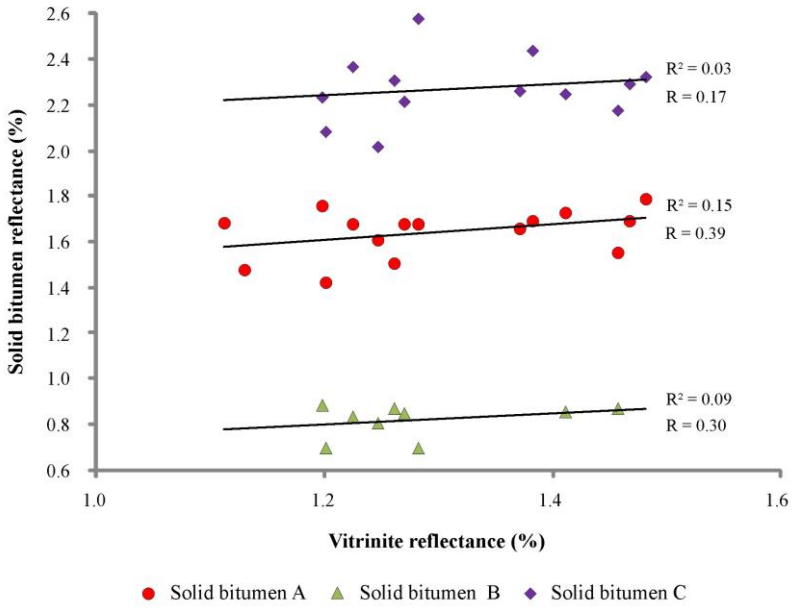

Figure 38. Correlation between vitrinite reflectance (%) and solid bitumens reflectance (%).

Furthermore, plotting the mean random reflectance of vitrinite and bitumen versus depth (Fig. 39), it was noticed that vitrinite and bitumen reflectance values do not display a linear depth-thermal maturity trend. In fact, the values of mean random reflectance of the bitumen do not show significant increase with the burial depth. It was expected that the reflectance of autochthonous bitumens increases with increasing of depth while the reflectance of allochthonous bitumens remains more or less constant (Gentzis and Goodarzi, 1990). This behavior is exhibited by the three groups of the bitumens studied (Fig. 39).

2.2.4. Solid bitumen in the Lusitanian Basin: where is their source?

The solid bitumens observed in this study are allochthonous bitumens (“migrabitumen”, Jacob, 1989), i.e., bitumens that had suffered migration processes. Some bitumens can migrate hundreds of miles to get trapped in a reservoir rock (e.g., Jacob, 1989;

Landis and Castaño, 1995; Petersen et al., 2013). The presence of several bitumens in the same rock can be related with various thermal events and/or different temporal pulses of hydrocarbons migration (e.g., Gentzis and Goodarzi, 1990; Stasiuk, 1997).

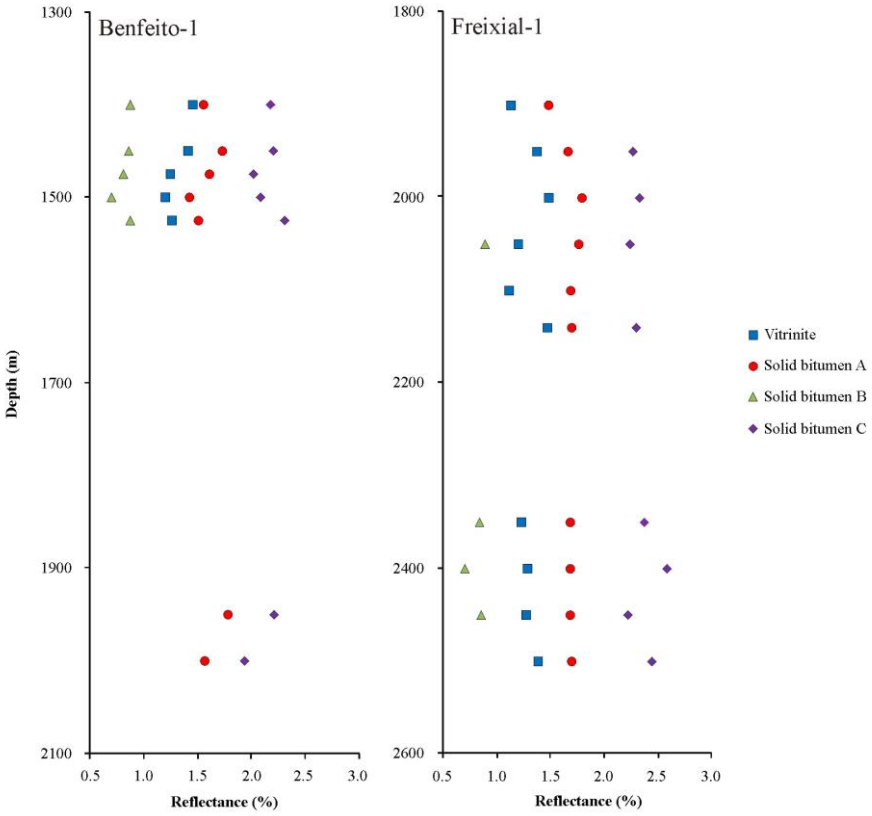

Figure 39. Bitumen and vitrinite reflectance (%) versus depth (m) of Benfeito-1 and Freixial-1 boreholes.

Different processes like biodegradation and/or weathering, thermal cracking, gas deasphalting of bitumen or preexistent oil hydrocarbons, or precipitation of preexistent oil in a reservoir can lead to the production of solid bitumens (e.g., Curiale, 1986; Hwang et al, 1998; Schoenherr et al., 2007; Kelemen et al., 2008, 2010). Geochemical studies are needed to permit the identification of the process that gave rise to the solid bitumen identified in the Arruda sub-basin (Lusitanian Basin). Based on the petrographic observation, seems that the origin of the solid bitumens A, B and C is not related with weathering once no petrographic evidences such as cracks and oxidation rims around the particles were detected.

Although the Lusitanian Basin show evidence of a potential source rocks of Jurassic age (Lower - Middle Jurassic and Oxfordian), several studies pointed out an immature stage for the organic matter (e.g., Duarte et al., 2012; Gonçalves et al., 2013; Poças Ribeiro et al., 2013; Silva et al., 2014). However some boreholes (on- and offshore) have revealed good

evidence of hydrocarbons (DPEP, 2014) but their source rock remains unknown. So far, no economics oil and/or gas occurrences have been discovered in the Lusitanian Basin neither in others sedimentary basins in Portugal.

2.2.5. Conclusions

Solid bitumens were identified in samples from Candeeiros and Cabaços Formations in the Arruda sub-basin (Lusitanian Basin) and are the purpose of this study. The following conclusions were drawn:

1) The Candeeiros and Cabaços Formations from Freixial-1 and Benfeito-1 boreholes have an irregular distribution of solid bitumens, which occur filling voids, veins and fracture, and dispersed in the mineral matrix;

2) Three types of bitumens were distinguished according their optical characteristics: (i) solid bitumen A - identified in all samples both in transmitted and reflected white lights, and mean random reflectance ranging between 1.42 and 1.79%R_r; (ii) solid bitumen B - irregular and dark grey surface with intense fluorescence (mean reflectance 0.91%R_r); and, (iii) solid bitumen C - smooth surfaces with mean random reflectance > 2.0%R_r;

3) No relationship between bitumen and vitrinite reflectance was established. The mean random reflectance of bitumen is more or less constant with the depth. These facts are indicative of migrated hydrocarbons and consequently they are allochthonous bitumen;

4) In this basin, solid bitumen reflectance cannot be used as a maturity parameter for the samples devoid of vitrinite;

5) The presence of allochthonous bitumen is an indicator of hydrocarbon generation and/or migration in the Lusitanian Basin or in neighbor basins.

References

Alves, T.M., Gawthorpe, R.L., Hunt, D.W., Monteiro, J.H., 2002. Jurassic tectono-sedimentary evolution of the Northern Lusitanian Basin (offshore Portugal). Marine and Petroleum Geology 19, 727 - 754.

Azerêdo, A.C., Duarte, L.V., Henriques, M.H., Manuppella, G., 2003. Da dinâmica continental no Triásico aos mares do Jurássico Inferior e Médio. Cadernos de Geologia de Portugal. Instituto Geológico e Mineiro, Lisboa. ISBN 972-98469-9-5.

Azerêdo, A.C., Wright, V.P., Ramalho, M.M., 2002. The Middle - Late Jurassic forced regression and disconformity in central Portugal: eustatic, tectonic and climatic effects on a carbonate ramp system. Sedimentology 49, 1339 - 1370.

Bertrand, R., 1990. Correlations among the reflectances of vitrinite, chitinozoans, graptolites and scolecodonts. Organic Geochemistry 15, 565 - 574.

Bertrand, R., 1993. Standardization of solid bitumen reflectance to vitrinite in some Paleozoic sequences of Canada. Energy Sources 15, 269 - 287.

Bertrand, R., Héroux, Y., 1987. Chitinozoan, graptolite and scolecodont reflectance as an alternative to vitrinite and pyrobitumen reflectance in Ordovician and Silurian Strata, Anticosti Island, Quebec, Canada. American Association of Petroleum Geologists Bulletin 71, 951 - 957.

Bertrand, R., Malo, M., 2012. Dispersed organic matter reflectance and thermal maturation in four hydrocarbon exploration wells in the Hudson Bay Basin: regional implications. Geological Survey of Canada, Open File 7066, 52 p.

Carvalho, J., Matias, H., Torres, L., Manupella, G., Pereira, R., Mendes-Victor, L. 2005. The structural and sedimentary evolution of the Arruda and Lower Tagus sub-basins, Portugal. Marine and Petroleum Geology 22, 427 - 453.

Curiale, J.A., 1986. Origin of solid bitumens, with emphasis on biological marker results. Organic Geochemistry 10, 559 - 580.

Curiale, J.A., Harrison, W.E., Smith, G., 1983. Sterane distribution of solid bitumen pyrolyzates. Changes with biodegradation of crude oil in Ouachita Mountains, Oklahoma. Geochimica et Cosmochimica Acta 47, 517 - 523.

DPEP, Divisão para a Pesquisa e Exploração de Petróleo. Ministério da Economia, Governo de Portugal. http://www.dgeg.pt/dpep/en/history.htm (retrieved 9th January 2014).

Duarte, L.V., Silva, R.L., Mendonça Filho, J.G., Poças Ribeiro, N., Chagas, R.B.A., 2012. High-resolution stratigraphy, palynofacies and source rock potential of the Água de Medeiros formation (Lower Jurassic), Lusitanian basin, Portugal. Journal of Petroleum Geology 35, 105 - 126.

Fowler, M.G., Kirste, D.M., Goodarzi, F., Macqueen, R.W, 1993. Optical and geochemical classification of Pine Point bitumens and evidence for their origin from two separate source rocks. Energy Sources 15, 315 - 337.

Gentzis, T., Goodarzi, F., 1990. A review of the use of bitumen reflectance in hydrocarbon exploration with examples from Melville Island, Arctic Canada, in: V.F. Nuccio and C.E.

Barker (Eds.). Applications of thermal maturity studies to energy exploration: SEPM, Rocky Mountain Section, 23 - 36.

George, S.C., Volk, H., Ahmed, M., Pickel, W., Allan, T., 2007. Biomarker evidence for two sources for solid bitumens in the Subu wells: Implications for the petroleum prospectivity of the East Papuan Basin. Organic Geochemistry 38, 609 - 642.

Gonçalves, P.A., Mendonça Filho, J.G., Mendonça J.O., Silva, T.F., Flores, D., 2013. Paleoenvironmental characterization of a Jurassic sequence on the Bombarral sub-basin (Lusitanian basin, Portugal): Insights from palynofacies and organic geochemistry. International Journal of Coal Geology 113, 27 - 40.

Gonçalves, P.A., Mendonça Filho, J.G., Silva, T.F., Mendonça J.O., Flores, D., 2014. The Mesozoic-Cenozoic organic facies in the Lower Tagus sub-basin (Lusitanian Basin, Portugal): Palynofacies and organic geochemistry approaches. Marine and Petroleum Geology 52, 42 - 56.

Huc, A.Y., Nederlof, P., Debarre, R., Carpentier, B., Boussafir, M., Laggoun-Défarge, F., Lenail-Chouteau, A., Bordas-Le Floch, N., 2000. Pyrobitumen occurrence and formation in a Cambro–Ordovician sandstone reservoir, Fahud Salt Basin, North Oman. Chemical Geology 168, 99 - 112.

Hwang, R.J., Teerman, S.C., Carlson, R.M., 1998. Geochemical comparison of reservoir solid bitumens with diverse origins. Organic Geochemistry 29, 505 - 517.

ISO 7404-2, 2009. Methods for the petrographic analysis of coals - Part 2: Methods of preparing coal samples. International Organization for Standardization. 12pp.

Jacob, H., 1989. Classification, structure, genesis and practical importance of natural solid oil bitumen (“migrabitumen”). International Journal of Coal Geology 11, 65 - 79.

Kelemen, S.R., Walters, C.C., Kwiatek, P.J., Afeworki, M., Sansone, M., Freund, H., Pottorf, R.J., Machel, H.G, Zhang, T., Ellis, G.S., Tang, Y., Peters, K.E., 2008. Distinguishing solid bitumens formed by thermochemical sulfate reduction and thermal chemical alteration. Organic Geochemistry 39, 1137 - 1143.

Kelemen, S.R., Walters, C.C., Kwiatek, P.J., Freund, H., Afeworki, M., Sansone, M., Lamberti, W.A., Pottorf, R.J., Machel, H.G, Peters, K.E., Bolin, T., 2010. Characterization of solid bitumens originating from thermal chemical alteration and thermochemical sulfate reduction. Geochimica et Cosmochimica Acta 74, 5305 - 5332.

Landis, C.R., Castaño, J.R., 1995. Maturation and bulk chemical properties of a suite of solid hydrocarbons. Organic Geochemistry 22, 137 - 149.

Leinfelder, R.R., Wilson, R.C.L., 1989. Seismic and sedimentologic features of Oxfordian-Kimmeridgian syn-rift sediments on the eastern margin of the Lusitanian Basin. Geologische Rundschau 79, 81 - 104.

Littke, R., Klussmann, U., Krooss, B., Leythaeuser, D., 1991. Quantification of loss of calcite, pyrite, and organic matter due to weathering of Toarcian black shales and effects on kerogen and bitumen characteristics. Geochimica et Cosmochimica Acta 55, 3369 - 3378.

Mendonça Filho, J.G., Menezes, T.R., Mendonça, J.O., Oliveira, A.D., Silva, T.F., Rondon, N.F., Silva, F.S., 2012. Organic Facies: Palynofacies and Organic Geochemistry Approaches, in: Panagiotaras, D. (Org.), Geochemistry Earth's system processes. InTech, Patras, ISBN 978-9-53-510586-2, vol. 1, pp. 211 - 245.

Mendonça Filho, J.G., Menezes, T.R., Mendonça, J.O., Oliveira, A. D., Souza, J.T., Sant'Anna, A.J., 2011. Kerogen: Composition and Classification. Chapter 3 in: ICCP Training Course on Dispersed Organic Matter, ISBN 978-9-89-826567-8, pp. 17 - 24.

Peters, K.E., Cassa, M.R., 1994. Applied source rock geochemistry, in: Magoon, L.B., Dow, W.G. (eds.), The petroleum system – from source to trap, AAPG Memoir 60, Tulsa, pp. 93 - 120.

Petersen, H.I., Schovsbo, N.H., Nielsen, A.T., 2013. Reflectance measurements of zooclasts and solid bitumen in Lower Paleozoic shales, southern Scandinavia: Correlation to vitrinite reflectance. International Journal of Coal Geology 114, 1 - 18.

Poças Ribeiro, N., Mendonça Filho, J.G., Duarte, L.V., Silva, R.L., Mendonça, J.O., Silva, T.F., 2013. Palynofacies and organic geochemistry of the Sinemurian carbonate deposits in the western Lusitanian Basin (Portugal): Coimbra and Água de Madeiros formations. International Journal of Coal Geology 111, 37 - 52.

Riediger, C.L., 1993. Solid bitumen reflectance and Rock-Eval T_{max} as maturation indices: an example from the "Nordegg Member", Western Canada Sedimentary Basin. International Journal of Coal Geology 22, 295 - 315.

Schoenherr, J., Littke, R., Urai, J.L., Kukla, P.A., Rawahi, Z., 2007. Polyphase thermal evolution in the Infra-Cambrian Ara Group (South Oman Salt Basin) as deduced by maturity of solid reservoir bitumen. Organic Geochemistry 38, 1293 - 1318.

Shalaby, M.R., Hakimi, M.H., Abdullah, W.H., 2012. Geochemical characterization of solid bitumen (migrabitumen) in the Jurassic sandstone reservoir of the Tut Field, Shushan Basin, northern Western Desert of Egypt. International Journal of Coal Geology 100, 26 - 39.

Silva, R. L., Mendonça Filho, J.G., Azerêdo, A., Duarte, L.V., 2014. Palynofacies and TOC analysis of marine and non-marine sediments across the Middle - Upper Jurassic boundary in the central-northern Lusitanian Basin (Portugal). Facies 60, 255 - 276.

Stasiuk, L.D., 1997. The origin of pyrobitumens in Upper Devonian Leduc Formation gas reservoirs, Albert, Canada: an optical and EDS study of oil to gas transformation. Marine and Petroleum Geology 14, 915 - 929.

Sun, Y.Z., Püttmann W., Speczik, S., 1995. Differences in the depositional environment of basal Zechstein in southwest Poland: implication for base metal mineralization. Organic Geochemistry 23, 819 - 835.

Tissot, B., Welte, D.H., 1984. Petroleum formation and occurrence, second ed. Springer Verlag, Hidelberg.

Tyson, R.V., 1995. Sedimentary Organic Matter. London, Chap. & Hall.

Walters, C.C., Kelemen, S.R., Kwiatek, P.J., Pottorf, R.J., Mankiewicz, P.J., Curry, D.J., Putney, K., 2006. Reactive polar precipitation via ether cross-linkage: A new mechanism for solid bitumen formation. Organic Geochemistry 37, 408 - 427.

Wilson, R.C.L., 1979. A reconnaissance study of Upper Jurassic sediments of the Lusitanian basin. Ciências da Terra, Universidade Nova Lisboa 5, 53 - 84.

Wilson, R.C.L., 1988. Mesozoic Development of the Lusitanian Basin, Portugal. Revista Sociedad Geológica de España 1, 393 - 407.

2.3. The presence of zooclasts and zoomorphs in the carbonate Candeeiros formation (Arruda sub-basin, Lusitanian Basin, Portugal): paleoenvironmental evidence

Adapted from Paula Alexandra Gonçalves, João Graciano Mendonça Filho, Joalice Mendonça Oliveira, Deolinda Flores

Comunicações Geológicas

Accepted

Abstract

Zooclasts correspond to animal-derived organic particles such as crustacean eggs, tintinnids, insect cuticles fragments and other arthropods fragments. Zoomorph subgroup is composed by animal-derived palynomorphs including foraminiferal linings, chitinozoa and scolecodonts. Due to their characteristics, it is very rare to find these organic particles in the kerogen assemblage of ancient marine sediments. The Candeeiros formation (informal unit), corresponds to sediments of the inner part of a carbonate ramp developed in the Middle Jurassic, showed in some layers the presence of degraded remains of particulate organic matter classified as zooclasts and foraminiferal test-linings (zoomorphs). The fact that such amounts of zooclasts and zoomorphs were preserved is indicative of high zooplankton productivity and consequently high primary productivity. To allow the survival of these organisms the water column must be oxygen rich. Despite the high primary productivity, the accumulation and preservation of the organic matter in the sediments was weak as evidenced by the lower total organic carbon content (less than 0.16wt.%).

2.3.1. Introduction

Zooclasts are a group of organic matter that comprised animal-derived organic particles having, in most of the cases, specific morphological characteristics. This group includes fish spines and scales, arthropod exoskeletal debris, tintinnids, insect cuticles fragments, organic linings from some bivalve shells, ostracod carapaces, graptolite fragments and crustacean eggs. Zooclasts are rarely found in the kerogen assemblage from ancient marine sediments (Tyson, 1995). Its rarity has two reasons: i) its biomass is much lower than the phytoplankton (the “ecological transfer efficiency” between phytoplankton and zooplankton is about 10%); and ii) they have more proteinaceous animal organic matter which is more easily and rapidly degraded (Tyson, 1995). So, it is much less probable that

these organic particles are preserved, principally in recognizable form, than the phytoplankton. Zoomorph subgroup is composed by animal-derived palynomorphs (discrete unitary animal derived particles, whether whole or damaged, are classified as zoomorph palynomorphs) including foraminiferal test-linings, chitinozoa and scolecodonts. It is identifiable as fragmented zoomorph palynomorphs (Tyson, 1989, 1995).

The Middle Jurassic Candeeiros formation (informal unit), from the Lusitanian Basin (LB), comprises limestones, dolomitic limestone, dolomites and oobioclastic/oncolitic /fenestral limestones (e.g., Azerêdo et al., 2002). According to Azerêdo et al. (2002), this formation corresponds to sedimentation on an inner to mid-carbonate ramp where normal marine and restricted micro- and macrofauna are present. Azerêdo (1999) refers that the Candeeiros formation has a rich microfossil assemblage comprising mainly agglutinated benthic foraminifera, calcareous algae and porostromates. Studies in the Maciço Calcário Estremenho allowed Azerêdo (2007) and Azerêdo et al. (2003) to define 5 formations for this period of time: Fórnea Formation (Lower Jurassic - basal Lower Aalenian), Barranco do Zambujal Formation (Lower Aalenian - Lower Bajocian), Chão das Pias Formation (Lower Bajocian to Upper Bajocian), Serra de Aire Formation (Bathonian) and Santo António-Candeeiros Formation (Bathonian to Callovian).

The aims of this paper are: i) to describe the kerogen assemblage of some levels from the carbonate Candeeiros formation in the region of the central LB usually defined as Arruda sub-basin; and ii) to point out the importance of the zooclasts and zoomorphs for paleoenvironmental reconstruction.

2.3.2. Samples and Methodologies

This study focused on the organic matter (OM) present in sediments from the Candeeiros formation, represented in cutting samples (Table 23) belonging to the Freixial-1 and Benfeito-1 boreholes (Arruda sub-basin, Lusitanian Basin). According to the geological report, Freixial-1 samples correspond to micritic limestone, finely recrystallized or with a grainstone/packstone texture. The report from Benfeito-1 borehole indicates that the samples correspond to limestone (sometimes grainstone/packstone), dolomitic and oolitic/pseudoolitic limestone with lithoclastic and bioclasts, and some layers of dolomite. Bajocian (?) - Bathonian age are assigned to these samples (see Table 23; data from the geological reports).

Table 23. Palynofacies and geochemical data from Candeeiros formation samples (Benfeito-1 and Freixial-1 boreholes, Arruda sub-basin, Lusitanian Basin). For samples 2050, 2100, 2150 and 2250 no palynofacies data is available due to the low organic residue recovered.

Age	Depth (m)	Phy (%)	AOM (%)	Pal (%)	Zooclast (%)	TOC (wt.%)	TS (wt.%)	IR (%)
Freixial-1 borehole								
Bathonian	2350	43.18	13.07	4.55	39.20	<0.16	0.04	<0.5
	2400	84.24	3.03	3.64	9.09		0.04	
	2450	63.58	15.56	1.66	19.21		0.11	
	2500	45.06	4.58	2.41	47.95		0.02	
Benfeito-1 borehole								
Bajocian? to Bathonian	2000	32.04	12.94	0.32	54.69	<0.12	0.06	<1
	2050	-	-	-	-		0.06	
	2100	-	-	-	-		0.07	
	2150	-	-	-	-		0.02	
	2200	60.86	31.25	0.66	7.24		0.02	
	2250	-	-	-	-		0.01	
	2300	80.40	18.94	0.66	0		0.03	
	2350	54.98	28.94	0.32	15.76		0.02	

TOC: Total organic carbon (wt.%); TS: Total sulfur (wt.%); IR: Insoluble residue (%); PHY: Phytoclast (%); AOM: Amorphous organic matter (%); PAL: Palynomophs (%).

Please see section 1.2.1 on Part II for description of the determination of total organic carbon, total sulfur content and insoluble residue.

Please see section 1.1.1 on Part II for detailed description of the palynofacies analysis.

In total, 12 (kerogen concentrate) samples were performed however 4 of them were not used due to their low content of organic matter (less than 300 particles).

2.3.3. Results

2.3.3.1. Geochemical analyses

The studied carbonate material from Candeeiros formation showed a very low content of OM. The TOC values range between 0.07 and 0.20 wt.% (Table 23), with a mean value of 0.10wt.%. TOC content represents the organic richness of sedimentary rocks (Jarvie, 1991) and its quantity depends of three primary variables: the influx of organic matter, the preservation and the dilution by the mineral matrix (Tyson, 1995). The TS content varied

between 0.02 wt.% and 0.19 wt.% (Table 23). The IR values (Table 23) in all the samples were lower than 1% pointing out to pure carbonate samples.

2.3.3.2. Palynofacies

In general, samples from Candeeiros formation have small amounts of particulate organic matter for counting and revealed a severely degraded appearance (Fig. 40). The palynofacies of Candeeiros formation have a mixture of terrestrial and marine organic matter. In the majority of the samples the phytoclast group prevailed (Table 23). Opaque phytoclasts represent approximately 20% (in average) of the total organic matter. Striate phytoclasts and non-biostructured non-opaque phytoclasts have also important contributions. The amorphous organic matter (AOM) is mostly homogeneous with diffuse outlines, is orange to brown in color (under white transmitted light) and exhibited very weak fluorescence (brown color) under incident blue light (Fig. 40D). Some AOM seems to be the result of zooclast reworking. Sporomorphs, freshwater and marine microplankton were rare or absent. Foraminiferal test-lignin (zoomorph subgroup), when present, revealed a several degraded aspect (Fig. 40E - F) or is fragmented. The zooclasts (Fig. 40A - C) represent approximately 24% (mean value) of the total organic matter; however, in two samples (Table 23) they represent more than 40% of the OM preserved. A few samples were impregnated with black solid bitumen.

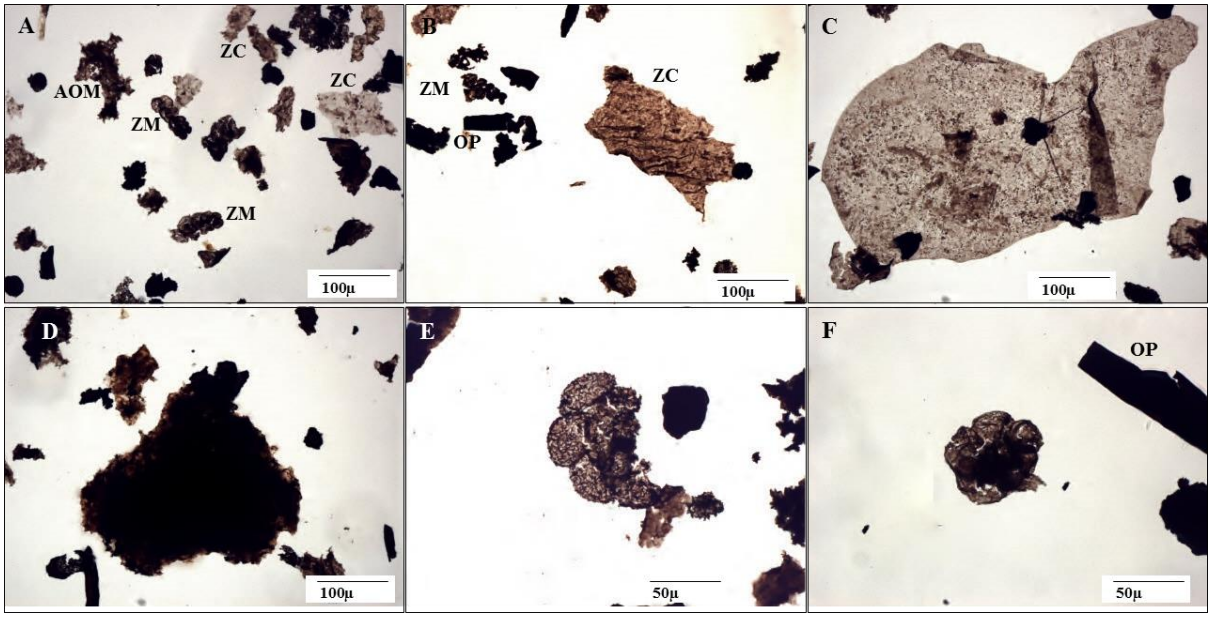

Figure 40. Photomicrographs taken under transmitted white light of the studied Candeeiros formation samples (Benfeito-1 and Freixial-1 boreholes, Arruda sub-basin, Lusitanian Basin). A: General view; B-C: Zooclasts; D: Amorphous organic matter (AOM); E-F: foraminiferal test-linings (zoomorphs). OP: opaque phytoclast; ZM: zoomorph; ZC: zooclast.

2.3.4. Zooclasts and zoomorphs: paleoenvironmental evidence

The presence of marine organic matter in sediments is influenced by the primary productivity, oxygenation rates, diagenetic processes and sedimentation accumulation rates (e.g., Tyson, 1995). Autotrophic phytoplankton is the major producer of organic matter in these environments. According to Tissot & Welte (1984), there is a relationship between autotrophic phytoplankton and heterotrophic zooplankton regarding their occurrence and distribution. The same authors indicate that there is a tendency for the biomass of zooplankton to be higher in areas where there is high productivity of phytoplankton. To enable the development of these organisms it is necessary a rich-oxygen water column. Thus, it is expected that the oxygen was available during the deposition of Candeeiros formation allowing the development of important zooplankton populations that consumed a large part of the phytoplankton existing in the system. These new data are according to the literature which states a rich microfossil assemblage as well the presence of macrofauna in this formation (Azerêdo, 1999).

The preservation of the organic matter depends of several factors, some related with the OM characteristics and others associated with the depositional environment characteristics, such as the redox condition (e.g., Martin & Sayles, 2005; Tissot & Welte, 1984). Tissot and Welte (1984) referred that low TOC content in sediments can be related with the oxicity of the depositional environment, and affects the amount and elemental composition of the stored OM. Also, low sediment accumulation rates under oxic conditions led to a minimal preservation of the OM (Tyson, 1995). Furthermore, during diagenetic processes, in oxic and suboxic environments, there is an important loss (complete or <60%) of organic matter which will reflect in TOC contents (Müller, 1977 in Tyson, 1995).

Attending to the above, it can be suggested that the low TOC contents in the Candeeiros formation are due the high productivity, high oxygen in the system and consequently low OM preservation. The preservation of zooclasts and zoomorphs, contrary to what would be expected, was, probably, due to the great increase of these type of organisms during the Bajocian(?) - Bathonian.

2.3.5. Conclusions

Qualitative and quantitative characteristics of the palynological content of zooclasts and zoomorphs are indicative that the studied succession of the informal Candeeiros formation was deposited in an oxic environment, which represents unfavorable conditions for the preservation of the OM. Nevertheless, the preservation of zooclasts and zoomorphs implies great concentration of zooplankton. Low TOC content and the preservation of

remains of zooclasts and zoomorphs in Candeeiros formation suggest a period of high primary productivity in an oxic water column that led to a boom of the zooplankton. The supply of OM derived from phytoplankton to the bottom of the deposition basin was small due the presence of zooplankton forms of OM.

References

Azerêdo, A.C., 1999. Etudes micropaléontologiques dans les séries carbonatées du Jurassique moyen du Bassin Lusitanien (Portugal). Comun. Inst. Geol. Mineiro, 86, 59 - 84.

Azerêdo, A.C., 2007. Formalização da Litostratigrafia do Jurássico Inferior e Médio do Maciço Calcário Estremenho (Bacia Lusitânica). Comunicações Geológicas, 94, 29 - 51.

Azerêdo, A.C., Duarte, L.V., Henriques, M.H., Manuppella, G., 2003. Da dinâmica continental no Triásico aos mares do Jurássico Inferior e Médio. Cadernos de Geologia de Portugal. Instituto Geológico e Mineiro, 43.

Azerêdo, A.C., Wright, V.P., Ramalho, M.M., 2002. The Middle-Late Jurassic forced regression and disconformity in central Portugal: eustatic, tectonic and climatic effects on a carbonate ramp system. Sedimentology, 49, 1339 - 1370.

Jarvie, D.M., 1991. Total organic carbon (TOC) analysis: Chapter 11: geochemical methods and exploration. In: Merril, R.K. (Ed.). Source and Migration Processes and Evaluation Techniques, Tulsa, Treatise of Petroleum Geology. AAPG, pp. 113 - 118.

Martin, W.R., Sayles, F.L., 2005. The recycling of biogenic material at the seafloor. In: Mackenzie, F.T. (Ed.), Sediments, diagenesis and sedimentary rocks, 7. Treatise on Geochemistry, Holland, H.D. and Turekian, K.K. (Eds.). Elsevies-Pergamon, Oxford, 37 - 65.

Mendonça Filho, J.G., Menezes, T.R., Mendonça, J.O., 2011b. Organic Composition (Palynofacies Analysis). Chapter 5. In: ICCP Training Course on Dispersed Organic Matter, 33 - 81.

Mendonça Filho, J.G., Menezes, T.R., Mendonça, J.O., Oliveira, A.D., Souza, J.T., Sant'Anna, A.J., 2011a. Kerogen: Composition and Classification. Chapter 3. In: ICCP Training Course on Dispersed Organic Matter, 17 - 24.

Mendonça Filho, J.G., Menezes, T.R., Mendonça, J.O., Oliveira, A.D., Silva, T.F., Rondon, N.F., Silva, F.S., 2012. Organic Facies: Palynofacies and Organic Geochemistry Approaches. In: Panagiotaras, D. (Org.), Geochemistry Earth's system processes. In: Tech, Patras, ISBN 978-9-53-510586-2, vol. 1, pp. 211 - 245.

Tissot, B., Welte, D.H., 1984. Petroleum formation and occurrence, second ed. Springer Verlag, Hidelberg, 540p.

Tyson R.V., 1995. Sedimentary Organic Matter. London, Chap. & Hall, 615p.

Tyson, R.V., 1989. Late Jurassic palynofacies trends, Piper and Kimmeridge Clay Formation, UK onshore and northern North Sea. In: Batter, D.J., Ken, M.C. (Eds.), Northwest European Micropalaeontology and Palynology, British Micropalaeontological Society Series, Ellis Horwood, Chichester, pp. 135 - 172.

3. Lower Tagus sub-basin

3. 1. The Mesozoic - Cenozoic organic facies in the Lower Tagus sub-basin (Lusitanian Basin, Portugal): Palynofacies and organic geochemistry approaches

Adapted from Paula Alexandra Gonçalves, João Graciano Mendonça Filho, Taís Freitas da Silva, Joalice Oliveira Mendonça, Deolinda Flores

Marine and Petroleum Geology (2014) 52, 42 - 56

Accepted 25th January 2014

Abstract

Studies of the Mesozoic and Cenozoic sequence crossed by the Barreiro-4 borehole provide an improved understanding of the organic matter deposited in the Lower Tagus sub-basin (Lusitanian Basin, Portugal) and the implications for the potential source rock and depositional environment. This study focused on 43 samples (Middle Jurassic to Neogene) that were subjected to palynofacies and organic geochemistry analyses (Total Organic Carbon, Rock-Eval pyrolysis and molecular biomarker analysis). The palynofacies data indicate that the sequence contains mainly phytoclasts (non-opaque phytoclasts). However, the Middle Jurassic samples are dominated by Amorphous Organic Matter (AOM). Continental and/or marine palynomorphs are present in all the samples. The Cretaceous samples are characterized by small amounts of kerogen that have high contents of solid bitumen. The Total Organic Carbon (TOC) content is generally less than 1 wt.%. The Rock-Eval S1 and S2 parameters vary from 0.01 to 3.50 mgHC/g rock and 0.15 to 34.03 mgHC/g rock, respectively, with the highest values corresponding to the Cretaceous samples. The hydrogen index (HI) and oxygen index (OI) values range from 35 to 552 mgHC/g TOC and 4 to 180 mgHC/g TOC, respectively. The T_{max} values range from 416 to 437ºC. The biomarker analysis showed that *n*-alkanes with 15-30 carbon atoms are present and usually have a unimodal distribution with predominance of low to medium molecular weight compounds. The CPI values range between 0.63 and 3.65, and the pristane/phytane ratios vary between 0.48 and 1.64, indicating alternation of oxic-anoxic conditions along the sequence. The distribution of terpanes shows small amounts of tricyclic and tetracyclic terpanes in most of the samples (except for some Cretaceous samples) and a predominance of pentacyclic terpanes. The amount of 17α (H),22,29,30-trisnorhopane (Tm) usually exceeds the amount of 18α (H),22,29,30-trinorneohopane (Ts). The 20S/(20S + 20R) and αββ/(ααα + αββ) ratios of the

C29 steranes generally have values below the range of equilibrium, indicating an immature stage of the OM.

3.1.1. Introduction

The accumulation and preservation of the organic matter (OM) depends on several conditions, such as primary productivity, transport, sedimentation rates and oxygenation of the water column. Part of the OM may be transformed into hydrocarbons depending on the geological events that occur over time (e.g., Hunt, 1979; Tissot and Welte, 1984). Palynofacies and geochemical parameters are important tools for studying OM in ancient sediments and allow the assessment of potential source rocks and paleoenvironmental reconstructions.

Numerous studies have been published about the OM in sediments from the North and Central Sectors of the Lusitanian Basin. They contributed to the recognition of specific intervals as potential source rocks (e.g., Duarte et al., 2012; Oliveira et al., 2006; Poças Ribeiro et al., 2013; Silva et al., 2014); the identification of large-scale perturbations of the carbon cycle (Silva et al., 2011); and, to better understanding the paleoenvironmental context (e.g., Duarte et al., 2010, 2011; Gonçalves et al., 2013; Silva et al., 2012). These studies were focused on onshore Jurassic deposits and revealed immature organic matter preserved in a marine environment under variable redox conditions. Two stratigraphic intervals (upper Sinemurian - late Pliensbachian and Oxfordian) have been identified as potential hydrocarbon source rocks (e.g., Duarte et al., 2011, 2012; Silva et al., 2014). However, no data are available for the Lower Tagus sub-basin in the southern part of the Lusitanian Basin.

This study presents a detailed overview of the OM that is present in the sediments of the Lower Tagus sub-basin. Samples were collected from several stratigraphic units (Middle Jurassic to Neogene) in this sub-basin. Palynofacies and geochemical evaluations of forty-three samples from the Barreiro-4 borehole (hereinafter called Br-4) were performed to determine: 1) the origin of the organic matter; 2) the thermal maturity; 3) the hydrocarbon potential; and 4) the depositional environment. Due to the aims of this study, preference was given to the informal names of the formations because they are used by the oil companies operating in Portugal.

3.1.2. Geological setting

Please see section 6 on Part I for detailed description geological setting.

3.1.3. Lithostratigraphy of the study area

The study area is located in the southern part of the Lusitanian Basin (Fig. 41). The Lower Tagus sub-basin developed as a NNW-SSW elongated saucer-shaped basin. Sedimentological and seismic data indicate that this sub-basin was a platform (Middle Oxfordian - Late Kimmeridgian) that was most likely controlled by the Setúbal-Pinhal Novo fault (Carvalho et al., 2005). During the Late Cretaceous, the sub-basin had the geometry of a foredeep basin as a result of the extensional tectonics induced by NW-SE compressive episodes of the Alpine orogeny (Carvalho et al., 2005; Rasmussen et al., 1998; Ribeiro et al., 1990). During this period, the sub-basin was filled with more than 2 km of siliciclastic sediments that alternate from coarse sandstones to silty mudstones.

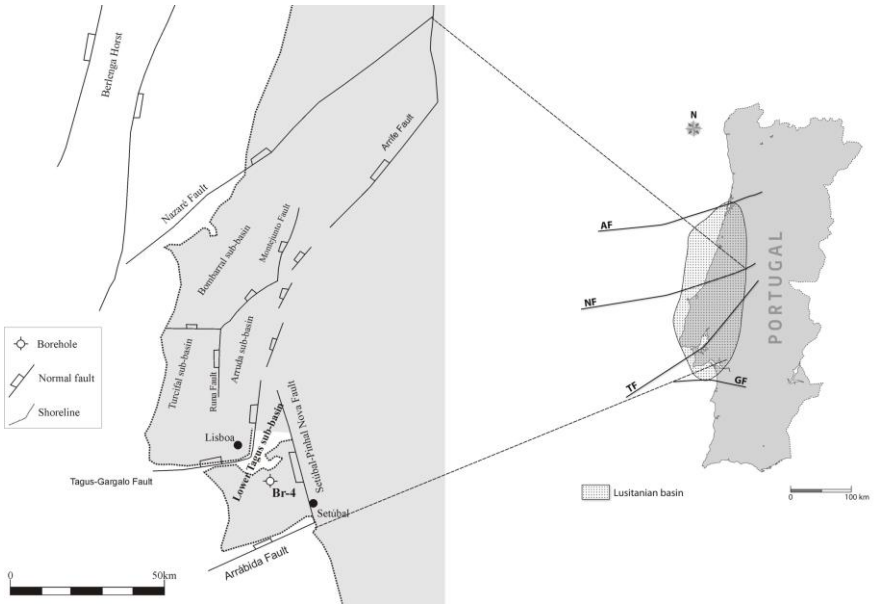

Figure 41. Geographic and tectonic settings of the Lusitanian basin (modified from Alves et al., 2002; Wilson et al., 1989) and location of Barreiro-4 (Br-4) borehole. AF: Aveiro Fault; NF: Nazaré Fault; TF: Tagus Fault; GF: Grândola Fault.

3.1.3.1. Mesozoic

3.1.3.1.1. Jurassic

The sedimentary record (Fig. 42) of the top of the Lower Jurassic is difficult to identify in the Lower Tagus sub-basin (Carvalho et al., 2005). The oldest record recognized in the Br-4 sequence (Fig. 43) belongs to the Brenha Formation (Bathonian to Callovian). In the Barreiro area, the Bathonian sediments are characterized by dolomitic limestones with layers of clay that were deposited in a shallow open carbonate platform. Fossiliferous and/or

bioturbated marls, marly limestones and compact limestones are present in other parts of the sub-basin (Azerêdo et al., 2002, Carvalho et al., 2005).

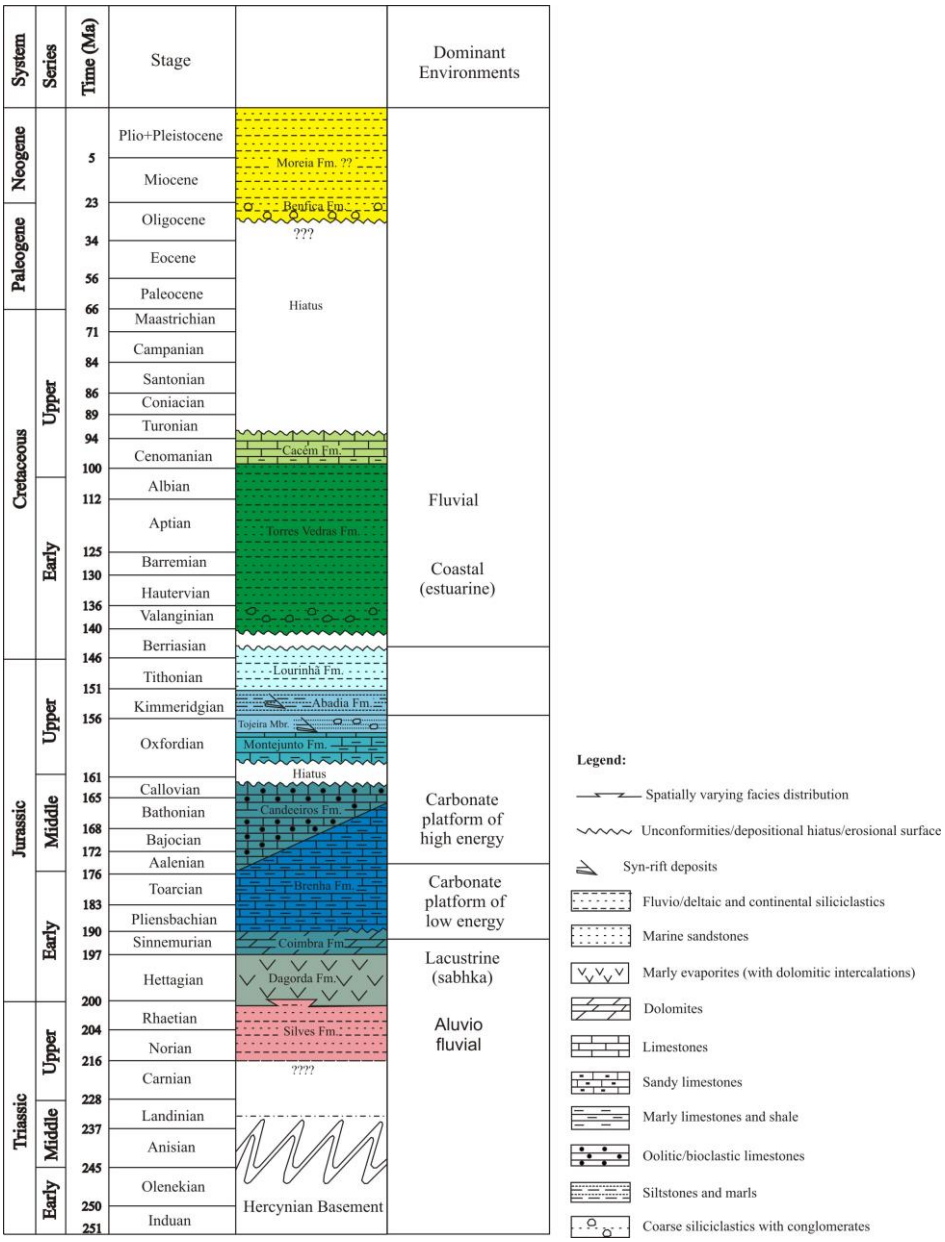

Figure 42. General stratigraphy of the southern Lusitanian basin (modified from Cunha, 2008).

The transition to the Callovian corresponds to a stratigraphic gap. The Callovian limestones reveal progressive dolomitization and were deposited on a high energy continental shelf at a relatively constant depth (Carvalho et al., 2005). The Montejunto Formation (Middle to Late Oxfordian) directly overlies the Middle Jurassic limestones, and the Cabaços Formation is missing.

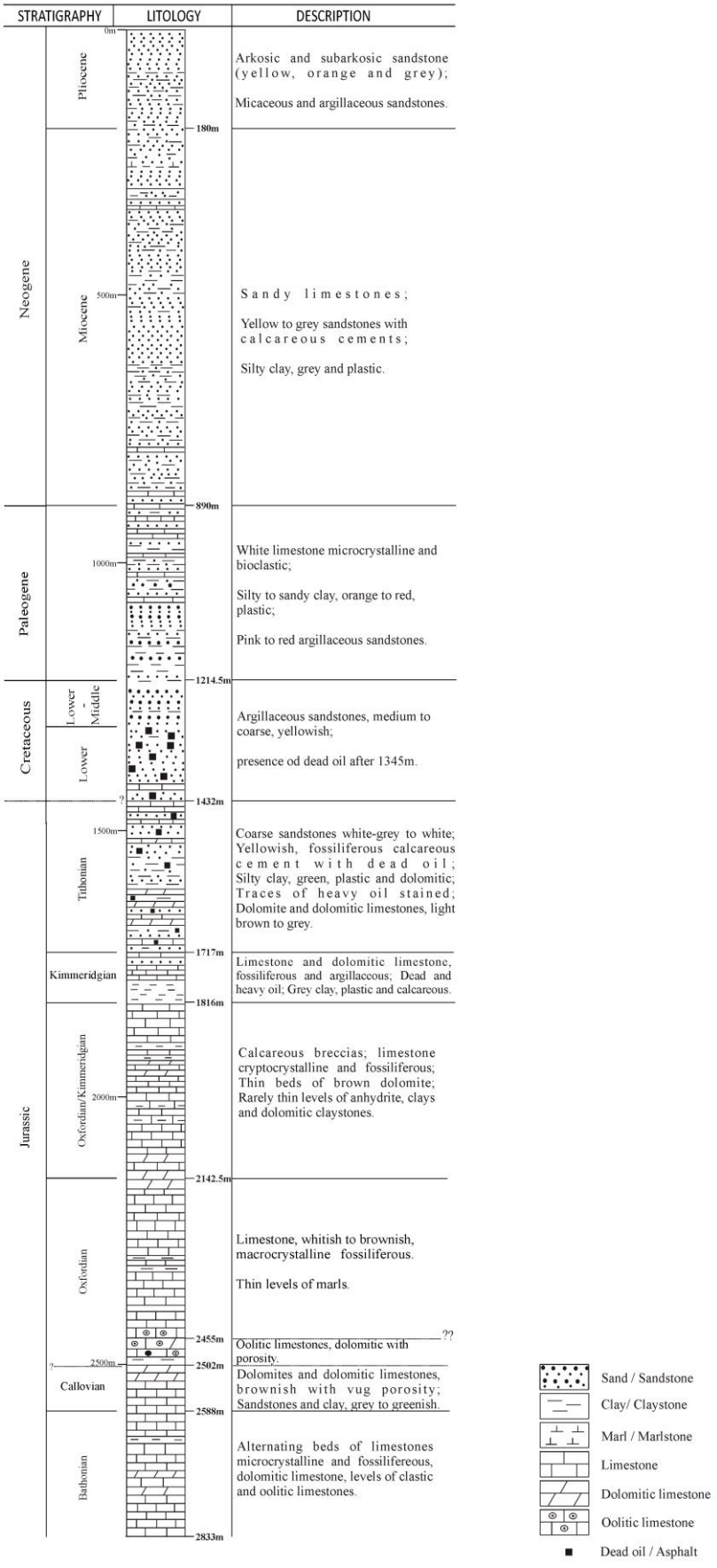

Figure 43. Simplified stratigraphic column of the sedimentary sequence by the Br-4 borehole (data from the geological report, which is available upon request at the DPEP).

The Montejunto Formation generally corresponds to a shelf carbonate facies (Carvalho et al., 2005). In the Barreiro area, it is characterized by a reef facies, whereas shallow water limestones facies are present in other locations. The Abadia Formation (Kimmeridgian age) is mostly a siliciclastic unit, is predominantly marly - detritic, and is interpreted as the result of prograding submarine fans (Kullberg et al., 2013). However, in the Lower Tagus sub-basin, carbonate sedimentation continued during this period. According to seismic studies (e.g., Ellis et al., 1990), the Lower Tagus sub-basin was a stable platform, although deep-water carbonate facies are present (in peri-diapiric zones) during the Kimmeridgian. In the Br-4 borehole, the Abadia Formation (Fig. 43) comprises brechoid para-reef limestones with detritic intercalations and clayish cement. The Amaral Formation (late Kimmeridgian) corresponds to a carbonate facies that was the result of shallow-water shelf carbonates coincident with a regressive episode (Carvalho et al., 2005; Kullberg et al., 2013). In contrast, the Lourinhã Formation (Upper Kimmeridgian to Tithonian) is characterized by sandstones and marls with rare layers of limestones that were deposited in a lacustrine to marine environment. Significant inputs of clastic sediments can be observed in the Barreiro area (Kullberg et al., 2013).

3.1.3.1.2. Cretaceous

The Valanginian to early Aptian succession in the Barreiro area corresponds to the Torres Vedras Formation and consists mainly of continental sediments that were deposited in fluvial environments (Kullberg et al., 2006; Rasmussen et al., 1998). A transgressive phase occurred after this period (Cenomanian-Turonian) and led to the deposition of shallow marine limestones and shales known as the Cacém Formation (Rasmussen et al., 1998). According to Rasmussen et al. (1998), the latest Cretaceous sediments are absent in the southern part of the Lusitanian Basin.

3.1.3.2. Cenozoic

The Lower Tagus sub-basin began to be filled with alluvial sediments in the Paleogene (Cunha et al., 2009; Kullberg et al., 2006). The deposits are characterized by interbedded layers of clay, silts and sands (sometimes cemented) and some limestones (Antunes and Pais, 1993). The deposition of sandstones with occasional limestone intercalations was the result of alluvial fans located on the footwalls of faults (Carvalho et al., 2005). The deposition of sediments during the Neogene was controlled by tectonic pulses and was sometimes related to glacio-eustatic sea-level curves, with the maximum transgression occurring in the Serravallian (Rasmussen et al., 1998). The Atlantic Ocean

invaded the basin at the beginning of the Miocene (Kullberg et al., 2006; Pais et al., 2012), and the marine and brackish water affected the depositional environment (Antunes and Pais, 1993). However, the deposition was predominately marine between Lisbon and the Arrábida hills (Carvalho et al., 2005). The Pliocene is characterized by a regressive trend (Kullberg et al., 2013). High-energy marine and fluvial environments allowed the deposition of feldspathic sandstones, coarse sandstones, gravels and conglomerates (Carvalho et al., 2005).

3.1.4. Samples and methods

Forty-four samples were collected from the Barreiro-4 borehole, which encountered a sedimentary sequence (siliciclastic and carbonate) that extended from the Middle Jurassic (Bathonian) to the Neogene (Fig. 43). The geological report of this borehole is available upon request at the Divisão para a Pesquisa e Exploração de Petróleo (DPEP).

Please see section 1.1. on Part II for detailed description of the palynofacies procedures.

Please see section 1.2. on Part II for detailed description of the geochemical analyses procedures.

3.1.5. Results and discussion

3.1.5.1. Jurassic

3.1.5.1.1. Palynofacies

Brenha Formation

A high abundance of AOM groups (all particulate organic components that appear to lack structure at the scale of light microscopy; Tyson, 1995) was observed in the Brenha Formation samples, but the abundance decreased from the bottom to the top (Table 24). The majority of the AOM (Fig. 44A - B) was homogeneous and was pale brown in transmitted white light and yellow to brownish in incident blue light. However, heterogeneous AOM was common and contained inclusions of palynomorphs, phytoclasts and pyrite. These types of AOM are the result of microbial reworking of phytoplankton or bacteria in reducing conditions (Mendonça Filho et al., 2012; Tyson, 1995).

Table 24. Palynofacies results from Br-4 borehole samples.

	Formation	Depth (m)	Sample	OP (%)	NOP (%)	AOM (%)	SPO (%)	FWM (%)	MAR (%)
Neogene		200	Br1	n.r.	n.r.	n.r.	n.r.	n.r.	n.r.
		400	Br2	23.00	39.33	12.00	7.33	0.00	18.33
		600	Br3	17.61	41.86	30.90	5.32	0.00	4.32
		800	Br4	10.20	62.97	25.66	0.29	0.00	0.87
Paleogene		1000	Br5	12.96	67.44	14.95	2.99	0.00	1.66
		1200	Br6	25.91	22.92	39.53	9.97	1.33	0.33
			Mean	*17.94*	*46.91*	*24.61*	*5.18*	*0.27*	*5.10*
Cretaceous	Torres Vedras	1225	Br7	n.r.	n.r.	n.r.	n.r.	n.r.	n.r.
		1250	Br8	n.r.	n.r.	n.r.	n.r.	n.r.	n.r.
		1275	Br9	22.12	44.55	27.10	5.92	0.00	0.31
		1300	Br10	20.46	49.83	27.72	1.65	0.00	0.33
		1325	Br11	7.81	57.66	20.42	6.01	0.00	8.11
		1350	Br12	n.r.	n.r.	n.r.	n.r.	n.r.	n.r.
		1375	Br13	n.r.	n.r.	n.r.	n.r.	n.r.	n.r.
		1400	Br14	n.r.	n.r.	n.r.	n.r.	n.r.	n.r.
		1425	Br15	19.48	46.10	23.38	10.71	0.00	0.32
			Mean	*17.47*	*49.54*	*24.66*	*6.07*	*0.00*	*2.27*
Upper Jurassic	Lourinhã	1450	Br16	26.56	39.02	15.41	13.11	0.00	5.90
		1500	Br17	26.71	45.03	9.32	13.35	0.00	5.59
		1550	Br18	20.25	67.41	5.70	4.75	0.00	1.90
		1600	Br19	n.r.	n.r.	n.r.	n.r.	n.r.	n.r.
		1650	Br20	27.53	60.44	2.85	8.54	0.00	0.63
		1700	Br21	18.21	62.65	14.81	4.32	0.00	0.00
			Mean	*23.85*	*54.91*	*9.62*	*8.82*	*0.00*	*2.80*
	Amaral	1750	Br22	7.85	69.37	16.49	6.28	0.00	0.00
		1800	Br23	18.88	67.55	4.42	8.85	0.00	0.29
			Mean	*13.37*	*68.46*	*10.46*	*7.57*	*0.00*	*0.15*
	Abadia	1850	Br24	16.00	72.00	7.50	4.50	0.00	0.00
		1900	Br25	25.00	59.21	8.68	7.11	0.00	0.00
		1950	Br26	7.21	82.45	4.39	5.96	0.00	0.00
		2000	Br27	6.95	84.12	4.96	3.72	0.00	0.25
		2050	Br28	1.99	84.72	8.64	4.65	0.00	0.00
		2100	Br29	8.82	33.53	24.41	11.76	1.47	20.00
			Mean	*10.95*	*69.34*	*9.76*	*6.28*	*0.25*	*3.38*
	Montejunto	2150	Br30	n.r.	n.r.	n.r.	n.r.	n.r.	n.r.
		2200	Br31	3.19	78.91	8.95	5.75	0.00	3.19
		2250	Br32	2.27	75.32	15.91	3.57	0.00	2.92
		2300	Br33	2.29	67.32	7.19	14.05	4.25	4.90
		2350	Br34	3.50	67.64	9.91	10.20	2.04	6.71
		2400	Br35	4.11	53.96	10.56	16.72	5.57	9.09
		2450	Br36	1.66	52.98	11.26	20.20	2.65	11.26
			Mean	*2.84*	*66.02*	*10.63*	*11.75*	*2.42*	*6.35*
Middle Jurassic	Brenha	2500	Br37	n.r.	n.r.	n.r.	n.r.	n.r.	n.r.
		2550	Br38	3.08	65.64	15.38	13.59	0.26	2.05
		2600	Br39	0.00	23.33	67.00	7.33	1.67	0.67
		2650	Br40	0.59	37.87	33.73	23.08	1.48	3.25
		2700	Br41	0.96	21.73	54.63	15.02	0.00	7.67
		2750	Br42	2.56	36.36	44.89	13.35	1.70	1.14
		2800	Br43	4.41	32.35	45.29	10.00	1.18	6.76
			Mean	*1.93*	*36.21*	*43.49*	*13.73*	*1.05*	*3.59*

OP: Opaque phytoclasts; NOP: Non-opaque phytoclasts; AOM: Amorphous organic matter; SPO: Sporomorphs; FWM: Freshwater microplankton; MAR: Marine palynomorphs. n.r.: not recoverable.

Some AOM showed euhedral craters that resulted from the dissolution of carbonate minerals by the HCl treatment. This type of AOM is considered to be bacterially derived and is generally related to lower TOC values (Mendonça Filho et al., 2010). The majority of the phytoclasts (tissues derived from terrestrial higher plants; Bostick, 1971) were non-biostructured non-opaque and biostructured (banded). Opaque phytoclasts, cuticles and membranes were rare or absent. Sporomorphs were the dominant type of palynomorphs (organic-walled microfossils), especially pollen grains of the genus *Classopollis*. These plants were adapted to hot and dry climates and to a wide range of salinity conditions (Mendonça Filho et al., 2011b; Tyson, 1995).

Marine palynomorphs were identified mainly in samples of Bathonian age, especially the foraminiferal test linings. According to several authors (e.g., Tyson, 1995), these palynomorphs are good indicators of marine conditions. They were well conserved, varied in color from pale brown to brown under transmitted white light and were brown when observed in blue light. The presence of dinoflagellate cysts and algae of the genus Tasmanites confirmed the marine conditions.

Montejunto Formation

Montejunto Formation is characterized by the presence of phytoclasts followed by the palynomorph group. The phytoclasts increase from the bottom to the top, while the distribution of palynomorphs was the opposite (Table 24). Non-biostructured non-opaque phytoclasts (Fig. 44C - F) are dominant, but the striate and banded phytoclasts increase towards the top of the formation; this was most likely related to a slight increase in distance from the terrestrial source area. In the palynomorph group, the sporomorph subgroup (Fig. 44D - E) was more abundant than the algae. In the sporomorph subgroup, pollen grains were most common in the organic matter assemblage, but their relative percentages decreased towards the top of the formation. The pollen grains had various forms, sizes and colors (pale yellow to yellow under white light and intense yellow to dark yellow under blue light).

Several samples (Br33 - Br36) contained agglomerates (dyads, tetrads) of the genus *Classopollis*. Spores with different sizes, shapes (from oval to triangular and some winged spores) and ornamentations were also present (Table 24).The samples from the bottom contained *Zygnema*-type zygospores and green algae from the Desmidiales Order (Fig. 44C and F), but they were absent at the top (Table 24). Marine palynomorphs were also present, but they decreased in abundance from the bottom to the top (see also Table 24). Dinoflagellate cysts (Fig. 44G - H), acritarchs and Prasinophyte algae were present in small

amounts. As in the Brenha Formation, foraminiferal test-linings (Fig. 44I) were the major marine palynomorphs.

AOM (Fig. 44C and 44F) was also present; it had a homogeneous aspect, without inclusion and was brown in both transmitted white and incident blue light, which most likely resulted from the diagenesis of macrophyte tissues (Mendonça Filho et al., 2012, 2011b, 2010; Tyson, 1995). The samples from this formation contained solid bitumen (Br32 - Br36), which decreased in abundance from the bottom to the top.

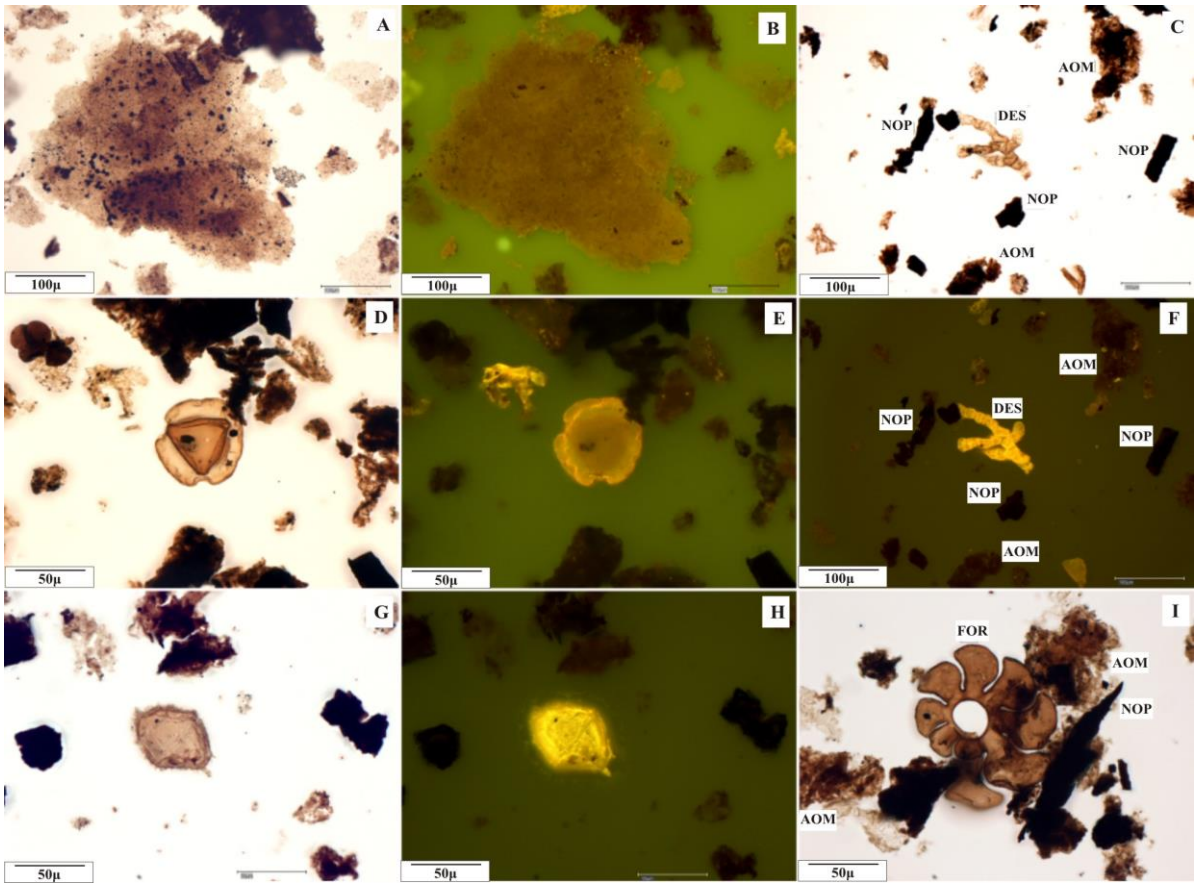

Figure 44. Photomicrographs of Jurassic particulate organic matter taken under transmitted white light (TL) and fluorescence mode (FM). A - B: AOM (Br39); C and F: algae from the Desmidiales Order (DES), non-opaque phytoclast (NOP) and AOM (Br34); D - E: spores (Br34); G - H: Dinoflagellate cyst (Br34); I: foraminiferal test-linings (Br34). TL: A, C, D, G, I; FM: B, D, F, H.

Abadia and Amaral Formations

The Abadia Formation is characterized almost exclusively by terrestrial organic matter (except for sample Br29) with a high abundance of non-opaque phytoclasts and sporomorphs (Table 24). The biostructured non-opaque phytoclasts dominated the OM assemblage and were represented mainly by the striate and banded tissues. The color of the

sporomorphs (spores and pollen grains) varied from orange to orange - brown in white transmitted light, and the fluorescence varied from yellow to dark yellow. Some of the pollen grains were from the genus *Classopollis*. Low percentages of homogeneous AOM showing fluorescence were found (Table 24). Marine microplankton was rare, and freshwater microplankton was absent. The exception was sample Br-29 (bottom of the formation), which contains a different assemblage of organic matter; AOM and palynomorph (continental and marine) groups represent more than 50% of the total organic matter.

The Amaral Formation overlies the Abadia Formation and is only represented by two samples (Br22 and Br23, Table 24), which are dominated by the phytoclast group. Non-biostructured, striate and banded non-opaque phytoclasts are the most common within this group. Some biostructured phytoclasts fluoresce. The homogeneous AOM usually has a brown fluorescence color. Spores, sometimes with ornamented walls, and pollen grains were observed. Freshwater and marine microplankton was rare.

Lourinhã Formation

The palynofacies of the Lourinhã Formation have a terrestrial character that is dominated by the phytoclast group. Opaque phytoclasts (Table 24) represent approximately 23% (mean value) of the total organic matter, indicating oxic depositional environments. The lath/equidimensional and corroded phytoclasts had no internal structure and clear to diffuse outlines, respectively. Striate phytoclasts, non-biostructured non-opaque phytoclasts, cuticles and membranes were observed (Fig. 44). The abundance of phytoclasts decreases from the bottom to the top, while the AOM and palynomorphs group (sporomorphs and marine microplankton) increase (Table 24). The AOM is mostly homogeneous with diffuse outlines, is pale brown to brown in color (under white transmitted light) and exhibited moderate fluorescence (yellow to orange color) under incident blue light. Resin particles, which are natural products of higher terrestrial plants (Tyson, 1995), were present at the top of this formation.

Freshwater microplankton was absent. Marine palynomorphs were identified at the top of the formation (Table 24) and included mainly dinoflagellate cysts, Prasinophyte algae and some foraminiferal test linings. The marine microplankton was pale yellow to brown in white transmitted light and yellow (sometimes intense) to orange - brown under blue light. The samples from this formation were impregnated with solid bitumen (with intense yellow fluorescence color) that sometimes represented more than 50% of the organic matter (Br19 and Br20).

3.1.5.1.2. Total Organic Carbon (TOC) and Rock-Eval Pyrolysis

The geochemical data are listed in Table 25. The TOC values are generally low, ranging between 0.07 and 0.65 wt.% with a mean of 0.24 wt.%, indicating poor to fair organic carbon content according to the limits suggested by Peters and Cassa (1994).

Table 25. Geochemical data of Br-4 borehole samples.

Sample	Depth (m)	TOC	IR	S1	S2	HI	OI	T_{max}
Br1	200	0.10	98					
Br 2	400	0.18	80					
Br 3	600							
Br 4	800	0.41	56	0.02	0.15	37	180	416
Br 5	1000	0.003	45					
Br 6	1200							
Br 7	1225							
Br 8	1250							
Br 9	1275							
Br 10	1300	0.06	100					
Br 11	1325	0.07	78					
Br 12	1350	6.16	95	3.5	34.03	552	4	428
Br 13	1375	0.39	91					
Br 14	1400	0.50	88					
Br 15	1425	0.53	70	0.31	2.06	386	39	422
Br 16	1450	0.34	51					
Br 17	1500	0.54	59	0.08	0.7	130	65	427
Br 18	1550	0.33	77					
Br 19	1600	0.37	93					
Br 20	1650	0.40	87					
Br 21	1700	0.11	83					
Br 22	1750	0.32	14					
Br 23	1800	0.65	58	0.01	0.23	35	166	422
Br 24	1850	0.13	13					
Br 25	1900	0.20	14					
Br 26	1950	0.07	22					
Br 27	2000	0.09	13					
Br 28	2050	0.08	10					
Br 29	2100	0.10	7					
Br 30	2150	0.09	9					
Br 31	2200	0.13	11					
Br 32	2250	0.06	8					
Br 33	2300	0.16	6					
Br 34	2350	0.25	5					
Br 35	2400	0.25	7					
Br 36	2450	0.37	5					
Br37	2500	0.15	7					
Br38	2550	0.56	8	0.03	0.72	129	84	437
Br39	2600	0.15	4					
Br40	2650	0.18	4					
Br41	2700	0.15	3					
Br42	2750	0.15	2					
Br43	2800	0.27	3					

TOC: Total Organic Carbon (wt. %); IR: Insoluble residue (%); S1 and S2: Peak 1 and Peak 2 (mgHC/g rock); HI: hydrogen index (mgHC/g TOC); OI: Oxygen index (mgCO2/g TOC); T_{max}: pyrolysis maximum temperature (ºC).

The Jurassic samples had HI values ranging from 35 to 130 mgHC/g TOC, and the OI values varied between 65 and 166 mgHC/g TOC. The HI values indicate that the organic matter of the samples consists of type II/III kerogen (Fig. 45), corresponding to mixed terrestrial and marine OM, which is consistent with the palynofacies data. The low T_{max} values (between 422 and 437ºC) indicate the immature to early mature character of the OM.

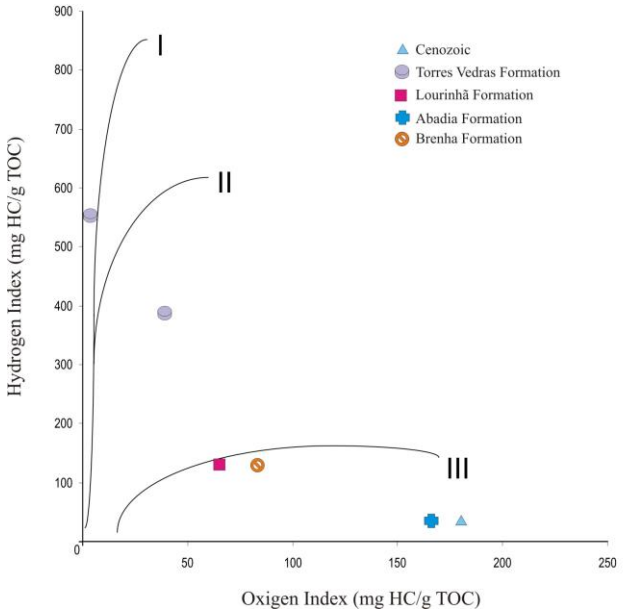

Figure 45. Van Krevelen type diagram for Br-4 samples.

3.1.5.1.3. Normal alkanes and isoprenoids

The *m/z* 85 chromatogram shows the presence of *n*-alkanes with 15-30 carbon atoms (Fig. 46) and the predominance of low to medium molecular weight compounds (*n*C15 to *n*C23) consisting of algal and/or microorganism sources and some continental contribution (Tissot and Welte, 1984). The exception was sample Br19 (Fig. 46F), which contained *n*-alkanes in the range of *n*C22 - *n*C34; these are characteristic of a terrestrial origin for the OM (Peters et al., 2005; Tissot and Welte, 1984).

The main acyclic isoprenoids, pristane (Pr) and phytane (Ph), were present in all the samples. Most of the samples from the Montejunto, Amaral and Abadia Formations had Pr > Ph. In contrast, almost all the samples from the Brenha and Lourinhã Formations had Pr < Ph (Table 26). The Pr/Ph ratio is usually used as an indicator of redox conditions in the depositional environment but should be interpreted carefully due to the interference of other factors, such as the origin and maturity of the OM (Peters et al., 2005; Waples and Machihara, 1991). According to several authors (e.g., Brooks et al., 1969; Didyk et al., 1978; Peters et al., 2005), Pr/Ph<1 is indicative of reducing conditions, while 1>Pr/Ph<3 reflects

oxic conditions. Ratios >3 are related to terrestrial sediments (Hunt, 1979). Oxic conditions are apparent in the Montejunto, Amaral and Abadia Formations, while the other formations indicated more reducing environments during early diagenesis (Fig. 46). The data from the Lourinhã Formation contradict the palynofacies results that indicate a more oxic environment. This might be explained by the presence of large amounts of solid bitumen. The increase in the amount of solid bitumen from the bottom to the top is accompanied by decreasing Pr/Ph ratios. Because it is not possible to distinguish biomarkers for autochthonous and migrated bitumens, the data obtained for this formation have mixed biomarker signatures.

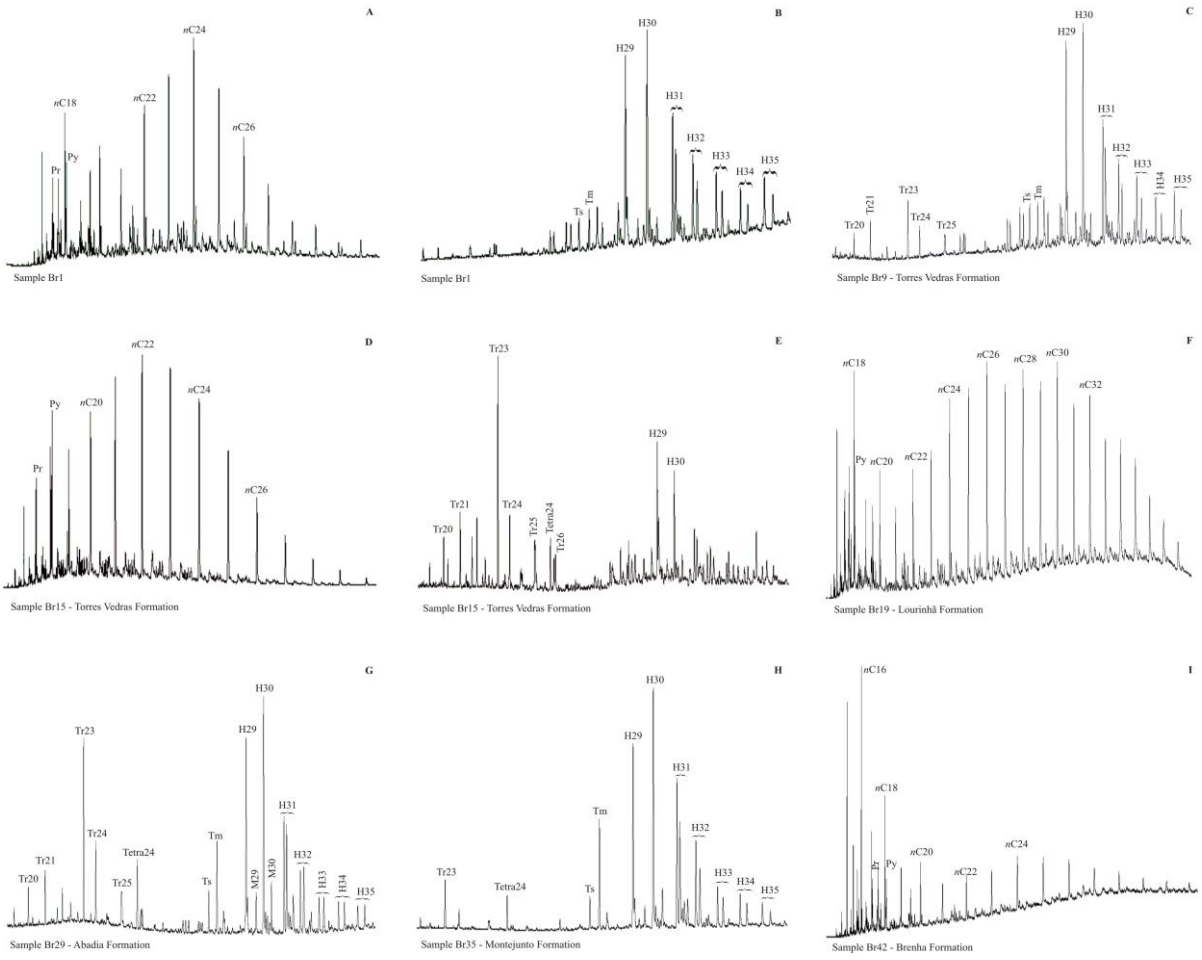

Figure 46. Gas chromatograms (*m/z 85*) and (*m/z* 191) of saturated fractions showing the distributions of *n*-alkanes and acyclic isoprenoids (A, D, F, I) and terpanes (B, C, E, G, H) of selected samples from the Barreiro-4 borehole. Tr 20 to Tr 26: C20 to C26 tricyclic terpane; Tetra 24: C24 tetracyclic terpane; Ts: 22,29,30-trisnorneohopane; Tm: 22,29,30-trisnorhopane; H29: 17α(H),21β(H)-30-norhopane; H30: 17α(H),21β(H)-hopane; H31(22S and 22R): 17α(H),21β(H)-homohopane; H32: 17α(H),21β(H)-bishomohopane (22S and 22R); H33: 17α(H),21β(H)-trishomohopane (22S and 22R); H34: 17α(H),21β(H)-tetrakishomohopane (22S and 22R); H35: 17α(H),21β(H)-pentakishomohopane (22S and 22R); M29: 17β(H),21α(H)-30-normoretane; M30: 17β(H),21α(H)-hopane (moretane).

The carbon preference index (CPI) is affected by the source and maturity of the OM. It is obtained from the sum of the *n*-alkanes with odd numbers of carbons versus the sum of the *n*-alkanes with even numbers of carbons from *n*C22 to *n*C30 (Tissot and Welte, 1984). The CPI values for the Jurassic samples range from 0.63 to 1.00 with a mean value of 0.86 (Table 26). Peters et al. (2005) found that CPI values substantially larger or smaller than 1 are indicative of low thermal maturity and that CPI values <1 are unusual and are related to immature oil and bitumen from carbonate or hypersaline environments. With increasing maturity, the CPI approaches 1 (CPI≈1), where there is no preference for even or odd numbers of carbons. These values can also be affected by the OM source (Peter et al., 2005).

3.1.5.1.4. Terpanes and steranes

In the majority of the samples, the tricyclic and tetracyclic terpanes (Fig. 46G - H) are nearly absent or occur in low abundances, whereas the pentacyclic terpanes are present in high abundances. Pentacyclic terpanes are related to prokaryotes and higher plants (Peter et al., 2005), while tricyclic terpanes are associated with constituents that exist in prokaryote membranes (Ourisson et al., 1982). C29 30-norhopane and C30 hopane are the most abundant pentacyclic terpanes. The hopane distribution is dominated by the C29 30-norhopane in the Lourinhã, Amaral and Abadia Formations and by the C30 hopane in the Montejunto (Fig. 46H) and Brenha Formations, with the C29/C30 17α-hopane ratios ranging between 0.59 and 1.71 (Table 26). The predominance of C29 30-norhopane is frequently associated with anoxic carbonate or marl source rocks (e.g., Peters et al., 2005; Waples and Machihara, 1991) but in some cases can be associated with terrestrial plant input (e.g., Brooks, 1986; Rinna et al., 1996). The extended hopanes C31-C35 are present in all the samples and occur as doublets; this stereoisomeric pair decreases in abundance with increasing molecular weight in most of the samples. 22,29,30-Trisnorhopane (Tm) predominates over 22,29,30-Trisnorneohopane (Ts), and the Ts/Tm ratio varies from 0.12 to 0.59 (Table 26). Ts is more resistant to thermal degradation than Tm; thus, the Ts/Tm ratio increases with increasing thermal evolution, but it also depends on the source of the organic matter (Seifert and Moldowan, 1978). In the Jurassic samples, the Ts/Tm ratio decreases with depth and was most likely influenced by the source lithology. This behavior was also observed in the sequence crossed by the Ramalhal-1 borehole, which was located in the Central Sector of the Lusitanian Basin (Gonçalves et al., 2013).

Table 26. Molecular parameters derived from biomarkers assemblage.

Formation	Sample	EOM	*n*-Alkanes				Terpanes						Steranes		
		(mg/g rock)	Pr/Ph	Pr/*n*-C17	Ph/*n*-C18	CPI	Ts/Tm	H32 S/(S+R)	Gama Index	H29/H30	H34/H35	Ster/17α-Hop	C27/C29 sterane	C29 S/(S + R)	C29 ββ/(αα+ββ)
	Br1	0.05	0.67	2.32	0.95	1.00	0.82	0.58	7.47	0.94	0.92	0.14	0.56	0.25	0.59
	Br2	0.11	1.39	0.60	0.21	1.04	0.96	0.59	3.94	1.12	0.93	0.16	1.06	0.18	0.54
	Br3	0.08	1.29	2.60	0.23	2.33	0.71	0.60	6.98	0.98	0.91	0.17	0.48	0.08	0.41
	Br4	0.16	1.21	3.67	0.38	3.65	0.67	0.57	12.54	0.83	0.84	0.24	1.21	0.08	0.54
	Br5	0.06	1.08	3.84	0.57	1.21	0.83	0.56	11.47	0.85	0.96	0.19	0.74	0.10	0.52
	Br6	0.08	1.16	4.74	0.54	1.01	1.23	0.59	11.49	0.88	0.83	0.19	0.58	0.14	0.41
Torres Vedras	Br7	0.05	0.93	2.63	0.46	0.95	0.88	0.61	10.71	0.89	0.84	0.17	0.53	0.20	0.55
	Br8	0.03	0.68	1.47	0.53	1.26	1.40	0.57	7.71	0.90		0.39	1.01	0.17	0.47
	Br9	0.03	1.16	1.62	0.37	1.53	1.13	0.58	6.68	0.78	0.88	0.29	0.85	0.10	0.37
	Br10	0.06	0.80	1.49	0.59	1.17	0.91	0.56	9.93	0.92	0.88	0.16	0.65	0.16	0.53
	Br11	0.05	1.44	0.66	0.17	2.02	0.80	0.59	7.09	0.98	0.85	0.22	0.86	0.09	0.55
	Br12	41.36	0.74	1.04	0.75	0.90									
	Br13	4.16	0.68	1.63	0.72	0.98									
	Br14	4.92	0.78	1.98	1.21	0.98									
	Br15	4.49	0.48	1.31	1.53	1.00	0.85	0.61	0.00	1.05	0.67	0.17	0.62	0.27	0.58
Lourinhã	Br16	2.66	0.56	1.54	1.94	0.99	1.01	0.62	6.44		0.78	0.15	0.71	0.28	0.61
	Br17	0.84	0.74	1.21	1.30	1.00	0.82	0.59	10.30	1.34	0.98	0.17	0.65	0.28	0.62
	Br18	1.63	0.59	1.09	0.67	0.94	1.46	0.68	0.00	1.71	0.73	0.00	0.26		
	Br19	0.83	0.80	1.37	0.58	0.89	1.29	0.61	0.56	1.07	0.61	0.10	0.21	0.47	0.54
	Br20	0.48	0.82	1.07	0.68	0.89	1.05	0.60	0.51	0.95	0.60	0.11	0.56	0.42	0.58
	Br21	0.27	0.87	0.84	0.63	0.86	0.84	0.53	0.00	1.50	0.93	0.09	0.23	0.39	0.61
Amaral	Br22	1.22	0.99	2.21	0.52	0.90	0.96	0.62	13.08	1.39	1.37	0.11	0.07	0.43	0.61
	Br23	0.22	1.62	0.94	0.19	0.97	0.89	0.59	10.61	1.35	1.13	0.12	0.52	0.30	0.64

(Continue on next page)

Table 26 (cont.). Molecular parameters derived from biomarkers assemblage.

Formation	Sample	EOM	*n*-Alkanes				Terpanes						Steranes		
		(mg/g rock)	Pr/Ph	Pr/*n*-C17	Ph/*n*-C18	CPI	Ts/Tm	H32 S/(S+R)	Gama Index	H29/H30	H35/H34	Ster/17α-Hop	C27/C29 sterane	C29 S/(S + R)	C29 ββ/(αα+ββ)
Abadia	Br24	0.13	1.64	1.86	0.36	0.90	0.80	0.58	12.29	1.26	1.04	0.17	0.31	0.31	0.64
	Br25	0.08	1.33	0.99	0.34	0.89	0.39	0.60	16.49	1.57	1.19	0.11	0.44	0.29	0.62
	Br26	0.04	1.49	1.20	0.21	0.84	0.52	0.59	14.31	1.21	1.18	0.11	0.33	0.27	0.60
	Br27	0.10	1.38	0.92	0.28	0.91	0.56	0.60	13.81	1.34	0.98	0.14	0.29	0.29	0.61
	Br28	0.05	1.54	1.81	0.32	0.86	0.46	0.59	10.05	1.15	1.24	0.16	0.30	0.26	0.60
	Br29	0.05	0.93	5.31	0.57	0.88	0.47	0.49	5.42	0.72	1.22	0.35	0.76	0.12	0.33
Montejunto	Br30	0.09	0.93	0.87	0.59	0.92	0.60	0.57	14.48	0.94	0.91	0.20	0.65	0.21	0.62
	Br31	0.05	1.05	2.51	0.57	0.74	0.73	0.56	7.56	0.87	1.08	0.19	0.55	0.22	0.52
	Br32	0.04	0.97	1.70	0.37	0.69	0.85	0.59	4.53	0.95	1.51	0.15	0.55	0.21	0.54
	Br33	0.22	1.17	1.31	0.50	0.78	0.13	0.63	9.38	1.31	0.88	0.09	0.55	0.31	0.64
	Br34	0.13	1.13	3.86	0.40	0.63	0.22	0.55	3.55	0.65	1.41	0.15	0.65	0.16	0.37
	Br35	0.11	1.01	4.21	0.52	0.88	0.40	0.56	7.70	0.68	1.05	0.16	0.58	0.23	0.49
	Br36	0.21	1.48	2.77	0.31	0.81	0.30	0.60	4.86	0.69	1.42	0.14	0.59	0.32	0.42
Brenha	Br37	0.13	1.00	2.01	0.53	0.88	0.36	0.61	4.12	0.59	1.81	0.05	0.33	0.29	0.50
	Br38	0.35	0.97	0.84	0.45	0.91	0.60	0.57	10.26	0.74	0.98	0.23	0.74	0.23	0.58
	Br39	0.07	0.98	1.09	0.37	0.77	0.41	0.57	5.34	0.69	1.28	0.11	0.66	0.21	0.45
	Br40	0.07	0.98	1.06	0.36	0.74	0.33	0.57	1.93	0.62	2.51	0.06	0.52	0.23	0.34
	Br41	0.09	0.85	1.39	0.39	0.85	0.33	0.59	1.61	0.63	2.31	0.05	0.57	0.38	0.39
	Br42	1.30	0.78	0.67	0.52	0.92	0.65	0.57	11.07	0.74	0.90	0.18	0.80	0.22	0.61
	Br43	0.07	0.87	1.06	0.45	0.86	0.40	0.58	3.05	0.63	1.60	0.06	0.40	0.32	0.43

EOM: extractable organic matter; Pr: Pristane; Ph: Phytane; CPI: Carbon Preference Index [2*(C23+C25+C27+C29)/C22+2*(C24+C26+C28)+C30]; Ts: 22,29,30-Trisnorneohopane; Tm: 22,29,30-Trisnorhopane; H29: 17α(H),21β(H)-30-norhopane; H30: 17α(H),21β(H)-Hopane; H32: 17α(H), 21β(H)-bishomohopane; (Ster/17α-hop): regular steranes consist of C27, C28, C29 ααα(20S + 20R) and αββ(20S + 20R) / 17α-hopanes consist of the C29-C33 pseudo-homologue (including 22S and 22R epimers); H34: 17α(H),21β(H)-tetrakishomohopane (22S - 22R); H35: 17α(H), 21β(H)-pentakishomohopane (22S - 22R); C27/C29 sterane: C27ααα 20R/C29ααα 20R; C29 (%): content of C29 ααα (20S +20R).

Gammacerane was present in most of the samples (except in samples Br18 and Br21), and the gammacerane index ranges between 0.51 and 16.49 (Table 26). The origin of the gammacerane is unclear, but it may have formed by the reduction of tetrahymanol, which is a lipid that is present in the membranes of certain protozoa (e.g., ten Haven et al., 1989). This compound is more resistant to biodegradation than the hopanes and is usually related to water-column stratification, which commonly results from hypersalinity at depth in marine and non-marine source rock depositional environments (Peters et al., 2005; Sinninghe Damsté et al., 1995).

The regular steranes/17α-hopanes ratio is related to the input of eukaryotic (mainly algae and higher plants) versus prokaryotic organisms during deposition (e.g., Chakhmakchev et al., 1996; Marynowski et al., 2000). These ratios are very low in the studied samples (Table 26), which is indicative of terrigenous and/or microbially reworked organic matter.

The relative distribution of the C27, C28 and C29 steranes showed that the C29 sterane was more abundant than the C28 and C27 steranes. The C27/C29 sterane ratio ranged between 0.07 and 0.80 (Table 26). The C29 steranes are commonly associated with a contribution from terrestrial higher plants, whereas the predominance of C27 and C28 steranes is indicative of a major contribution of planktonic organic matter (Huang and Meinschein, 1979). However, the abundance of C29 steranes can also be related to a prokaryotic origin of the OM (e.g., Volkman, 1988) or some brown and green algae (Hunt, 1979). Some authors (e.g., Hunt, 1979; Peters et al., 2005) have identified high amounts of C29 steranes in hydrocarbons derived from marine sources. Based on these associations, these data (C29>C28>C27) indicate a mix of terrestrial and marine organic matter, which is consistent with the palynofacies data previously described (see 3.1.5.1.1).

The C32 22S/(22S + 22R) homohopane, 20S/(20S + 20R) C29 sterane and ββ/(αα + ββ) C29 sterane ratios can be used as indicators of source rock maturity. The 22S/(22R + 22S) homohopane ratio is a useful tool to determine the OM maturation, principally in the immature to early mature stages (e.g., Seifert and Moldowan, 1980). In this case, the ratio 22S/(22S + 22R) epimer of the C32 homohopanes varied between 0.49 and 0.68 (Table 26), and some of the samples reached the equilibrium values proposed by Seifert and Moldowan (1980). The 20S/(20S + 20R) and ββ/(αα + ββ) isomerization ratios in the C29 sterane (Table 26) ranged between 0.12 and 0.47 and 0.33 - 0.64, respectively. The plot of 20S/(20S + 20R) versus ββ/(αα + ββ) for the C29 sterane (Fig. 47) indicates that all the samples are in an immature stage

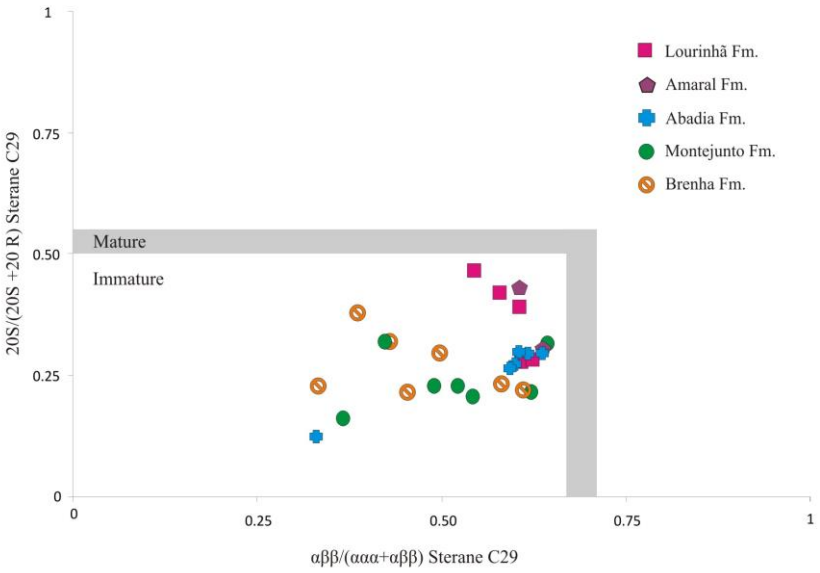

Figure 47. 20S/(20S + 20R) C29 sterane versus ββ/(αα + ββ) C29 sterane, indicating the thermal maturity of the studied samples.

3.1.5.2. Cretaceous

3.1.5.2.1. Palynofacies

All the Cretaceous samples (Fig. 48) were from the Torres Vedras Formation and contained small amounts of kerogen, most of which were impregnated with large amounts of solid bitumen (Fig. 48D - E). In some samples (Br12 - Br15), solid bitumen represents more than 55% of the particulate matter. The characteristic OM assemblage of this period is dominated by degraded phytoclasts (up to 65% of each sample), especially non-opaque non-biostructured phytoclasts, as well as striate phytoclasts, cuticles (increasing from the bottom to the top; Fig. 48A - B) and membranes. The occurrence of opaque phytoclasts, most of which are corroded, can indicate a more oxidizing environment. Homogeneous AOM was present and was pale yellow to brown color under white transmitted light and moderately to intensely fluorescent (yellow to orange) under incident blue light. Sporomorphs were also observed and increased towards the top of the sequence, especially ornamented spores and bisaccate pollen grains (Fig. 48C and F). Fungal spores are also present and reflect the proximity to the terrestrial source area (Tyson, 1995); they are brown-orange in both white and blue incident light. Freshwater microplankton was absent, and very small amounts of marine microplankton were present, except for sample Br11, which contained dinocysts and acritarchs (approximately 8% of the total organic matter).

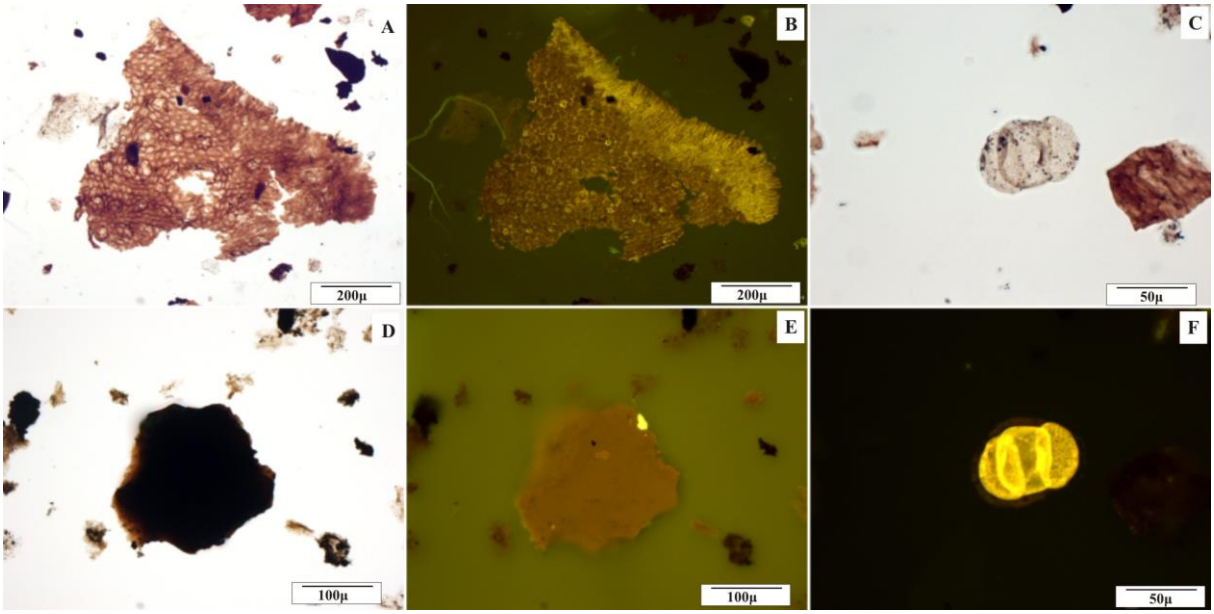

Figure 48. Photomicrographs of Cretaceous particulate organic matter taken under transmitted white light (TL) and fluorescence mode (FM). A - B: cuticle (Br10); C and F: bisaccate pollen grain (Br11); D - E: solid bitumen (Br12). TL: A, C, D; FM: B, E, F.

3.1.5.2.2. Total Organic Carbon (TOC) and Rock-Eval pyrolysis

The TOC values of the Cretaceous samples varied between 0.06 and 6.16 wt.% (Table 25). Rock-Eval pyrolysis performed on samples Br12 and Br 15 revealed S2 values of 34.03 and 2.06 mgHC/g rock, respectively. The HI showed values > 300 mgHC/g TOC (Fig. 45) and T_{max} between 422 and 428ºC. The low T_{max} values can be associated with contamination by migrated hydrocarbons (Peter and Cassa, 1994), which is consistent with the palynofacies analysis.

3.1.5.2.3. Rock extract

Samples Br12 - Br15 (Table 26) showed the highest amounts of extractable OM (EOM) (4.16 - 41.36 mg/g rock), which indicate large amounts of bitumen and is consistent with the data obtained by palynofacies and pyrolysis. Liquid chromatography revealed that the rock extracts are mainly represented by polar compounds (between 60.87% and 98.82%) and smaller amounts of the saturate fraction and aromatic hydrocarbons (0.09% - 17.39% and 0.00 - 21.42%, respectively).

3.1.5.2.4. Normal alkanes and isoprenoids

The *n*-alkane patterns showed a dominance of short chains (*n*C16 - *n*C20) in samples Br7 - Br11. In contrast, the samples that contained migrated bitumen (Br12 - Br15) showed a

different pattern. In these samples, the *m/z* 85 chromatograms display a full suite of saturated hydrocarbons between C15 - C33 *n*-alkanes with a clear predominance of the C20 - C26 chain *n*-alkanes (Fig. 46D). Phytane is the predominant acyclic isoprenoid in the studied samples, except for samples Br9 and Br11. The average Pr/Ph ratio was 0.86. The highest value was 1.44 and was found in sample Br9 (Table 26). The CPI varied between 0.90 and 2.02 (Table 26); samples Br8-Br11 had CPI values >1, while the other samples were close to 1.

3.1.5.2.5. Terpanes and steranes

The terpane distributions of samples Br7 - Br 11 were characterized by low contents of tricyclic and tetracyclic terpanes and the presence of pentacyclic terpanes, with C30 hopane prevailing over C29 norhopane (Fig. 46C). The C29/C30 17α-hopane ratio (Table 26) varied between 0.78 and 1.05 and can be associated with clay - rich source rocks (Gürgey, 1999). This is corroborated by the lithology and/or the insoluble residue data (Fig. 43, Table 25). In contrast, samples Br12 - Br15 showed the presence of tricyclic and tetracyclic terpanes (Fig. 46E). Tricyclic terpanes are usually associated with lacustrine or marine source rocks in which C23 terpane is the most abundant compound (Peters et al., 2005). The content of C24 tetracyclic terpane exceeds that of C26 tricyclic terpane. The absence of pentacyclic terpanes can be attributed to the maturity because tricyclic terpanes seem to be more stable than pentacyclic terpane (e.g., Peter et al., 2005; Snowdon et al., 1987).

The Ts/Tm ratio (Table 26) decreases with depth and varies between 0.80 - 1.40 with a mean value of 1. The behavior of the samples appears to be influenced more by lithology and source input than maturity. Gammacerane was not detected in the samples that contain high amounts of bitumen (Br12 to Br15; Table 26). Gammacerane was found in the other samples and, as discussed above, can be indicative of the stratification of the water column during deposition (Peters et al., 2005; Sinninghe Damsté et al., 1995).

C29, C28 and C27 steranes were not measured in all the samples (Table 26). C29 sterane predominates over C28 and C27 steranes (except in samples Br8 and Br9). The C27/C29 ratio ranges from 0.53 to 1.01 (Table 26).

The C32 22S/(22S + 22R) terpane values range between 0.56 and 0.61 (Table 26), reflecting an early mature to mature thermal maturity. Relative to the steranes, the C29 20S/(20S + 20R) ratio varies between 0.09 and 0.27, and the C29 ββ/(αα + ββ) ranges between 0.37 and 0.58 (Table 26).

3.1.5.3. Cenozoic

3.1.5.3.1. Palynofacies

The palynofacies demonstrated the terrestrial character of the Cenozoic samples. Phytoclasts and sporomorphs represent more than 58% of the total organic matter. However, there was an increase of marine influence during the Neogene (Table 24). Non-opaque phytoclasts (Fig. 49A) were the principal organic particles found in the samples, followed by opaque phytoclasts, especially corroded phytoclasts. Cuticles were also present, especially at the bottom of the sequence, and they are sometimes degraded. Sporomorphs (especially spores with ornamentations - Fig. 49E and F - and bisaccate pollen grains) were also present; they decrease during the Paleogene and increase during the Neogene (see Table 24).

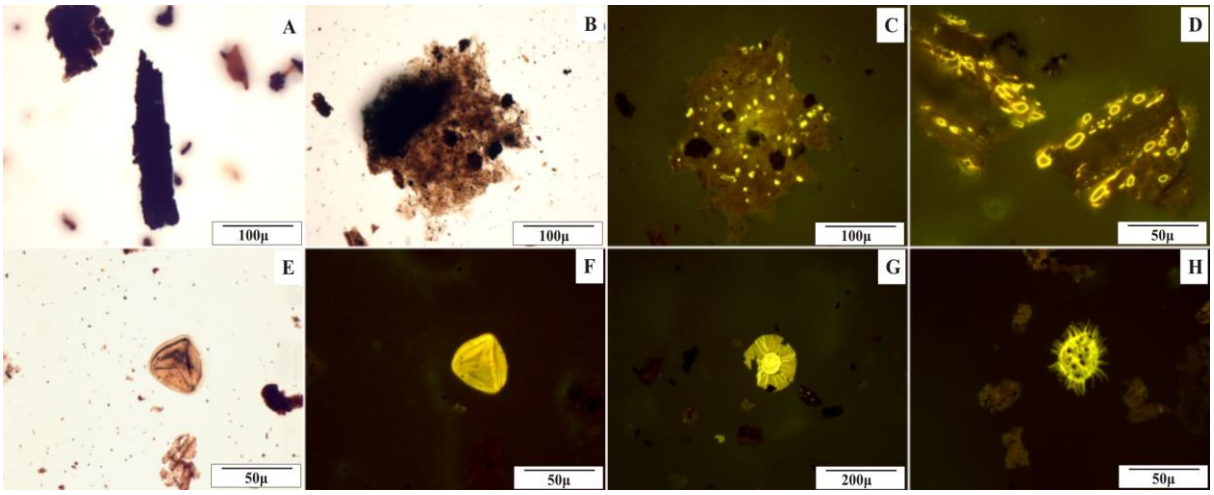

Figure 49. Photomicrographs of Cenozoic particulate organic matter taken under transmitted white light (TL) and fluorescence mode (FM). A: Non-biostructured non-opaque phytoclast (Br4); B to D: AOM with drops of oil (Br4); E- F: spore (Br4); G: Prasinophyte algae (Br3); H: Acritarch. TL: A, B, E; FM: C, D, F, G, H.

AOM was also present (Fig. 49B - C) and represented approximately 25% of the organic matter (Table 24). Freshwater microplankton was rare or absent, and marine microplankton (Fig. 49G - H) increased from the bottom to the top and reached approximately 18% of the OM present in sample Br2 (Table 24). The marine microplankton is represented by acritarchs and rare dinocysts. The decrease of terrestrial input associated with the increase of marine microplankton can be related to the increasing distance from the terrestrial source and/or an increase in productivity of the marine biomass (e.g., Gorin and Steffen, 1991; Tyson, 1995) as a result of a transgressive episode. Solid bitumen and oil drops (Fig. 49 C - D) were also observed.

3.1.5.3.2. Total Organic Carbon (TOC) and Rock-Eval pyrolysis

Low TOC content between 0.003 and 0.41 wt.% (Table 25) are characteristic of this period. The HI and OI values for sample Br4 are 37 and 180 mgHC/g TOC, respectively, corresponding to a type III kerogen (Fig. 45) that is derived primarily from terrestrial higher plants. T_{max} reaches 416ºC. However, the low S2 value indicates that the data from this sample, including the HI and T_{max} values, are unreliable (Bordenave et al., 1993; Peters and Cassa, 1994).

3.1.5.3.3. Normal alkanes and isoprenoids

The *n*-alkane patterns showed the dominance of short chains (*n*C16 - *n*C20) and exhibited a unimodal distribution. The exception was sample Br1, which showed a bimodal distribution (Fig. 46A).

The two main acyclic isoprenoids (Pr and Ph) are present in the analyzed samples. The Pr/Ph ratios range from 0.67 to 1.39 and have a mean value of 1.13 (Table 26). These data suggest oxic conditions during the deposition of the Paleogene and Neogene sediments, except for sample Br1, which was deposited in a more anoxic environment. The *n*C18 concentrations always predominate over the phytane and, other than sample Br2, the *n*C17 concentrations are lower than pristane, indicating a more continental contribution. This observation is also corroborated by the CPI values (Table 26), which are ≥ 1 in all samples, indicating a terrestrial contribution.

3.1.5.3.4. Terpanes and steranes

Tricyclic and tetracyclic terpanes are nearly absent, and the pentacyclic terpanes of the hopane series are dominated by C30 hopane (Fig. 46B). The C29/C30 ratio was < 1 for most of the samples (see Table 26).

The Ts/Tm ratios varied between 0.67 and 1.23. As described above, this ratio depends on both maturity and source (e.g., Seifert and Moldowan, 1978; Peters et al., 2005) and in these samples is more closely related to the source input or the depositional environment than the maturity.

The extended hopanes C31 - C35 are present and occur as doublets that decrease in abundance with increasing molecular weight. The C34/C35 homohopane ratios varied from 0.83 to 0.96 (Table 26). The concentration of C34 and C35 homohopanes can be used as an indicator of the organic matter type and of redox conditions; low concentrations of C35 homohopane are an indicator of anoxic marine conditions, whereas high concentrations are

commonly related to oxic conditions in the water column during deposition (Peters et al., 2005; Peters and Moldowan, 1991).

Gammacerane was present in all the samples. The gammacerane index varied between 3.94 and 12.54 (Table 26). The concentration of gammacerane remained stable during the Paleogene and decreased during the Neogene, reaching the lowest value at 400 m (Br2; Table 26), after which it began to increase again.

The distributions of the C27, C28 and C29 steranes for the Paleogene and some Neogene samples are similar (C29 > C28 > C27). The C27/C29 sterane ratios range from 0.48 to 1.21 (Table 26). Samples Br2 and Br 4 had a predominance of C27 sterane, which is indicative of a major contribution of planktonic organic matter. The palynofacies in sample Br2 confirm these data (see Table 24). As in the Jurassic and Cretaceous samples, these data are indicative of a mixed terrigenous and marine origin of the OM. The regular steranes/17α-hopanes (Table 26) ratios were lower and varied between 0.14 and 0.24 (Table 26).

The ratio of the 22S/(22S + 22R) epimer of C32 homohopanes revealed that the majority of the samples had reached equilibrium (Table 26). The 20S/(20S + 20R) and ββ/(αα + ββ) isomerization ratios in C29 sterane had ranges of 0.08-0.25 and 0.41-0.59, respectively (Table 26).

3.1.6. Paleoenvironmental characterization

The paleoenvironmental reconstruction is primarily based on the kerogen composition and geochemical data. Due to the lack of palynofacies and biomarker data for the Cretaceous, the paleoenvironmental characterization focuses only on the Jurassic samples.

The sedimentary sequence crossed by the Br-4 borehole starts with a marine carbonate platform of Bathonian age that corresponds to the deposition of the Brenha Formation. The kerogen assemblage is dominated by the AOM and is associated with significant percentages of phytoclasts (21.73 - 37.87%) and continental or marine palynomorphs (9.67 - 27.81%). The different types of AOM suggest periods of reworking by bacterial activity and other primary productivity. The presence of dinocysts, Prasinophyte algae and foraminiferal test-linings confirm the marine conditions during sedimentation. The organic geochemical parameters suggest that OM sedimentation occurred under anoxic conditions in a stratified water column. The decline in AOM abundance accompanied by phytoclast enrichment (≈ 68%) in the uppermost Brenha Formation (Callovian age) indicates a change in the depositional environment. The increase of phytoclasts reveals a major continental influence, possibly in a relatively deep and energetic continental shelf

environment. These conditions might have been the result of a drop in sea - level, which allowed more terrestrial components (phytoclasts) to be transported deeper into the basin. This interpretation is consistent with some authors (e.g., Azerêdo et al., 2002) who have reported the occurrence of a complex regression that led to several variations in the carbonate ramp environment at the end of the Middle Jurassic. The transition between the latest Callovian and the end of the early Oxfordian contains an important basin - wide disconformity (e.g., Mouterde et al., 1979; Wilson, 1988). A stratigraphic gap is present in this part of the basin, which causes the Montejunto Formation limestones (Middle - Late Oxfordian) to directly overlie the Middle Jurassic limestones. Deposition of the Montejunto Formation occurred in a shallow marine carbonate platform with sporadic clay inputs (Kullberg et al., 2013; Wilson, 1988) under variable energy conditions and oscillations in the water column. These conditions controlled the fluctuations in oxygen content, leading to oxic to suboxic environments. The presence of sporomorphs (mainly pollen grains of the genus *Classopollis*) and freshwater algae can be related to the presence of fluvial systems along the coastline, which carried these organic particles to marine depositional areas. In the upper part of this sequence, the increase of biostructured phytoclasts indicates increased continental influence compared to the base of the formation. Carbonate sedimentation continued during the deposition of the Abadia Formation. Continental organic matter is dominant (Table 24) and is principally composed of non-opaque phytoclasts. This translucent fraction is most biodegraded in the coastal sections and is an indication of the proximity and oxic conditions (Tyson, 1995). The increase of opaque phytoclasts supports the idea of oxic conditions. Detrital inputs (increases in insoluble residue), mainly clays, occur at the top of the sequence, as well an increase in continental influence (more than 90% terrestrial organic matter). Carbonate sedimentation continued during the deposition of the Amaral Formation and occurred in an intertidal to subtidal environment with some marine influences (e.g., Kullberg et al., 2013). This formation had only a minor expression in the study area. The continental influence (phytoclasts) prevailed, but the AOM increased relative to the previous formation. The biomarker data suggests a suboxic environment that allowed preservation of the OM. The Jurassic ended with the deposition of the Lourinhã Formation, which took place in oxic conditions. The deposition occurred in a lacustrine to marginal marine environment (Kullberg et al., 2013) that was influenced both by seawater and freshwater and was often subaerially exposed. The increase of the opaque fraction (mean value of ≈ 24%; Table 24) may be the result of regressive periods in which the organic matter was exposed, resulting in an increase in oxidation rates. The presence of resin and cuticles, some of which have stomata and others which have a preserved inner part of the epidermis, confirms the proximity to the terrestrial source area. The biomarker data for this formation is ambiguous due the presence of solid bitumen.

3.1.6. Conclusions

Palynofacies and geochemical data from the Br-4 borehole allow the characterization of the OM in the study area to determine its origin and variation during the Mesozoic and Cenozoic as well as the hydrocarbon potential of the sequence. The kerogen had low TOC contents (<1 wt.%) and was predominantly characterized by continental organic matter punctuated by marine palynomorphs that were preserved in a marine environment under anoxic - oxic conditions. The sequence showed several depositional environments, from carbonate platform to coastal environments that are marked by marine transgressive and regressive phases. The results (low values of TOC, S2 and HI) show that the Jurassic sequence has poor potential as an oil source rock, with small amounts of organic matter and predominantly type III and scarce type II kerogens. The maturity indicators [T_{max}, C29 20S/(20S + 20R) sterane, C29ββ/(αα + ββ) sterane] suggest an immature stage for the extracted bitumen. The Montejunto Formation and the Tithonian-Cretaceous age samples confirm the presence of solid bitumen, and the Rock-Eval pyrolysis data (low T_{max}, high S1, TOC and HI) indicate that the bitumen has undergone migration.

References

Alves, T.M., Gawthorpe, R.L., Hunt, D.W., Monteiro, J.H., 2002. Jurassic tectono-sedimentary evolution of the Northern Lusitanian Basin (offshore Portugal). Marine and Petroleum Geology 19, 727 - 754.

Antunes, M.T., Pais, J., 1993. The Neogene of Portugal. Ciências da Terra, Universidade Nova Lisboa, 12, 7-22. ISSN 0254-055x.

Azerêdo, A.C., Duarte, L.V., Henriques, M.H., Manuppella, G., 2003. Da dinâmica continental no Triásico aos mares do Jurássico Inferior e Médio. Cadernos de Geologia de Portugal. Instituto Geológico e Mineiro, Lisboa. ISBN 972-98469-9-5.

Azerêdo, A.C., Wright, V. P., Ramalho, M.M., 2002. The Middle - Late Jurassic forced regression and disconformity in central Portugal: eustatic, tectonic and climatic effects on a carbonate ramp system. Sedimentology 49, 1339 - 1370.

Behar, F., Beaumont, H.L., Penteado, H.L., 2001. Rock-Eval 6 Technology: Performance and Developments. Oil & Gas Science and Technology-Revue de l'Institut Français du Pétrole 56, 111 - 134.

Bordenave, M.L., Espitalié, L., Leplat, P., Oudin, J.L., Vandenbroucke, M., 1993. Screening techniques for source rock evaluation, in: Bordenave, M.L. (Ed.), Applied Petroleum Geochemistry. Editions Technip, Paris, pp. 217 - 278.

Bostick, N.H., 1971. Thermal alteration of clastic organic particles as an indicator of contact and burial metamorphism in sedimentary rocks. Geosciences & Man, Baton Rouge 3, 83 - 92.

Brooks, J. D., Gould, K., Smith, J. W., 1969. Isoprenoid hydrocarbons in coal and petroleum. Nature 222, 257 - 259.

Brooks, P.W., 1986. Unusual biological marker geochemistry of oils and possible source rocks, offshore Beaufort-Mackenzie Delta, Canada. Organic Geochemistry 10, 401 - 406.

Carvalho, J., Matias, H., Torres, L., Manupella, G., Pereira, R., Mendes-Victor, L., 2005. The structural and sedimentary evolution of the Arruda and Lower Tagus sub-basins, Portugal. Marine and Petroleum Geology 22, 427 - 453.

Chakhmakchev, A., Suzuki, N., Suzuki, M., Takayama, K., 1996. Biomarker distributions in oils from the Akita and Niigata Basins, Japan. Chemical Geology 133, 1 - 14.

Cunha, P., Pais, J., Legoinha, P., 2009. Evolução geológica de Portugal continental durante o Cenozóico – sedimentação aluvial e marinha numa margem continental passiva (Ibéria ocidental) in: Abstracts, 6º Simposio sobre el Margen Ibérico Atlántico MIA09 (Oviedo, España), p. xi-xx.

Cunha, T., 2008. Gravity anomalies, flexure and the thermo-mechanical evolution of the West Iberia Margin and its conjugate of Newfoundland. PhD Thesis, Department of Earth Sciences, University of Oxford.

Didyk, B.M., Simoneit, B.R.T., Brassell S.C., Eglinton, G., 1978. Organic geochemical indicators of palaeoenvironmental conditions of sedimentation. Nature 272, 216 - 222.

Duarte, L.V., Silva, R.L., Mendonça Filho, J.G., 2011. The Lower Jurassic of the west coast of Portugal: stratigraphy and organic matter in carbonate sedimentation, in: Flores, D., Marques, M.M. (Eds.). 63rd ICCP Annual Meeting – Field Trip, Porto, Memória nº 17. ISSN 087.1607.

Duarte, L.V., Silva, R.L., Mendonça Filho, J.G., Poças Ribeiro, N., Chagas, R.B.A., 2012. High-resolution stratigraphy, palynofacies and source rock potential of the Água de Medeiros Formation (Lower Jurassic), Lusitanian Basin, Portugal. Journal of Petroleum Geology 35, 105 - 126.

Duarte, L.V., Silva, R.L., Oliveira, L.C.V., Comas-Rengifo, M.J., Silva, F., 2010. Organic - rich facies in the Sinemurian and Pleinsbachian of the Lusitanian Basin, Portugal: Total organic carbon distribution and relation to transgressive-regressive facies cycles. Geologica Acta 8, 325 - 340.

Ellis, P.M., Wilson, R.C.L., Leinfelder, R.R., 1990. Controls on Upper Jurassic carbonate buildup development in the Lusitanian Basin, Portugal. IAS special publications 9, 169 - 202.

Espitalié, J., Laporte, J. L., Madec, M., Marquis, F., Leplat, P., Paulet, J., Boutefeu, A., 1977. Méthode rapide de caractérisation des roches mètres, de leur potentiel pétrolier et de leur degré d'évolution. Revue de l'Institut Français du Pétrole 32, 23 - 42.

Gonçalves, P.A., Mendonça Filho, J.G., Mendonça J.O., Silva, T.F., Flores, D., 2013. Paleoenvironmental characterization of a Jurassic sequence on the Bombarral sub-basin (Lusitanian basin, Portugal): Insights from palynofacies and organic geochemistry. International Journal of Coal Geology 113, 27 - 40.

Gorin, G.E., Steffen, D., 199l. Organic facies as a tool for recording eustatic variations in marine fine-grained carbonates - example of the Berriasian stratotype at Berrias (Ardèche, SE France). Palaeogeography, Palaeoclimatology, Palaeoecology 85, 303 - 320.

Gürgey, K., 1999. Geochemical characteristics and thermal maturity of oils from the Thrace Basin (Western Turkey) and Western Turkmenistan. Journal of Petroleum Geology 22, 167 - 189.

Huang, W.Y., Meinschein, W, G., 1979. Sterols as ecological indicators. Geochimica et Cosmochimica Acta 43, 739 - 745.

Hunt, J. M., 1979. Petroleum Geochemistry and Geology. Freeman, San Francisco.

Kullberg, J.C., Rocha, R.B., Soares, A.F., Rey, J., Terrinha, P., Azerêdo, A.C., Callapez, P., Duarte, L.V., Kullberg, M.C., Martins, L., Miranda, J.R., Alves, C., Mata, J., Madeira, J., Mateus, O., Moreira, M., Nogueira, C.R., 2013. III.3. A Bacia Lusitaniana: Estratigrafia, Paleogeografia e Tectónica, in: Geologia de Portugal, 2, ISBN: 978-972-592-364-1, pp. 195 - 347.

Kullberg, J.C., Terrinha, P., Pais, J., Reis, R.P., Legoinha, P., 2006. Arrábida e Sintra: dois exemplos de tectónica pós-rifting da Bacia Lusitaniana, in: Dias, R., Araújo, A., Terrinha, P., Kullberg, J.C. (Eds.), Geologia de Portugal no contexto da Ibéria, Universidade de Évora, ISBN: 972-778-094-6, pp. 369 - 396.

Leinfelder, M.R.R., Wilson, R.C.L., 1989. Seismic and sedimentologic features of Oxfordian-Kimmeridgian syn - rift sediments on the eastern margin of the Lusitanian Basin. Geologische Rundschau 79, 81 - 104.

Marynowski, L., Narkiewicz, M., Grelowski, C., 2000. Biomarkers as environmental indicators in a carbonate complex, example from the Middle to Upper Devonian, Holy Cross Mountains, Poland. Sedimentary Geology 137, 187 - 212.

Mendonça Filho, J.G., Chagas, R.B.A., Menezes, T.R., Mendonça, J.O., Silva, F.S., Sabadini-Santos, E., 2010. Organic facies of the Oligocene lacustrine system in the Cenozoic Taubaté Basin, Southern Brazil. International Journal of Coal Geology 84, 166 - 178.

Mendonça Filho, J.G., Menezes, T.R., Mendonça, J.O., 2011b. Organic Composition (Palynofacies Analysis). Chapter 5 in: ICCP Training Course on Dispersed Organic Matter, ISBN 978-9-89-826567-8, pp. 33 - 81.

Mendonça Filho, J.G., Menezes, T.R., Mendonça, J.O., Oliveira, A.D., Silva, T.F., Rondon, N.F., Silva, F.S., 2012. Organic Facies: Palynofacies and Organic Geochemistry Approaches, in: Panagiotaras, D. (Org.), Geochemistry Earth's system processes, inTech, Patras, ISBN 978-9-53-510586-2, vol. 1, pp. 211 - 245.

Mendonça Filho, J.G., Menezes, T.R., Mendonça, J.O., Oliveira, A. D., Souza, J.T., Sant'Anna, A.J., 2011a. Kerogen: Composition and Classification. Chapter 3 in: ICCP Training Course on Dispersed Organic Matter, ISBN 978-9-89-826567-8, pp. 17 - 24.

Montenat, C., Guery, F., Jamet, M., Berthou, P.Y., 1988. Mesozoic evolution of the Lusitanian Basin: comparison with the adjacent margin, in: Boillot, G., Winterer, E.L. (Eds.), Proceedings of the Ocean Drilling Program, Scientific Results 103, 757 - 775.

Mouterde, R., Rocha, R.B., Ruget, C., Tintant, H., 1979. Faciès, biostratigraphie et paléogéographie du Jurassique portugais. Ciências da Terra, Universidade Nova Lisboa 5, 29 - 52.

Oliveira, L.C.V., Rodrigues, R., Duarte, L.V., Lemos, V., 2006. Avaliação do potencial gerador de petróleo e interpretação paleoambiental com base em biomarcadores e isótopos estáveis do carbono da seção Pliensbaquiano-Toarciano inferior (Jurássico inferior) da região de Peniche (Bacia Lusitânica, Portugal). Boletim de Geociências da Petrobras 14, 207 - 234.

Ourisson, G., Albrecht, P., Rohmer, M., 1982. Predictive microbial biochemistry from molecular fossils to prokaryotic membranes. Trends in Biochemical Sciences 7, 236 - 239.

Pais, J., Cunha, P., Moreira, D., Legoinha, P., Dias, R., Moura, D., Silveira, A.B., Kullberg, J.C., González-Delgado, J., 2012. The Paleogene and Neogene of Western Iberia. A Cenozoic Record in the European Atlantic Domain. Springer Verlag.

Peters, K.E., Moldowan, J.M., 1991. Effects of source, thermal maturity and biodegradation on the distribution and isomerization of homohopanes in petroleum. Organic Geochemistry 17, 47 - 61.

Peters, K.E., Cassa, M.R., 1994. Applied source rock geochemistry, in: Magoon, L.B., Dow, W.G. (eds.), The petroleum system – from source to trap, American Association of Petroleum Geologists Memoir 60, Tulsa, pp. 93 - 120.

Peters, K.E., Walters, C.C., Moldowan, J.M., 2005. The Biomarker Guide, vol. 2, Biomarkers and Isotopes in Petroleum Exploration and Earth History, second ed. Cambridge University Press, London.

Poças Ribeiro, N., Mendonça Filho, J.G., Duarte, L.V., Silva, R.L., Mendonça, J.O., Silva, T.F., 2013. Palynofacies and organic geochemistry of the Sinemurian carbonate deposits in the western Lusitanian Basin (Portugal): Coimbra and Água de Madeiros formations. International Journal of Coal Geology 111, 37 - 52.

Rasmussen, E.S., Lomholt, S., Andersen, C., Vejbæk, O.L., 1998. Aspects of the structural evolution of the Lusitanian Basin in Portugal and the shelf and slope area offshore Portugal. Tectonophysics 300, 199 - 225.

Ribeiro, A., Kullberg, M.C., Kullberg, J.C., Manuppella, G., Phipps, S., 1990. A review of alpine tectonics in Portugal - foreland detachment in basement and cover rocks. Tectonophysics 184, 357 - 366.

Rinna, J., Rullkötter, J., Stein, R., 1996. Hydrocarbons as indicators for provenance and thermal history of organic matter in late Cenozoic sediments from hole 909c, Fram Strait, in: Thiede, J., Myhre, A.M., Firth, J.V., Johnson, G.L., Ruddiman, W.F. (Eds.). “Proceedings of the Ocean Drilling Program, Scientific Results”, Vol. 151, College Station, TX (Ocean Drilling Program), 407 - 414.

Seifert, W. K., Moldowan, J. M., 1978. Applications of steranes, terpanes and monoaromatics to the maturation, migration and source of crude oils. Geochimica Cosmochimica Acta 42, 77 - 95.

Seifert, W.K., Moldowan, J.M., 1980. The effect of thermal stress on source-rock quality as measured by hopane stereochemistry. Physics and Chemistry of the Earth 12, 229 - 237.

Silva, R.L., Mendonça Filho, J.G., Azerêdo, A., Duarte, L.V., 2014. Palynofacies and TOC analysis of marine and non-marine sediments across the Middle-Upper Jurassic boundary in the central-northern Lusitanian Basin (Portugal). Facies 60, 255 - 276.

Silva, R.L., Duarte, L.V., Comas-Rengifo,M.J., Mendonça Filho, J.G., Azerêdo, A.C., 2011. Update of the carbon and oxygen isotopic records of the Early - Late Pliensbachian (Early Jurassic, 187 Ma): Insights from the organic-rich hemipelagic series of the Lusitanian Basin (Portugal). Chemical Geology 283, 177 - 184.

Silva, R.L., Mendonça Filho, J.G., Silva, F.S., Duarte, L.V., Silva, T.F., Ferreira, R., Azeredo, A.C., 2012. Can biogeochemistry aid in the palaeoenvironmental/early diagenesis reconstruction of the ~187 Ma (Pliensbachian) organic-rich hemipelagic series of the Lusitanian Basin (Portugal)?. Bulletin of Geosciences 87, 373 - 382.

Sinninghe Damsté, J.S., Kenig, F., Koopmans, M.P., Köster, J., Schouten, S., Hayes, J.M., Leeuw, J.W., 1995. Evidence for gammacerane as an indicator of water column stratification. Geochimica et Cosmochimica Acta 59, 1895 - 1900.

Snowdon, L.R., Brooks, P.W., Williams, G.K., and Goodarzi, F., 1987. Correlation of the Canol Formation source rock with oil from Norman Wells. Organic Geochemistry 11, 529 - 548.

ten Haven, H.L., Rohmer, M, Rullkötter, J., Bisseret, P., 1989. Tetrahymanol, the most likely precursor of gammacerane, occurs ubiquitously in marine sediments. Geochimica et Cosmochimica Acta 53, 3073 - 3079.

Tissot, B., Welte, D.H., 1984. Petroleum formation and occurrence, second ed. Springer Verlag, Hidelberg.

Tyson, R.V., 1995. Sedimentary Organic Matter. London, Chap. & Hall.

Volkman, J.K., 1988. Biological marker compounds as indicators of the depositional environments of petroleum source rocks. in: Kelts, K. et al., (Eds), Lacustrine Petroleum Source Rocks, Geological Society Special Publication 40, 103 - 122.

Waples, D.W., Machihara, T., 1991. Biomarkers for Geologists: A Practical Guide to the application of Steranes and Triterpanes in Petroleum Geology. American Association of Petroleum Geologists, Methods in Exploration, Series 9.

Wilson, R. C. L., 1988. Mesozoic Development of the Lusitanian Basin, Portugal. Revista de la Sociedad Geológica de España 1, 393 - 407.

Wilson, R.C.L., Hiscott, R.N., Willis, M.G., Gradstein, F.M., 1989. The Lusitanian Basin of west central Portugal: Mesozoic and Tertiary tectonics, stratigraphy, and subsidence history, in Tankard, A.J., Balkwill, H.R. (Eds.), Extensional Tectonics and Stratigraphy of the North Atlantic Margins. American Association Petroleum Geologists Memoir 46, 341 - 361.

Part IV - General Conclusions

This thesis involved bulk organic petrology and geochemical analyses of the Jurassic sequences from the Lusitanian Basin. The main objectives has been to characterize the organic matter content, the level of thermal maturity, the organic facies and the source potential of the Jurassic sedimentary sequences. For this propose carbonate and pelitic rock samples were selected belonging to four boreholes drilled in the Lusitanian Basin. The results obtained were divided into three chapters according with location (sub-basin) where the boreholes were drilled. The general conclusions are presented below.

Bombarral sub-basin

- Rock-Eval pyrolysis and palynofacies data reveal a terrestrial origin for the organic matter (type III kerogen);
- The phytoclast dominance, mainly the non-opaque non-biostructured phytoclasts, in the kerogen assemblage suggests a higher terrigenous input due to the greater proximity to the continental source area. This proximity is more marked in the Lourinhã and Abadia Formations. Montejunto Formation revealed the major contributions of marine phytoplankton of all the sequence and corresponds to a period of major input of salt water in the system reflecting a more distal environment;
- The organic matter was preserved in a proximal - distal environment and oxic conditions. These environment characteristics are directly related to the input of phytoclasts in the system;
- The maturity parameters [T_{max}, C29 20S/(20S + 20R) sterane, C29ββ/(αα + ββ) sterane, H32 22S/(22S + 22R) and other biomarker maturity] suggest an immature to early mature stage for the organic matter;
- In general, all formations contain lower values of TOC, S2 and HI, indicating that they are not potential source rocks for oil;
- Solid bitumen were observed in Brenha and Montejunto Formations.

Arruda sub-basin

- Palynofacies and geochemical data indicate both marine and terrestrial organic matter where the phytoclast predominated despite an important contribution of the amorphous organic matter (predominantly types III and IV, and minor type II kerogens);

- The organic matter was deposited in a marine environment with variations in the redox condition (anoxic to oxic).
- Candeeiros Formation (informal formation) revealed an important contribution of zooclasts and zoomorphs pointing to oxic condition during the deposition;
- Vitrinite reflectance values, 22S/(22S + 22R) epimer of C32 homohopanes ratio and 20S/(20S + 20R) and ββ/(αα + ββ) isomerization ratios in C29 sterane indicate that the organic matter reached the oil window;
- According to its characteristics the majority of the samples are classified as being poor to fair as regards the generative potential. However, some samples of the Abadia, Montejunto, Cabaços and Brenha Formations can be considered potential source rocks for hydrocarbons (gas and/or oil) in this section of the Lusitanian Basin;
- Three families of solid bitumen were identified in the Candeeiros and Cabaços Formations; according to the data, they are allochtonous bitumen and cannot be used as maturity parameter.

Lower Tagus sub-basin

- Palynofacies and geochemical data was pointing to continental organic matter punctuated by marine palynomorphs (predominantly type III and scarce type II kerogens);
- The organic matter was preserved in a marine environment under anoxic - oxic conditions. The sequence showed several depositional environments, from carbonate platform to coastal environments that are marked by marine transgressive and regressive phases;
- The maturity indicators [T_{max}, C29 20S/(20S + 20R) sterane, C29ββ/(αα + ββ) sterane] suggest an immature stage for the organic matter;
- The results (low values of TOC, S2 and HI) show that the Jurassic sequence has poor potential as an oil source rock;
- Solid bitumens were also observed in this sub-basin mainly in Montejunto Formation and in the samples from the Upper Jurassic (Tithonian age) and Cretaceous.

The integration of organic petrology and geochemistry studies proved important during this study however the correlation between optical and geochemical data was not always

possible due the presence of solid bitumens. In these cases the biomarker data were not reliable once it was not possible to distinguish between autochthones and allochtonous bitumens. Optical observations (transmitted and reflected light, and fluorescence mode) proved to be an asset in the study of organic matter dispersed in sedimentary rocks.

In order to improve our current understanding of the deposition and evolution of the organic matter in the Lusitanian Basin, as well as provide data for future modelling, it is necessary:

- Reduce the distance between samples in order to allow a better assessment of the vertical variation pattern in organic matter characteristics in some of the studied formations (e.g., Coimbra, Brenha, Cabaços and Montejunto);
- Study the influence of salt (Cabaços Formation) in thermal maturation and in retention of bitumen;
- Deepening the study of solid bitumen: identification of the different families of solid bitumens in others sub-basins and to determine their origin;
- Use basin modelling to outline the burial and thermal histories of the studied sub-basins.

Part V - Petrographic Atlas

The aim of this atlas is to present microscopic aspects, on transmitted and reflected lights, incident blue light and SEM, of the studied samples that were not included in Part III - Results and Discussion.

This part includes four chapters. The first three correspond to the main groups of kerogen in transmitted white light - Phytoclast, Amorphous Organic Matter and Palynomorphs. The last chapter is dedicated to solid bitumen.

The characterization of the kerogen assemblage on transmitted and incident blue lights follows the classification system proposed by Tyson (1995), Vicent (1995), Mendonça Filho (1999) and Mendonça Filho et al. (2010, 2011, 2012). The photomicrographs were taken using transmitted and incident blue lights using a Carl Zeiss Axio Imager A1 microscope at the Palynofacies and Organic Facies Laboratory (LAFO) and a Leica DM 2500P microscope with a Discus software at the Department of Geosciences, Environment and Spatial Planning (DGAOT).

The petrographic characterization on reflect light of solid bitumen was performed following standard procedures (ASTM D7708, 2011 and ISO 7404-2, 2009). The photomicrographs were taken in reflected white and blue incident lights using a Leica DM4000 microscope using a 50x oil immersion objective at the DGAOT.

The SEM images present in this atlas were taken using a Scanning Electron Microscope model MA10 Zeiss at LAFO. SEM observations were only carried out in the samples (Fx25, Fx26 and Fx29) where large amount of solid bitumen were observed in the palynofacies analysis.

Legend:

Transmitted light - TL

Incident blue light (fluorescence mode) - FM

Reflect light - RL

Differential interference contrast light - DIC

1. Phytoclasts Group

Phytoclasts correspond to fragments of tissues derived from terrestrial higher plants and fungi (Bostick, 1971). For more information about nomenclature and/or petrographic features see section 1.1.1.3. on Part II of this thesis.

1.1. Palynofacies features

1.1. A - Opaque phytoclast, lath (Bf64; TL).

1.1. B - Opaque phytoclast, equidimensional (Bf71; TL).

1.1. C - Non-opaque biostructured phytoclast, banded (Fx2; TL).

1.1. D - Non-opaque biostructured phytoclast, striate (Bf8; TL).

1.1. E - Non-opaque biostructured phytoclast, striped (Bf23; TL).

1.1. F - Non-opaque biostructured phytoclast, pitted (Fx22; TL).

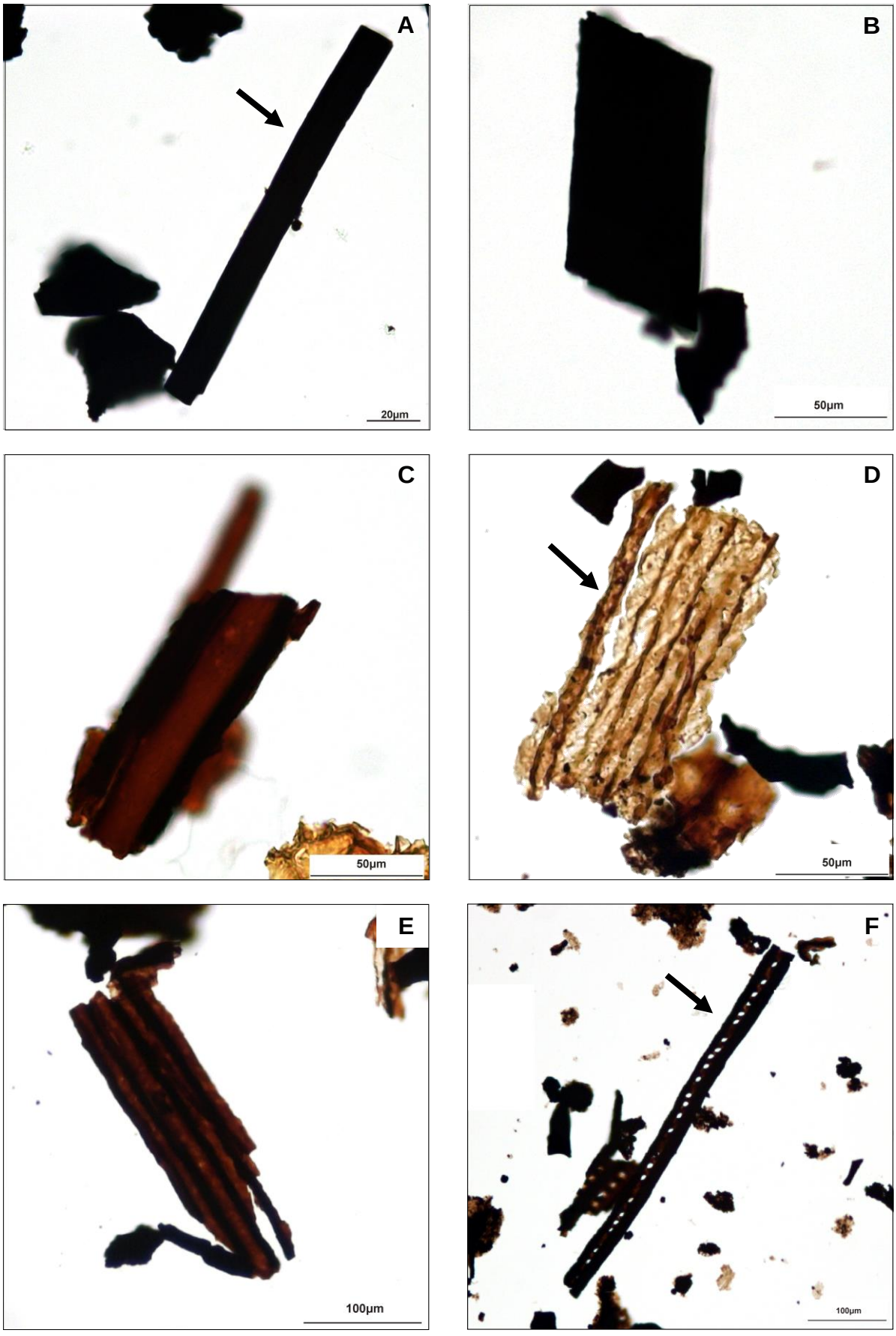
A
20µm
B
50µm
C
50µm
D
50µm
E
100µm
F
100µm

1.1 G - Non-opaque phytoclast, cuticle (Fx8; TL).

1.1 H - Non-opaque phytoclast, cuticle (Fx8; FM).

1.1 I - Non-opaque phytoclast, membrane (Am.7; TL).

1.1 J - Non-opaque phytoclast, membrane (Am.7; FM).

1.1 K - Particular Case, structured phytoclast: cross-hatch structure (Am.26; FM).

1.1 L - Sclereid (Fx12; TL).

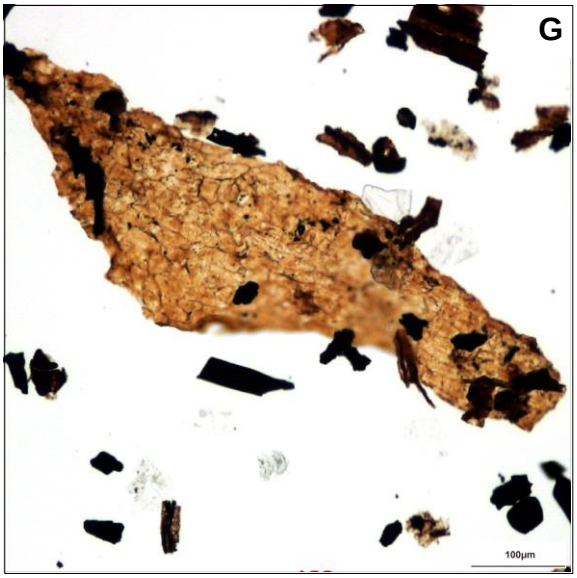
G
100µm

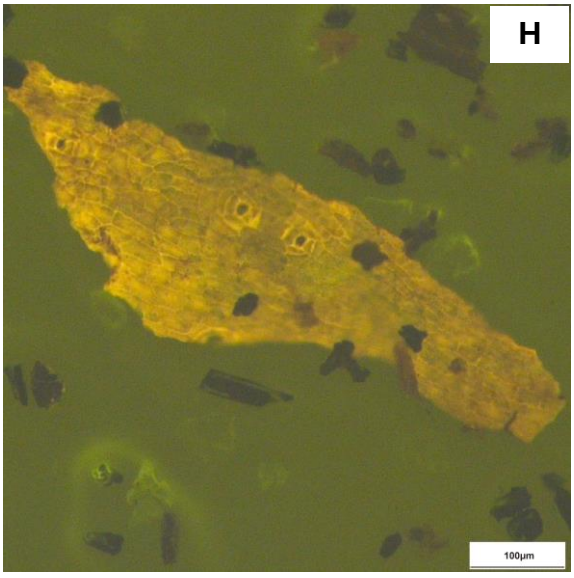
H
100µm


I
500 µm

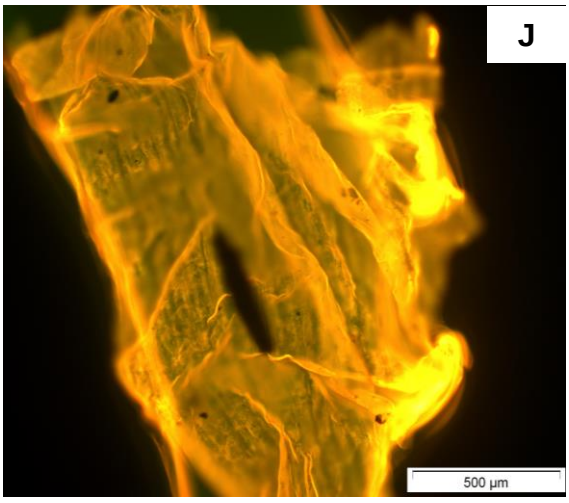
J
500 µm

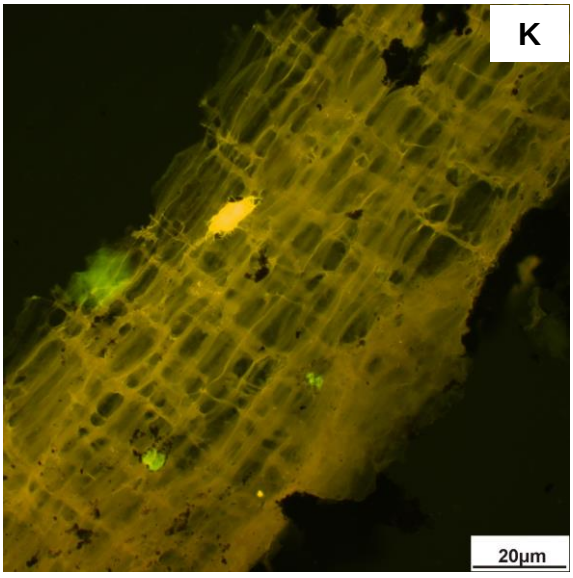
K
20µm

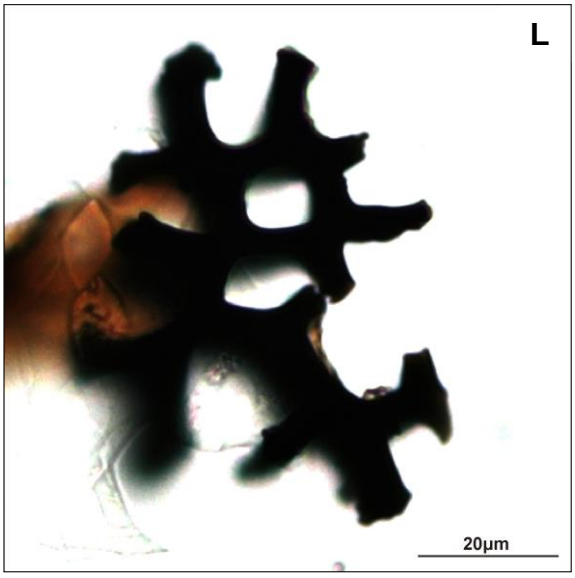
L
20µm

1.2. SEM aspects

1.2. A - Non-opaque biostructured phytoclast (Fx29).

1.2. B - Non-opaque biostructured phytoclast, banded (Fx25).

1.2. C - Non-opaque biostructured phytoclast, pitted (Fx25).

1.2. D - Non-opaque biostructured phytoclast, striped (Fx25).

1.2. E - Non-opaque biostructured phytoclast (Fx25).

1.2. F - Non-opaque phytoclast, cuticle (Fx25).

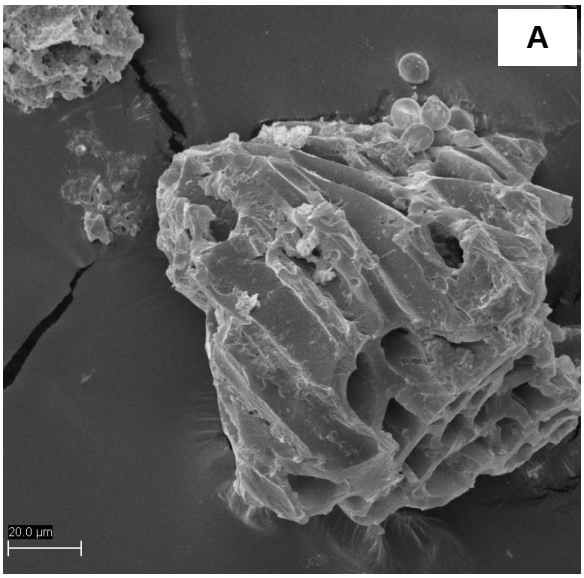
A
20.0 µm

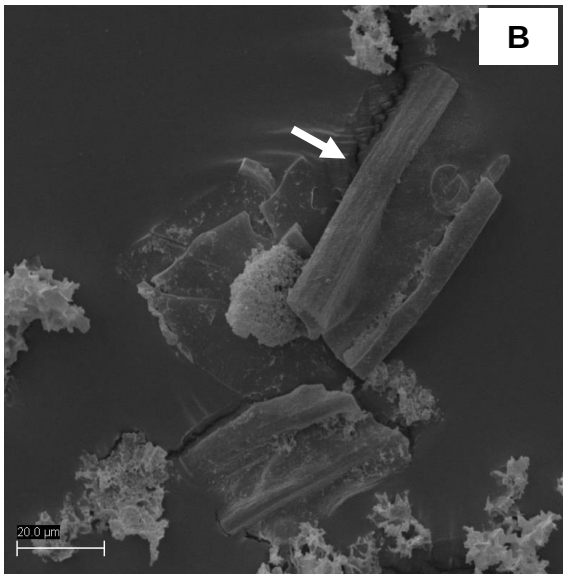
B
20.0 µm

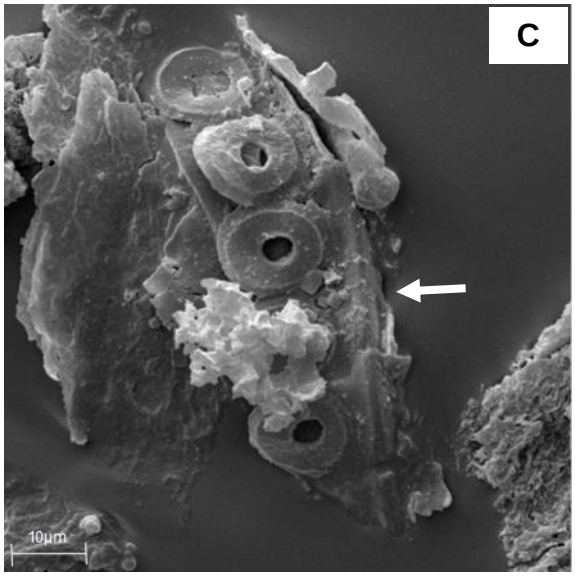
C
10µm

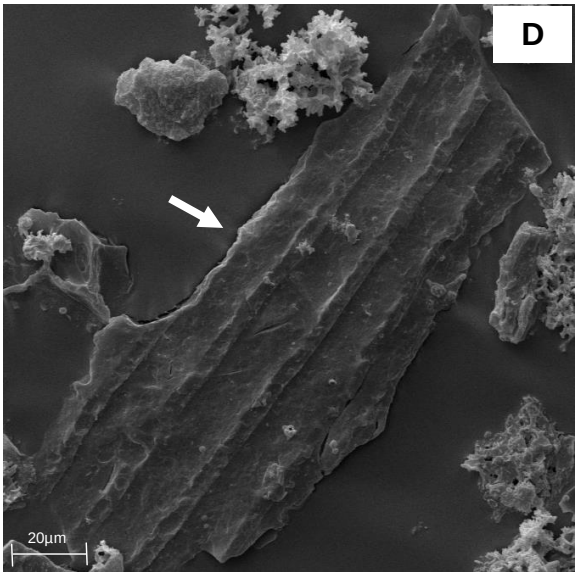
D
20µm

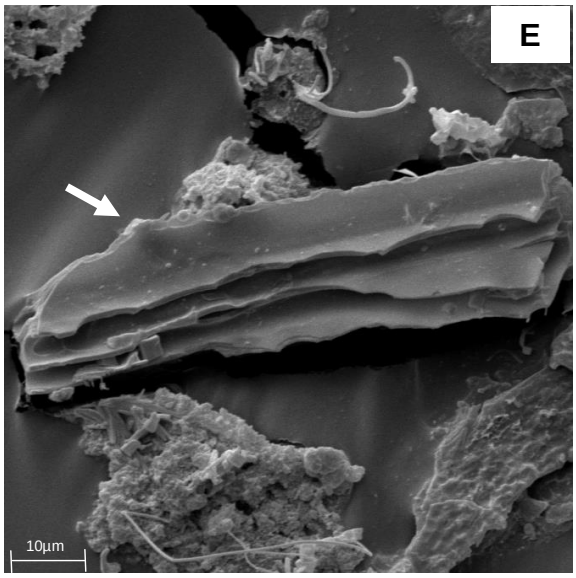
E
10µm

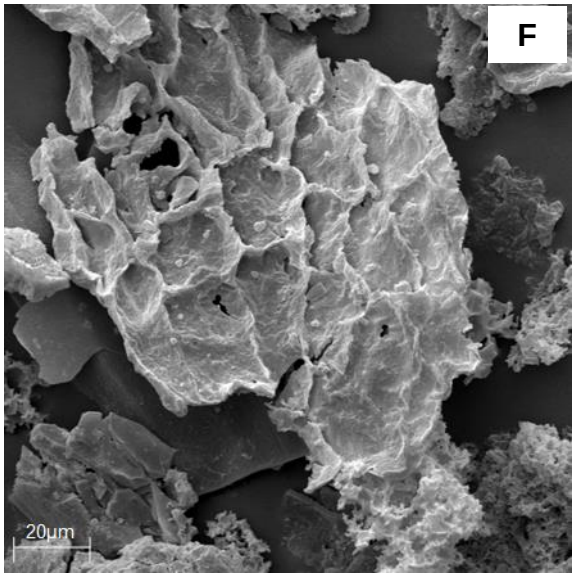
F
20µm

2. Amorphous Group

The Amorphous group included of all particulate organic components that appear structureless at the scale of the optical microscopy (Tyson, 1995). For more information about nomenclature and/or petrographic features see section 1.1.1.3 on Part II of this thesis.

2.1. Palynofacies features

2.1. A - Phytoplankton or bacterially derived amorphous organic matter (Br39; TL).

2.1. B - Phytoplankton or bacterially derived amorphous organic matter (Br39; FM).

2.1. C - Phytoplankton or bacterially derived amorphous organic matter (Fx29; TL).

2.1. D - Phytoplankton or bacterially derived amorphous organic matter (Fx29; FM).

2.1. E - Phytoplankton or bacterially derived amorphous organic matter (Br39; TL).

2.1. F - Phytoplankton or bacterially derived amorphous organic matter (Br39; FM).

2.1. G - Phytoplankton or bacterially derived amorphous organic matter, without fluorescence (Bf35; TL).

2.1. H - Resin (Bf5; FM).

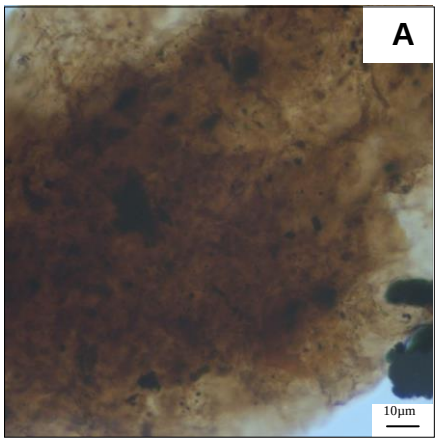
A
10µm

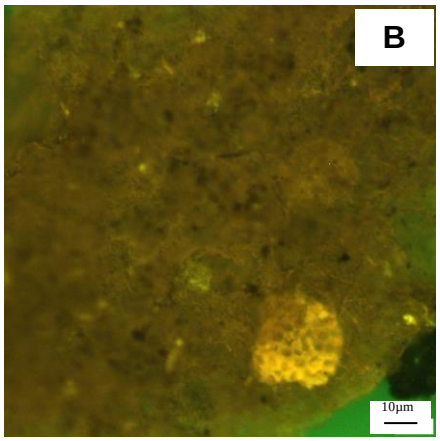
B
10µm

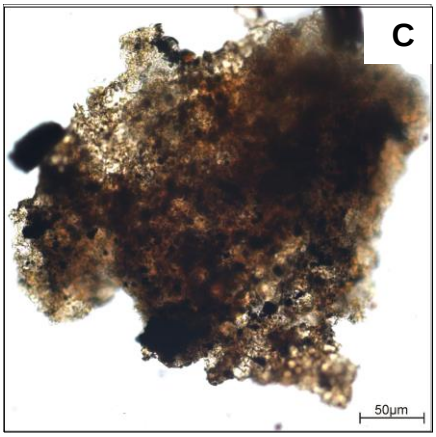
C
50µm

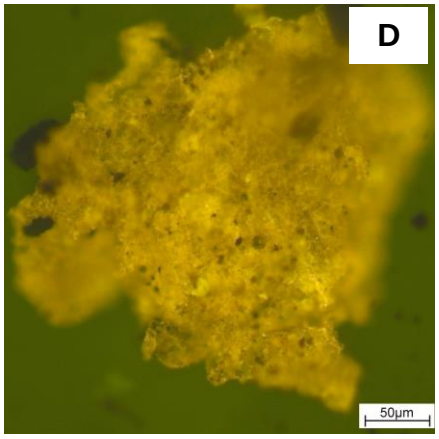
D
50µm

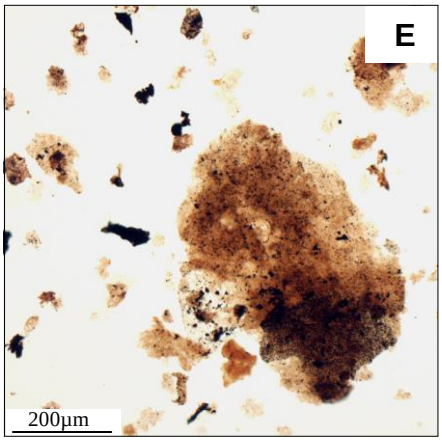
E
200µm

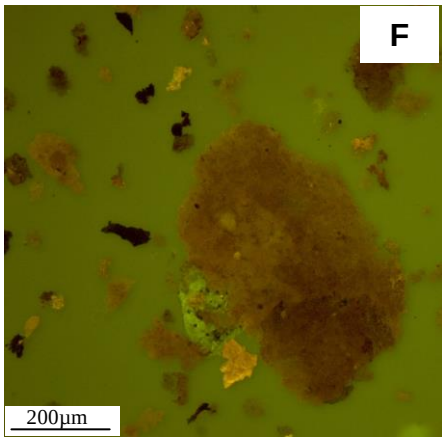
F
200µm

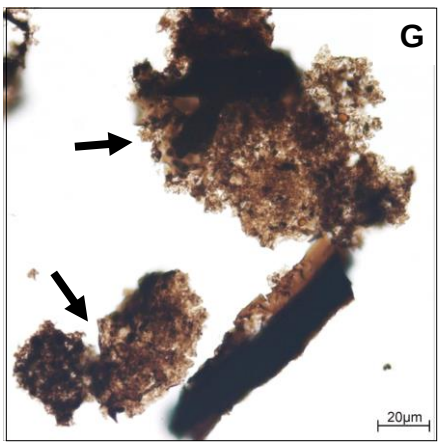
G
20µm

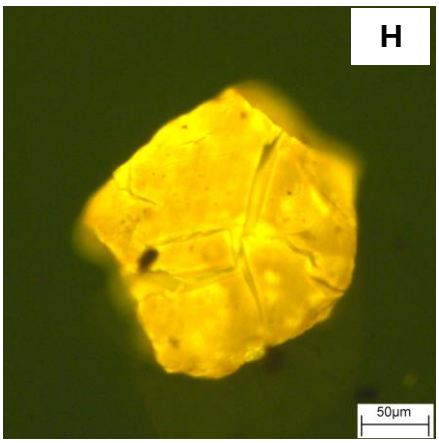
H
50µm

3. Palynomophs Group

Palynomorph group includes all discrete HCl and HF - resistant, organic-walled microfossil (Tchudy, 1961). For more information about nomenclature and/or petrographic features see section 1.1.1.3. on Part II of this thesis.

3.1. Palynofacies features

3.1.1. Sporomorphs - Spores

3.1.1. A - Spore with visible trilete (Bf3; TL).

3.1.1. B - Spore with visible trilete (Bf3; FM).

3.1.1. C - Ornamented spore (Fx9; TL).

3.1.1. D - Ornamented spore (Fx9; FM).

3.1.1. E - Ornamented spore (Bf14; TL).

3.1.1. F - Ornamented spore (Bf14; FM).

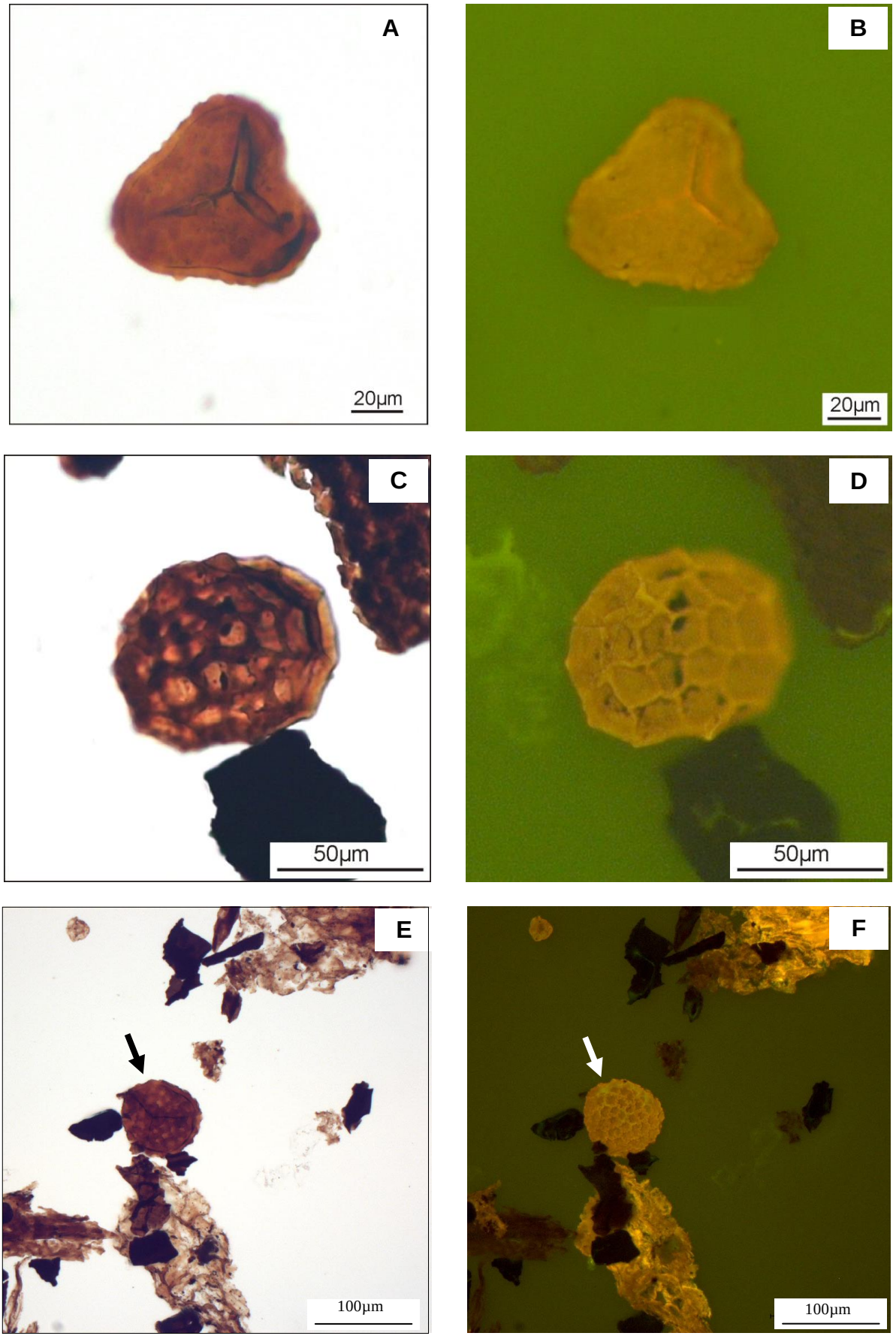
A
20µm
B
20µm
C
50µm
D
50µm
E
100µm
F
100µm

3.1.1. G - Ornamented spore (Bf16; TL).

3.1.1. H - Ornamented spore (Bf16; FM).

3.1.1. I - Ornamented spore with visible trilete (Bf23; TL).

3.1.1. J - Ornamented spore with visible trilete (Bf23; FM).

3.1.1. K - Spore with visible trilete (Fx10; TL).

3.1.1. L - Spore with visible trilete (Fx10; FM).

3.1.1. M - Ornamented spore (Rm9; TL).

3.1.1. N - Ornamented spore (Rm9; FM).

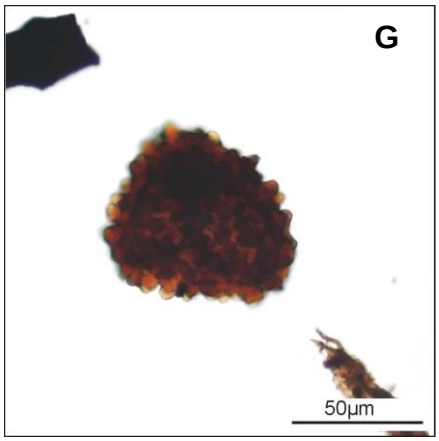
G
50µm

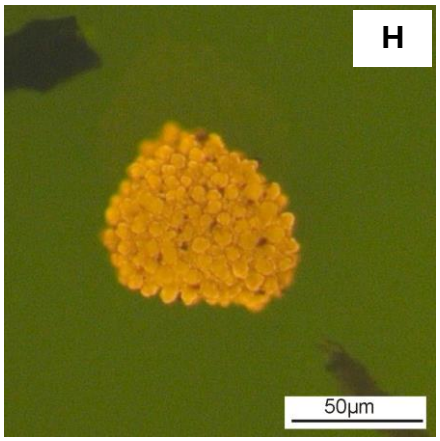
H
50µm

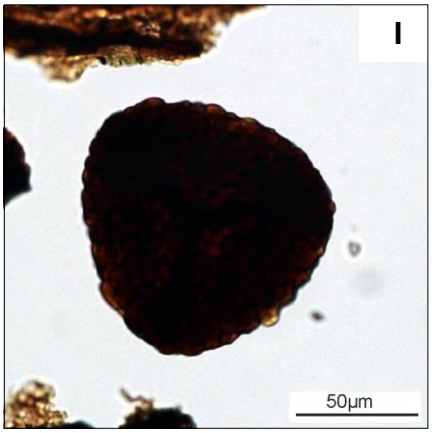
I
50µm

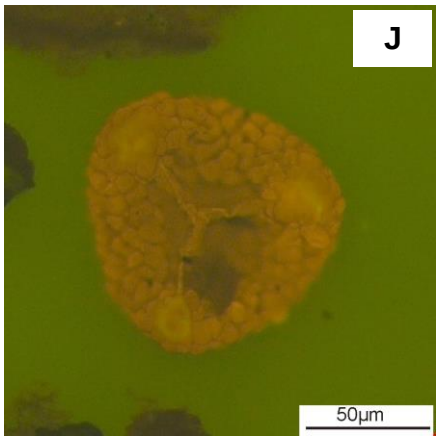
J
50µm

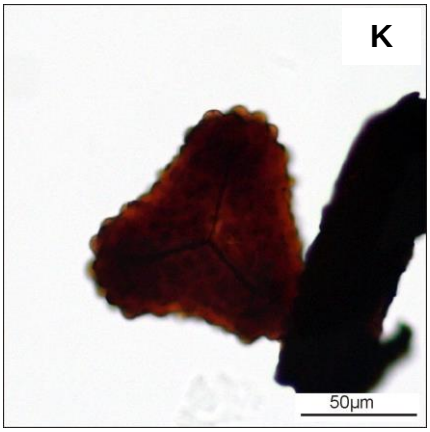
K
50µm

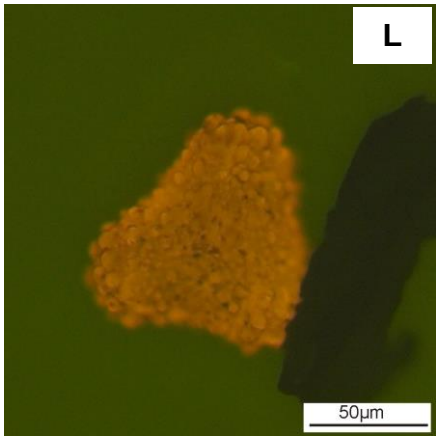
L
50µm

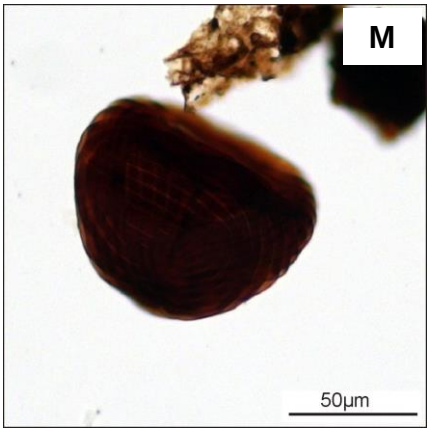
M
50µm

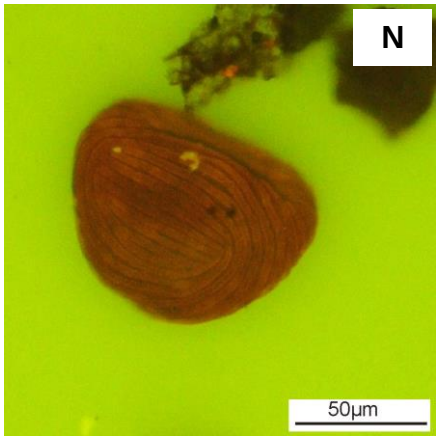
N
50µm

3.1.1. O - Winged spore (Br34; TL).

3.1.1. P - Winged spore (Br34; FM).

3.1.1. Q - Winged spore (Br34; TL).

3.1.1. R - Winged spore (Br34; FM).

3.1.1. S - Winged spores (Br34; DIC).

3.1.1. T - Fungal spore (Br1; TL).

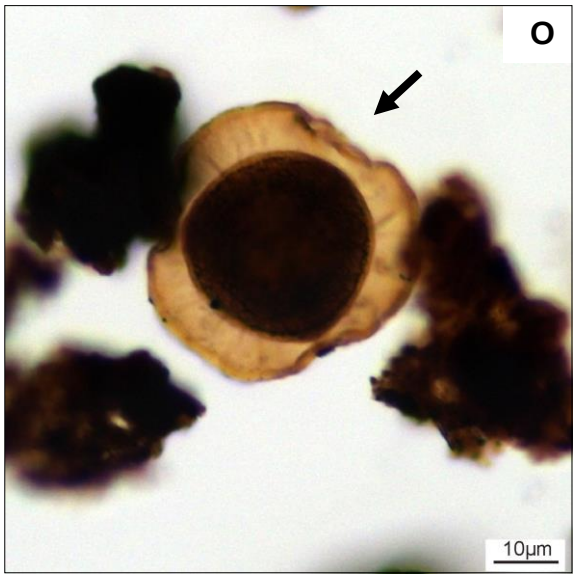
O
10µm

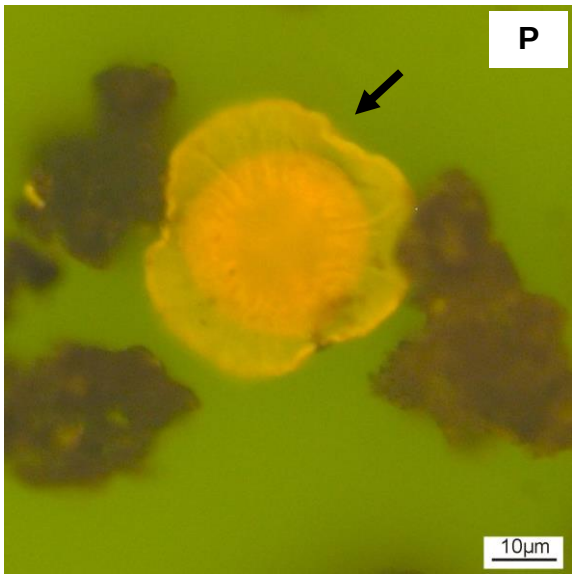
P
10µm

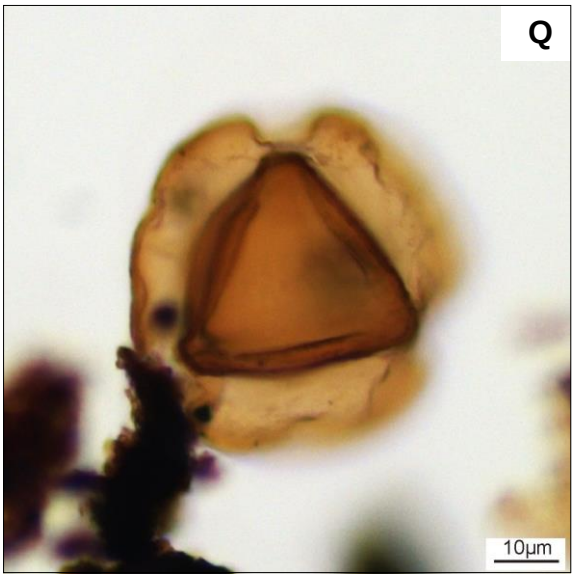
Q
10µm

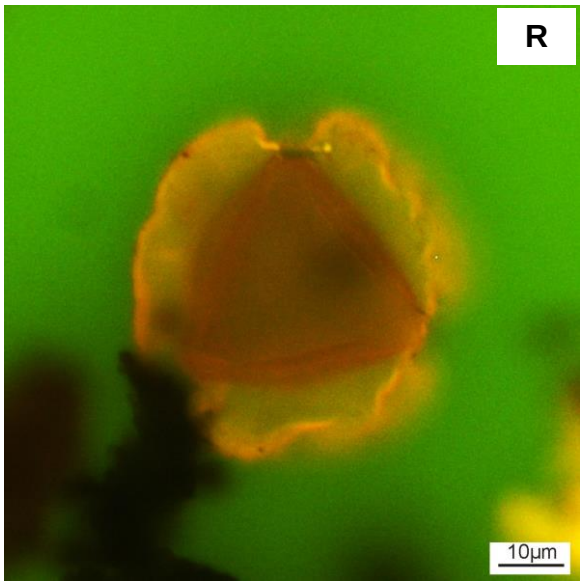
R
10µm


S
10µm

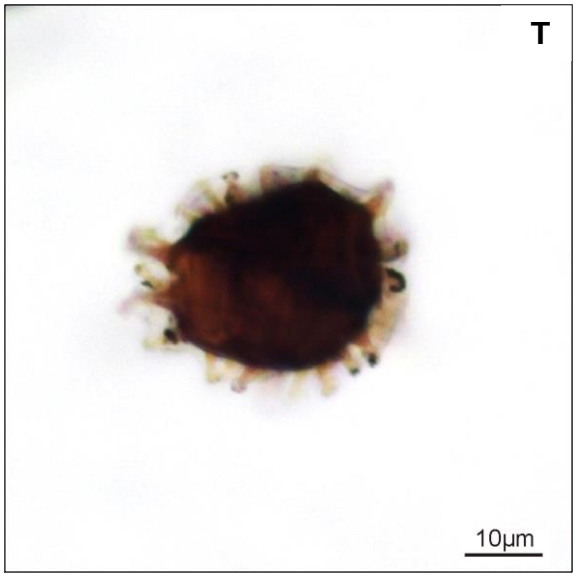
T
10µm

3.1.2. Sporomorphs - Pollen Grain and Polyads

3.1.2. A - Bisaccate pollen (Br33; TL).

3.1.2. B - Bisaccate pollen (Br33; FM).

3.1.2. C - Bisaccate pollen (Bf47; TL).

3.1.2. D - Bisaccate pollen (Br11; FM).

3.1.2. E - Tetrad of the genus *Classopollis* (Bf27; FM).

3.1.2. F - Polyad covered by bacteria (dots with higher fluorescence intensity) (Bf8; FM).

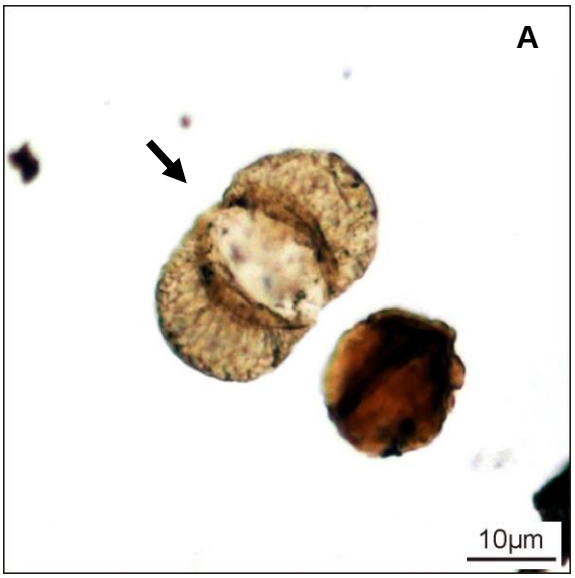
A
10µm

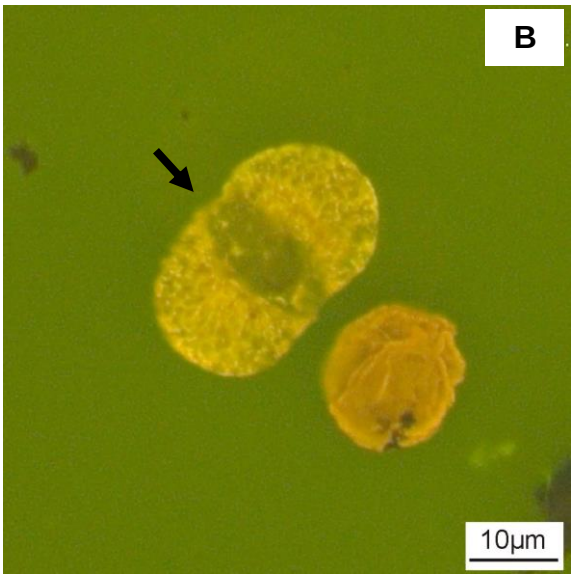
B
10µm


C
20µm

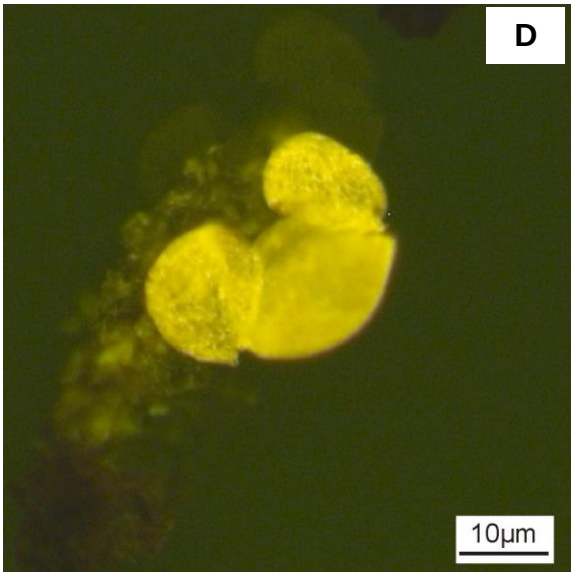
D
10µm

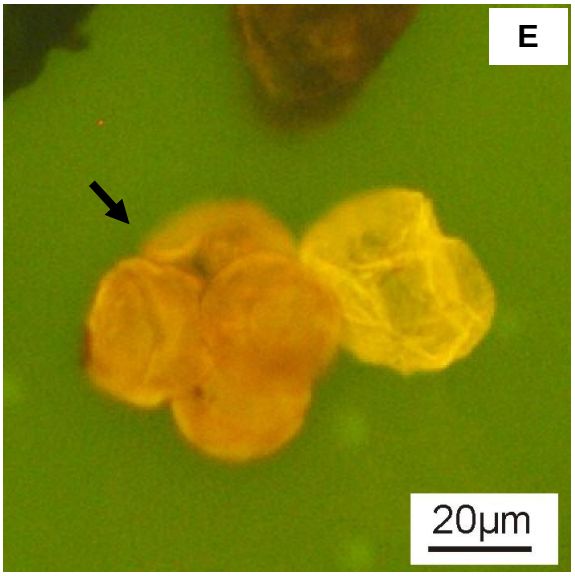
E
20µm

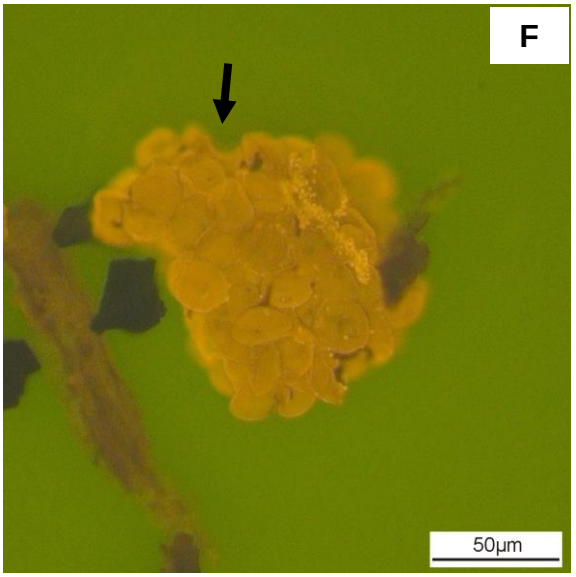
F
50µm

3.1.3. Freshwater microplankton

3.1.3. A - Green algae from the Desmidiales Order (Br38; TL).

3.1.3. B - Green algae from the Desmidiales Order (Br38; FM).

3.1.3. C - Zygospores of *Zygnema*-type (Fx16; TL).

3.1.3. D - Zygospores of *Zygnema*-type (Fx16; FM).

3.1.3. E - Zygospores of *Zygnema*-type (Fx21; TL).

3.1.3. F - Zygospores of *Zygnema*-type (Fx21; FM).

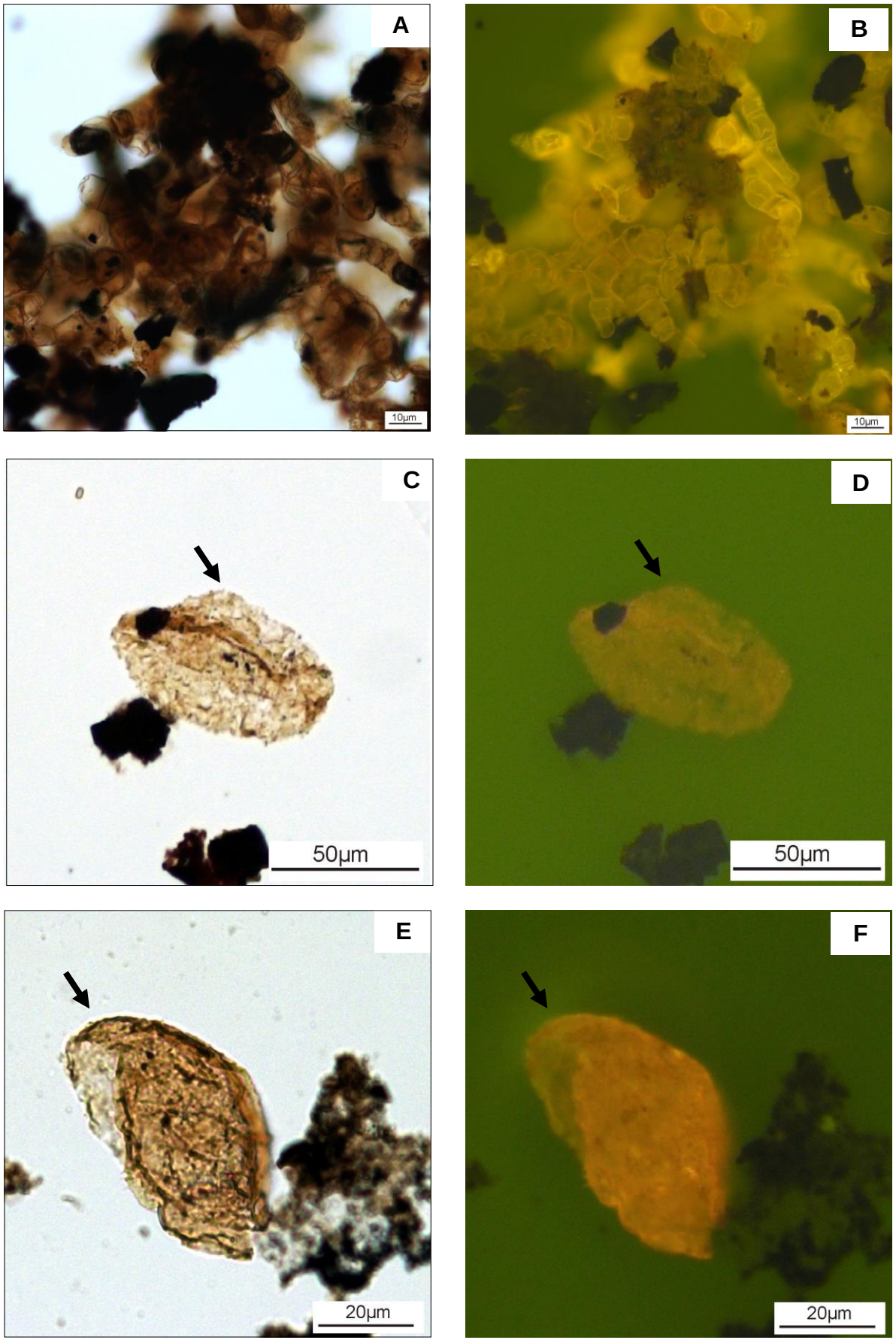
A
10µm
B
10µm
C
50µm
D
50µm
E
20µm
F
20µm

3.1.4. Marine microplankton

3.1.4. A - Cyst of dinoflagellate (Fx16; TL).

3.1.4. B - Cyst of dinoflagellate (Fx16; FM).

3.1.4. C - Cyst of dinoflagellate (Fx20; TL).

3.1.4. D - Cyst of dinoflagellate (Fx20; FM).

3.1.4. E - Cyst of dinoflagellate (Fx24; TL).

3.1.4. F - Cyst of dinoflagellate (Fx24; FM).

3.1.4. G - Prasinophyte phycomata, *Tasmanites* genus (Br38; FM).

3.1.4. H - Acritarch (Br8; FM).

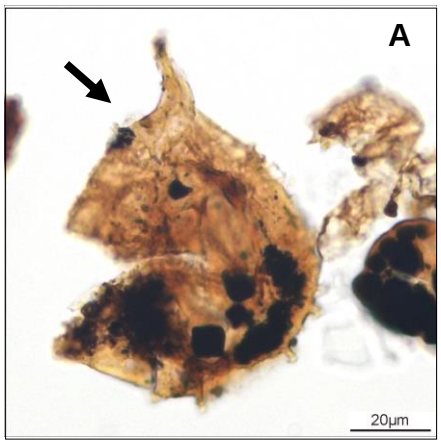
A
20µm

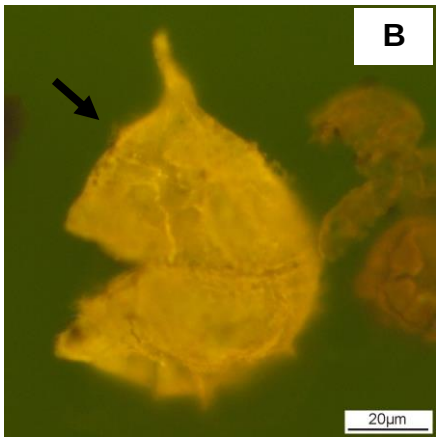
B
20µm

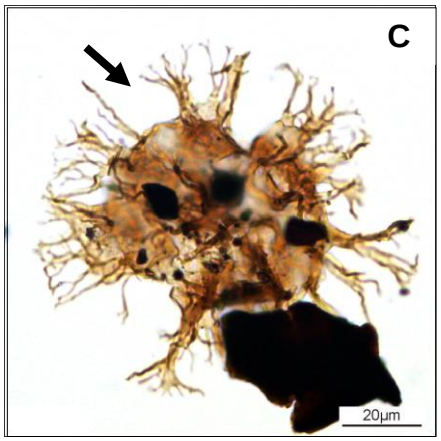
C
20µm

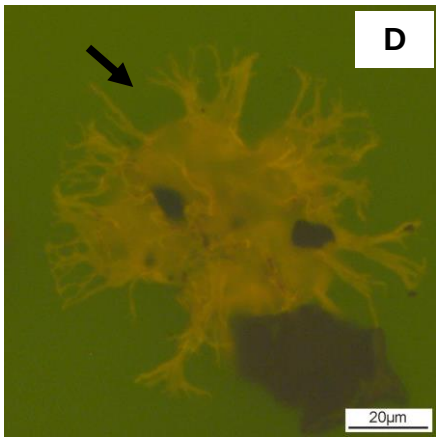
D
20µm

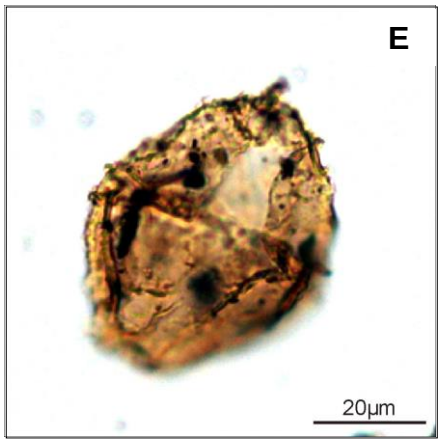
E
20µm

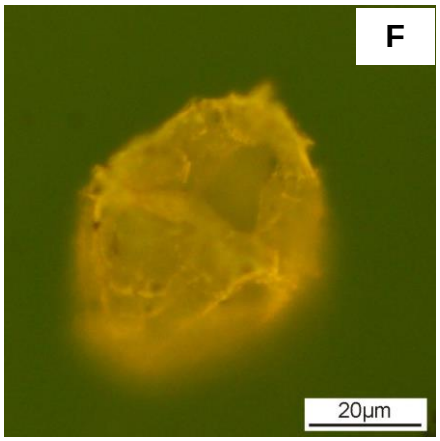
F
20µm

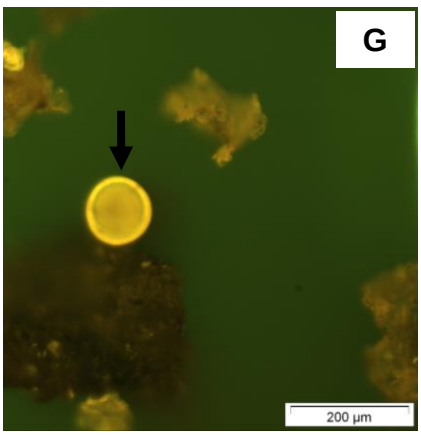
G
200 µm

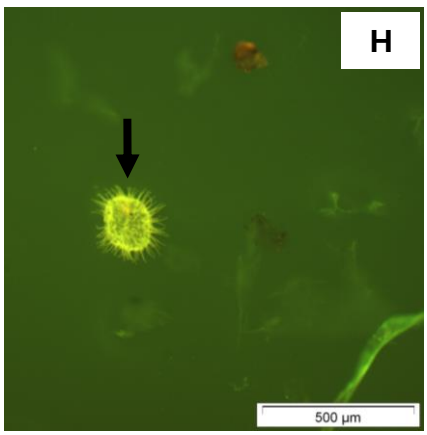
H
500 µm

3.1.5. Zoomorphs and Zooclasts

3.1.5. A - Zoomorph, foraminiferal test-linings (Fx18; TL).

3.1.5. B - Zoomorph, foraminiferal test-linings (Br33; TL).

3.1.5. C - Zoomorph, foraminiferal test-linings (Br34; TL).

3.1.5. D - Zoomorph, foraminiferal test-linings (Br36; TL).

3.1.5. E - Zoomorph, foraminiferal test-linings (Br38; TL).

3.1.5. F - Zoomorph, foraminiferal test-linings (Br41; TL).

3.1.5 G - Zooclasts (Fx33; TL).

3.1.5. H - Zooclasts (Fx36; TL).

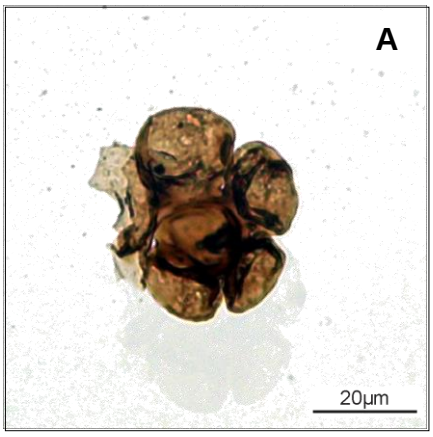
A
20µm

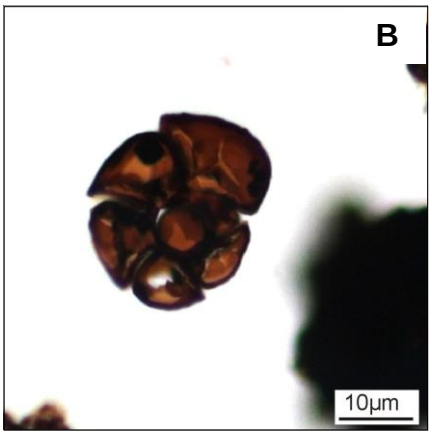
B
10µm

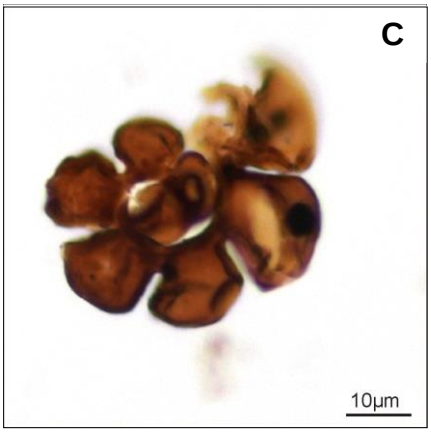
C
10µm

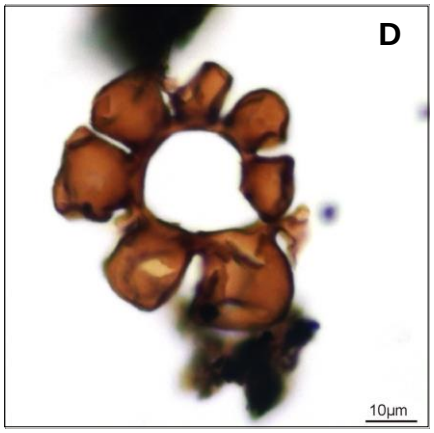
D
10µm

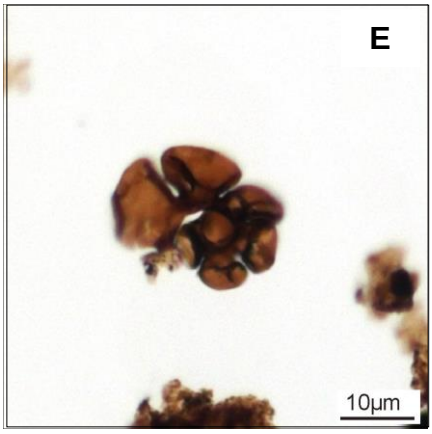
E
10µm


F
10µm

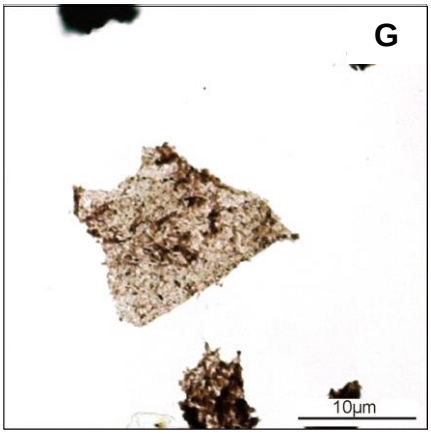
G
10µm

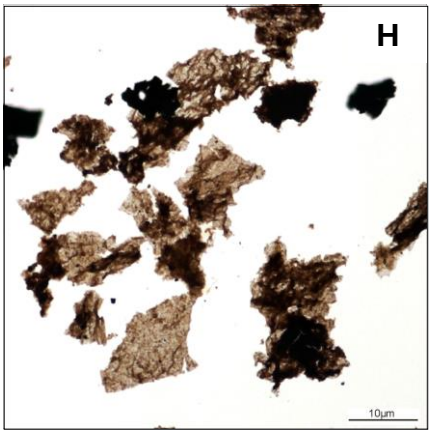
H
10µm

3.2. SEM aspects

3.2. A to E - Palynomorphs (Fx25).

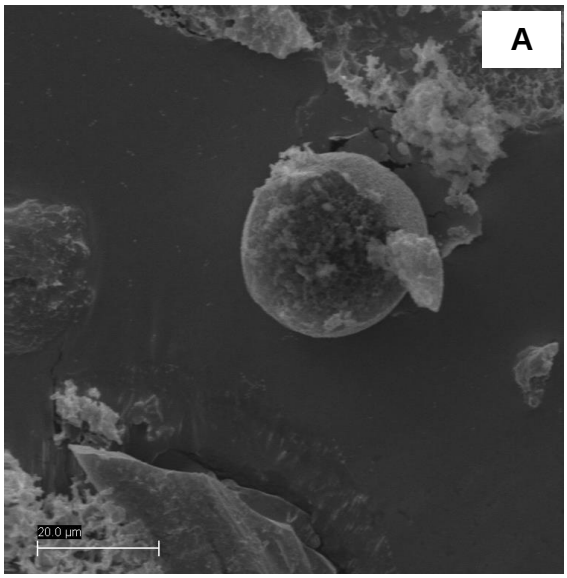
A
20.0 µm

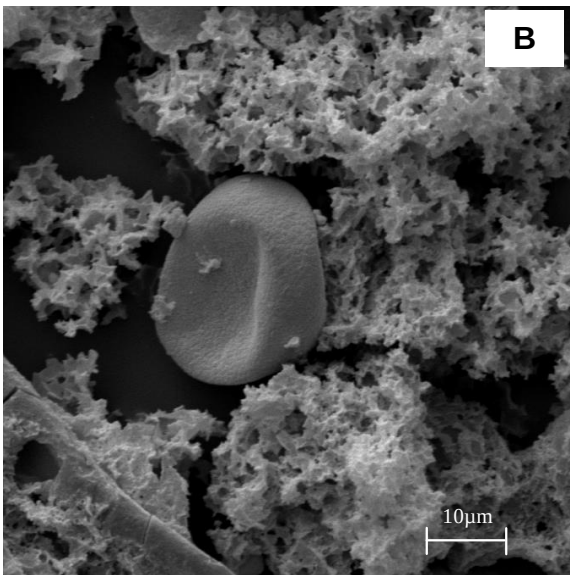
B
10µm

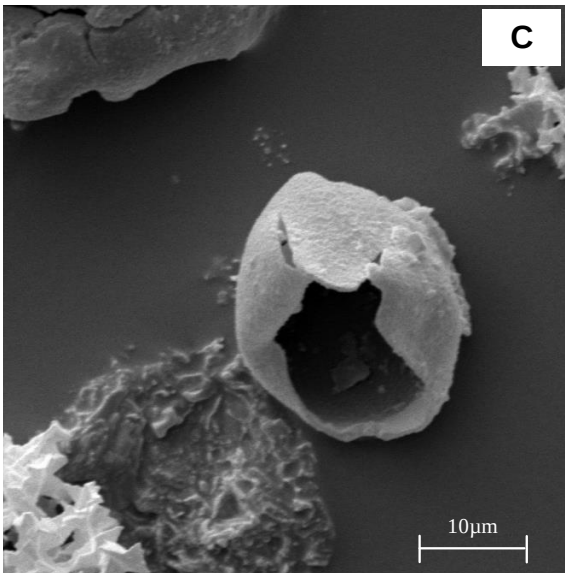
C
10µm

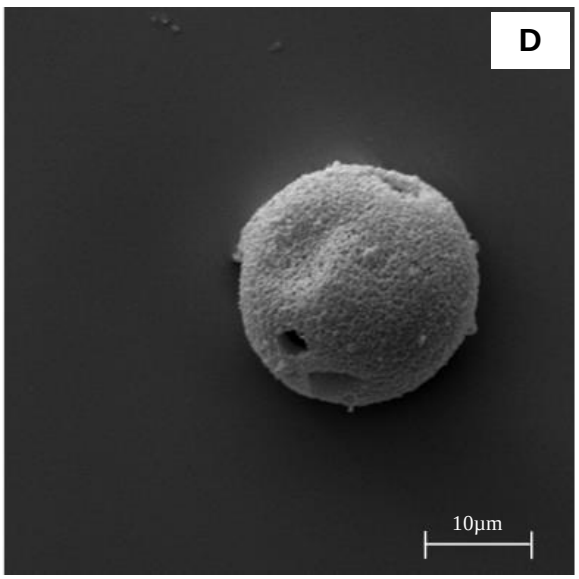
D
10µm

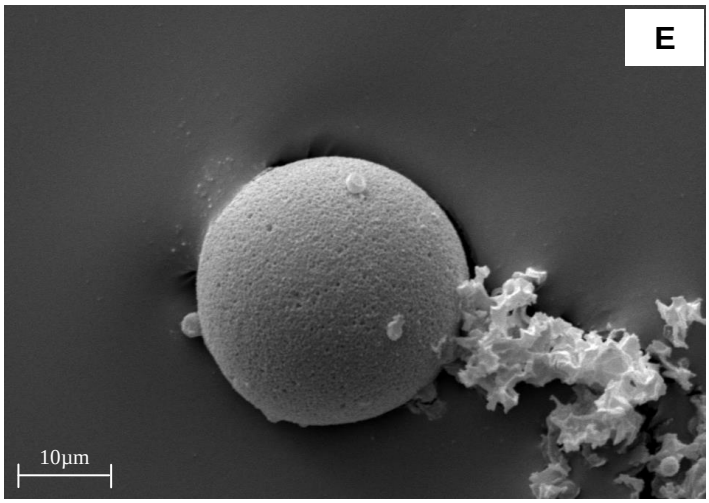
E
10µm

4. Solid bitumen

4.1. Palynofacies aspects

4.1. A - Black solid bitumen (Am.27; TL).

4.1. B to F - Black solid bitumen (Fx25; TL)

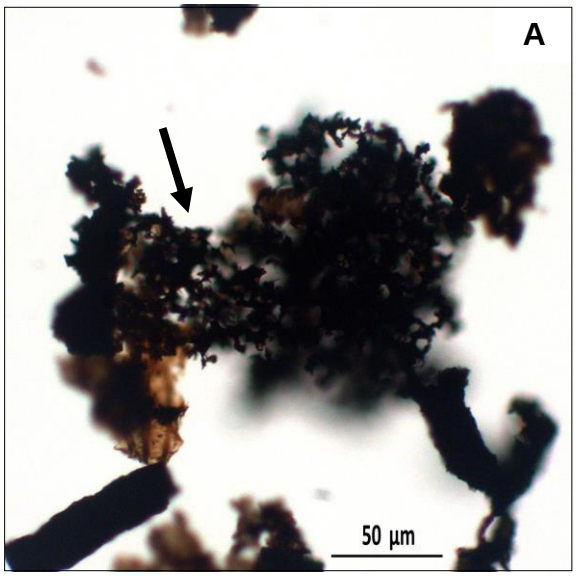
A
50 µm

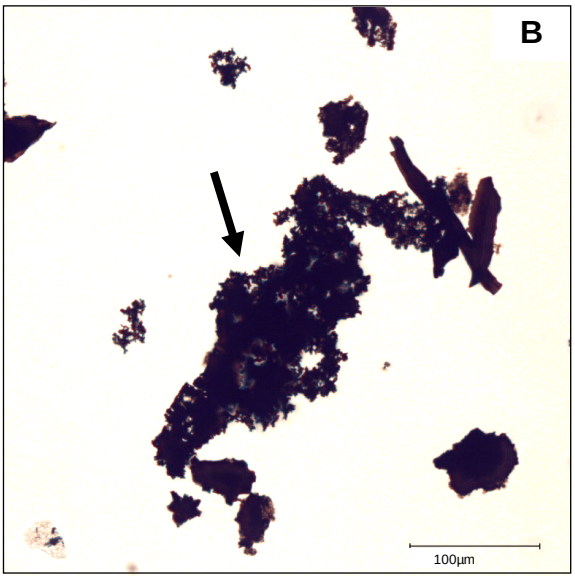
B
100µm

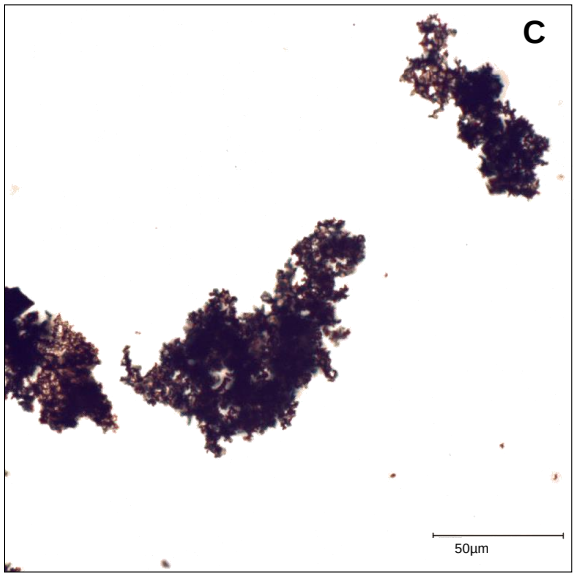
C
50µm

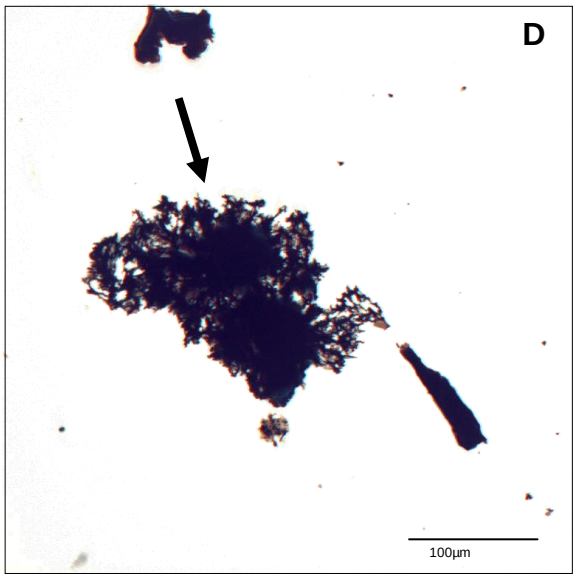
D
100µm

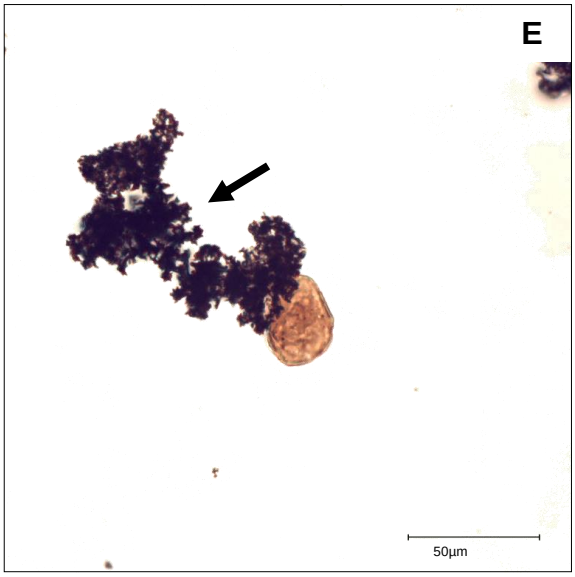
E
50µm

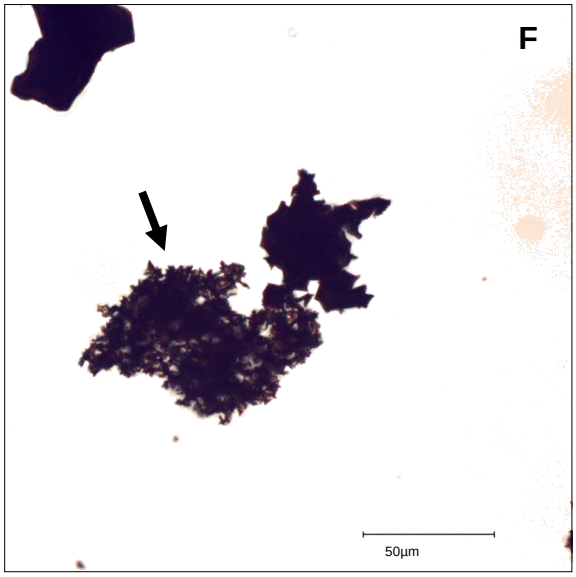
F
50µm

4.1. G - Solid bitumen (Br12; TL).

4.1. H - Solid bitumen (Br12; FM).

4.1. I - Solid bitumen (Br14; TL).

4.1. J - Solid bitumen (Br14; FM).

4.1. K - Solid bitumen (Br26; TL).

4.1. L - Solid bitumen (Br26; FM).

4.1. M - Solid bitumen (Bf77; TL).

4.1. N - Solid bitumen (Bf77; TL).

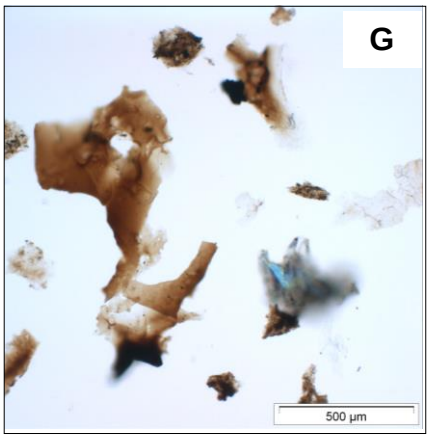
G
500 µm

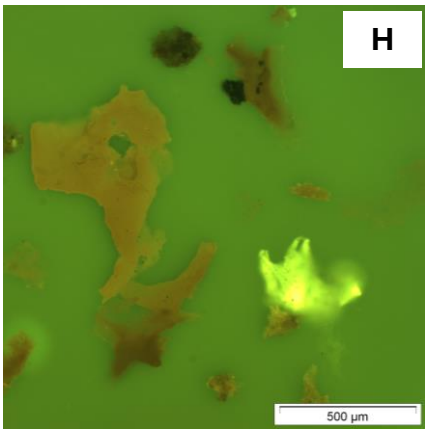
H
500 µm

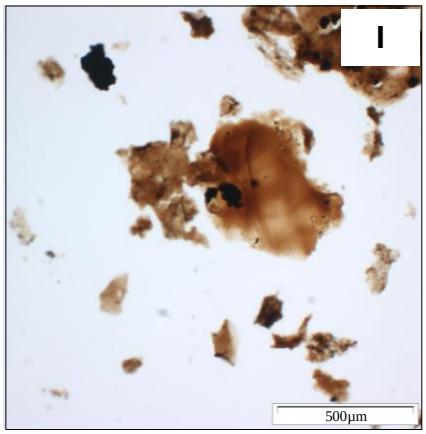
I
500µm

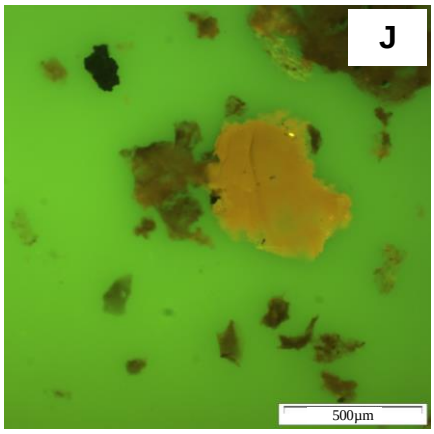
J
500µm

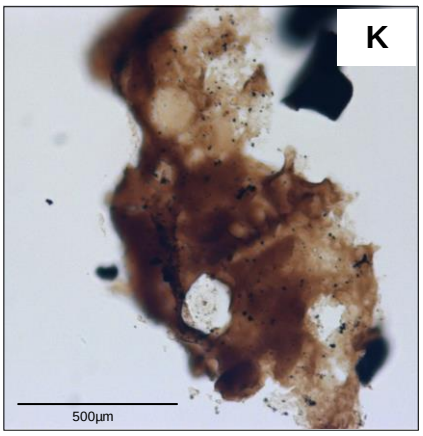
K
500µm

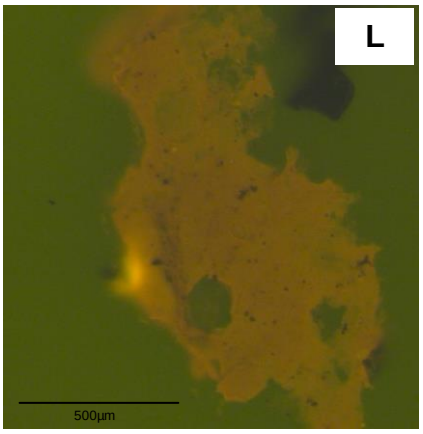
L
500µm

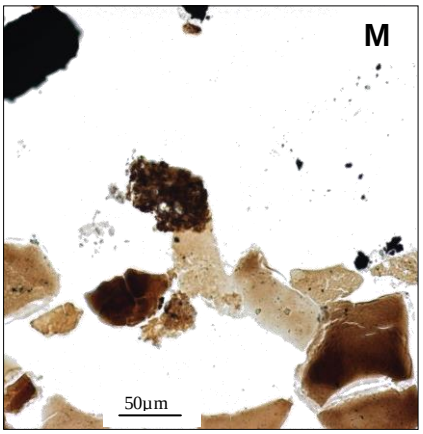
M
50µm

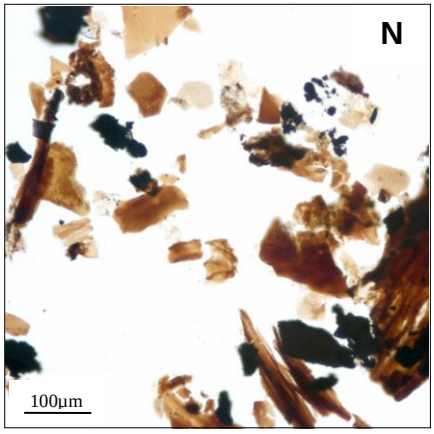
N
100µm

4.2. Whole rock features

4.2.1. Solid bitumen A

4.2.1. A - Solid bitumen A (Fx25; RL).

4.2.1. B - Solid bitumen A (Fx25; FM).

4.2.1. C - Solid bitumen A (Bf40; RL).

4.2.1. D - Solid bitumen A (Fx25; RL).

4.2.1. E - Solid bitumen A (Bf44; RL).

4.2.1. F - Solid bitumen A (Bf44; FM).

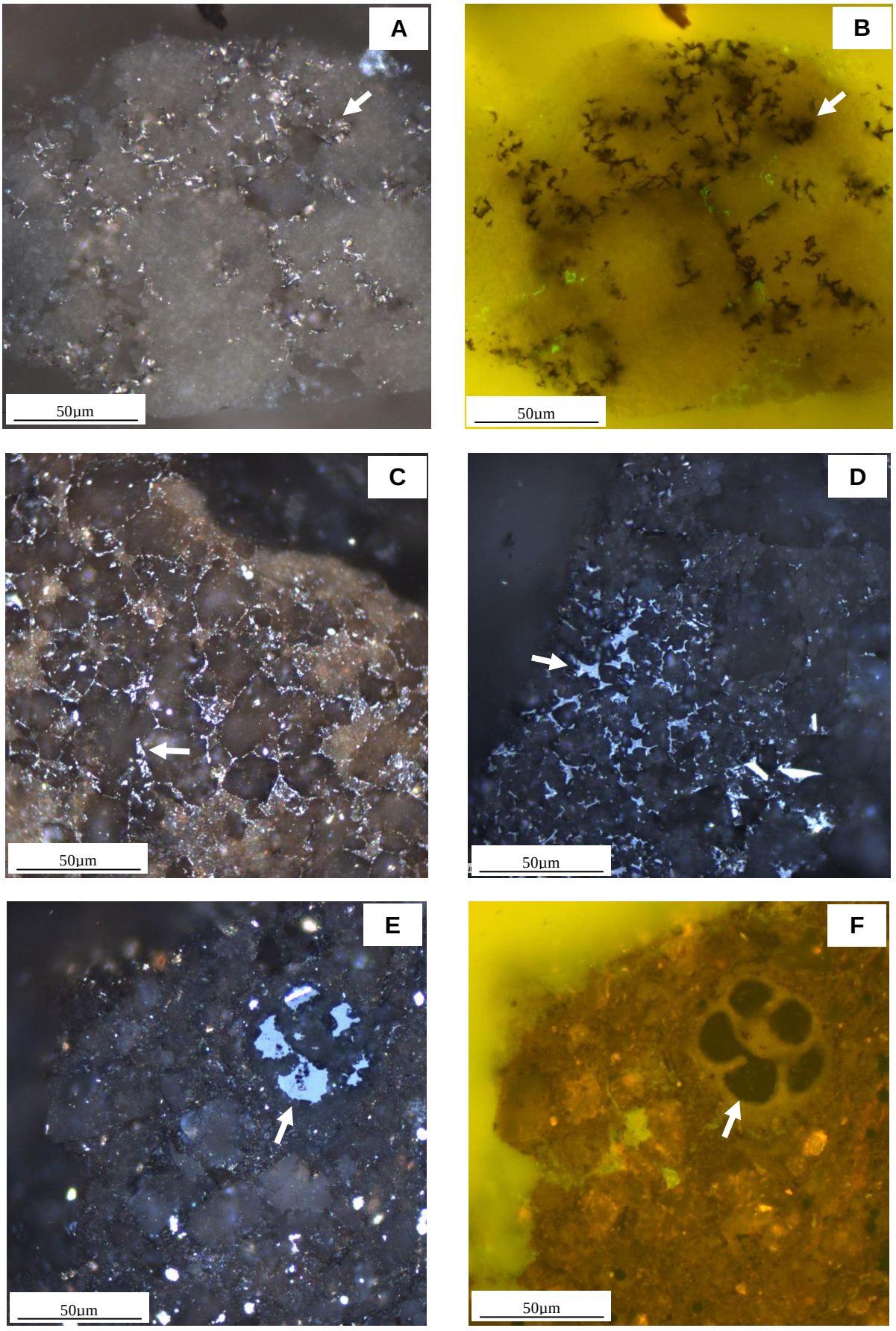
A
50µm
B
50µm
C
50µm
D
50µm
E
50µm
F
50µm

4.2.2. Solid bitumen B

4.2.2. A - Solid bitumen B (Bf38; RL).

4.2.2. B - Solid bitumen B (Bf38; FM).

4.2.2. C - Solid bitumen B (Fx32; RL).

4.2.2. D - Solid bitumen B (Fx32; FM).

4.2.2. E - Solid bitumen B (Fx32; RL).

4.2.2. F - Solid bitumen B (Fx32; FM).

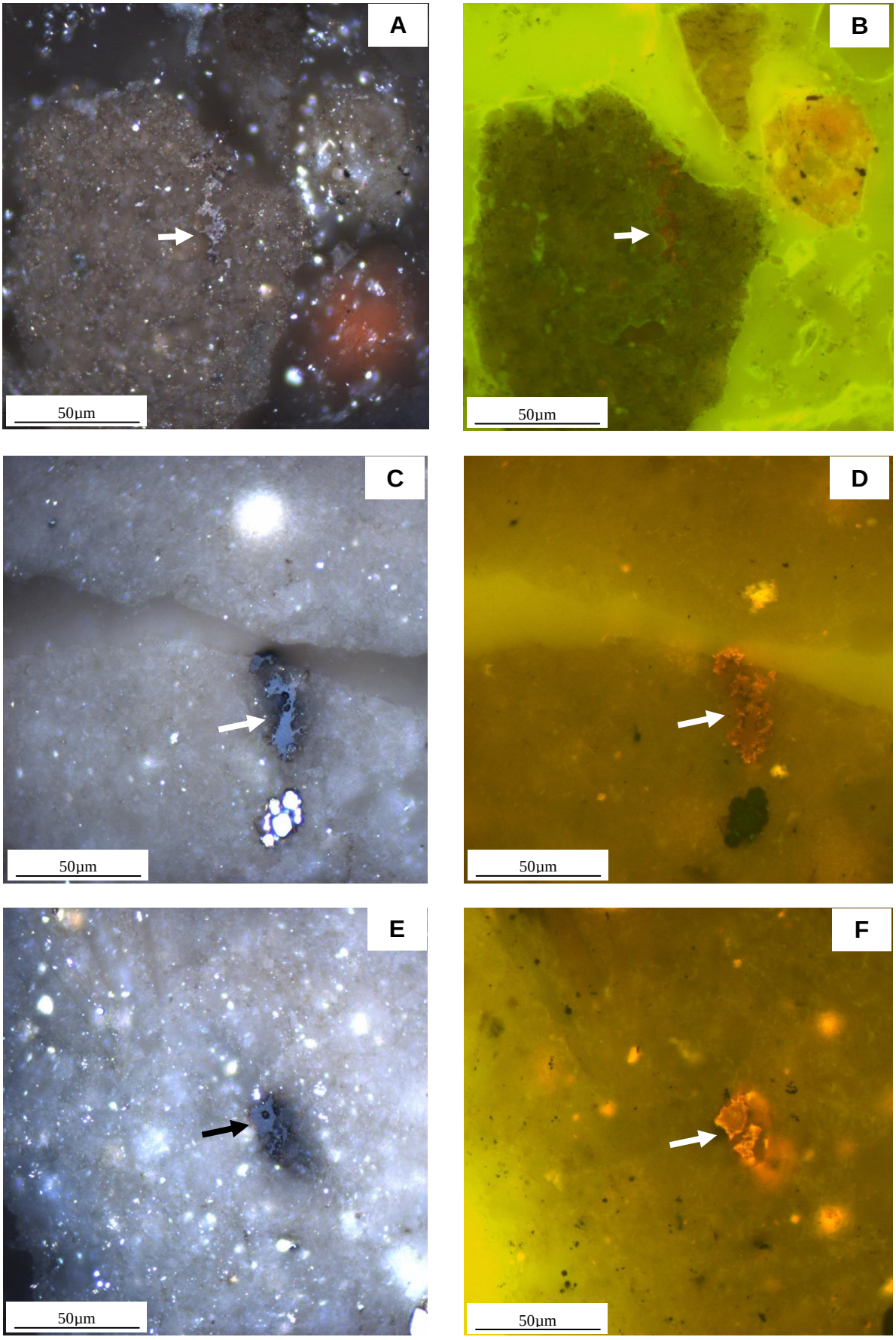
A
50µm
B
50µm
C
50µm
D
50µm
E
50µm
F
50µm

4.2.3. Solid bitumen C

4.2.3. A - Solid bitumen C (Bf53; RL).

4.2.3. B - Solid bitumen C (Bf53; FM).

4.2.3. C to F - Solid bitumen C (Fx25; RL).

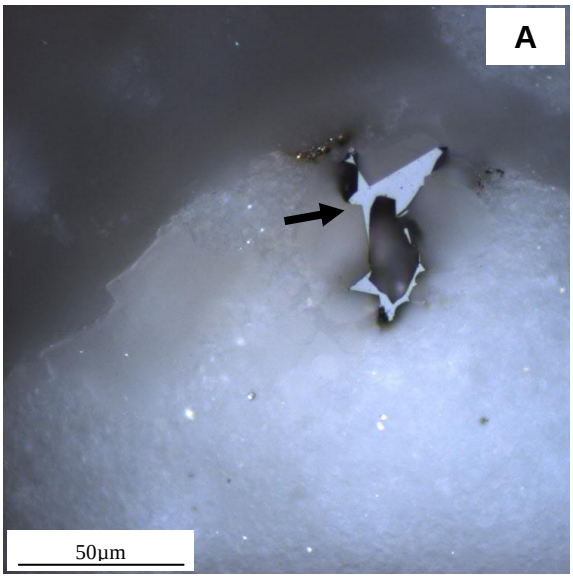
A
50µm

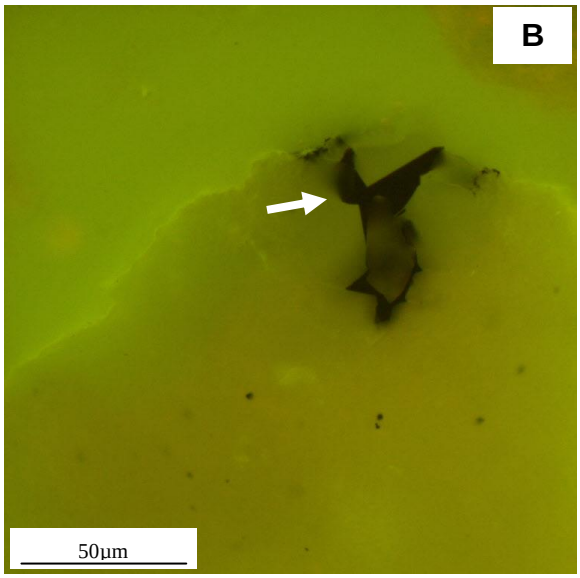
B
50µm

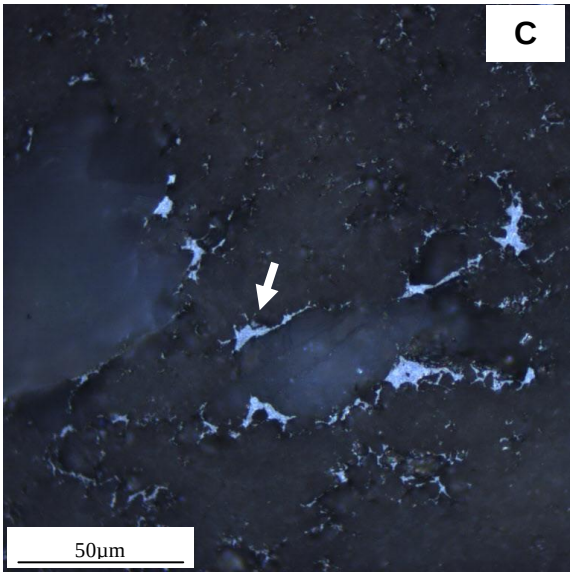
C
50µm

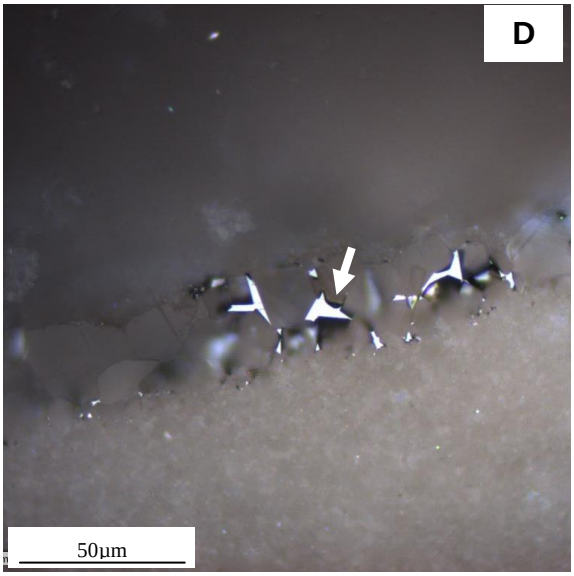
D
50µm

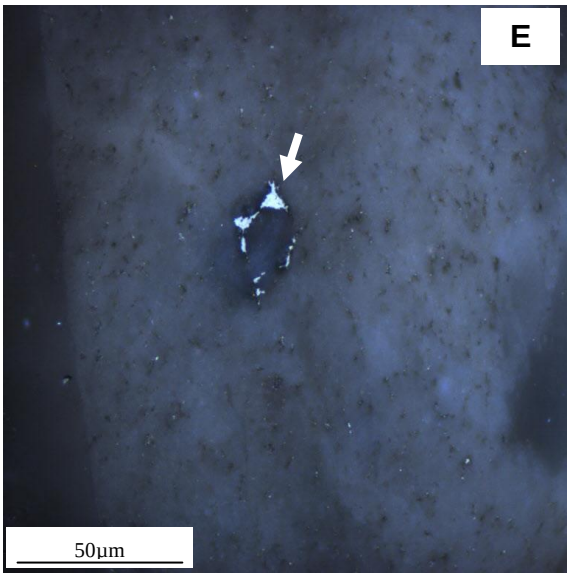
E
50µm

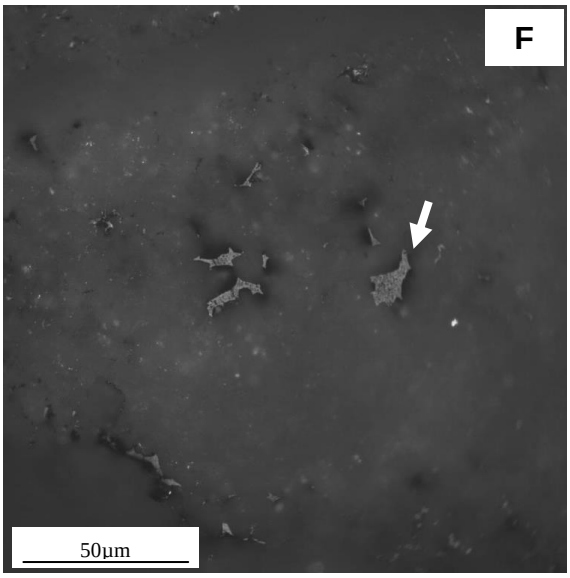
F
50µm

4.3. SEM aspects

4.3. A to F - Solid bitumen (Fx25)

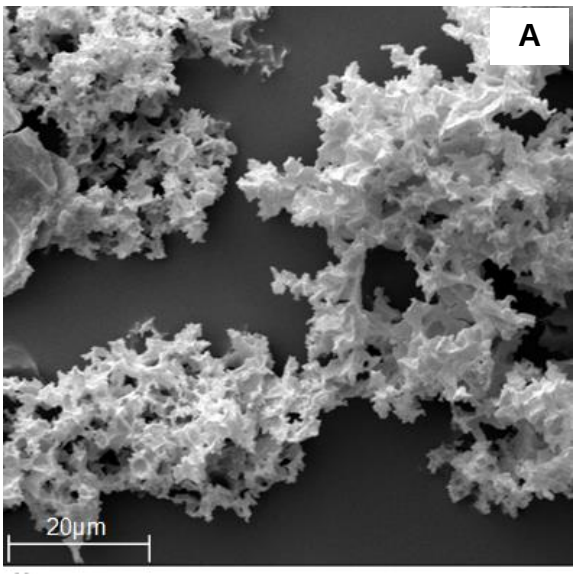
A
20µm

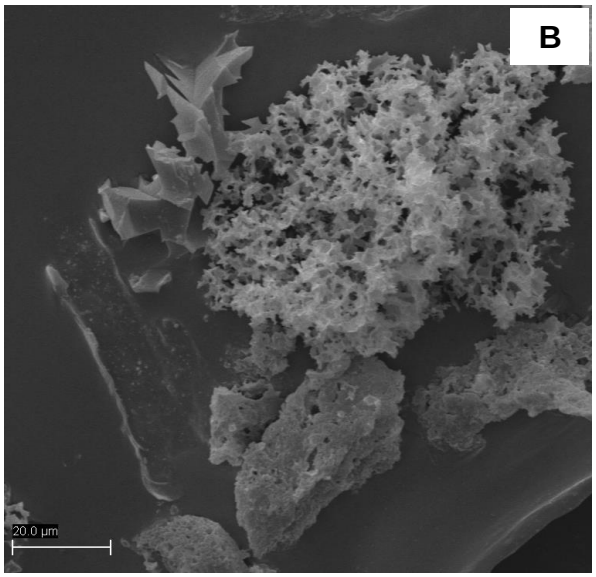
B
20.0 µm

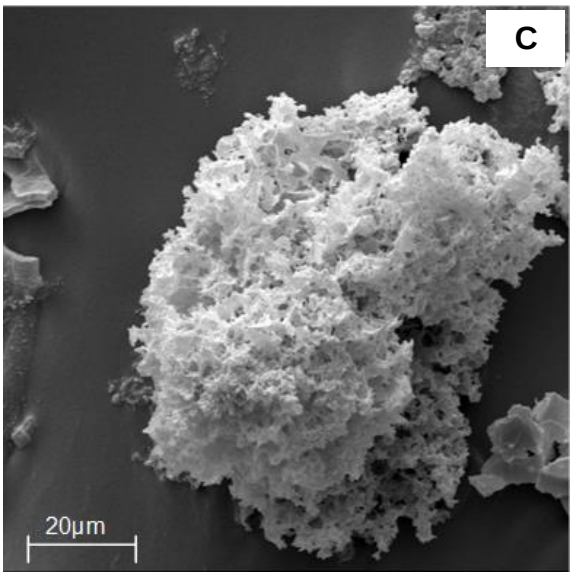
C
20µm

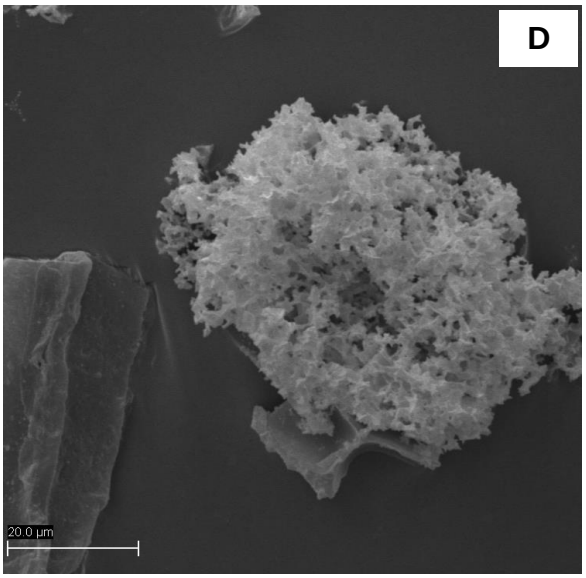
D
20.0 µm

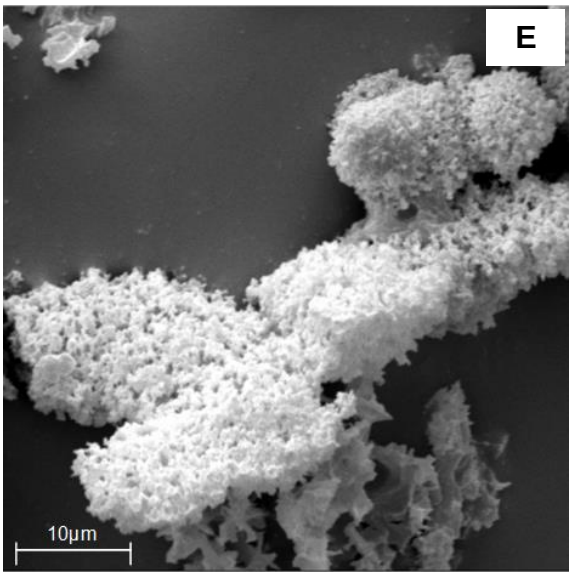
E
10µm

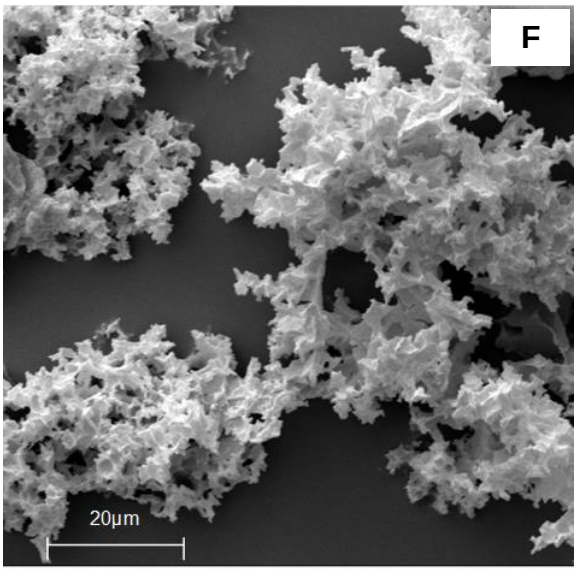
F
20µm

References

ASTM D7708, 2011. Standard Test Method for Microscopical Determination of Reflectance of Vitrinite Dispersed in Sedimentary Rocks. ASTM International, 8 pp.

Bostick, N.H., 1971. Thermal alteration of clastic organic particles as an indicator of contact and burial metamorphism in sedimentary rocks. Geosciences & Man, Baton Rouge 3, 83 - 92.

ISO 7404-2, 2009. Methods for the petrographic analysis of coals - Part 2: Methods of preparing coal samples. International Organization for Standardization. 12pp

Mendonça Filho, J.G., 1999. Aplicação de estudos de palinofácies e facies orgânica em rochas do Paleozóico da Bacia do Paraná, Sul do Brasil. Universidade Federal do Rio Grande do Sul. PhD thesis, 338 pp.

Mendonça Filho, J.G., Menezes, T.R., Mendonça, J.O., 2011. Organic Composition (Palynofacies Analysis). Chapter 5 in: ICCP Training Course on Dispersed Organic Matter, ISBN 978-9-89-826567-8, pp. 33 - 81.

Mendonça Filho, J.G., Menezes, T.R., Mendonça, J.O., Oliveira, A.D., Carvalho, M.A., Sant'Anna, A.J., Souza, J.T., 2010. Palinofácies, in: Sousa, C.I. (Ed.), Paleontologia. Rio de Janeiro, Interciência, pp.379 - 413

Mendonça Filho, J.G., Menezes, T.R., Mendonça, J.O., Oliveira, A.D., Silva, T.F., Rondon, N.F., Silva, F.S., 2012. Organic Facies: Palynofacies and Organic Geochemistry Approaches, in: Panagiotaras, D. (Org.), Geochemistry Earth's system processes. InTech, Patras, ISBN 978-9-53-510586-2, vol. 1, pp. 211 - 245.

Tchudy, R.H., 1961. Palynomorphs as indicators of facies environments in Upper Cretaceous and Lower Tertiary strata, Colorado and Wyoming. Wyoming Geological Society, 16*th* Annual Field Conference, Guidebook, 53 - 59.

Tyson, R.V., 1995. Sedimentary Organic Matter. Chap. & Hall, London.

Vicent, A.J., 1995. Palynofacies analysis of Middle Jurassic sediments from the Inner Hebrides. PhD Thesis, University of Newcastle upon Tyne. 475p.